AD-776 981

ANALYSIS OF MANEUVERABILITY EFFECTS ON ROTOR/WING DESIGN CHARACTERISTICS

R. D. Foster, et al

Bell Helicopter Company

Prepared for:

Army Air Mobility Research and Development Laboratory

February 1974

DISCLAIMER NOTICE

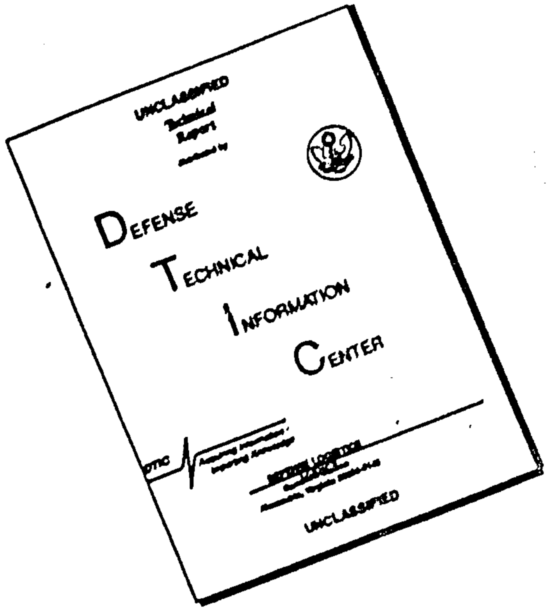

THIS DOCUMENT IS BEST QUALITY AVAILABLE. THE COPY FURNISHED TO DTIC CONTAINED A SIGNIFICANT NUMBER OF PAGES WHICH DO NOT REPRODUCE LEGIBLY.

Unclassified

Security Classification

AD776981

DOCUMENT CONTROL DATA - R & D

(Security classification of title, body of abstract and indexing annotation must be entered when the overall report is classified)

1. ORIGINATING ACTIVITY (Corporate author) Bell Helicopter Company Fort Worth, Texas	2a. REPORT SECURITY CLASSIFICATION Unclassified 2b. GROUP

3. REPORT TITLE

ANALYSIS OF MANEUVERABILITY EFFECTS ON ROTOR/WING DESIGN CHARACTERISTICS

4. DESCRIPTIVE NOTES (Type of report and inclusive dates)

5. AUTHOR(S) (First name, middle initial, last name)

R. D. Foster
J. C. Kidwell
C. D. Wells

6. REPORT DATE	7a. TOTAL NO. OF PAGES	7b. NO. OF REFS
February 1974	249	16

8a. CONTRACT OR GRANT NO. DAAJ02-70-C-0031 b. PROJECT NO. 1X164206D378 c. d.	9a. ORIGINATOR'S REPORT NUMBER(S) USAAMRDL Technical Report 74-26 9b. OTHER REPORT NO(S) (Any other numbers that may be assigned this report)

10. DISTRIBUTION STATEMENT

Approved for public release; distribution unlimited.

11. SUPPLEMENTARY NOTES	12. SPONSORING MILITARY ACTIVITY
	Eustis Directorate U.S. Army Air Mobility R&D Laboratory Fort Eustis, Virginia

13. ABSTRACT

A parametric study was conducted to determine the effects of maneuverability requirements on the design characteristics of rotors and wings for helicopters. The study was performed for both single-rotor helicopters and single-rotor winged helicopters. The study was conducted under the terms of Contract DAAJ02-70-C-0031.

Study results indicate that for typical UTTAS configurations, both winged and pure helicopters, designed for equal maneuvering capability, had equal payload capability. Therefore, for equal maneuvering capability, there was no discernible difference in weight or overall size. Winged configurations were more limited in their ability to achieve low (i.e., near zero) g, high-speed, maneuvering flight due to the difficulty in reducing wing lift sufficiently.

Designs optimized for maneuvering capabilities ranging from 1.50g at V_{NRP} to 2.00g at V_{NRP} resulted in design gross weight variations from 14,450 pounds to 15,980 pounds, respectively.

A recommended maneuvering requirement for UTTAS vehicles is shown to be closely related to the definition of required dive speeds and the resulting dive recovery characteristics. MIL-S-8698 dive speed definitions required a 2.00g maneuvering capability at V_{NRP}. A less stringent dive speed definition would allow a corresponding decrease in maneuvering capability required.

Identified technical risks include the definition of dive speeds for UTTAS vehicles; the low altitude, lightweight capability of a vehicle designed for a high maneuvering requirement; and the problem of pilot recognition of dynamic system structural limits during maneuvering flight.

252

DD FORM 1 NOV 65 1473 REPLACES DD FORM 1473, 1 JAN 64, WHICH IS OBSOLETE FOR ARMY USE.

Unclassified

Security Classification

Unclassified

Security Classification

14. KEY WORDS	LINK A		LINK B		LINK C	
	ROLE	WT	ROLE	WT	ROLE	WT
UTTAS						
Maneuverability effects						
Rotor/wing design characteristics						

1a

Unclassified

Security Classification

DEPARTMENT OF THE ARMY
U. S. ARMY AIR MOBILITY RESEARCH & DEVELOPMENT LABORATORY
EUSTIS DIRECTORATE
FORT EUSTIS, VIRGINIA 23604

This report presents the results of one study of the effects of maneuverability requirements on the design of pure and winged helicopters. The general objective was to present a rationale for a given maneuverability requirement for new Army helicopters in the utility class.

This report is published for the dissemination of information and the stimulation of new ideas.

The technical monitor for this contractual effort was Mr. Russell O. Stanton, UTTAS Project Officer, Systems Support Division.

Project 1X164206D378
Contract DAAJ02-70-C-0031
USAAMRDL Technical Report 74-26
February 1974

ANALYSIS OF MANEUVERABILITY EFFECTS ON ROTOR/WING DESIGN CHARACTERISTICS

Final Report

By

R. D. Foster
J. C. Kidwell
C. D. Wells

Prepared by

Bell Helicopter Company
Fort Worth, Texas

For

EUSTIS DIRECTORATE
U.S. ARMY AIR MOBILITY RESEARCH AND DEVELOPMENT LABORATORY
FORT EUSTIS, VIRGINIA

iii

SUMMARY

A parametric study was conducted to determine the effects of maneuverability requirements on the design characteristics of rotors and wings for helicopters. The study was performed for both single-rotored helicopters and single-rotored winged helicopters. The study was conducted under the terms of Contract DAAJ02-70-C-0031.

Study results indicate that for typical UTTAS configurations, both winged and pure helicopters, designed for equal maneuvering capability, had equal payload capability. Therefore, for equal maneuvering capability, there was no discernible difference in weight or overall size. Winged configurations were more limited in their ability to achieve low (i.e., near zero) g, high-speed, maneuvering flight due to the difficulty in reducing wing lift sufficiently.

Designs optimized for maneuvering capabilities ranging from 1.50g's at V_{NRP} to 2.00g's at V_{NRP} resulted in design gross weight variations from 14,450 pounds to 15,980 pounds, respectively.

A recommended maneuvering requirement for UTTAS vehicles is shown to be closely related to the definition of required dive speeds and the resulting dive recovery characteristics. MIL-S-8698 dive speed definitions required a 2.00g maneuvering capability at V_{NRP}. A less stringent dive speed definition would allow a corresponding decrease in maneuvering capability required.

Identified technical risks include the definition of dive speeds for UTTAS vehicles; the low altitude, lightweight capability of a vehicle designed for a high maneuvering requirement; and the problem of pilot recognition of dynamic system structural limits during maneuvering flight.

FOREWORD

This report describes the procedures and the results of a study conducted to investigate the effects of maneuverability requirements on the rotor/wing design characteristics of a UTTAS type vehicle. The work was performed by the Bell Helicopter Company from April 1970 to September 1970, under U. S. Army Air Mobility Research and Development Laboratory Contract DAAJ02-70-C-0031. USAAMRDL technical program direction was provided by Mr. R. Stanton.

Principal Bell Helicopter Company personnel associated with the program were Messrs. C. Cox, J. Duhon, R. Foster, K. Harvey, J. Kidwell, M. Schramm, and D. Wells.

Preceding page blank

TABLE OF CONTENTS

Preceding page blank

TABLE OF CONTENTS (Continued)

LIST OF ILLUSTRATIONS

LIST OF ILLUSTRATIONS - Continued

LIST OF TABLES

LIST OF TABLES - Continued

LIST OF SYMBOLS

A	rotor disc area, ft^2
C_L	wing lift coefficient
C_{L_m}	peak wing lift coefficient in pullup maneuver
$C_{L_{max}}$	maximum wing lift coefficient
C_{L_t}	wing lift coefficient in trimmed flight
D	rotor diameter, ft
g	normal load factor
GW	gross weight, lb
HP	horsepower
i_w	wing incidence angle, deg
KTAS	knots true airspeed
MRP	military rated power
NRP	normal rated power
R	rotor radius, ft
R/C	rate of climb, FPS
R/D	rate of descent, FPS
RHP	rotor horsepower
S_t	horizontal stabilizer area, ft^2
S_w	wing area, ft^2
SHP	shaft horsepower
T	rotor thrust, lb

V	airspeed, kt or FPS
V_H	airspeed at military rated power, kt
V_L	limit dive airspeed, kt
V_{NRP}	airspeed at normal rated power, kt
β	rotor flapping angle, deg
σ	rotor solidity, rotor blade area/rotor disc area
σ'	density ratio
Ω	rotor rotational speed, rad/sec
ΩR	rotor tip speed, FPS

INTRODUCTION

Under the terms of Contract DAAJ02-70-C-0031, the Bell Helicopter Company conducted an analysis of the effects of maneuverability requirements on rotor/wing design characteristics. The analysis was performed on single rotor helicopters, with and without wings. The objectives included evaluation of the impact of varying maneuverability requirements on the important design parameters and the identification of related areas of technical risk. This contract was an extension of work previously accomplished under Contract DAAJ02-69-C-0013.

The study effort was organized into four tasks.

Task I - Wingless Helicopter Study

Task II - Winged Helicopter Study

Task III - Optimized Designs for Three Maneuverability Levels

Task IV - Technical Risk Analysis

During Task I, five pure helicopter configurations with varying maneuvering capabilities were synthesized. The effects of varying rotor tip speed and rotor solidity were examined. Performance and payload capability was established for configurations with a constant design gross weight. Each design met some fundamental stability criteria such as positive dynamic stability and positive control gradients. The maneuvering response of each configuration was examined by use of both digital and hybrid computer programs. Time history plots and summarizing graphs are presented in the report.

During Task II, the effects of adding wings to three of the helicopter configurations of Task I were examined. Considering the various wing and rotor combinations, 18 different designs were included in this phase of the study. Again, the maneuvering response to each configuration was examined and appropriate data is included in this report.

Task III was based on the data developed during Tasks I and II. Three designs were developed as optimum to meet the requirements of 1.50g, 1.75g, and 2.00g cyclic-only maneuvering capabilities at their respective maximum level flight airspeeds attainable with normal rated power. From the results of studying the maneuvering characteristics of these vehicles and other considerations, recommendations concerning the maneuvering load factor requirements for UTTAS designs were formulated.

Finally, in Task IV, the areas of technical risk and concern were identified and related to the results of this study.

For all configurations, the maneuvers performed included pullups, pushovers, constant-airspeed turns, and constant-altitude turns. The range of speeds investigated varied from hovering flight to 195 KTAS. Also included in this report is an analysis of noise characteristics along with rotor loads and stress analysis for the critical conditions for the largest and smallest rotor configurations.

TASK I - WINGLESS HELICOPTER STUDY

SCOPE AND GROUND RULES

The purpose of the Task I phase of this study--wingless helicopter configurations--was to investigate the effects of rotor configuration on maneuverability. The rotor chosen for this investigation was a four-bladed design with a hingless flexbeam hub. The blades have double-swept tips to improve performance and reduce noise. To determine the aircraft size (component weights and dimensions) and engine requirements, the following design ground rules were established:

1. Constant disc loading = 6.0 pounds per square foot
2. Constant Basic Design Gross Weight = 15,600 pounds
3. All performance requirements for 4000 feet - 95°F
4. Equal mission endurance capability
5. Engine performance based on typical advanced technology engine characteristics
6. Fuselage size and weight constant
7. Main rotor blades to have Wortmann airfoil

These ground rules are consistent with the design baseline requirements of Appendix A of RFQ DAAJ02-70-Q-0049.

It is recognized that there would be some impact in power-limited maneuvers because of disc loading variations, but these are limited to the low-speed regime and are considered to be secondary to the effects of blade loading, advance ratio, and Mach number. In assessing low-speed effects due to change in disc loading, the key parameter for power-limited maneuvering is the <u>difference</u> between level flight power required and power available. Since the installed power available is primarily a function of the disc loading (assuming reasonable wing areas) and is determined by the hovering climb requirement, the steady maneuver capability that results from the difference between power required and available for the various disc loadings that might be applicable to a UTTAS design will not vary significantly. During high-speed maneuvers, based on past contractor experience, power limits are not a significant factor in transient maneuver capability. The design gross weight of 15,600 pounds resulted from sizing a baseline configuration to satisfy the desired payload requirement of 2640 pounds, using a rotor configuration which had a solidity of

0.11 and an operating tip speed of 725 feet per second. The Wortmann airfoil is an improved state-of-the-art airfoil independently developed by Bell Helicopter Company. The airfoil, designated by FX69-H-098, is a 9.8-percent-thick, cambered section which has been tested in the two-dimensional facilities of the United Aircraft Research Laboratories. A more detailed discussion of this airfoil will be given in a later section when maneuver results are presented comparing the FX69-H-098 and the NACA 0012.

Using the above ground rules, five wingless configurations were investigated in the Task I phase of this study. Including the baseline configuration, the five configurations had rotor solidity and tip speed variations as follows:

Baseline Configuration	$\sigma = 0.11$	$\Omega R = 725$ FPS
Low-Solidity Configuration	$\sigma = 0.09$	$\Omega R = 725$ FPS
High-Solidity Configuration	$\sigma = 0.13$	$\Omega R = 725$ FPS
Low Tip Speed Configuration	$\sigma = 0.11$	$\Omega R = 675$ FPS
High Tip Speed Configuration	$\sigma = 0.11$	$\Omega R = 775$ FPS

The effects of these rotor configurations on payload and performance--as dictated by the design ground rules--will be discussed in the following sections.

STABILITY AND CONTROL ANALYSIS - TASK I

Because of the large number of configurations investigated in this maneuverability study, it was not feasible to analyze the stability and control characteristics of each configuration in detail. The vertical stabilizer was sized to provide static directional stability with no tail rotor contribution so that level flight could be sustained at minimum power without exceeding a sideslip angle of 20 degrees. This criterion is more stringent than the MIL-H-8501A requirements, so no effort was made to examine lateral stability characteristics. However, the longitudinal stability of each configuration was checked to insure that the following minimum criteria were satisfied:

1. Positive static stability
2. Positive or neutral dynamic stability at the aft cg without benefit of a stability augmentation system at cruise airspeeds (150 KTAS and V_{NRP})

3. Minimum 12-inch cg range

4. Trimmed level flight rotor flapping less than 1 degree at cruise airspeeds

5. Positive longitudinal cyclic stick gradients with adequate forward stick margins

To satisfy the static and dynamic stability criteria, a minimum horizontal stabilizer area of 45 square feet was required. The flapping criterion was satisfied by using a linear rigging between the longitudinal cyclic stick and the horizontal stabilizer incidence. Parabolic rigging was used in subsequent analysis and will be discussed in Task III. The configurations investigated in this study had similar airframe characteristics. The basic dimensional characteristics of the wingless configurations are given in Table I.

PERFORMANCE - TASK I

Power Available

The engine data used in this study was based on typical advanced technology engine characteristics. Allowances were made for installation losses, including inlet temperature rise, inlet pressure losses, accessory power losses, and transmission losses.

Hover

The hovering power required was calculated for the five helicopters of Task I. The rotor horsepower required to hover was calculated on Bell Helicopter Company computer program F35 (Reference 1) using the Wortmann airfoil data. In hover no improvement due to the swept tip blades has been taken into account. Hover power required is shown on Figures 1 and 2. Data shown on these figures are presented as horsepower/density ratio versus gross weight/density ratio for a temperature of 95°F. This method of presentation allows the determination of power required at any altitude as long as the density ratio is determined for the proper altitude and 95°F.

An estimate of 45.5 horsepower for the accessory power required has been made based on an assumed typical UTTAS configuration and typical mission requirements. In addition, the transmission losses have been estimated to be three percent of the main rotor horsepower. The tail rotor power required was calculated on computer program F35 based on the required thrust to counteract hover torque. For all configurations, a tail rotor diameter of 13 feet and solidity of 0.12 were used. The tip speed of the tail rotor was assumed to be the same as the tip speed of the main rotor.

TABLE I. TASK I - DIMENSIONAL CHARACTERISTICS OF WINGLESS HELICOPTER CONFIGURATIONS

Fuselage Length	690 Inches
Fuselage Height	150 Inches
Fuselage Width	100 Inches
CG Range - Station Line	
Forward	221 Inches
Mid*	227 Inches
Aft	233 Inches
Main Rotor Hub	
Station Line	232 Inches
Waterline	161 Inches
Horizontal Stabilizer	
Area	45 $Feet^2$
Station Line	582 Inches
Waterline	90 Inches
Vertical Fin	
Area	54 $Feet^2$
Station Line	642 Inches
Waterline	107.5 Inches

*All maneuvers run at mid-cg

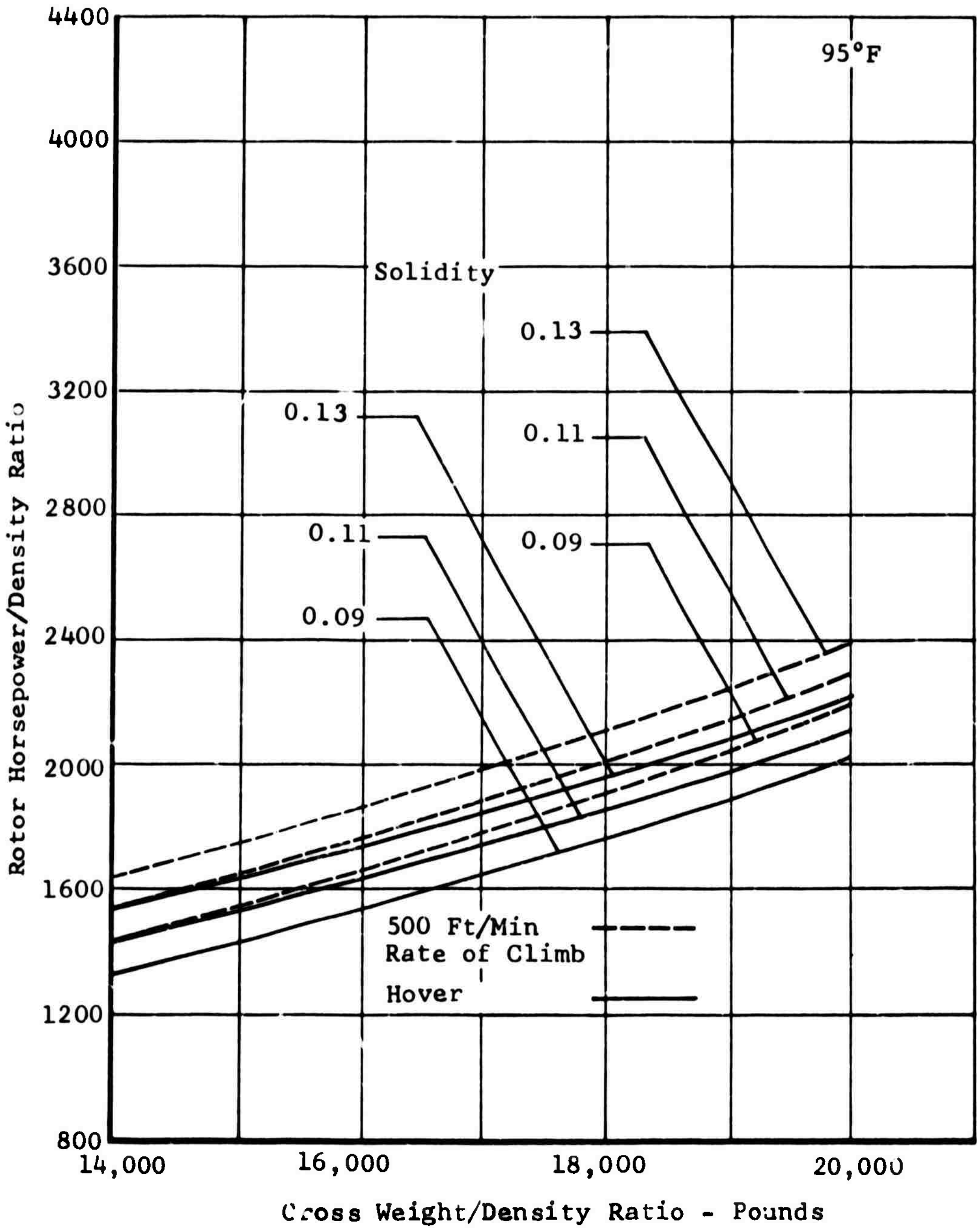

Figure 1. Task I - Wingless Helicopter, Hover Power Required, Tip Speed = 725 FPS.

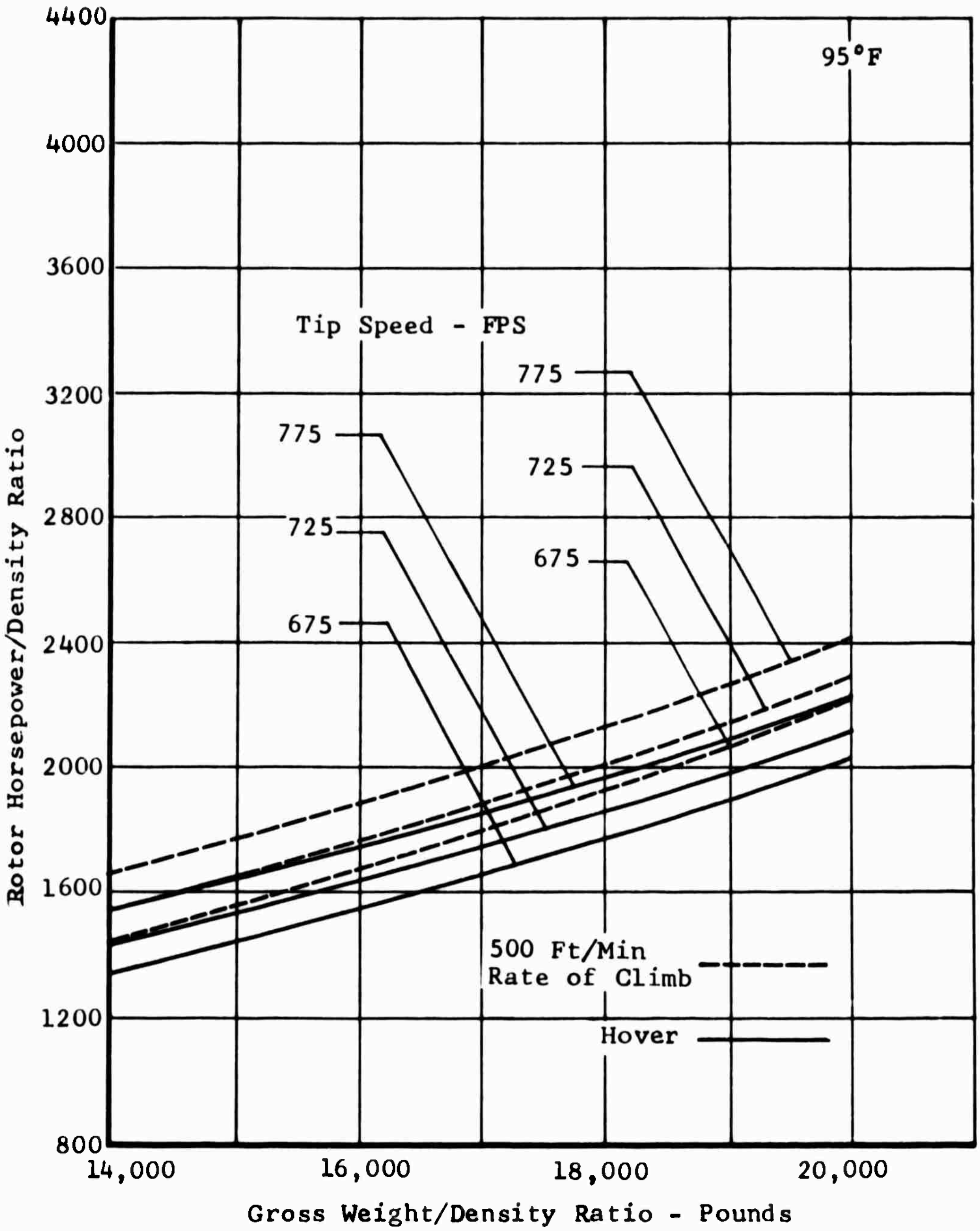

Figure 2. Task I - Wingless Helicopter, Hover Power Required, Solidity = 0.11.

The excess power necessary to perform a vertical climb of 500 feet per minute has been calculated and is shown on Figures 1 and 2. The installed power was determined from the vertical climb power requirement by using the engine altitude and temperature variations to obtain the required power at sea level on a standard day. The uninstalled power was then determined by adding the installation losses and is shown in Table II.

TABLE II. TASK I - ENGINE POWER REQUIRED

ΩR (FPS)	σ	Uninstalled Engine HP Rating S.L. Std Day
725	0.11	2825
725	0.09	2700
725	0.13	2950
675	0.11	2735
775	0.11	2970

Forward Flight

The forward flight power required was also calculated on F35 for the same configurations as the hovering data. The equivalent flat-plate drag area for all configurations was taken to be 11.43 square feet. This drag estimate has been verified by wind-tunnel tests of a 1/6 scale model of the Bell Model D268 in the LTV low-speed wind tunnel in November, 1969. The swept tip improvement was determined to be equivalent to 2.34 square feet of drag area. This value was determined from flight tests of prototype swept tip blades on the UH-1 series and is believed to be a conservative estimate for the UTTAS type helicopter. For calculation purposes the 2.34 square foot swept tip effect is subtracted from the drag area of 11.43 square feet. The efficiency factor in forward flight was 92.5 percent, which included allowances for the transmission losses and the tail rotor power required. In addition, 45.5 horsepower was included for operation of accessories. The speed power polars for the five configurations at 4000 feet, 95°F are shown on Figures 3 and 4 for the design gross weight of 15,600 pounds. The military and normal rated powers

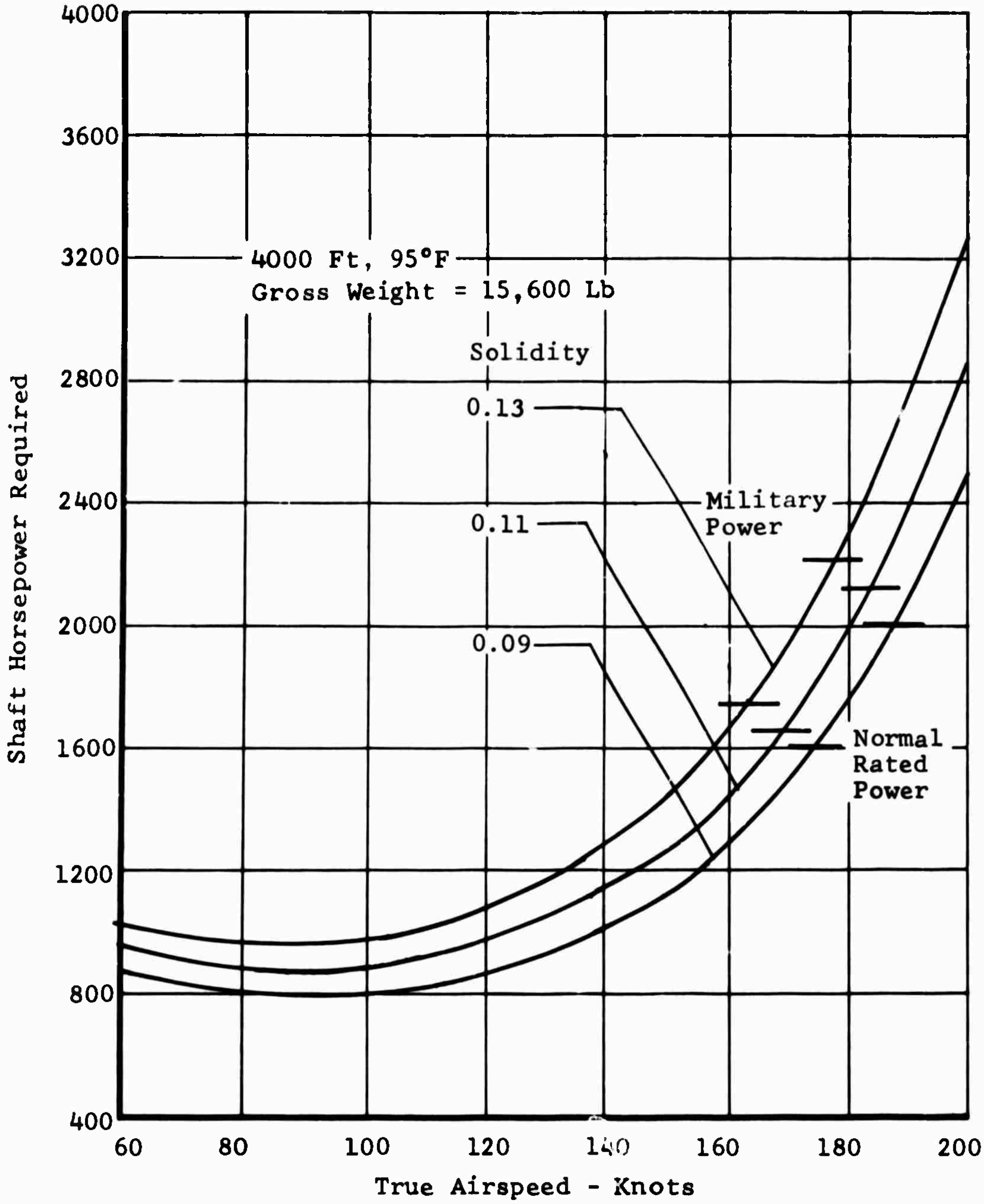

Figure 3. Task I - Wingless Helicopter, Speed Power Polar, Tip Speed = 725 FPS.

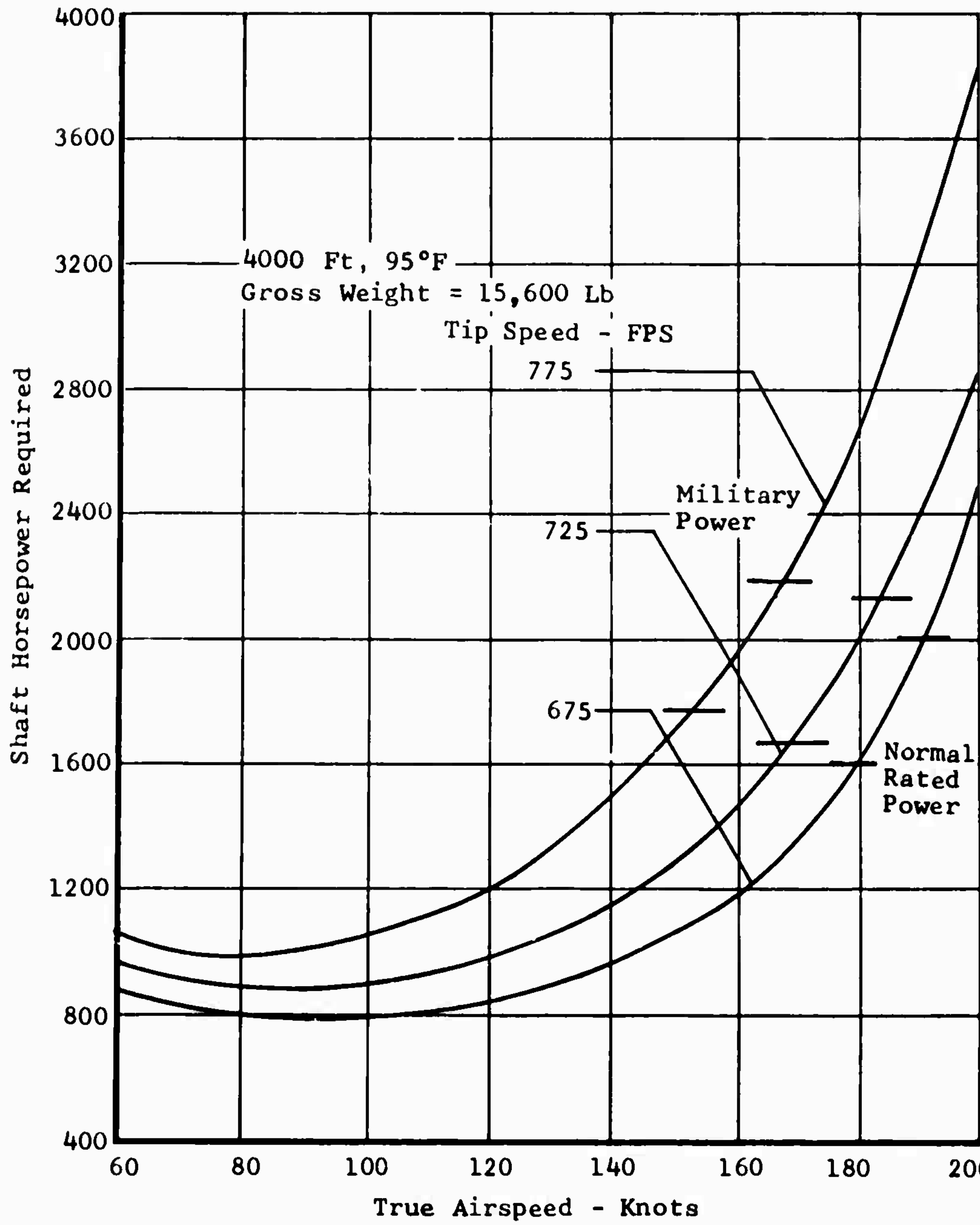

Figure 4. Task I - Wingless Helicopter, Speed Power Polar, Solidity = 0.11.

available are also shown on these figures. The maximum speeds are found from Figures 3 and 4 and are shown in Table III. Normal rated power speeds were found to be greater than 150 knots for all cases. Additional speed power polars for a range of gross weights for each configuration are given on Figures 94 through 98 of Appendix I.

TABLE III. TASK I - MAXIMUM TRUE AIRSPEED, 4000 FT, 95°F

ΩR (FPS)	σ	V_{NRP} (KTAS)	V_H (KTAS)
725	0.11	169	184
725	0.09	175	188
725	0.13	163	178
675	0.11	180	191
775	0.11	153	168

The specific range at 4000 feet, 95°F was calculated using the data of Figures 94 through 98 and the specific fuel consumption of a typical advanced technology engine. The specific range data is shown on Figures 99 through 103 of Appendix I. The military rated power, normal rated power, and long-range cruise speeds are also shown on these plots.

Weights

The component weights in this study were determined using the theoretical and empirical equations for major components which have been developed by Bell Helicopter Company. The weights of equipment and furnishings were based on actual components or on vendor data. A summary weight statement for the five configurations studied in this section is given in Table IV.

Mission Analysis

In order to compare the mission capability of the different designs, the following mission was selected:

TABLE IV. TASK I - WINGLESS HELICOPTERS SUMMARY WEIGHT STATEMENT

Design Gross Weight, Pounds		15,600		15,600		15,600		15,600		15,600
Engines (No. and Type)		2 ADV.		2 ADV.		2 ADV.		2 ADV.		2 ADV.
SHP - Uninstalled		2825		2700		2950		2735		2970
Main Rotor(s) Diameter, Feet		57.5		57.5		57.5		57.5		57.5
Solidity		0.11		0.09		0.13		0.11		0.11
Tip Speed, FPS		725		725		725		675		775
Weights, Pounds										
Rotor Group		2607		2277		2920		2607		2607
Wing Group		-		-		-		-		-
Tail Group		187		187		187		187		187
Body Group		1946		1946		1946		1946		1946
Alighting Gear		468		468		468		468		468
Flight Controls		715		714		717		714		717
Fixed	413		418		419		418		419	
Rotating	297		296		298		296		298	
Eng. Section Nacelles		176		176		176		176		176
Propulsion		2377		2311		2502		2314		2593
Engine Install	574		561		595		565		597	
Induction System	64		62		66		62		66	
Exhaust	74		71		80		73		80	
Fuel System	367		355		414		342		448	
Controls	32		32		32		32		32	
Starting	39		38		40		38		40	
Rotor Brake	47		47		50		47		50	
Trans and Drive System	1180		1145		1225		1155		1232	
Passive Defense		200		200		200		200		200
Instruments		73		73		73		73		73
Hydraulics		93		93		93		93		93
Electrical		281		281		281		281		281
Avionics		411		411		411		411		411
Furnishings and Equipment		658		658		658		658		658
Air Conditioning		121		121		121		121		121
APU		93		93		93		93		93
Armament		175		175		175		175		175
Weight Empty		10,581		10,186		11,021		10,521		10,624
Crew	600		600		600		600		600	
Payload (Pass or Cargo)	2640		3111		2006		2836		2249	
Fluids	61		61		61		61		61	
Survival Equipment										
Passive Defense										
Armament										
Fuel	1718		1642		1912		1582		2066	
Miscellaneous										
Useful Load		5019		5414		4579		5079		4976
Mission Weight		15,600		15,600		15,600		15,600		15,600

8 minutes at idle power

40 minutes at normal rated power

78 minutes at cruise power

30 minutes reserve at cruise power

156 minutes total

The cruise speed was 150 knots for all configurations. Since the gross weight for all configurations was fixed at 15,600 pounds, the variable for the mission evaluation was payload. The effect of the design parameters on payload and fuel is shown in Table V. The effect of these parameters on maneuvering capability is discussed in the following sections.

TABLE V. TASK I - PAYLOAD COMPARISON

ΩR (FPS)	σ	Fuel (Lb)	Payload (Lb)
725	0.11	1718	2640
725	0.09	1642	3111
725	0.13	1912	2006
675	0.11	1582	2836
775	0.11	2066	2249

ROTORCRAFT FLIGHT SIMULATION ANALYSIS

The Rotorcraft Flight Simulation Analysis--independently developed by Bell Helicopter Company and designated as computer program C81--was used in this study to simulate maneuvering flight and to investigate blade airload characteristics in both the trimmed and maneuvering conditions. Essentially, the program consists of a rotor aerodynamic and dynamic analysis coupled with a fuselage analysis which includes all six rigid-body degrees of freedom. Detailed descriptions of program C81 can be found in References 2, 3, and 4; a brief description is presented herein.

Program C81 has the capability to consider conventional single-rotor configurations, tandem or side-by-side configurations, and tilting rotor or coaxial rotor configurations. Four hub types may be considered--teetering, gimbaled, articulated, or rigid--with either two, three, or four blades. The rotor aerodynamic analysis includes the effects of compressibility, stall, and reversed flow, and is coupled with the dynamic analysis to calculate blade airloads. The inplane and out-of-plane blade deflections are coupled to insure accurate calculation of natural frequencies and forced responses.

The fuselage analysis requires a complete definition of the airframe--cg location, mast length and tilt, and the sizes and locations of wings, horizontal stabilizer, vertical fin, and pylon fairing. The contributions to lift, drag, and side forces and to pitching, yawing, and rolling moments are treated separately for each aerodynamic surface and for the fuselage itself.

Two versions of C81 were used in this study. A hybrid version was used to investigate maneuvering flight, and a digital version was used in the rotor stress analysis. On the hybrid version, the rotor analysis is on an analog computer and the fuselage analysis is on a digital computer. The analog rotor analysis allows continuous radial integration at azimuthal increments as small as 2 degrees, rather than the segmented radial integration and 30-degree azimuth increments of the digital rotor analysis. However, rotor stress analysis is restricted to the digital version of C81.

The hybrid version of C81 has several advantages over the digital:

1. The flight equations are continuously solved in approximately twice real time. One second of flight time requires only two seconds of hybrid time compared to about four minutes on the digital computer.

2. The simulated aircraft is controlled by a computerized autopilot which will execute maneuvers in rapid succession. This autopilot is simply a computing aid which simulates the pilot of the actual aircraft.

Once the operator has specified the desired operation, the autopilot will initiate any of the following:

1. Trim at a new airspeed (if the power required exceeds power available, the autopilot will find the rate-of-descent which corresponds to maximum power flight).

2. Perform a coordinated turn of any desired g-level.

3. Perform a pullup or pushover maneuver using preset control motions--collective and cyclic inputs, individually or in combination--which can be prescribed by input rate and magnitude, and by time phasing, if desired.

The autopilot instructions can be easily changed. If the desired maneuver is simple--a symmetrical pullup or pushover--as many as four or five maneuvers can be run in 1 minute.

Because two versions of program C81 (digital and hybrid) were used in this study, it was necessary to demonstrate the correlation between them. Figures 5 and 6 present two maneuver time histories--a cyclic pullup and a cyclic pushover--both for the baseline wingless configuration at 150 KTAS. The figures clearly show that the two versions of C81 are in excellent agreement. The agreement was found to be equally good for those maneuvers which approached stall.

SCOPE OF MANEUVERS INVESTIGATED - TASK I

The maneuvering flight capability of five configurations was investigated in the wingless helicopter phase (Task I) of this study. At constant gross weight (15,600 pounds) and constant disc loading (six pounds per square foot), the configurations included the following variations in rotor tip speed and solidity:

Constant Tip Speed ΩR = 725 feet/second	Constant Solidity σ = 0.11
σ = 0.09	ΩR = 675 feet/second
σ = 0.11	ΩR = 725 feet/second
σ = 0.13	ΩR = 775 feet/second

The maneuvers used to establish the capability of each configuration are described in Table VI. The maneuvers included pullups, pushovers, and coordinated turns at airspeeds ranging from hover to 195 KTAS. Three types of control inputs were applied--cyclic, collective, and combination cyclic plus collective inputs. At two intermediate airspeeds--89 KTAS and 150 KTAS--all three types of control inputs were applied in the pullup and pushover maneuvers. Above 150 KTAS, collective pitch was not used, and below 89 KTAS, cyclic pitch was used only in combination with collective pitch.

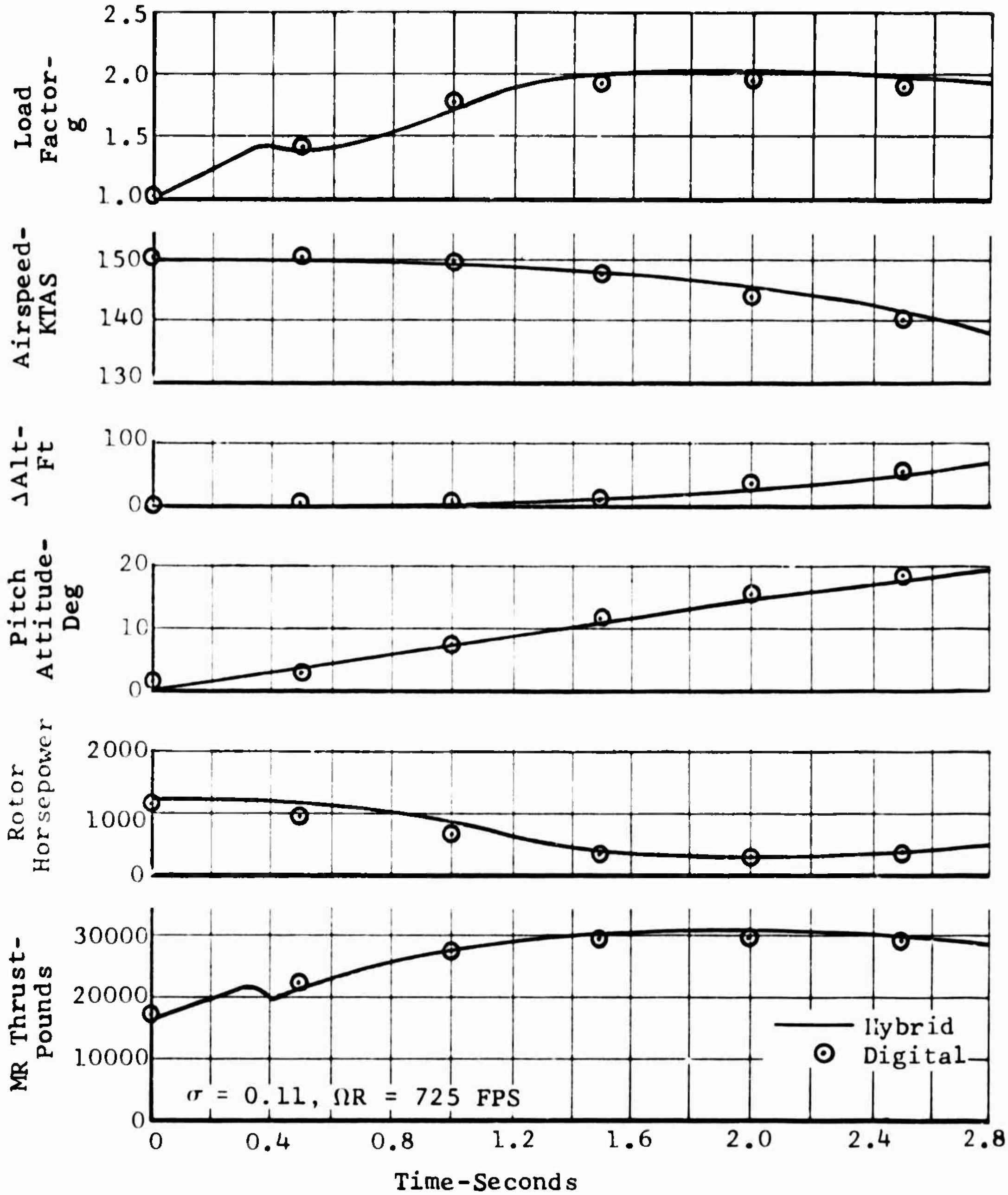

Figure 5. Comparison of Hybrid and Digital Maneuver, Baseline Wingless Configuration, 2.0-Degree Cyclic Pullup at 150 KTAS.

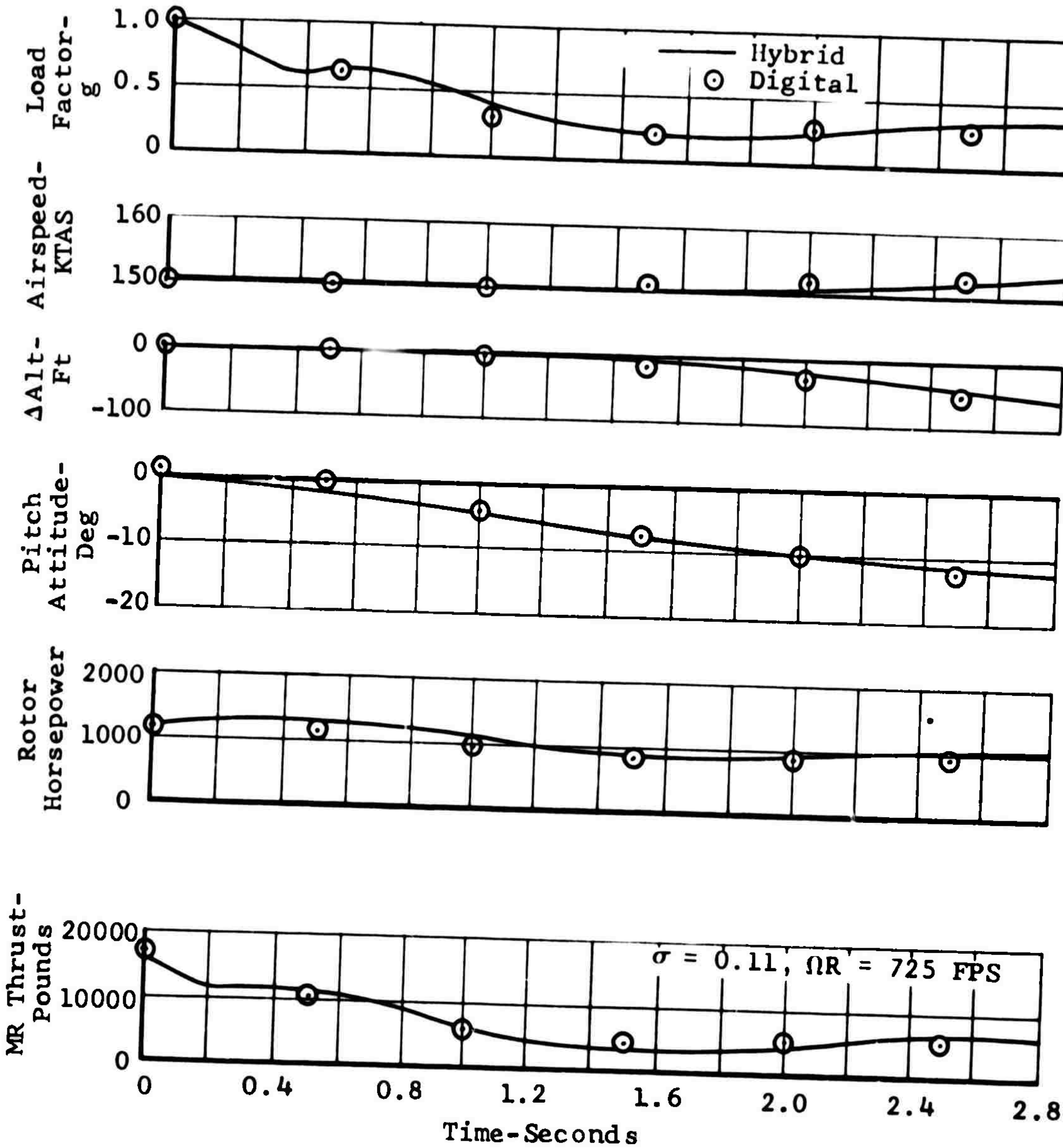

Figure 6. Comparison of Hybrid and Digital Maneuver Baseline Wingless Configuration, 2.0-Degree Cyclic Pushover at 150 KTAS.

TABLE VI. SUMMARY OF MANEUVERS INVESTIGATED

Maneuver	Control Input	True Airspeed - Knots					
Pullups	Cyclic			89	150	167	195
	Collective+Cyclic		56	89	150		
	Collective	0	56	89	150		
Pushovers	Cyclic			89	150	167	195
	Collective+Cyclic		56	89	150		
	Collective		56	89	150		
Coordinated Turns-Constant Altitude	Cyclic			89	150	167	195
	Collective+Cyclic		56	89	150		
Coordinated Turns-Constant Airspeed	Cyclic			89	150	167	195
	Collective+Cyclic		56	89	150		

MANEUVER LIMITING CRITERIA

Before establishing the maneuver capability of the subject configurations, those criteria which limit that capability had to be considered. The limiting criteria used in this study are presented in Table VII in two categories: flight path limits and rotor limits.

TABLE VII. CRITERIA USED FOR MANEUVER LIMITATIONS

Flight Path Limits	
Pitch Angle	± 50 Deg
Pitch Rate	± 20 Deg/Sec
Roll Angle	± 70 Deg
Roll Rate	± 60 Deg/Sec
Sideslip Angle	± 6 Deg
Sideslip Rate	± 25 Deg/Sec
Rotor Limits	
Flapping	± 4.5 Deg
Horsepower	Zero ⟶ Maximum Available

The flight path limits are based on Bell flight test experience. They represent the extreme flight conditions at which the pilot is likely to terminate a maneuver and initiate recovery. In actual rather than simulated flight, these limits would clearly be a function of the pilot's ability and his confidence in the aircraft. However, because most of the maneuvers in this study were limited by rotor considerations, particularly at high airspeeds, the arbitrary flight path limits became unimportant with respect to the results of this study.

The need for the horsepower limits is to prevent rotor rpm overspeed or underspeed during maneuver. The flapping limit of 4.5 degrees is based on Bell studies concerning the design of rigid rotor inboard flexures. A detailed discussion of this limit follows.

The Design of Flexures for Rigid Rotors

The flexure at the inboard end of the blade on hingeless flex-beam rotors must provide for blade flapping relative to the hub, transmit to the hub the moment which arises from this flapping, and have inplane stiffness which will place the natural frequency of the blade above one-per-rev.

The flexure should be designed to do most of the bending, leaving the inboard end of the blade comparatively free of oscillatory bending due to flapping. This requires that the flexure be rather thin and wide. The length of the flexure from the hub to the attachment at the inboard end of the blade is the primary parameter which may be varied in the design to control the flapping spring rate, or the amount of hub moment per degree of cyclic flapping. Practical investigations of the flapping spring rate have shown that increasing the flapping spring rate contributes to long-period pitching instabilities of the helicopter at high speeds.

This may be appreciated by a visualization of rotor-fuselage coupling through the flight regime. The coning rotor, while translating from the hover to high forward speeds, tends to blow back and requires progressively greater displacement of the control axis with increasing horizontal velocity. If the helicopter is speed-stable, its fuselage and control axis will pitch up at speeds above the trim speed, reducing the forward tilt of the disc and slowing the aircraft. At speeds below the trim speed, the fuselage and control axis will pitch down, increasing both the forward tilt of the rotor and the helicopter speed. The two-bladed teetering rotor, with weak coupling between the rotor and fuselage, allows the fuselage and control axis to be almost aerodynamically independent of rotor position, with resulting desirable stability characteristics.

The hub-moment or rigid rotor increases strength of the rotor-fuselage couple beyond that of the teetering rotor, and hence aerodynamic disturbances along the flight path, which cause displacement of the rotor from its trim position, make the fuselage tend to follow because of the pure moment transmitted through the rotor hub to its shaft. It is clear then that as the effective stiffness of the flapping increases, the tendency of the fuselage to follow the rotor is increased. As the fuselage pitches to follow the rotor, the control axis pitches with it in the same sense as the rotor, thereby tending to increase the control input in the direction of the rotor excursion, making it pitch even farther. In the absence of adequate horizontal tail loads on the fuselage to right the fuselage and control axis, the helicopter flight path becomes divergent. So, as rotor-flapping spring rate increases, the size and effectiveness of the horizontal tail must increase, until at the extreme, the completely rigid rotor, no practical tail size will provide sufficient control power to stabilize the helicopter, and quarter-wave divergence occurs. Therefore, the flexure should be designed to give just enough hub moment for the desired maneuvering control power.

An examination of all of the parameters of the flexure shows that for a given width of the flexure plate the material stresses from flapping are reduced by increasing the thickness of the flexure; but this makes the flexure stiffer, increasing the flapping spring rate only slightly, and transferring damaging moments to the root of the blade. This may be relieved by making the flexure longer, but this in turn increases the flapping spring rate and the accompanying tendency toward pitching instability. The flexure, therefore, should be designed as short, as wide, and as thin as possible. These qualities are limited at their extremes by inplane stiffness requirements, flapping spring rate requirement, and material strength limitations.

The design drive-torque for the rotor mast, when considered with the mast-bending moments, indicates an optimized mast diameter of approximately nine inches. Practically, the space reserved for attachment of the hub to the mast results in the location of the inboard end of the flexure about six inches from the axis of rotation of the rotor, as a minimum. For this study, the flexure was designed within these approximate constraints to provide the desired hub-spring rate, which was chosen because of helicopter stability considerations.

In order to make the flexure as soft as possible and to remain within the endurance limit while still maintaining flapping-control power, the design must use the highest available ratios of the materials bending endurance limit stresses to its modulus of elasticity. In metals considered practical for flexure application in view of cost, corrosion properties, and manufacturing considerations, this maximum ratio occurs in titanium, so it has been chosen as the flexural material. The material endurance limit must not be exceeded during maneuvers or gusts, since resulting damaging cycles would deny the component life objectives for UTTAS in its stringent operational role.

Studies at Bell have shown that, at the material endurance limit in titanium, the maximum bending angle for an appropriately sized flexure is approximately 4.5 degrees half amplitude for reversed bending, conservatively assuming that all bending occurs in the flexure.

MANEUVERING FLIGHT PROCEDURES

To establish the maneuvering capability of the five Task I configurations, each of the 34 maneuvers described in Table VI was run on the hybrid computer. The maneuvering capability was defined to be that load factor which could be sustained for one second or more without exceeding any of the limits in Table VII. This section describes the procedures used to establish the sustained g-level for the different types of maneuvers.

Pullup and Pushover Maneuvers

The maximum horsepower available was sufficient to allow entering all maneuvers from trimmed level flight except those at 195 KTAS, which were entered from a shallow dive at military rated power. The rate of application and magnitude of the desired control inputs were prescribed to the computer which used the autopilot to apply and hold the control input without attempting recovery. The maximum g-capability was found by progressively increasing the magnitude of the control input and repeating the maneuver until one of the limiting criteria was reached.

To illustrate this technique, hybrid time histories of two maneuvers at the limiting g-level are presented on Figures 7 and 8. These figures are typical of the hybrid computer time histories which are presented throughout this report. Fifteen parameters were plotted during each maneuver. With the exception of load factor, which had its own channel, each parameter was plotted in combination with one other on the same plotting channel. This double plotting was done by plotting one parameter for a fixed increment of time, then transferring to the other parameter to plot it for a different time increment. For example, Figure 7 shows collective pitch and rotor horsepower plotted alternately on the same channel. The rotor horsepower time increment is twice that for collective pitch. To enhance understanding of this double plotting technique, the curves of Figure 7 have been made continuous by dashing in those portions of the curves which were not machine plotted. On Figure 8 and all subsequent time histories presented herein, the curves are given exactly as they were machine plotted, without dashes.

Because the maneuvering flight data is plotted versus time, it was not possible to directly plot the blade flapping motions in terms of degrees. Instead, the blade motions are represented by plotting the tip deflection in units of feet. The tip deflection is measured relative to the blade precone position. The flapping angle, β, is easily found by expressing

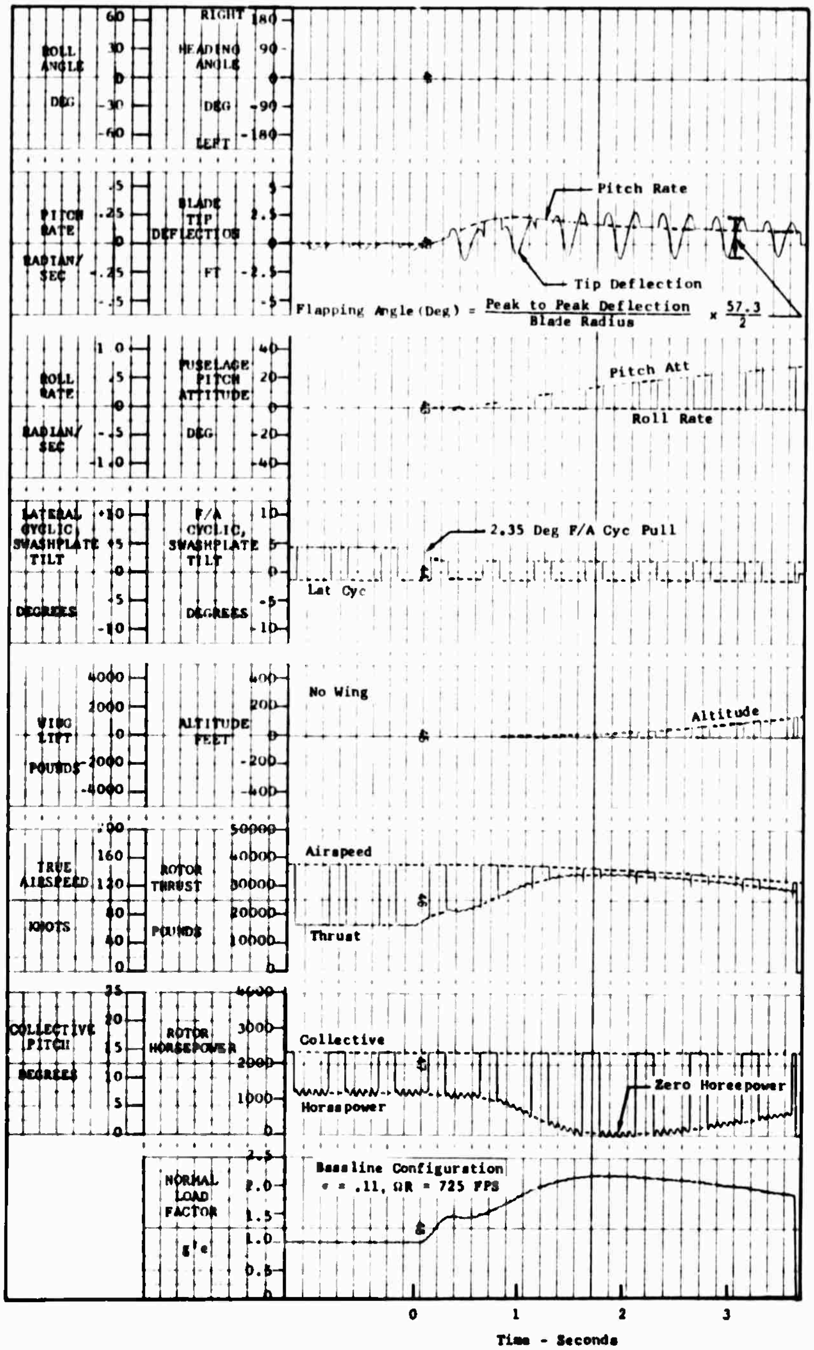

Figure 7. Maneuver Time History, F/A Cyclic Pullup, Maneuver Limited by Zero Horsepower.

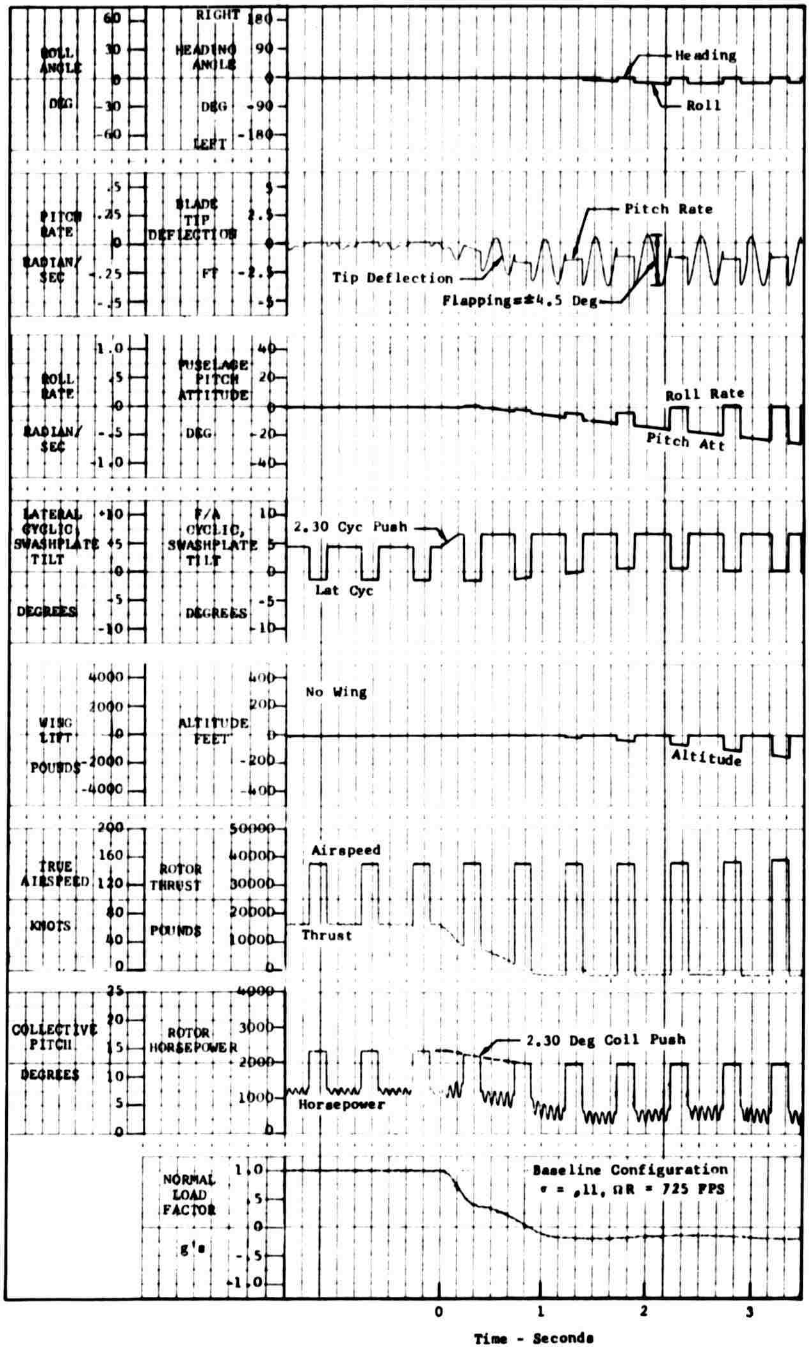

Figure 8. Maneuver Time History, Collective + F/A Cyclic Pushover, Maneuver Limited by Flapping.

the amplitude of the tip deflection in terms of degrees. As given on Figure 7, the amplitude of the tip deflection is simply one-half of the peak-to-peak deflection, and the flapping angle, β, is given by

$$\beta = \frac{\text{Peak-to-Peak Tip Deflection}}{\text{Blade Radius}} \times \frac{57.3}{2}$$

For the Task I baseline configuration ($\sigma = .11$, $\Omega R = 725$ fps), Figure 7 shows the response to a 2.35-degree cyclic pull initiated at 150 KTAS. This was a limited maneuver because the horsepower approached zero about 1.5 seconds into the maneuver. A larger cyclic pull would have resulted in exceeding the zero horsepower limit. The maneuver reached a peak load factor of 2.19 g's, but the sustained load factor was 2.12 g's.

Figure 8 shows the response to a 2.3-degree collective plus cyclic push at 150 KTAS, again for the Task I baseline configuration. The limiting criterion for this maneuver was flapping which approached 4.5 degrees at 2.0 seconds into the maneuver. The sustained load factor in the maneuver was -0.15 g.

Coordinated Turns

The techniques used in turning flight maneuvers required extensive use of a specially programmed autopilot. The desired load factor was prescribed to the autopilot which regulated the lateral cyclic control to maintain the bank angle required for the specified turn. The F/A cyclic and collective controls were prescribed as required to satisfy the flight path constraints--constant altitude or constant airspeed. To illustrate the relationship between the flight path constraints and the allowable control inputs, Figures 9 through 11 present the hybrid time histories of three coordinated turns.

For the Task I baseline configuration at 150 KTAS, Figure 9 gives a 1.75g cyclic-only turn. The flight path constraint was constant altitude, which was interpreted to mean that altitude must be maintained through a heading angle change of 180 degrees. In the turn presented, the aircraft climbed about 65 feet half-way through the turn. At the completion of the turn, the aircraft was only 15 feet higher than the entry altitude, but airspeed had dropped off to 124 KTAS.

The time history of a 1.75g cyclic-only turn with a constant airspeed constraint is given on Figure 10, again for the baseline configuration at 150 KTAS. To maintain airspeed

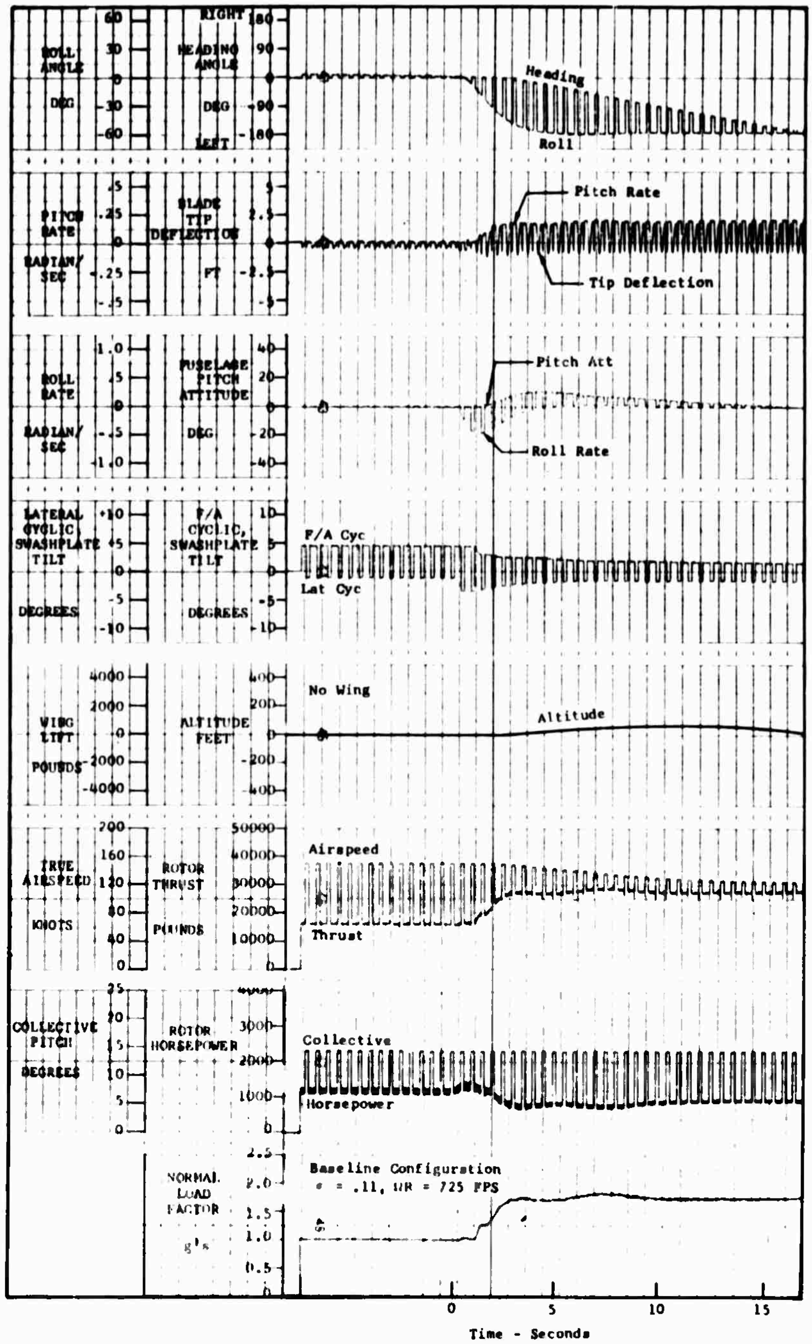

Figure 9. Maneuver Time History, 1.75g Coordinated Turn, Cyclic-Only, Constant Altitude.

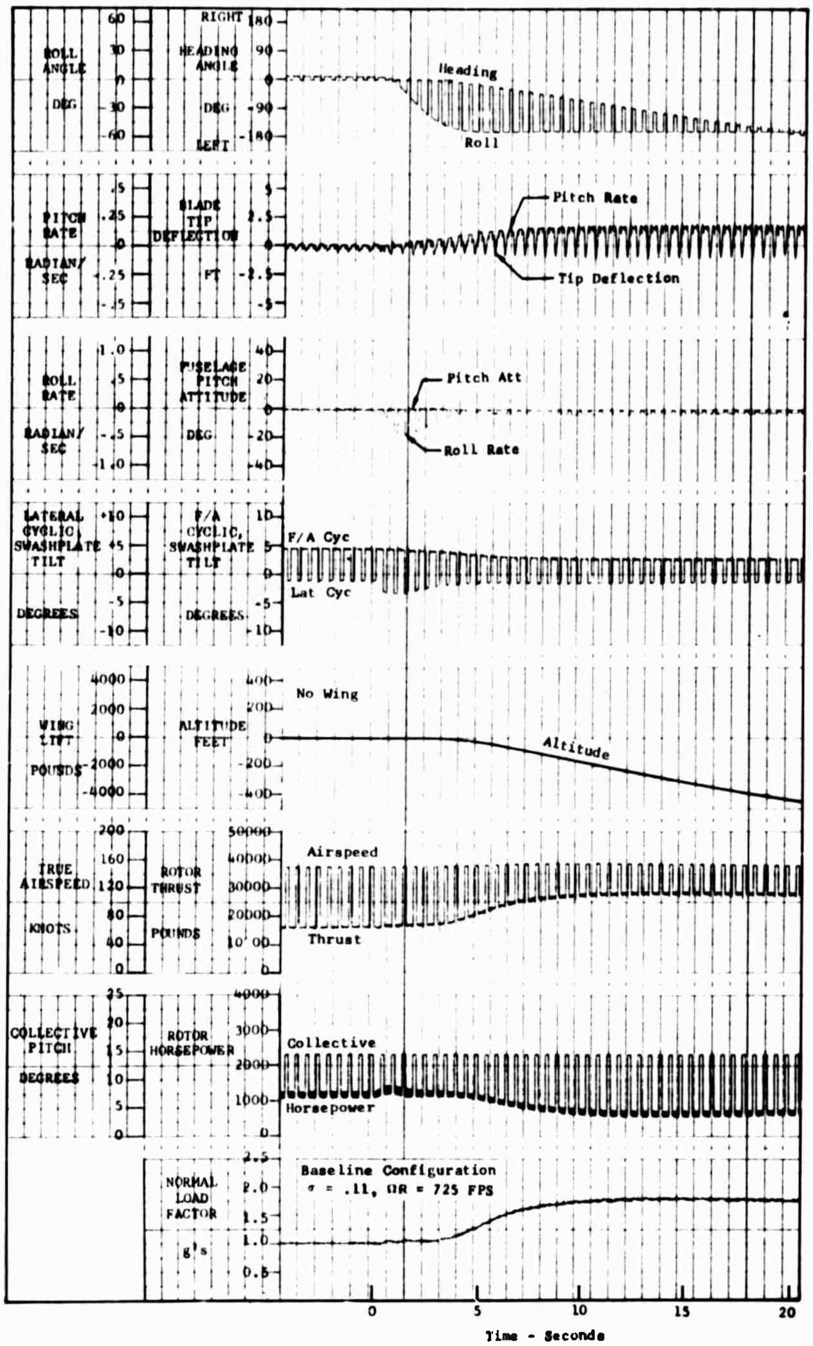

Figure 10. Maneuver Time History, 1.75g Coordinated Turn, Cyclic-Only, Constant Airspeed.

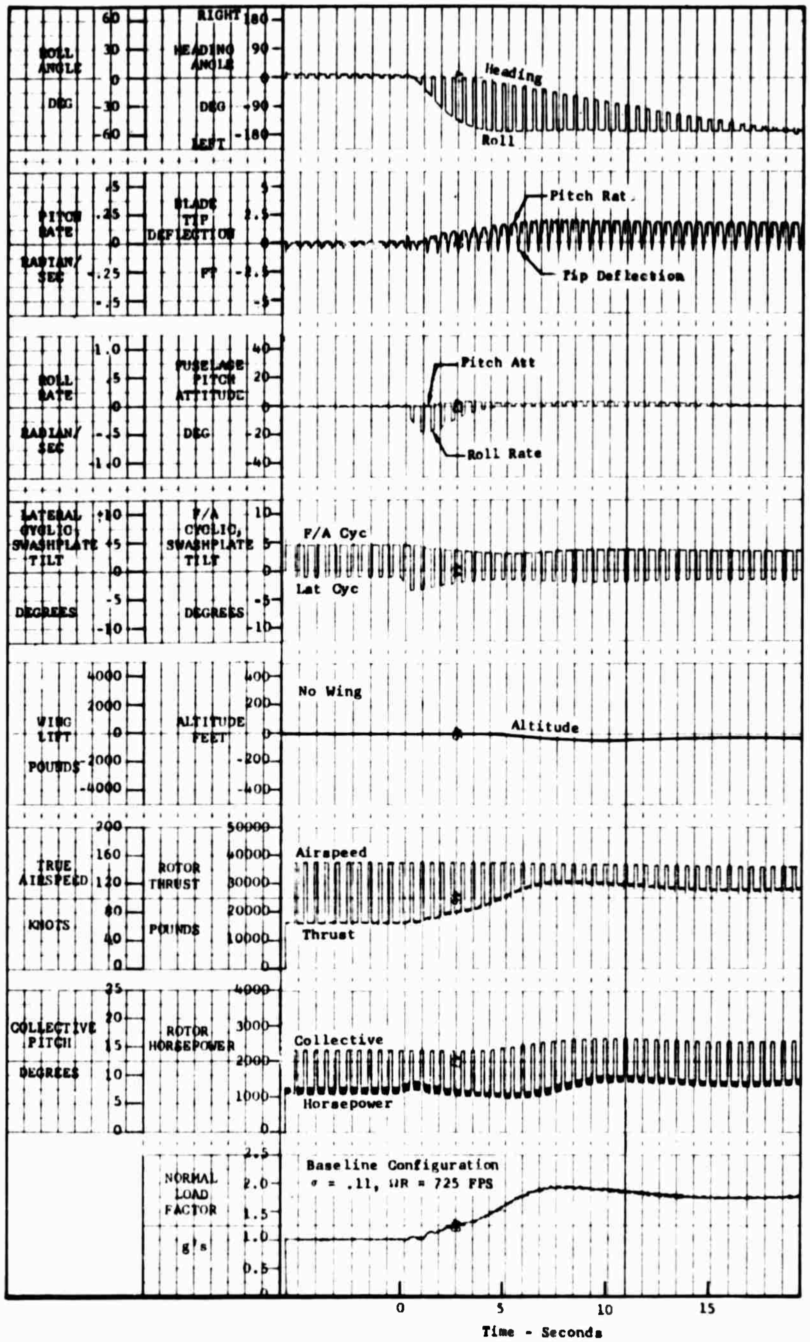

Figure 11. Maneuver Time History, 1.75g Coordinated Turn, Collective + Cyclic, Constant Altitude and Airspeed.

throughout a heading angle change of 180 degrees required an altitude loss of 460 feet. The aircraft rate of descent in the steady-state turn was 1320 feet per minute.

If both cyclic and collective could be used, and if the power available was sufficient, both constant airspeed and constant altitude were maintained throughout the turn. This type of turn is illustrated on Figure 11, which shows a 1.75g cyclic plus collective turn at 150 KTAS. If the power available was not sufficient to maintain both airspeed and altitude, the collective plus cyclic turns were run at maximum horsepower, thereby reducing the airspeed and altitude bleed-off requirements when compared to the cyclic-only turns.

Input Rate and Time Phasing Study

Prior to running the maneuvers, it was necessary to investigate the effects of control input rate and time phasing between cyclic and collective inputs on the obtainable load factors. Two criteria had to be considered: (1) what combination of input rate and time phasing gives the "maximum" load factor; (2) how does this optimum combination relate to the input techniques which a pilot is likely to use? The study was done by considering the Task I baseline configuration in pullup maneuvers, using various combinations of input rates and time phasing.

Cyclic-Only Maneuvers. Bell flight test experience has shown that for rapid cyclic pullup maneuvers, the input rates are usually rapid, about six inches per second. To determine the input rate which gives maximum sustained g's, pullup maneuvers were run at airspeeds from 56 to 167 KTAS, using cyclic input rates of 4, 6, and 8 inches per second (full range of cyclic was 12 inches, corresponding to 26 degrees of swashplate tilt). At all airspeeds considered, it was found that the input rate had little impact on the load factors attained. For example, at 150 KTAS, the maximum sustained load factor was 2.12 g's using 4 and 6 inches per second, and 2.10 g's using 8 inches per second. Consequently, 6 inches per second was chosen as the rate which best satisfies the criteria previously discussed. A complete data summary of the cyclic input rate study is given in Appendix II.

Collective Plus Cyclic Maneuvers. For combination collective plus cyclic maneuvers, there were two factors to consider--the collective input rate, and the time phasing between the cyclic and collective inputs. To investigate the effects of collective input rate and time phasing, pullup maneuvers were run with collective rates of 1.5, 3.0, and 4.5 inches per second (the full range of collective being 12 inches, corresponding to 20 degrees of blade pitch) in combination with time delays of 0, 0.5, and 1.0 seconds. The cyclic input rate was 6 inches per second. The data from this study is given in Appendix II along with the cyclic-only data.

The results were inconclusive in that no single combination of collective input rate and time phasing was the best throughout the airspeed range. At the highest speed considered, 150 KTAS, maximum g's were attained using the slowest input rate--1.5 inches per second. The g-capability was not increased by delaying the collective input. At the lower airspeeds, 56 and 89 KTAS, maximum g's were attained by delaying the collective input by 1.0 second, but the input rate used had little effect on the g-capability. At all airspeeds, the optimum combination of rate and time delay was only slightly better than the combination which gave the lowest g-capability. Therefore, to simplify the running technique on the computer, a single combination of collective rate and time delay--1.5 inches per second and zero seconds delay--was chosen to be used at all airspeeds.

MANEUVER RESULTS - TASK I

Using the techniques previously discussed, the sustained load factor capability of the five Task I configurations was determined for each of the 34 maneuvers described in Table VI. The results of the pullup and pushover maneuvers are presented on Figures 12 through 16, which also give the incipient stall limits of the configurations. Additionally, the results are given in Appendix II, which includes the magnitude of the control inputs and the limiting criteria for each maneuver.

Stall Effects

The incipient stall limits presented on Figures 12 through 16 represent the load factors at which evidence of rotor aerodynamic stall first appeared. The stall was characterized by a rapid increase in flapping and rotor horsepower required, an increased oscillation in the normal load factor, and in actual flight would probably be accompanied by increasing vibration levels. The incipient stall limit is important because it represents the maximum load factor which can realistically be sustained for more than brief periods of time. Although the incipient stall limit can be exceeded in transient maneuvers, it defines the potential maximum for sustained maneuvering flight which is the subject of this report.

The load factors actually achieved were less than the stall limited capability because of the flight path and rotor limits imposed on the maneuvers. The relationship of the actual to

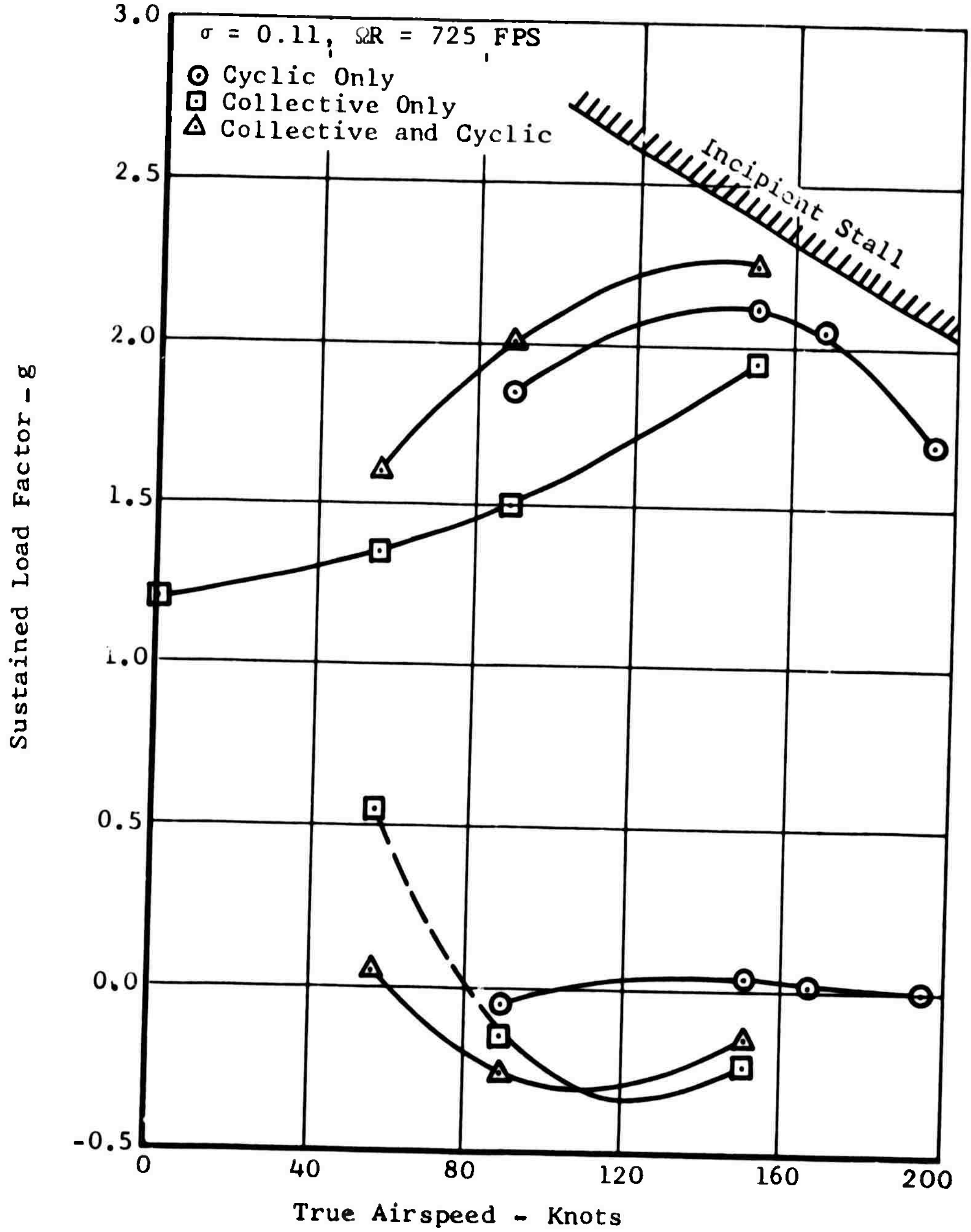

Figure 12. Task I - Maneuver Results, Baseline Configuration.

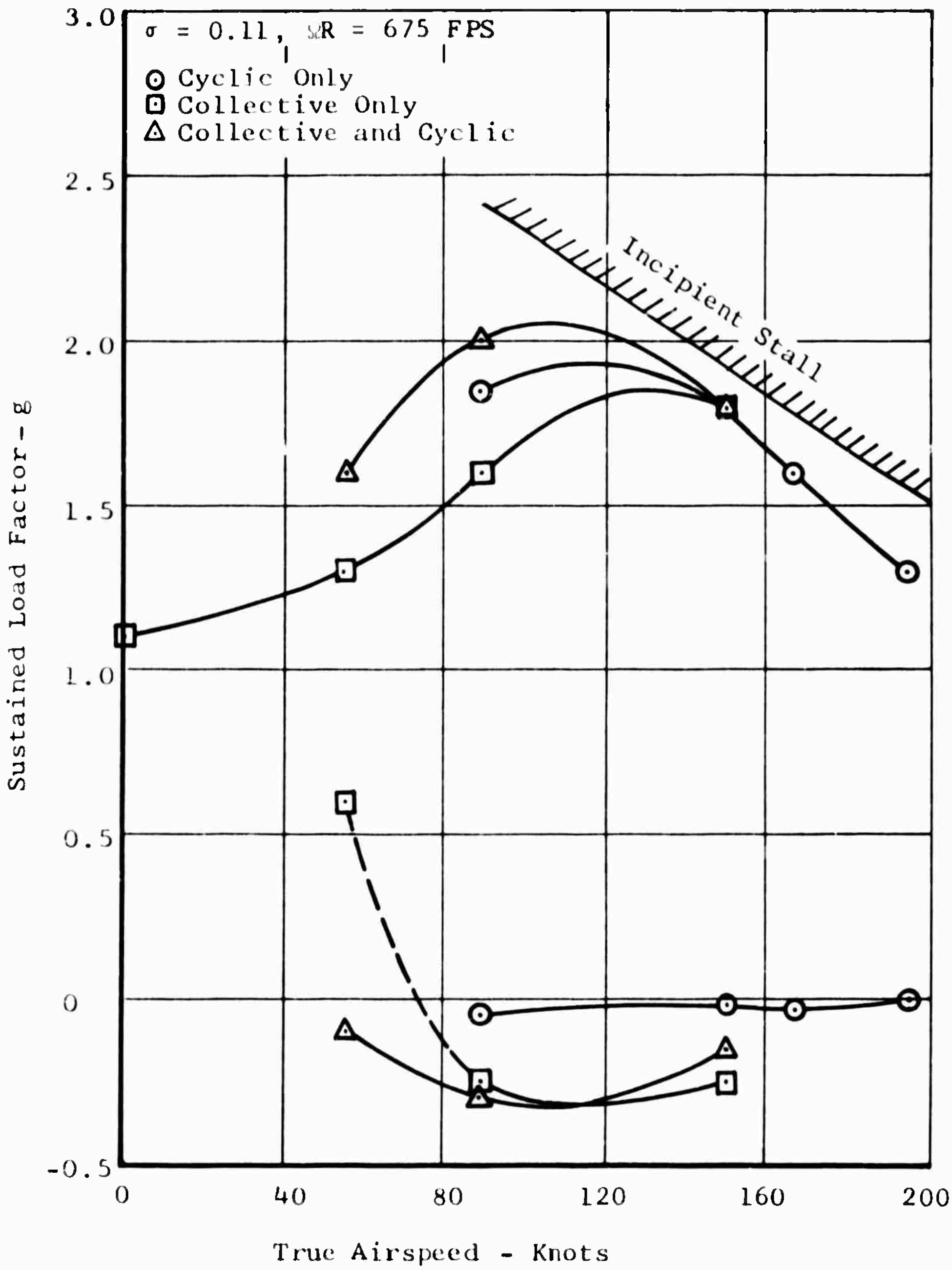

Figure 13. Task I - Maneuver Results, Low Tip Speed Configuration.

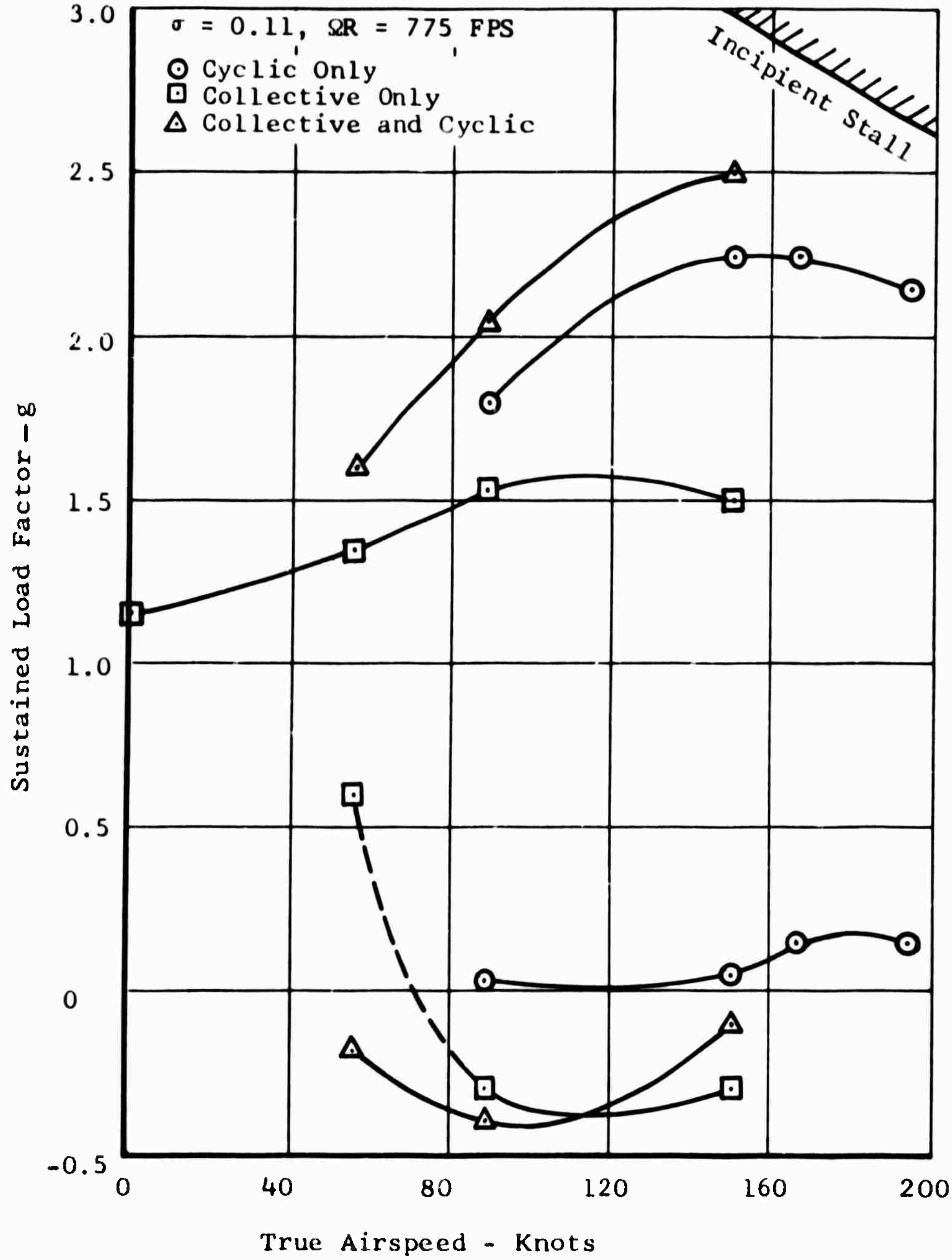

Figure 14. Task I - Maneuver Results, High Tip Speed Configuration.

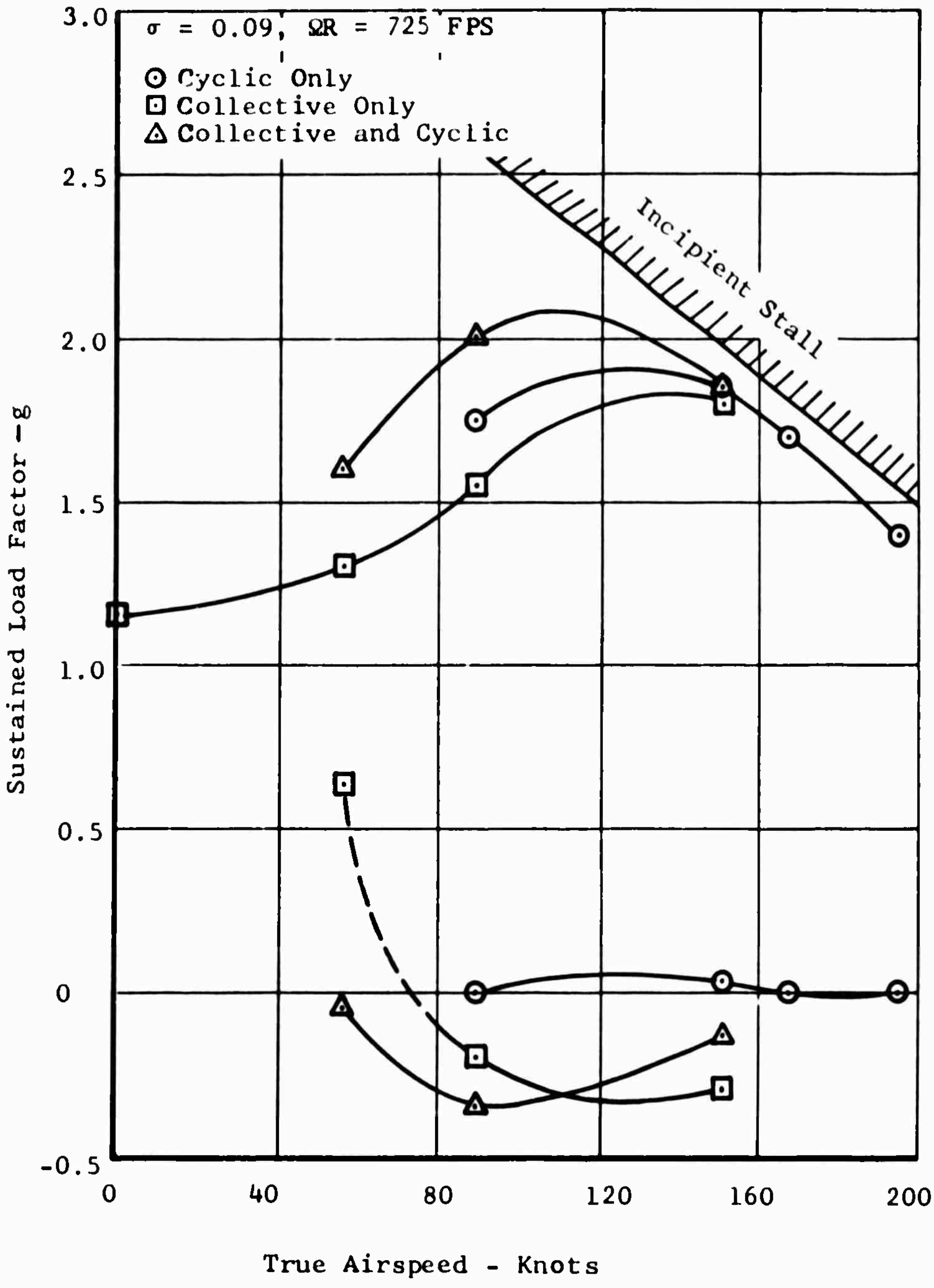

Figure 15. Task I - Maneuver Results, Low Solidity Configuration.

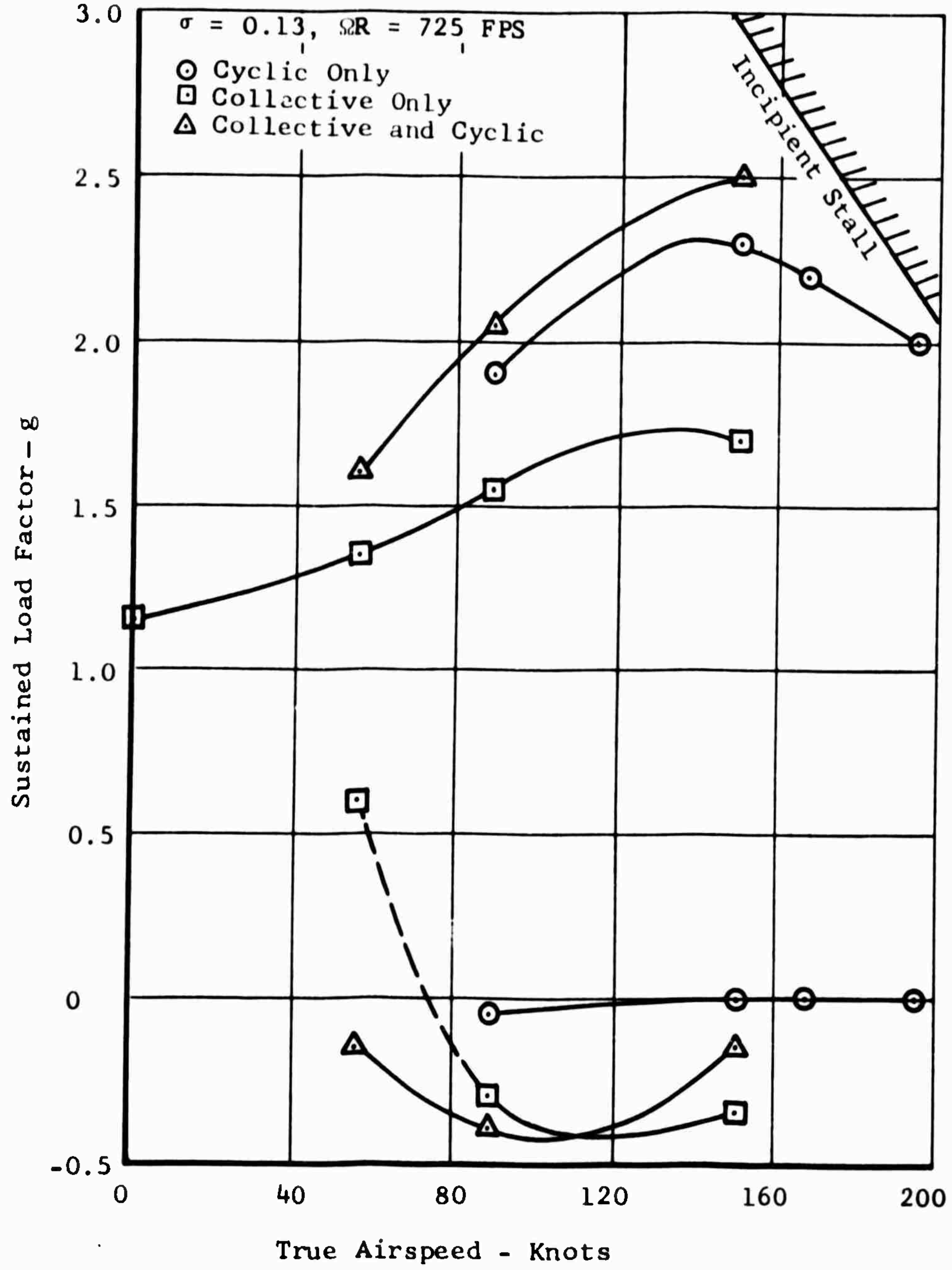

Figure 16. Task I - Maneuver Results, High Solidity Configuration.

potential capability was different for each configuration. For example, at 150 KTAS, the actual g-capability of the low tip speed configuration (Figure 13) was only 0.1 g below the potential capability. In comparison, the high tip speed configuration (Figure 14) was limited by flapping to about 0.5 g below the stall limit at 150 KTAS.

Effects of Limiting Criteria

With respect to the limiting criteria, the results for all five configurations were consistent. At high airspeeds, 150 KTAS and above, both the pullup and pushover maneuvers were normally limited by the rotor flapping criteria. At the lower airspeeds, 89 KTAS and below, the cyclic-only and combination collective plus cyclic maneuvers were limited by the flight path criteria, with pitch rate being the most common.

The collective pullup maneuvers were horsepower limited at all airspeeds. From hover, through the transition to a vertical climb, only 1.1-1.2 g's could be sustained without exceeding the maximum horsepower limit. However, in jump takeoff or autorotational landing maneuvers, transient load factors higher than 1.5 g's can be achieved. This is accomplished by supplementing engine power with the stored energy in the rotor.

In Appendix II, the limiting criteria for some of the low speed pushovers is given as "extreme flight conditions". These maneuvers were terminated from practical considerations rather than limited by the criteria of Table VII. For example, consider the low tip speed configuration (Figure 13) at 89 KTAS in a collective pushover maneuver. A collective push of 10 degrees was accomplished without exceeding any of the limiting criteria. However, four seconds into the maneuver the rate of descent was 5200 feet per minute, which is not realistically consistent with nap-of-the earth maneuvering flight. Consequently, the maneuver was terminated prior to exceeding any of the flight path or rotor limits.

Coordinated Turn Capability

For all configurations, the coordinated turn g-capability was found to be equal to the pullup capability. However, the important aspect of the coordinated turn maneuvers was not the effect of rotor configuration on turning capability, but rather the relationship between the turning g-level and the bleed-off of airspeed and altitude required to satisfy the turning flight path constraints--constant airspeed or constant altitude. For example, when comparing these configurations--

baseline (σ = .11, ΩR - 725 fps), high tip speed (σ = .11, ΩR = 775 fps), and high solidity (σ = .13, ΩR = 725 fps)--in a 2.0-g turn with a constant airspeed constraint, all three stabilized in the turn at the same rate of descent, 35 feet per second. More detailed information concerning the bleed-off of airspeed and altitude in turning flight will be presented in a later section of this report.

Effect of Airfoil Section on Maneuver Capability

The Bell-designed FX69-H-098 airfoil was used in this study. When compared to more conventional airfoils such as the NACA 0012, the FX69-H-098 has improved maximum lift capability without penalizing the high Mach number drag characteristics. Figure 17 compares the $C_{L_{max}}$ capability of the FX69-H-098 and NACA 0012 as a function of Mach number. The FX69-H-098 clearly offers a potentially significant increase in maximum rotor thrust capability. The design philosophy which resulted in development of the FX69-H-098 can be found in Reference 5.

When compared to the NACA 0012, the FX69-H-098 offers a "potential" increase in g-capability which is equal to the increase in the aerodynamic stall limit. However, the "actual" increase in g-capability is influenced by the limiting criteria of Table VII. To quantify the impact of airfoil capability on maneuver capability, the Task I baseline configuration was run in pullup maneuvers, using the NACA 0012 and the FX69-H-098 airfoils. The results of this airfoil comparison are shown on Figure 18. At high airspeeds, because of the limiting criteria of Table VII, the actual increase in pullup g-capability was less than the potential increase which is represented by the difference in stall limits. For example, at 167 KTAS, the potential increase was 0.26g, but the actual increase was 0.15g. At low airspeeds where the maneuvers were largely flight path limited, the airfoil used did not influence the g-capability.

Definition of Configuration g-Capability

The g-capability of a particular configuration was defined to be the maximum load factor which was reached and sustained at the configuration's normal rated power airspeed, V_{NRP}. It is important to remember that V_{NRP} is different for each configuration. Consequently, when comparing the g-capability of different configurations, the differences were influenced by airspeed as well as by rotor solidity and tip speed. Obtaining V_{NRP} for each configuration from Table III, and referring to Figures 12 through 16 for the maneuver results, the g-capability of each configuration was determined and is given in Table VIII.

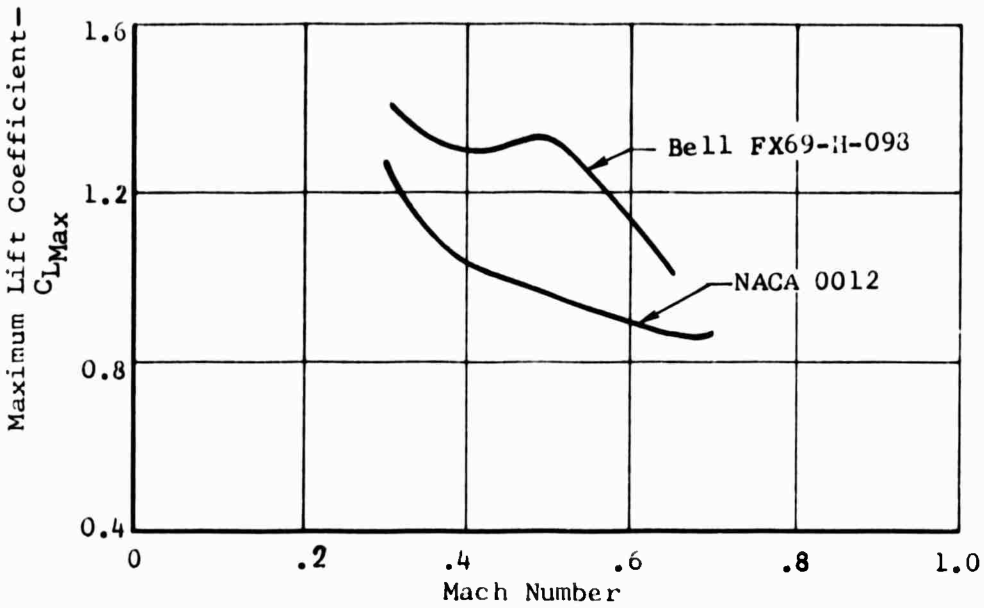

Figure 17. Comparison of Airfoil Maximum Lift Characteristics, Bell FX69-H-098 and NACA 0012.

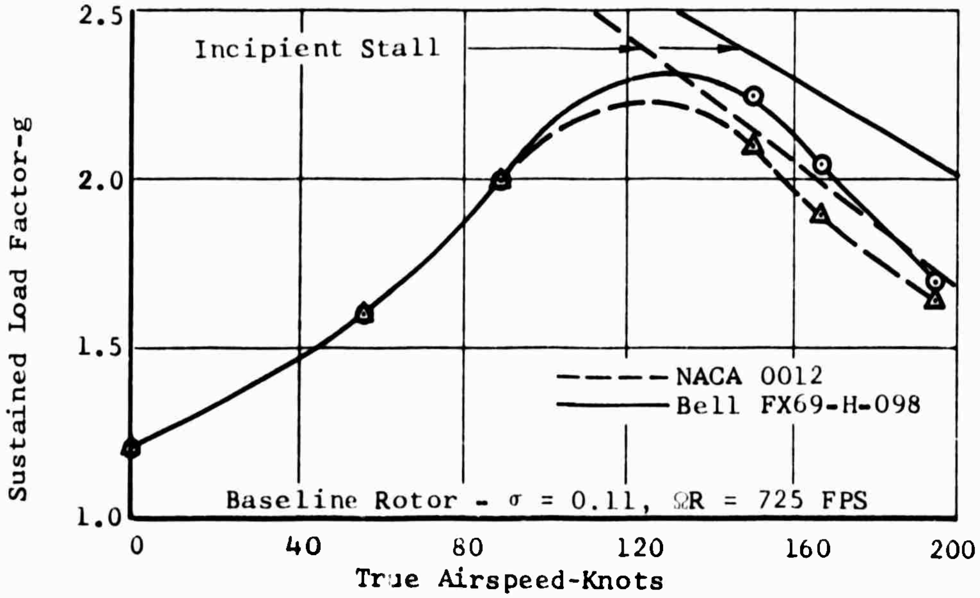

Figure 18. Effect of Main Rotor Airfoil Section on Maneuvering Flight Capability.

TABLE VIII. MANEUVER CAPABILITY - WINGLESS CONFIGURATIONS

Rotor Solidity	Tip Speed (FPS)	V_{NRP} (KTAS)	Load Factor @ V_{NRP} (g)
0.11	675	180	1.46
0.11	725	169	2.02
0.11	775	153	2.50
0.09	725	175	1.62
0.13	725	163	2.25

The data of Table VIII is given in carpet-plot form on Figure 19. To prevent unnecessary extrapolation, Figure 19 inclues data for two additional configurations-- $\sigma = 0.13$, ΩR - 675 fps and $\sigma = 0.09$, ΩR - 775 fps--which were investigated only at their normal rated power airspeeds in pullup maneuvers.

The first important conclusion from Figure 19 is that as rotor solidity and tip speed increase, the g-capability increases, as would be expected. However, as previously mentioned, these effects are exaggerated by the fact that as rotor solidity and tip speed increase, V_{NRP} decreases. If the configurations were compared at constant airspeed, the effects of rotor solidity and tip speed would be somewhat less than as shown in Figure 19.

The second conclusion to be drawn from Figure 19 is that within the frame work of solidities and tip speeds investigated, there are many configurations which define a given g-capability. For example, a 2.00g design could consist of a solidity of 0.09 and tip speed of 760 fps, or a solidity of 0.13 and a tip speed of 692 fps. Similar ranges exist for any specified g-capability. In this study, the g-levels of interest were 1.50, 1.75, and 2.00g's. Figure 19 can be used to define a locus of wingless configurations which satisfy these load factor requirements.

RELATIONSHIP OF MANEUVER CAPABILITY TO PERFORMANCE - TASK I

The previous section presented the maneuver results for each configuration, discussed how the maneuvers were influenced by the limiting criteria, and defined the maneuver capability of each Task I configuration. Attention is now turned to relating the configuration maneuver capability to the performance.

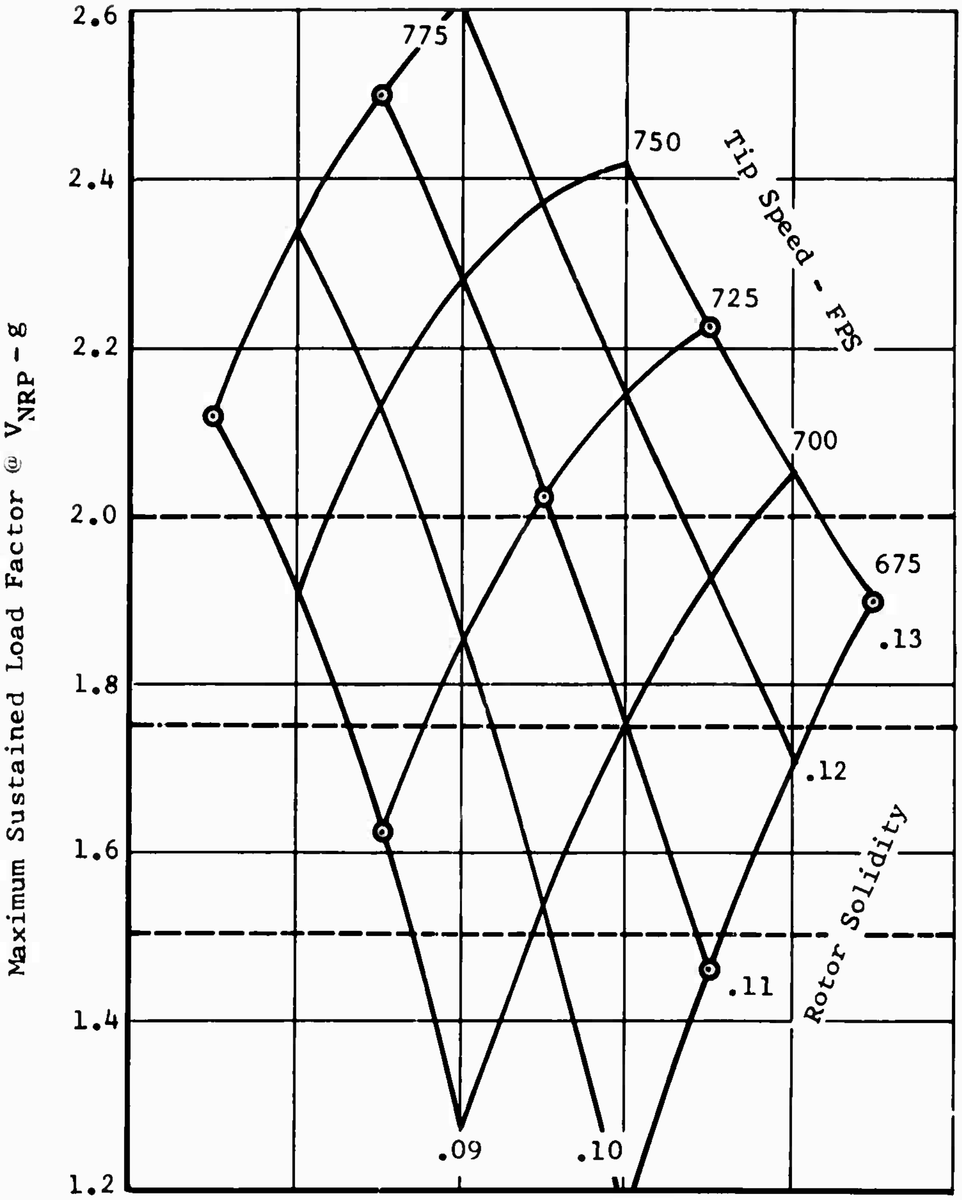

Figure 19. Effects of Rotor Solidity and Tip Speed on g-Capability at V_{NRP}.

Relationship of g-Capability to V_{NRP}

The effects of rotor solidity and rotor tip speed on the normal rated power airspeed, V_{NRP}, of the Task I wingless helicopters are presented on Figure 20. The figure clearly shows that as rotor solidity or tip speed was increased, the V_{NRP} capability was decreased.

Cross-plotted on the V_{NRP} curves of Figure 20 are the locus of configurations which satisfy 1.50g, 1.75g, and 2.00g levels of maneuverability. The first conclusion regarding the relationship of g-capability to V_{NRP} is that for a given design g-level, V_{NRP} is not significantly influenced by the choice of configuration which satisfies the given load factor requirement. That is, all the 1.50g configurations have about the same V_{NRP}, independent of the solidity and tip speed combination. The same is true for the 1.75g and 2.00g designs, although to a lesser degree for the 2.00g designs.

Second, as the g-level requirement is increased, the V_{NRP} capability is reduced. A 2.00g design will have a V_{NRP} about five KTAS less than a 1.75g design, and the same increment applies between the 1.75g and 1.50g designs.

Relationship of g-Capability to Payload

Payload (from Table V), as a function of rotor solidity and tip speed, is given on Figure 21 along with the locus of configurations which satisfy 1.50g, 1.75g, and 2.00g design requirements. As solidity, tip speed, or the design load factor was increased, the payload was reduced.

Figure 21 clearly shows that the configuration chosen to satisfy a particular maneuverability requirement has a significant effect on payload capability. For example, the maximum payload 2.00g configuration ($\sigma = 0.09$, $\Omega R =$ 765 fps) has 560 pounds more payload than the minimum payload 2.00g configuration ($\sigma = 0.13$, $\Omega R = 692$ fps).

The major impact of Figure 21 is that for any load factor capability, there are many configurations which meet or exceed the specified payload requirement of 2640 pounds. This offers the flexibility needed to consider noise, airspeed, control loads, blade life and other factors, being assured that the payload and design load factor requirements can be satisfied. An additional tradeoff to be considered is gross weight. Those configurations with payload capability greater than 2640 pounds can be reduced in gross weight, maintaining solidity and disc loading until the payload requirement is matched. Reducing the gross weight can be directly related to cost savings. This gross weight reduction is possible only if the engine size is also reduced. If this study had been conducted with a "fixed" engine, this conclusion would not be valid.

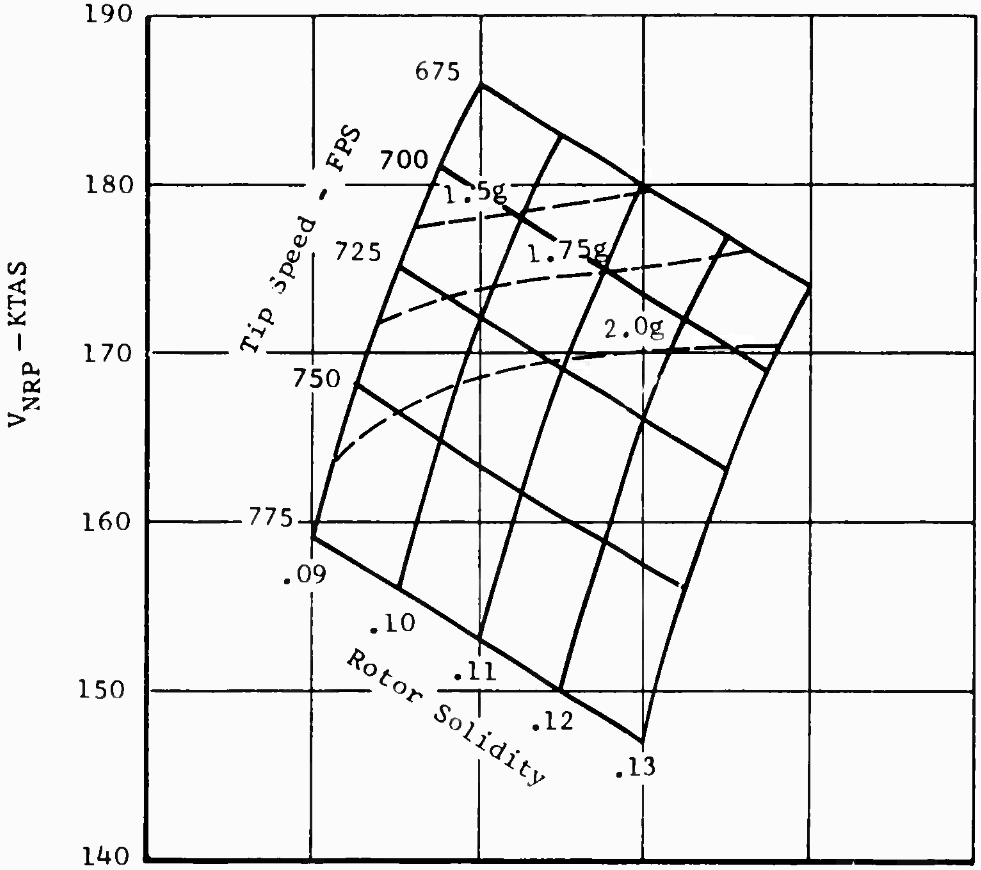

Figure 20. Effects of Rotor Solidity and Tip Speed on V_{NRP} and Design g-Capability.

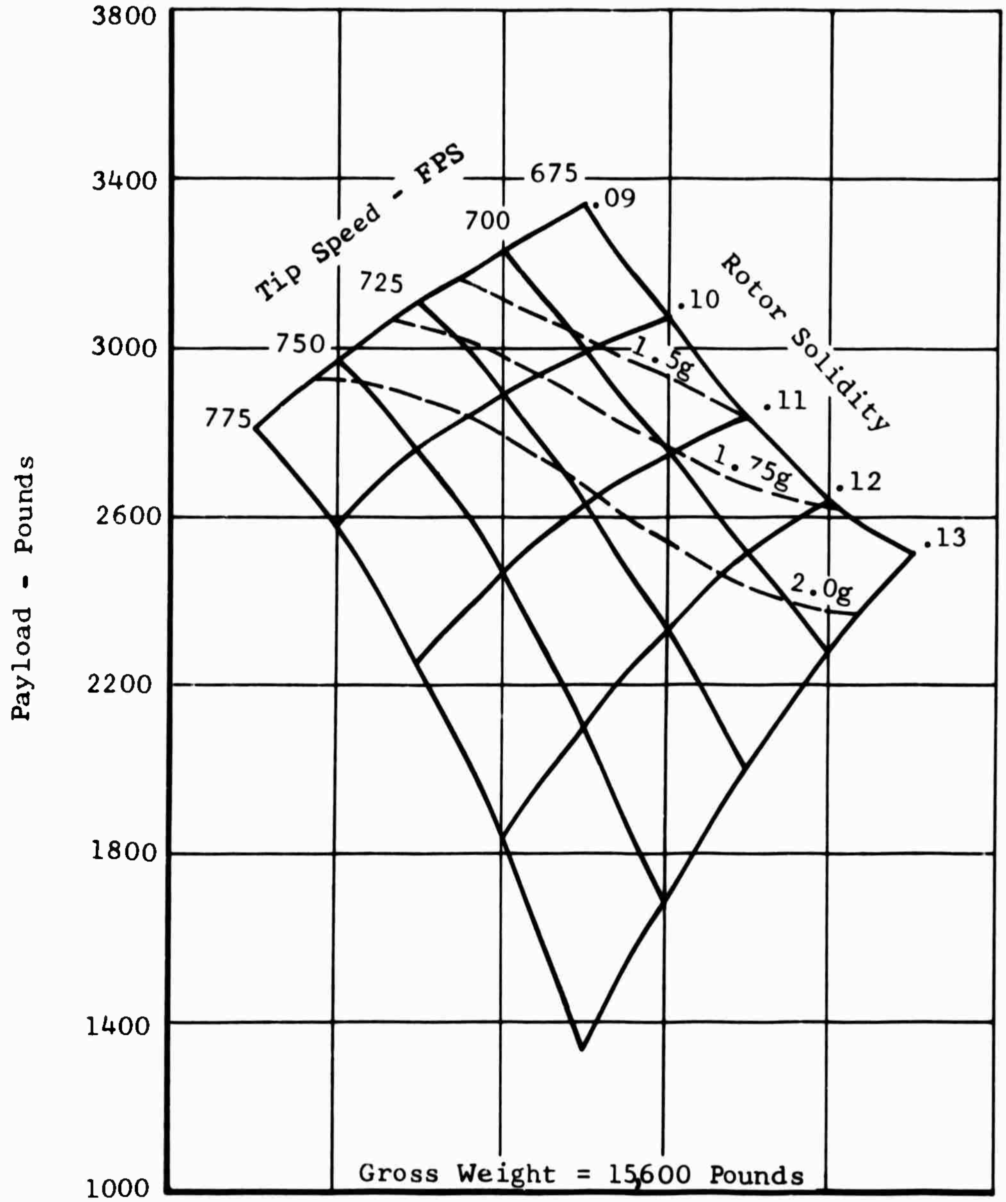

Figure 21. Effects of Rotor Solidity and Tip Speed on Payload and Design g-Capability.

TASK II - WINGED HELICOPTER STUDY

SCOPE AND GROUND RULES

The purpose of the Task II study was to investigate the effect of wings on the maneuverability of selected configurations from Task I. The ground rules given for Task I were used for the Task II study.

All the configurations selected for study had a rotor tip speed of 725 feet per second. The rotor solidity and wing parameters varied as given in Table IX.

TABLE IX. TASK II - CONFIGURATIONS

Description	Tip Speed (FPS)	Solidity	Wing Area (Ft^2)	Wing Incidence (Deg)
Baseline Rotor	725	0.11	70	6.5
				9.5
				12.5
			105	6.5
				9.5
				12.5
Low Solidity Rotor	725	0.09	70	6.5
				9.5
				12.5
			105	6.5
				9.5
				12.5
High Solidity Rotor	725	0.13	70	6.5
				9.5
				12.5
			105	6.5
				9.5
				12.5

The wing areas of Table IX represent the total area including the fuselage carry-through which was equal to 45 square feet. The wing incidences refer to the zero-lift-line angle relative to the fuselage waterline.

STABILITY AND CONTROL ANALYSIS - TASK II

A detailed stability and control analysis of all the winged helicopter configurations examined during Task II was not made because of the number of configurations involved. The two configurations which had the highest wing lift and the lowest wing lift were investigated in detail. The stability and control characteristics of these two boundary configurations were considered representative of the characteristics of all of the winged helicopter configurations studied in Task II.

The airframe characteristics of the winged helicopter configurations were basically the same as for the wingless helicopter configurations, with the addition of a wing with its aerodynamic center at the mid-cg location (Table I). The configurations for which data is presented had a solidity of 0.11, a tip speed of 725 feet per second, and a gross weight of 15,600 pounds. The low wing lift configuration had a wing area of 70 square feet and a wing incidence of 6.5 degrees. The wing area was 105 square feet, and the wing incidence was 12.5 degrees for the high wing lift configuration. Trimmed level flight wing lift values are shown in Figure 22 for these two configurations.

Main rotor total flapping is shown in Figure 23. Both configurations had less than 1.20 degrees of flapping at level flight cruise airspeeds (150 KTAS and V_{NRP}) at the mid-cg.

Hybrid computer data indicated that all winged configurations had neutral or positive dynamic stability characteristics at the aft cg.

MIL-H-8501A requires positive stick position and force stability with respect to speed at constant power for speeds up to V_H. These gradients are indicated with dashed lines through the trim points on Figure 24. The solid lines indicate the variable power, trim stick position with respect to airspeed gradients which are also positive. Adequate control margin at the speeds for both maximum continuous and military rated power are apparent in Figure 24.

These characteristics were achieved without electronic stabilization.

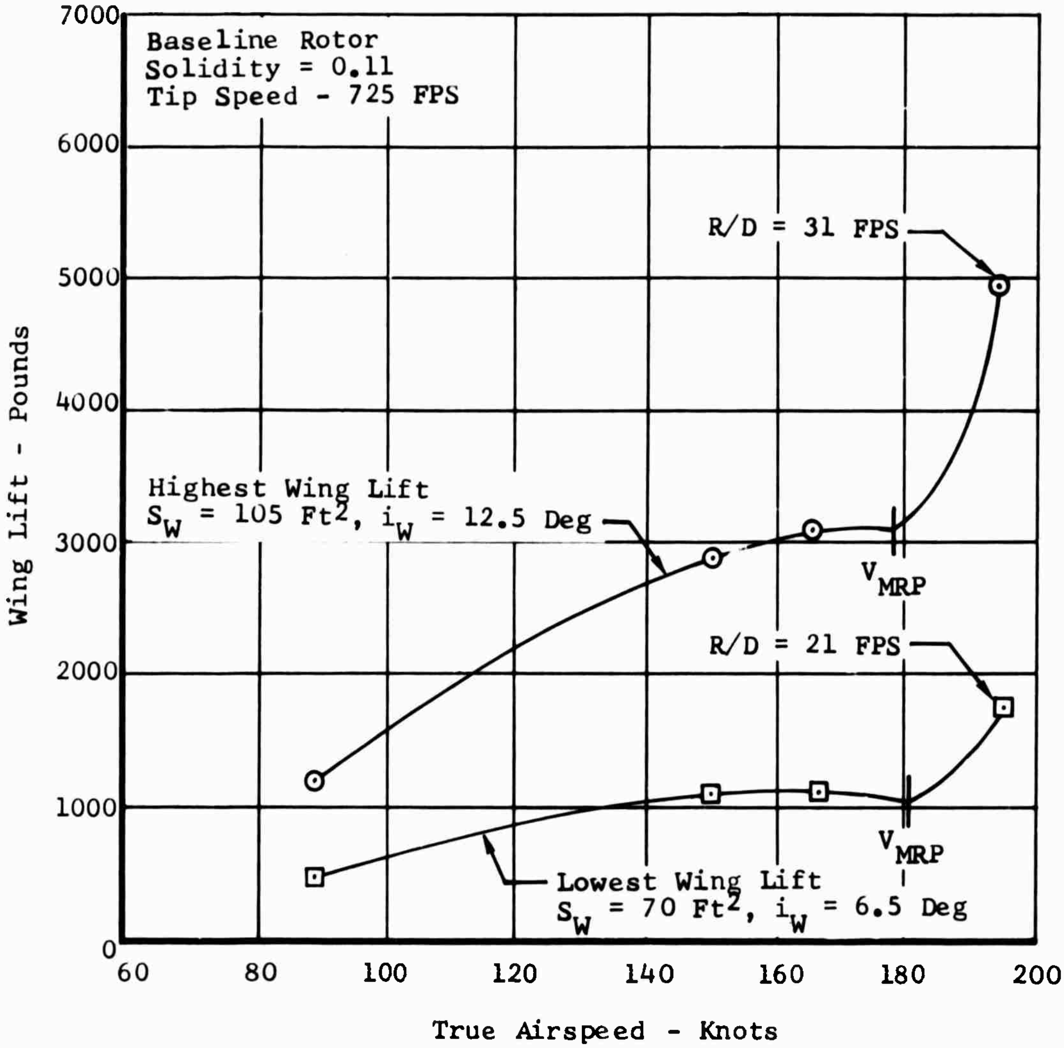

Figure 22. Wing Lift Versus True Airspeed for Task II Configurations.

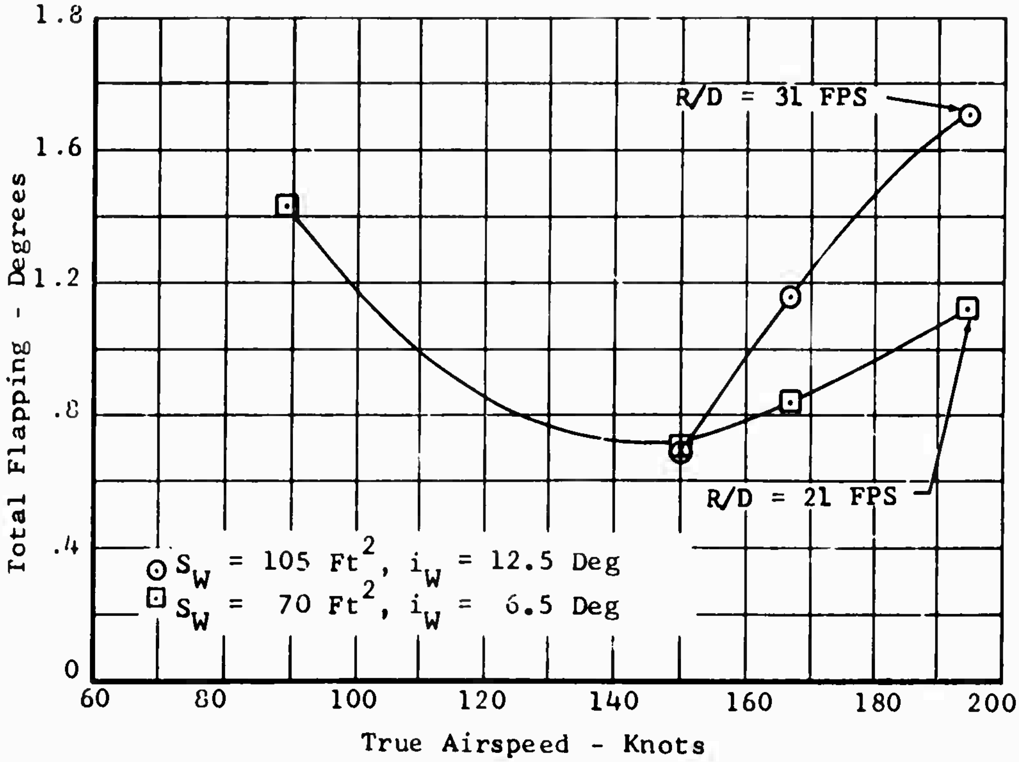

Figure 23. Task II Winged Configurations, Main Rotor Flapping.

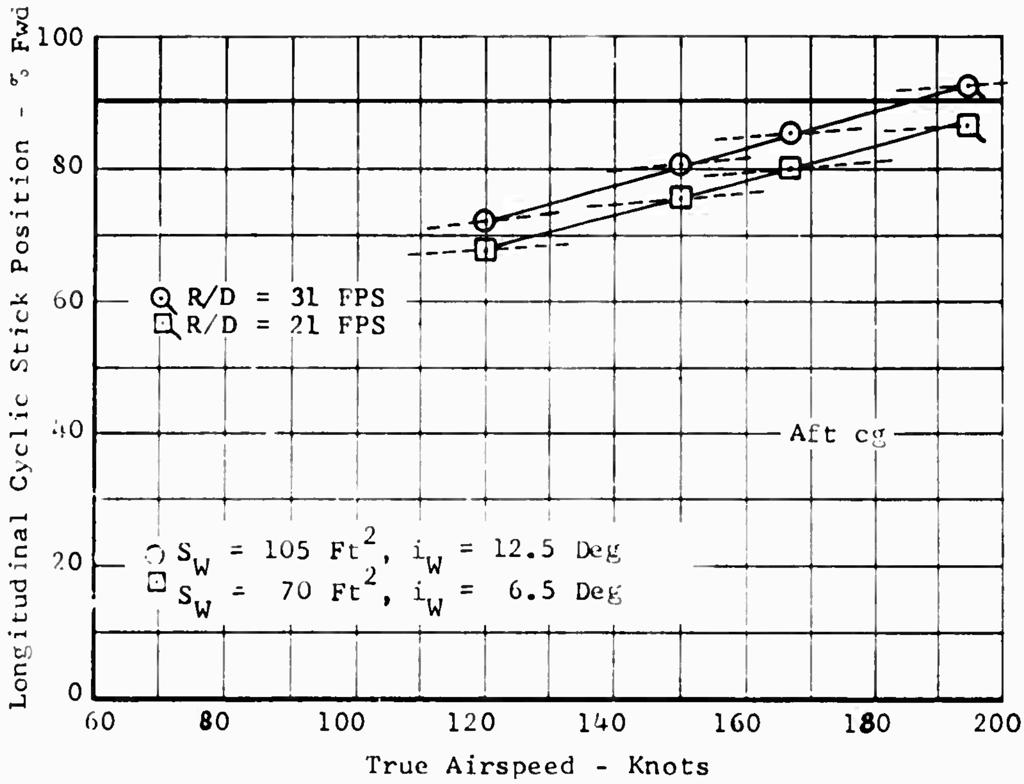

Figure 24. Task II Winged Configuration, Longitudinal Cyclic Stick Position Versus True Airspeed.

PERFORMANCE - TASK II

Power Available

The power available data used in Task II was based on an advanced technology engine with losses and allowances the same as used in Task I.

Hover

The rotor horsepower required data for the various configurations previously calculated in Task I and shown on Figure 1 was also used for the applicable winged configurations. Before entering Figure 1 to obtain hovering power required, the wing download was added to the gross weight to determine the net rotor thrust required. The download has been determined to be equal to 0.7 $\left(\frac{\text{Wing Area}}{\text{Rotor Disc Area}}\right)$. This value was determined from a 1/4 scale model test of the Bell Model XV-3, Reference 6.

The installation losses and tail rotor power required were the same as used in Task I. The excess power necessary to climb and the uninstalled power available were also determined as explained in Task I. The uninstalled power available is shown in Table X.

Forward Flight

The forward flight power required was calculated on F35 with allowance for the wing lift and drag. The wing lift for trimmed level flight was calculated on the hybrid computer for all of the configurations considered. Trimmed level flight wing lift is shown on Figures 25 through 27 for all 18 winged configurations. The variation with airspeed results from the combined effects of dynamic pressure and trimmed pitch attitude. At high level flight speeds, the trim pitch attitudes are increasing nose-down, resulting in a decrease in trim wing lift. In the maneuver study, however, trimmed flight at airspeeds greater than V_{MRP} were in a dive condition wherein the flight path angle contributes a positive angle of attack increment. Therefore, the wing lift increases with airspeed throughout the airspeed range as was shown on Figure 22. The values from Figures 25 through 27 were subtracted from the gross weight to find the rotor thrust at which the power required was calculated. The equivalent flat plate drag area for the helicopter with the wing added was estimated to be 12.61 square feet with the 70-square-foot wing, and 13.02 square feet with the 105-square-foot wing. In addition, the wing induced drag and the increased wing profile drag with

TABLE X. TASK II - ENGINE POWER REQUIRED

ΩR (FPS)	σ	S_{w_2} (Ft^2)	i_w (Deg)	Uninstalled Engine HP Rating S.L. Std Day
725	0.11	70	6.5	2890
			9.5	
			12.5	
		105	6.5	2925
			9.5	
			12.5	
	0.09	70	6.5	2760
			9.5	
			12.5	
		105	6.5	2800
			9.5	
			12.5	
	0.13	70	6.5	3020
			9.5	
			12.5	
		105	6.5	3055
			9.5	
			12.5	

angle of attack were included. These values were estimated from the results of the wind-tunnel test of a 1/6 scale model of the Bell Model D268 UTTAS configuration. The swept tip improvement and tail rotor, transmission, and accessory losses were the same as explained in Task I. Three values of wing incidence were studied for each wing area to determine the effect of trim wing lift on performance and maneuver capability. The speed-power polars at 4000 feet, 95°F for all the winged configurations at the design gross weight of 15,600 pounds are shown in Figures 28 through 33. The military and normal rated power available are also shown on these figures. The maximum speeds are found from Figures 28 through 33 and are shown in Table XI. Normal rated power speed was greater than 150 knots for all cases. Additional speed power polars

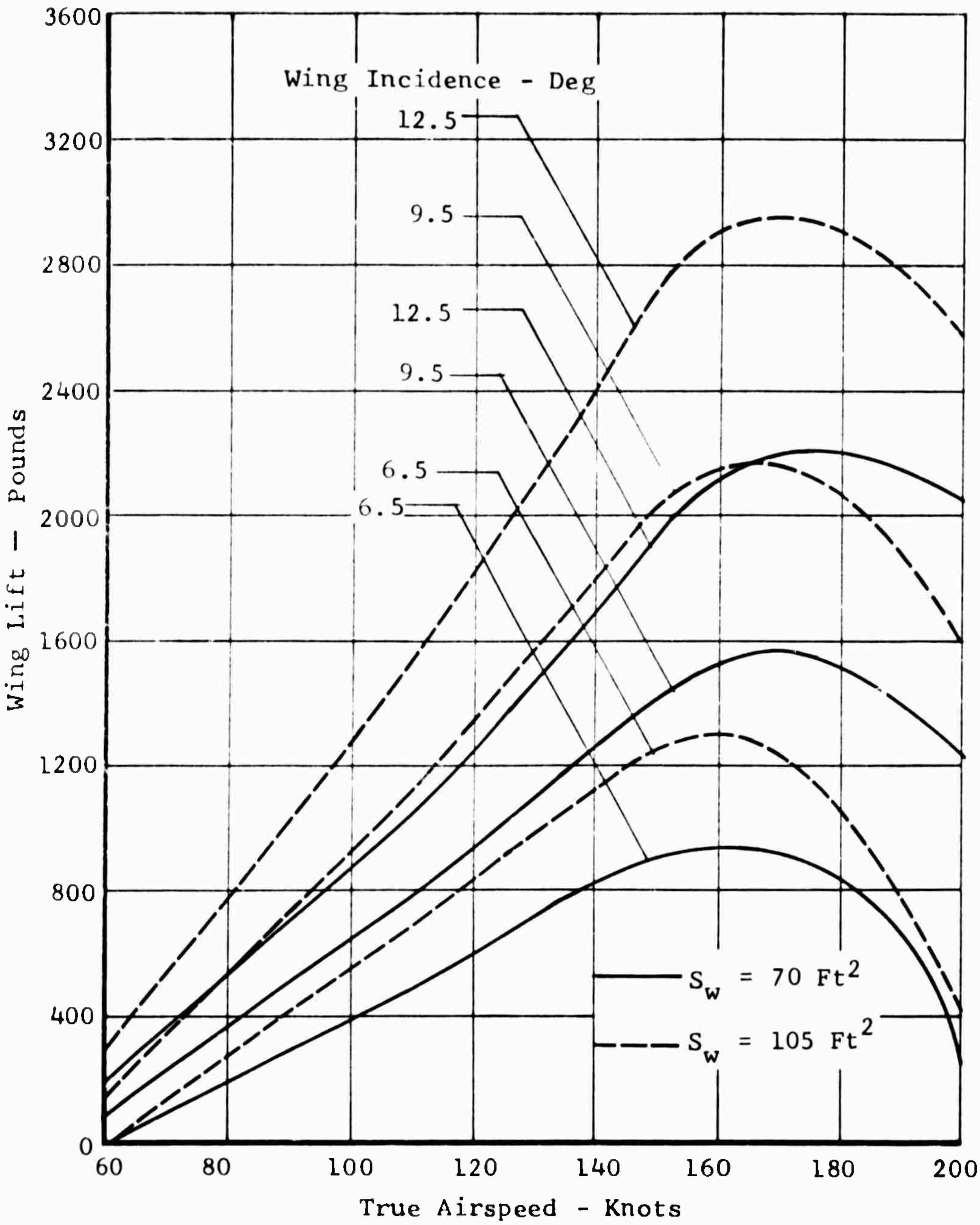

Figure 25. Task II - Winged Helicopter, Wing Lift Versus True Airspeed, Solidity = 0.11.

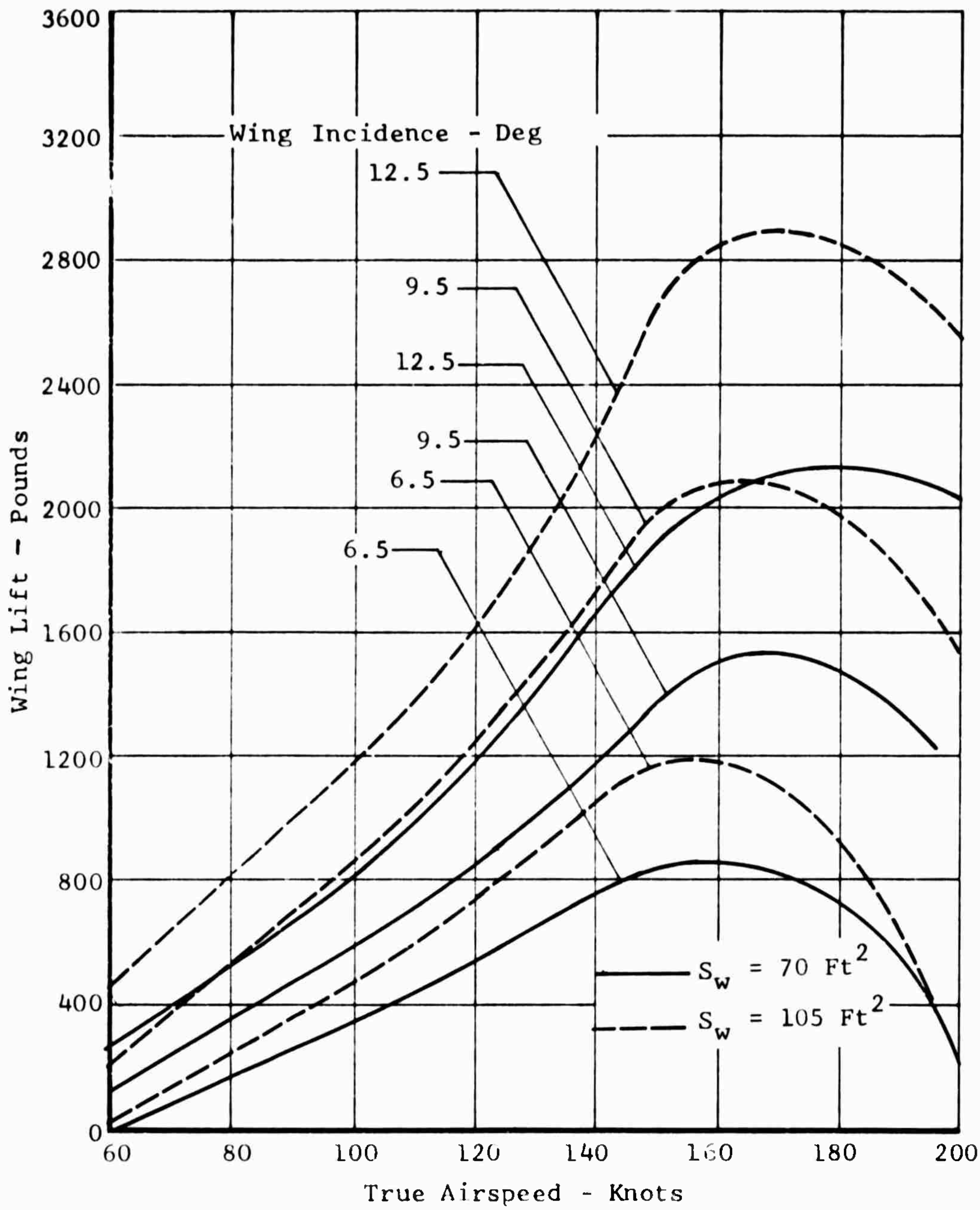

Figure 26. Task II - Winged Helicopter, Wing Lift Versus True Airspeed, Solidity = 0.09.

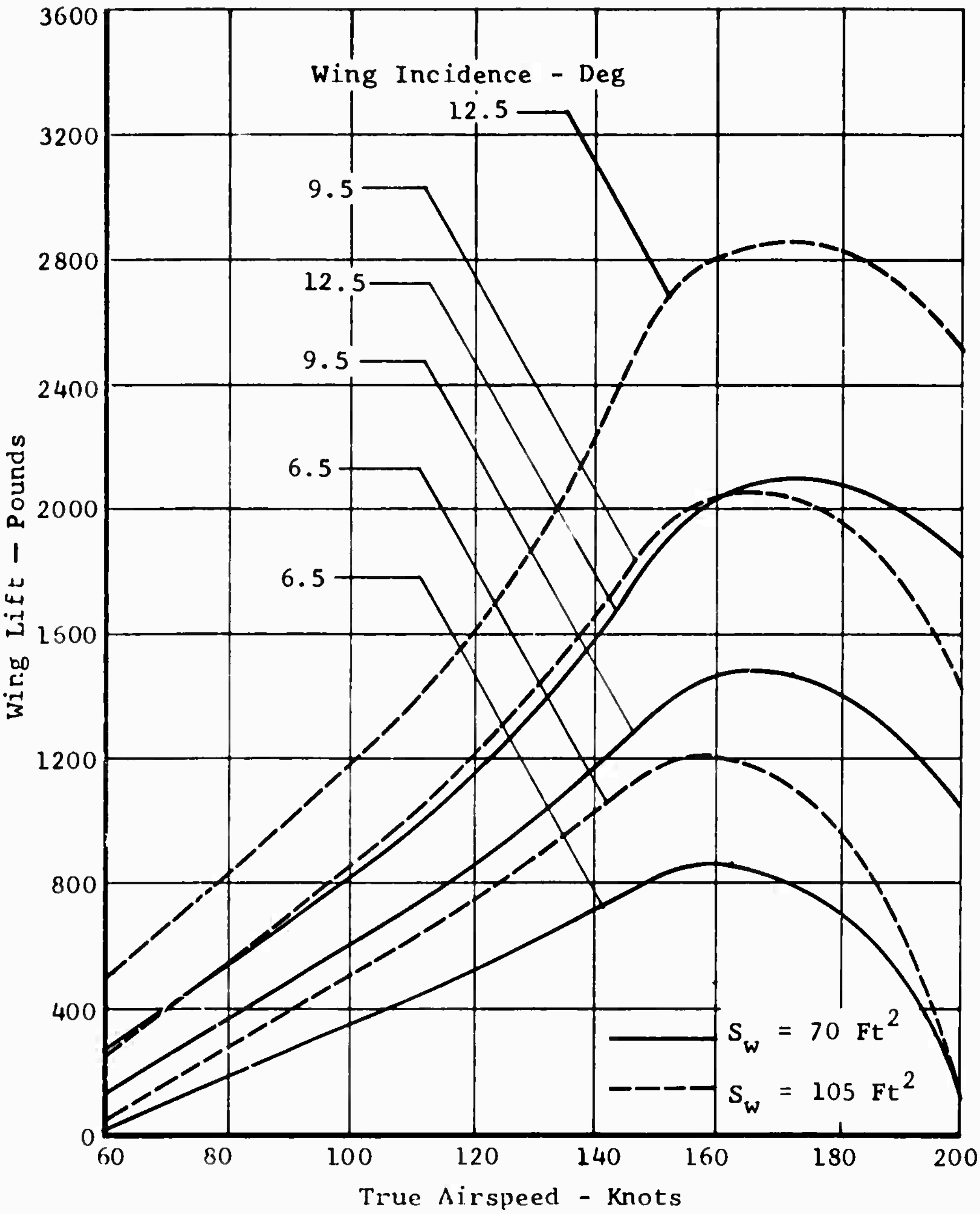

Figure 27. Task II - Winged Helicopter, Wing Lift Versus True Airspeed, Solidity = 0.13.

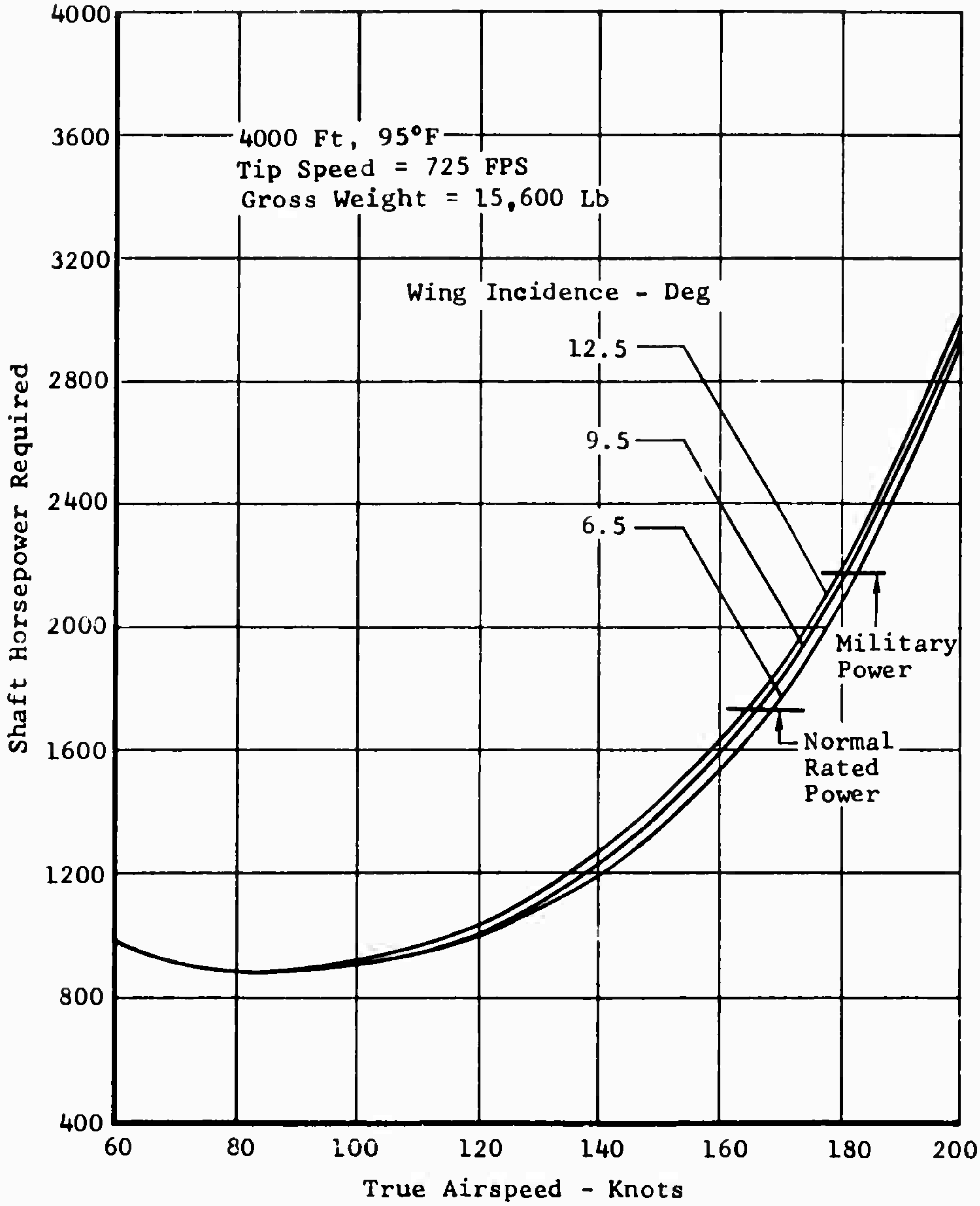

Figure 28. Task II - Winged Helicopter, Speed Power Polar, Solidity = 0.11, Wing Area = 70 Ft^2.

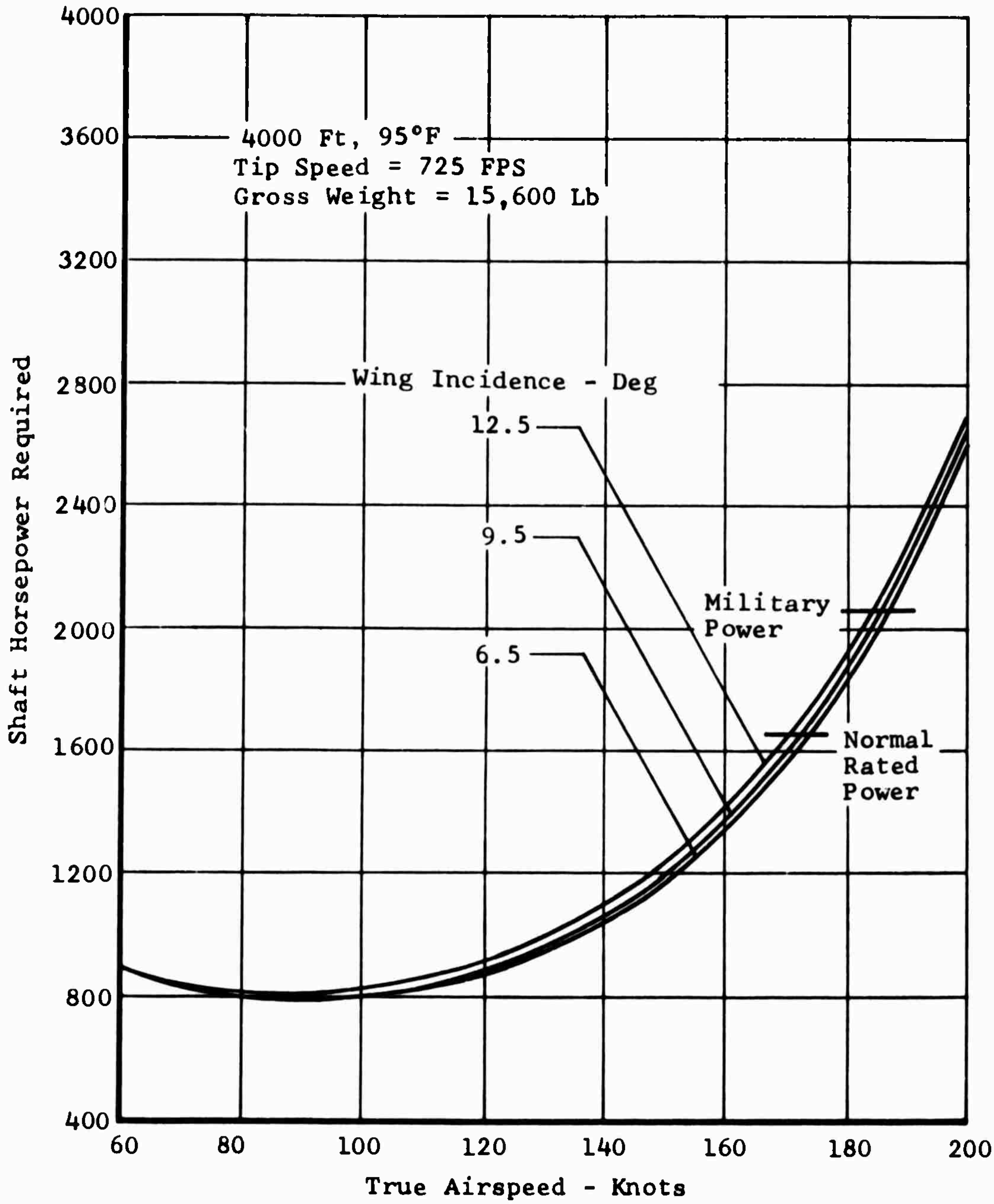

Figure 29. Task II - Winged Helicopter, Speed Power Polar, Solidity = 0.09, Wing Area = 70 Ft^2.

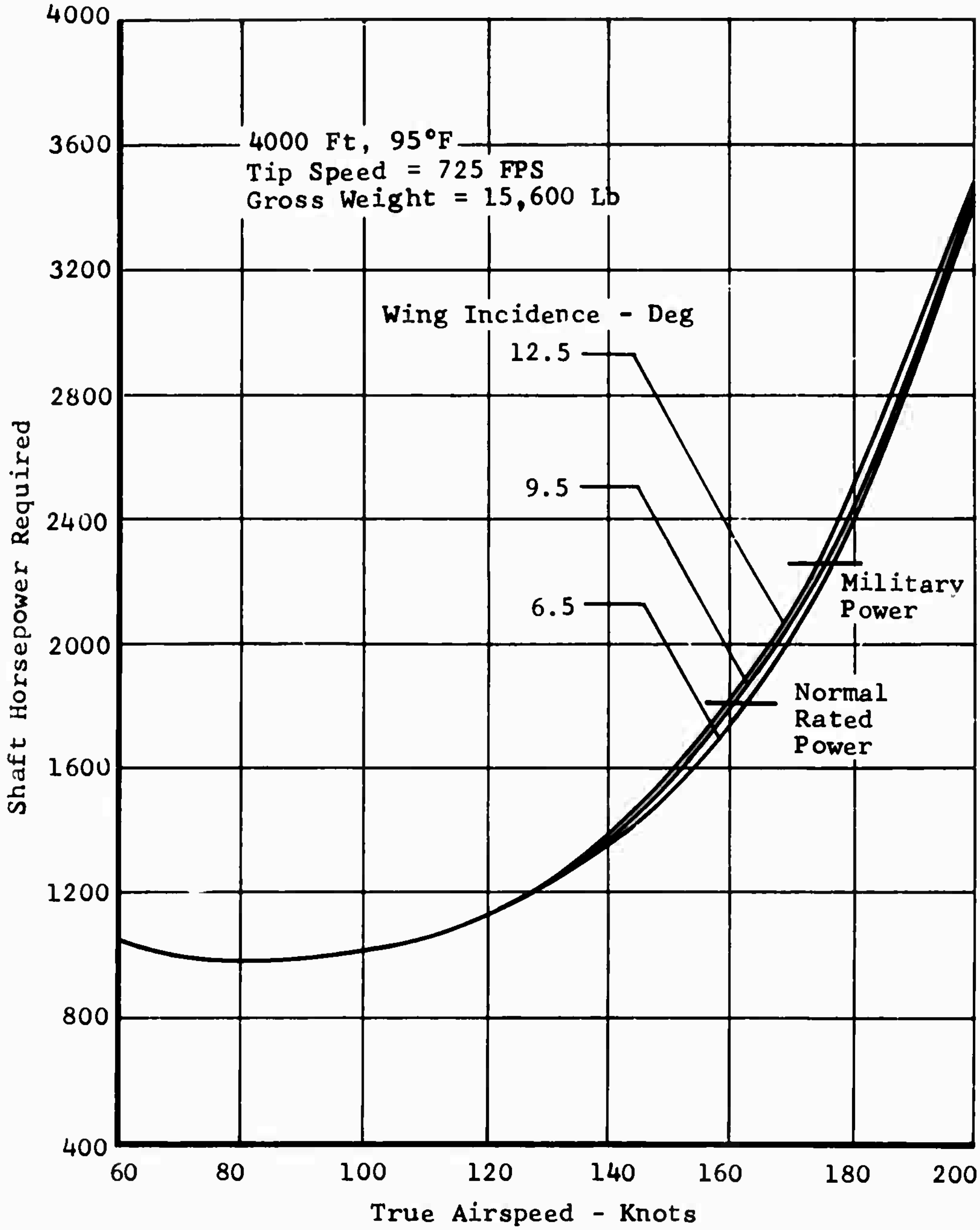

Figure 30. Task II - Winged Helicopter Speed Power Polar, Solidity = 0.13, Wing Area = 70 Ft^2.

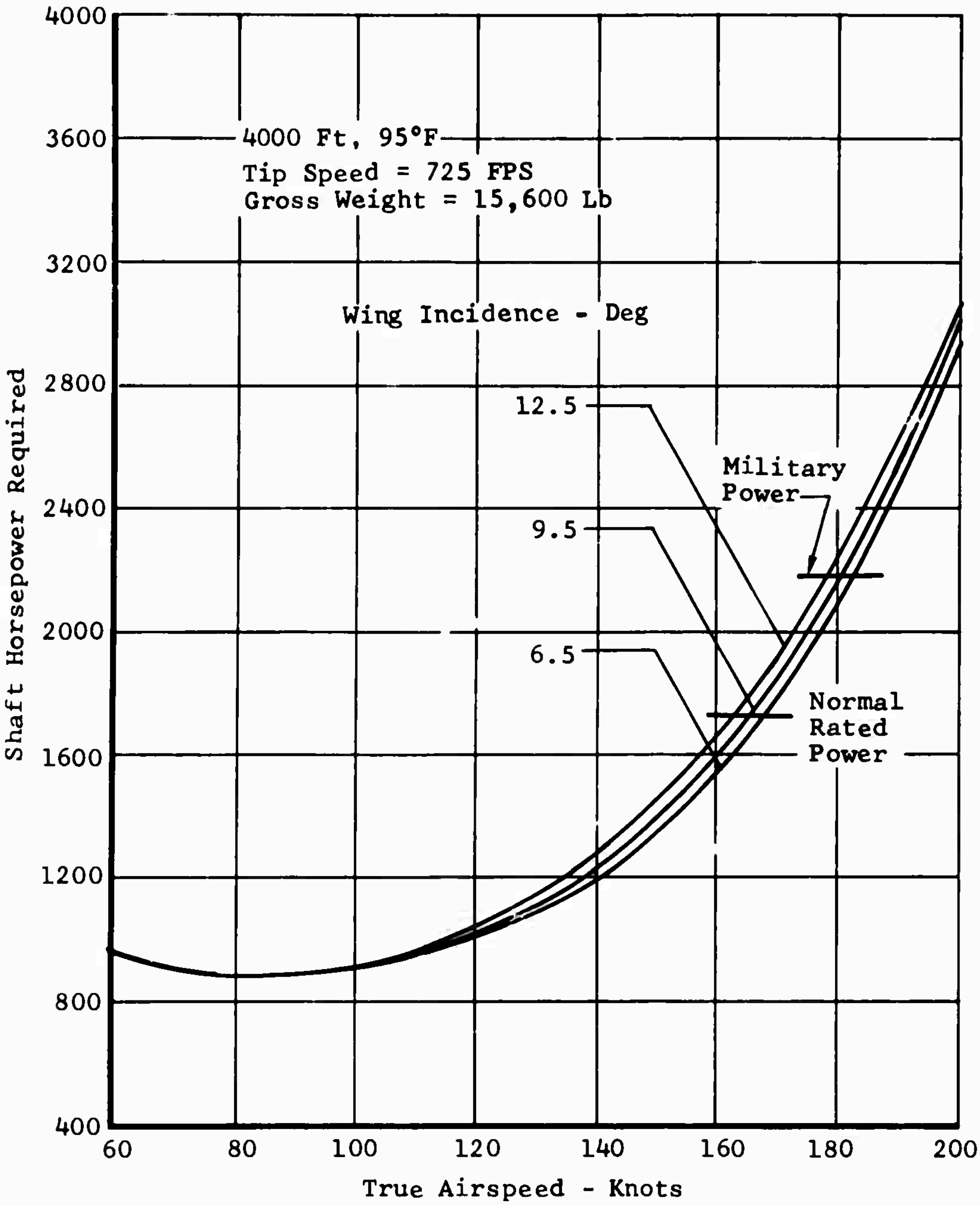

Figure 31. Task II - Winged Helicopter, Speed Power Polar, Solidity = 0.11, Wing Area = 105 Ft^2.

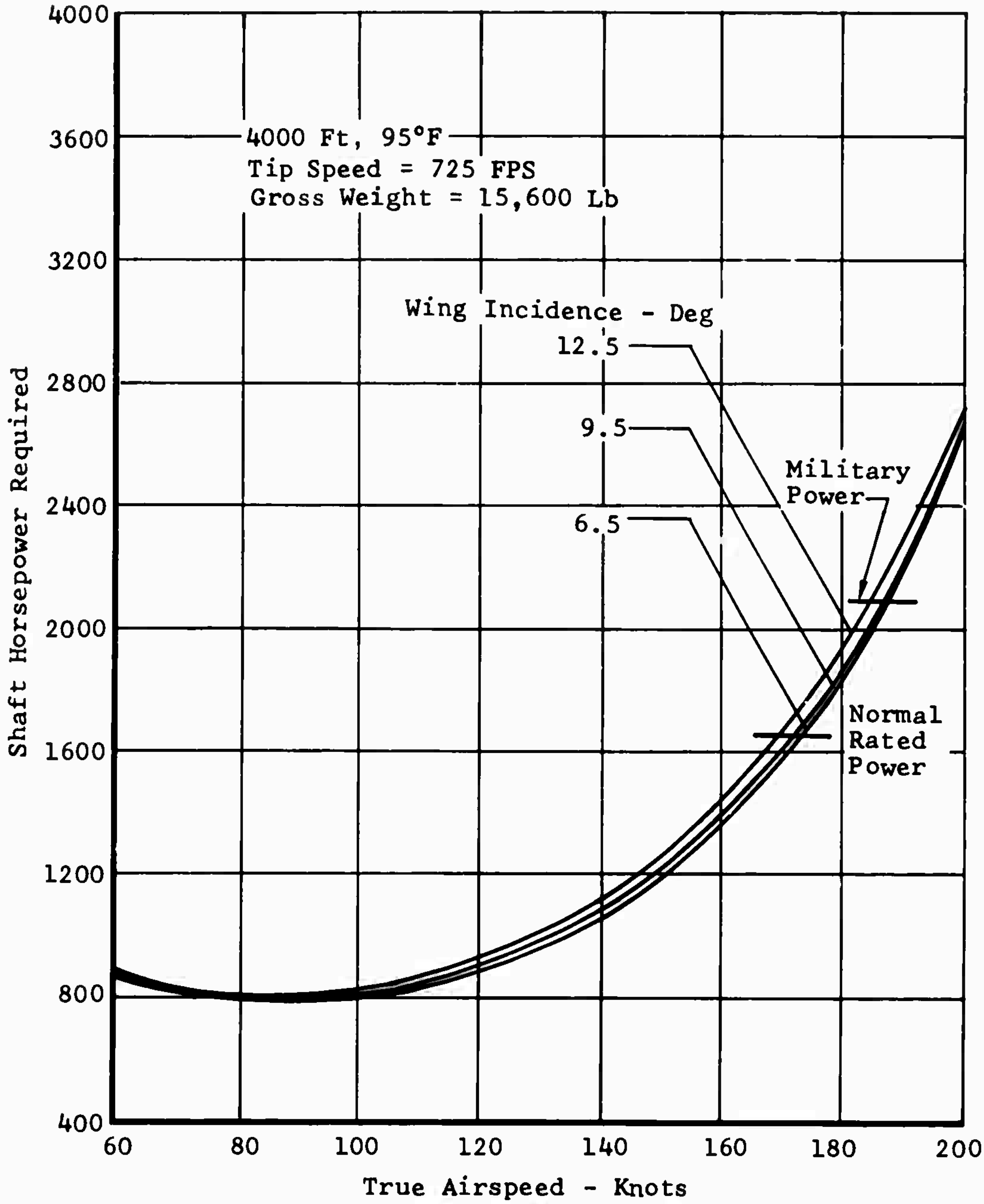

Figure 32. Task II - Winged Helicopter, Speed Power Polar, Solidity = 0.09, Wing Area = 105 Ft^2.

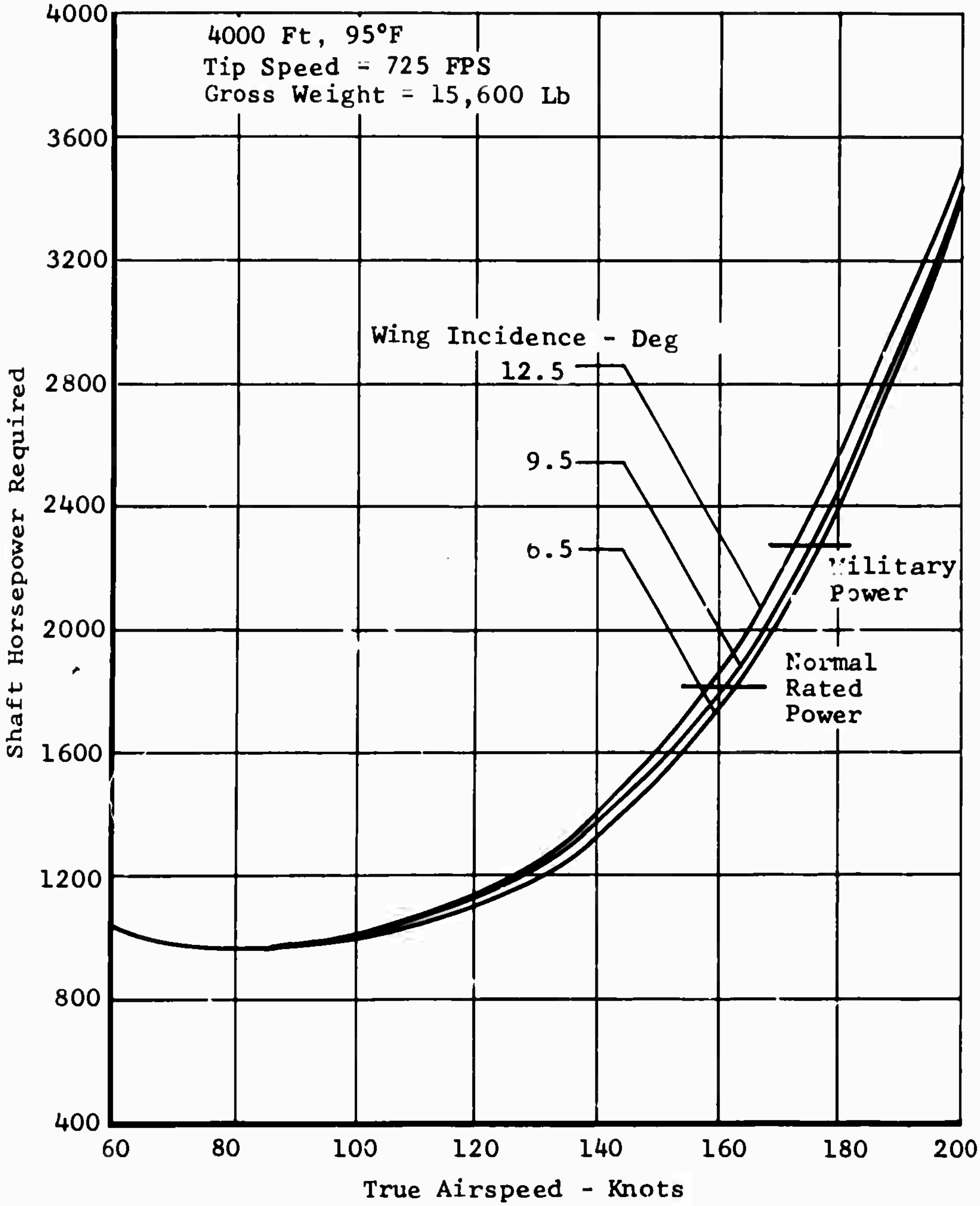

Figure 33. Task II - Winged Helicopter, Speed Power Polar, Solidity = 0.13, Wing Area = 105 Ft^2.

for a range of gross weights for each configuration are given on Figures 104 through 121 of Appendix III.

TABLE XI. TASK II - MAXIMUM TRUE AIRSPEED, 4000 FEET, 95°F

σ	S_w (Ft^2)	i_w (Deg)	V_{NRP} (KTAS)	V_H (KTAS)
0.11	70	6.5	168	182
		9.5	167	181
		12.5	164	180
	105	6.5	168	182
		9.5	166	181
		12.5	163	179
0.09	70	6.5	173	187
		9.5	173	187
		12.5	171	186
	105	6.5	173	187
		9.5	172	187
		12.5	170	185
0.13	70	6.5	163	177
		9.5	162	176
		12.5	160	174
	105	6.5	163	177
		9.5	160	175
		12.5	158	173

Specific range data for all the winged configurations were calculated and are shown in Figures 122 through 139 of Appendix III. Also shown on these plots are the military rated power, normal rated power, and long-range cruise speed.

Weights

The weights were estimated as in Task I and a summary weight statement for all configurations is shown in Tables XII through XIV.

TABLE XII. TASK II - WINGED HELICOPTERS SUMMARY WEIGHT STATEMENT, ROTOR SOLIDITY = 0.11

Design Gross Weight, Pounds		15,600		15,600		15,600		15,600		15,600		15,600
Engines (No. and Type)		2 ADV.		2 ADV.		2 ADV.		2 ADV.		2 ADV.		2 ADV.
SHP - Uninstalled		2890		2890		2890		2925		2925		2925
Main Rotor(s) Diameter, Feet		57.5		57.5		57.5		57.5		57.5		57.5
Solidity		0.11		0.11		0.11		0.11		0.11		0.11
Tip Speed, FPS		725		725		725		725		725		725
Wing Area, Ft^2		70		70		70		105		105		105
Wing Incidence, Deg.		6.5		9.5		12.5		6.5		9.5		12.5
Weights, Pounds												
Rotor Group		2607		2607		2607		2607		2607		2607
Wing Group		84		86		105		126		145		175
Tail Group		187		187		187		187		187		187
Body Group		1946		1946		1946		1946		1946		1946
Alighting Gear		468		468		468		468		468		468
Flight Controls		717		717		717		717		717		717
Fixed	419		419		419		419		419		419	
Rotating	298		298		298		298		298		298	
Eng. Section/Nacelles		176		176		176		176		176		176
Propulsion		2448		2454		2469		2473		2479		2487
Engine Install	587		587		587		591		591		591	
Induction System	64		64		64		66		66		66	
Exhaust	77		77		77		79		79		79	
Fuel System	393		399		414		397		403		411	
Controls	32		32		32		32		32		32	
Starting	39		39		39		40		40		40	
Rotor Brake	49		49		49		49		49		49	
Trans and Drive System	1207		1207		1207		1219		1219		1219	
Passive Defense		200		200		200		200		200		200
Instruments		73		73		73		73		73		73
Hydraulics		93		93		93		93		93		93
Electrical		281		281		281		281		281		281
Avionics (inc nav)		411		411		411		411		411		411
Furnishings and Equipment		658		658		658		658		658		658
Air Conditioning		121		121		121		121		121		121
APU		93		93		93		93		93		93
Armament		175		175		175		175		175		175
Weight Empty		10,738		10,746		10,780		10,805		10,830		10,868
Crew	600		600		600		600		600		600	
Payload (Pass or Cargo)	2386		2351		2284		2297		2245		2172	
Fluids	61		61		51		61		61		61	
Survival Equipment	-		-		-		-		-		-	
Passive Defense	-		-		-		-		-		-	
Armament	-		-		-		-		-		-	
Fuel	1815		1842		1875		1837		1864		1899	
Miscellaneous	-		-		-		-		-		-	
Useful Load		4862		4854		4820		4795		4770		4732
Mission Weight		15,600		15,600		15,600		15,600		15,600		15,600

TABLE XIII. TASK II - WINGED HELICOPTERS SUMMARY WEIGHT STATEMENT, ROTOR SOLIDITY = 0.09

Design Gross Weight, Pounds		15,600		15,600		15,600		15,600		15,600		15,600
Engines (No. and Type)		2 ADV.		2 ADV.		2 ADV.		2 ADV.		2 ADV.		2 ADV.
SHP - Uninstalled		2760		2760		2760		2800		2800		2800
Main Rotor(s) Diameter, Feet		57.5		57.5		57.5		57.5		57.5		57.5
Solidity		0.09		0.09		0.09		0.09		0.09		0.09
Tip Speed, FPS		725		725		725		725		725		725
Wing Area, Ft^2		70		70		70		105		105		105
Wing Incidence, Deg.		6.5		9.5		12.5		6.5		9.5		12.5
Weights, Pounds												
Rotor Group		2277		2277		2277		2277		2277		2277
Wing Group		84		86		106		126		144		173
Tail Group		187		187		187		187		187		187
Body Group		1946		1946		1946		1946		1946		1946
Alighting Gear		468		468		468		468		468		468
Flight Controls		714		714		714		716		716		716
Fixed	418		418		418		419		419		419	
Rotating	296		296		296		297		297		297	
Eng. Section/Nacelles		176		176		176		176		176		176
Propulsion		2348		2348		2357		2372		2377		2384
Engine Install	569		569		569		575		575		575	
Induction System	63		63		63		64		64		64	
Exhaust	74		74		74		75		75		75	
Fuel System	359		359		368		363		368		375	
Controls	32		32		32		32		32		32	
Starting	39		39		39		39		39		39	
Rotor Brake	47		47		47		48		48		48	
Trans and Drive System	1165		1165		1165		1176		1176		1176	
Passive Defense		200		200		200		200		200		200
Instruments		73		73		73		73		73		73
Hydraulics		93		93		93		93		93		93
Electrical		281		281		281		281		281		281
Avionics (inc nav)		411		411		411		411		411		411
Furnishings and Equipment		658		658		658		658		658		658
Air Conditioning		121		121		121		121		121		121
APU		93		93		93		93		93		93
Armament		175		175		175		175		175		175
Weight Empty		10,305		10,301		10,336		10,373		10,396		10,432
Crew	600		600		600		600		600		600	
Payload (Pass or Cargo)	2983		2963		2900		2886		2843		2772	
Fluids	61		61		61		61		61		61	
Survival Equipment	-		-		-		-		-		-	
Passive Defense	-		-		-		-		-		-	
Armament	-		-		-		-		-		-	
Fuel	1651		1669		1703		1680		1700		1735	
Miscellaneous	-		-		-		-		-		-	
Useful Load		5295		5293		5264		5227		5204		5168
Mission Weight		15,600		15,600		15,600		15,600		15,600		15,600

TABLE XIV. TASK II - WINGED HELICOPTERS SUMMARY WEIGHT STATEMENT, ROTOR SOLIDITY = 0.13

Design Gross Weight, Pounds		15,600		15,600		15,600		15,600		15,600		15,600
Engines (No. and Type)		2 ADV.		2 ADV.		2 ADV.		2 ADV.		2 ADV.		2 ADV.
SHP - Uninstalled		3020		3020		3020		3055		3055		3055
Main Rotor(s) Diameter, Feet		57.5		57.5		57.5		57.5		57.5		57.5
Solidity		0.13		0.13		0.13		0.13		0.13		0.13
Tip Speed, FPS		725		725		725		725		725		725
Wing Area, Ft^2		70		70		70		105		105		105
Wing Incidence, Deg.		6.5		9.5		12.5		6.5		9.5		12.5
Weights, Pounds												
Rotor Group		2920		2920		2920		2920		2920		2920
Wing Group		84		86		105		126		141		172
Tail Group		187		187		187		187		187		187
Body Group		1946		1946		1946		1946		1946		1946
Alighting Gear		468		468		468		468		468		468
Flight Controls		718		718		718		720		720		720
Fixed	419		419		419		420		420		420	
Rotating	299		299		299		300		300		300	
Eng. Section/Nacelles		176		176		176		176		176		176
Propulsion		2551		2560		2562		2570		2577		2587
Engine Install	605		605		605		609		609		609	
Induction System	66		66		66		67		67		67	
Exhaust	80		80		80		81		81		81	
Fuel System	427		436		438		429		436		446	
Controls	32		32		32		32		32		32	
Starting	40		40		40		40		40		40	
Rotor Brake	50		50		50		50		50		50	
Trans and Drive System	1251		1251		1251		1262		1262		1262	
Passive Defense		200		200		200		200		200		200
Instruments		73		73		73		73		73		73
Hydraulics		93		93		93		93		93		93
Electrical		281		281		281		281		281		281
Avionics (inc nav)		411		411		411		411		411		411
Furnishings and Equipment		658		658		658		658		658		658
Air Conditioning		121		121		121		121		121		121
APU		93		93		93		93		93		93
Armament		175		175		175		175		175		175
Weight Empty		11,155		11,166		11,187		11,218		11,240		11,281
Crew	600		600		600		600		600		600	
Payload (Pass or Cargo)	1810		1756		1726		1740		1682		1598	
Fluids	61		61		61		61		61		61	
Survival Equipment	-		-		-		-		-		-	
Passive Defense	-		-		-		-		-		-	
Armament	-		-		-		-		-		-	
Fuel	1974		2017		2026		1981		2017		2060	
Miscellaneous	-		-		-		-		-		-	
Useful Load		4445		4434		4413		4382		4360		4319
Mission Weight		15,600		15,600		15,600		15,600		15,600		15,600

Mission Analysis

The mission fuel and payload were calculated for all configurations for the mission described in Task I. The mission results are based on a takeoff gross weight of 15,600 pounds and a cruise speed of 150 knots. The resulting fuel and payload data is given on Table XV for all of the Task II configurations.

TABLE XV. TASK II - PAYLOAD COMPARISON

σ	S_{w_2} (Ft^2)	i_w (Deg)	Fuel (Lb)	Payload (Lb)
0.11	70	6.5	1815	2386
		9.5	1842	2351
		12.5	1875	2284
	105	6.5	1837	2297
		9.5	1864	2245
		12.5	1899	2172
0.09	70	6.5	1651	2983
		9.5	1669	2963
		12.5	1703	2900
	105	6.5	1680	2886
		9.5	1700	2843
		12.5	1735	2772
0.13	70	6.5	1974	1810
		9.5	2017	1756
		12.5	2026	1726
	105	6.5	1981	1740
		9.5	2017	1682
		12.5	2060	1598

SCOPE OF MANEUVERS INVESTIGATED - TASK II

In the winged helicopter phase (Task II) of this study, the maneuvering flight capability of 18 configurations was investigated. As described in Table IX, the configurations were composed of three rotor solidities (0.09, 0.11, and 0.13) at constant tip speed (725 fps) and two wing areas (70 and 105 square feet) at three incidences (6.5, 9.5, and 12.5 degrees).

As in Task I, the Rotorcraft Flight Simulation Analysis (computer program C81) was used to simulate maneuvering flight of the winged configurations. Excellent correlation existed between the hybrid and digital versions of C81 for the winged configurations. Figure 34 compares the hybrid and digital time histories of a 2.0-degree cyclic pullup maneuver at 167 KTAS for a typical winged configuration (baseline rotor-- $\sigma = 0.11$, $\Omega R = 725$ fps; large wing at high incidence--105 square feet, 12.5 degrees). For the same configuration, Figure 35 compares the hybrid and digital time histories of a 1.75-degree cyclic pushover maneuver at 167 KTAS. These two figures clearly show that the correlation between the hybrid and digital versions of C81 with winged configurations is equivalent to that which was shown for the wingless configurations.

The maneuvers used to establish the capability of the winged configurations were the same as those used in Task I, described in Table VI, except that airspeeds below 150 KTAS were not considered. The potential increase in load factor offered by the wing, even when at maximum lift ($C_{L_{max}} = 1.0$), was insufficient to justify the expense and time required to investigate the winged configurations at low airspeeds. To illustrate this point, Figure 36 presents the maximum potential increases in load factor for the large and small wings when operating at $C_{L_{max}}$. At 120 KTAS, the potential increase was only 0.25g with the large wing and 0.17g with the small wing. At 80 KTAS, the potential increases were reduced to 0.15g and 0.10g. Another point considered when omitting the low airspeeds was that in this study all the configurations are ultimately evaluated at their normal rated power airspeeds (V_{NRP}), which in all cases are significantly above 150 KTAS. Consequently, even if data were available at the low airspeeds, it would not influence the conclusions which result from comparing the maneuver capability at V_{NRP}.

The criteria used to limit the maneuvers in Task II were the same as those used in Task I, given on Table VII. The procedures used to establish the g-capability in each type of maneuver were also the same as those used in Task I. That is, for each maneuver, the maximum load factor was found which could be sustained for at least 1 second without exceeding any of the limiting criteria.

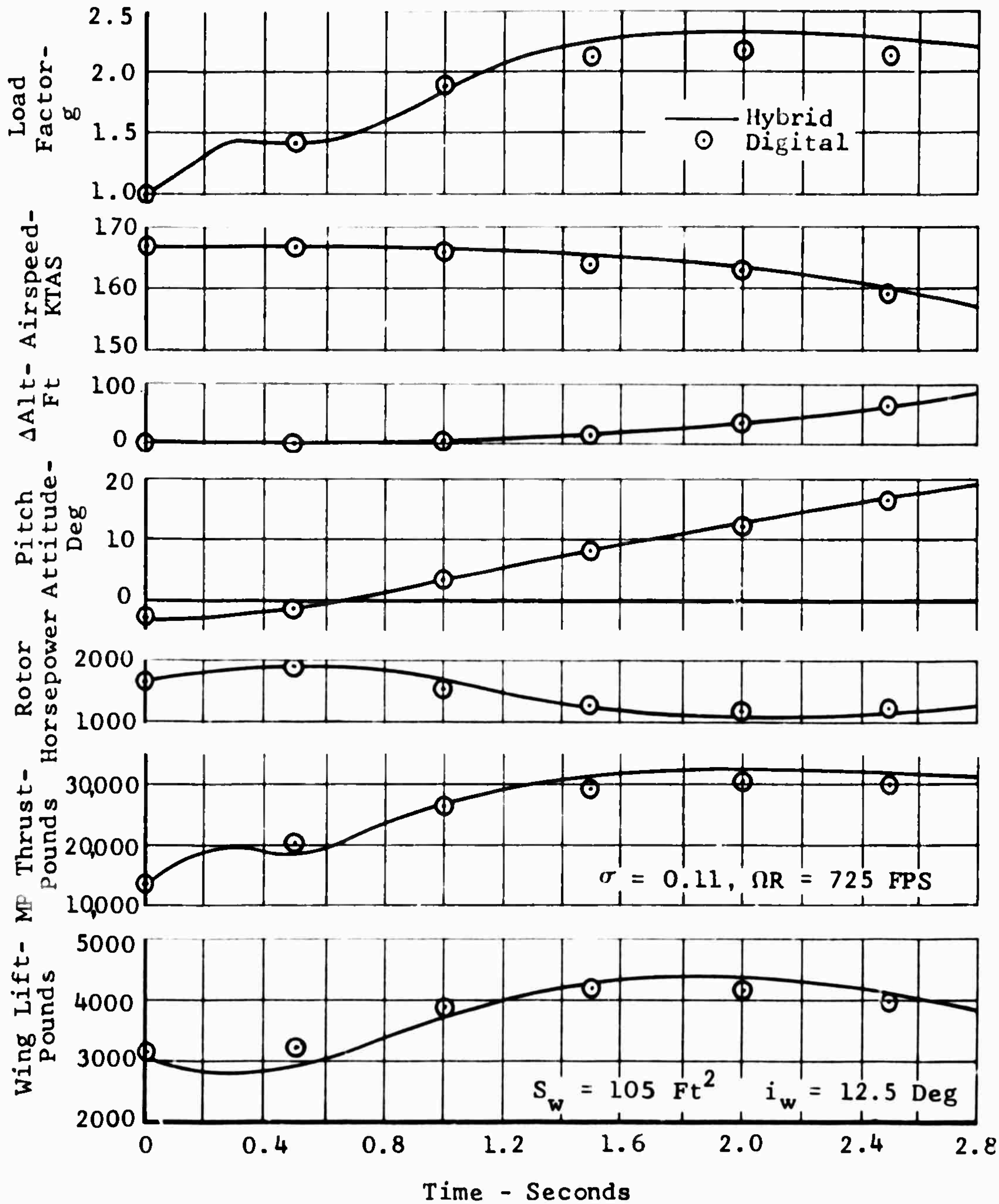

Figure 34. Comparison of Hybrid and Digital Maneuver, Baseline Rotor-Winged Configuration, 2.0-Degree Cyclic Pullup at 167 KTAS.

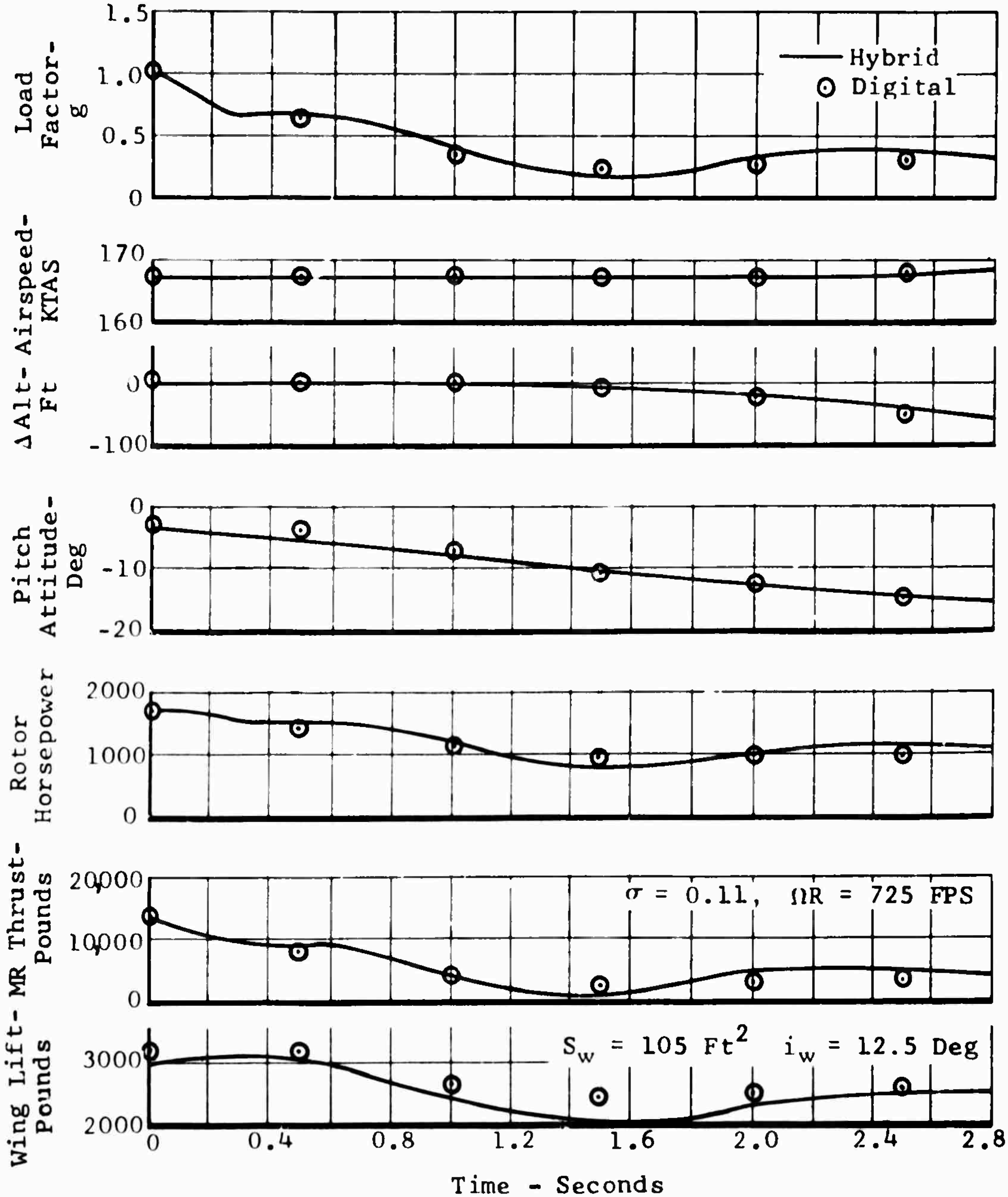

Figure 35. Comparison of Hybrid and Digital Maneuver, Baseline Rotor - Winged Configuration, 1.75-Degree Cyclic Pushover at 167 KTAS.

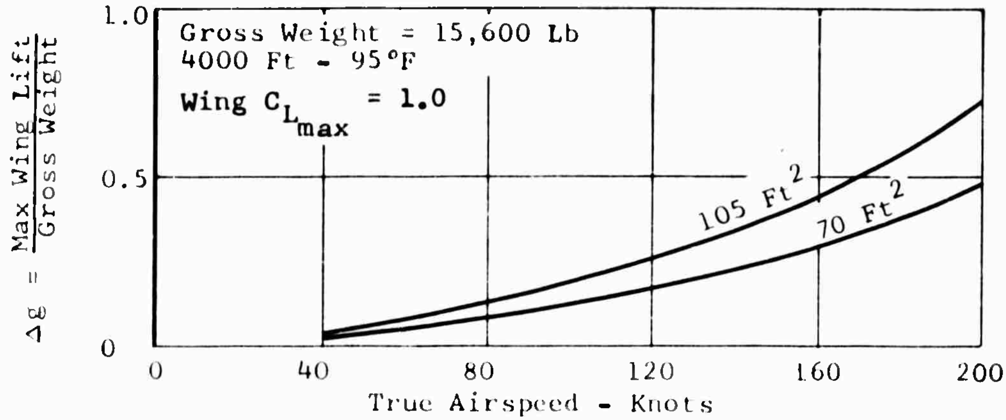

Figure 36. Potential Increase in Load Factor, Wing at Maximum Lift.

MANEUVER RESULTS - TASK II

Figures 37 through 42 summarize the results of the pullup and pushover maneuvers for all 18 winged configurations. The maneuvers which gave the maximum load factors in pullups and the minimum load factors in pushovers are compared to the results for the equivalent wingless configuration (same solidity and tip speed). A complete data listing of the Task II maneuvers is given in Appendix IV, including not only the load factors attained but also the control inputs required and the limiting criteria.

As was the case for Task I, the turning flight capability for the winged configurations was substantially the same as the pullup capability. Again, the key aspects of the coordinated turns were the airspeed and altitude bleed-off requirements which are essentially a function of the load factor, not the configuration, and will be discussed more fully in the Task III section.

Effects of Wings on Pullup Capability

Inspection of Figures 37 through 42 clearly shows that the wings increased the pullup load factor capability at all airspeeds considered. Furthermore, for a given rotor solidity and wing area, the g-capability was progressively increased as wing incidence was increased. To illustrate how the wings improved the pullup capability three time histories of cyclic pullup maneuvers at 167 KTAS are given in Figures 43 through 45 for these configurations:

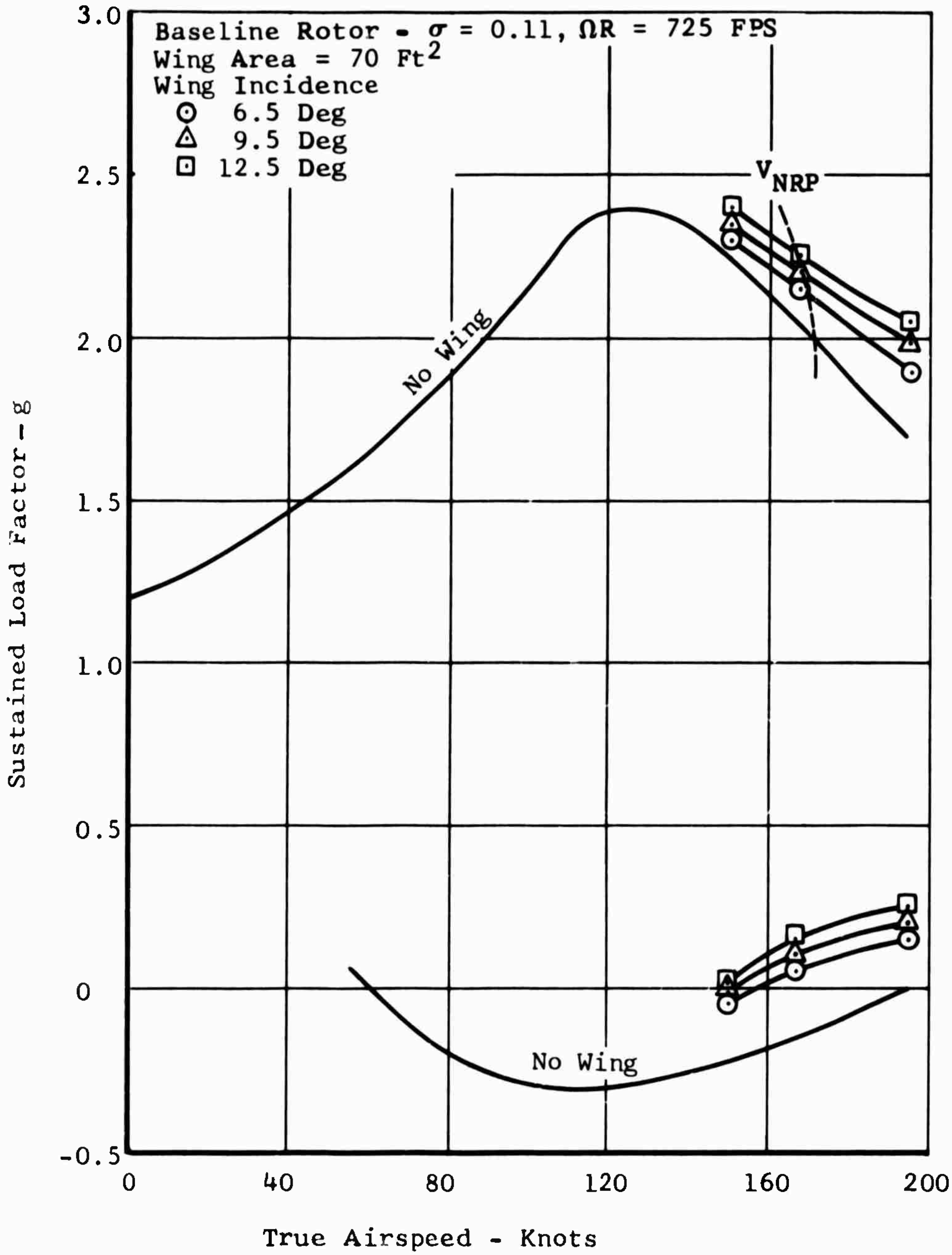

Figure 37. Task II - Maneuver Results, Baseline Rotor, Small Wing.

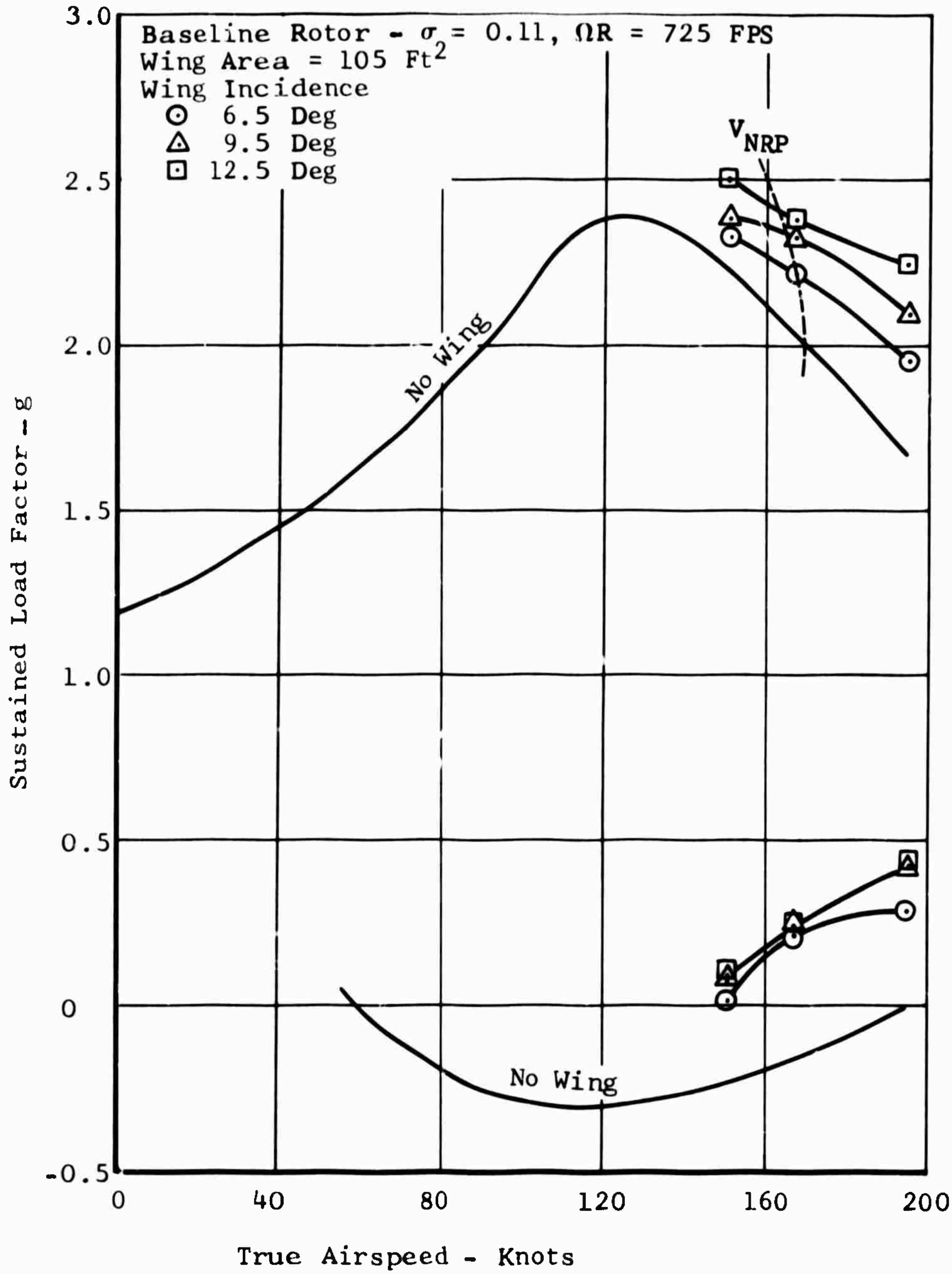

Figure 38. Task II - Maneuver Results, Baseline Rotor, Large Wing.

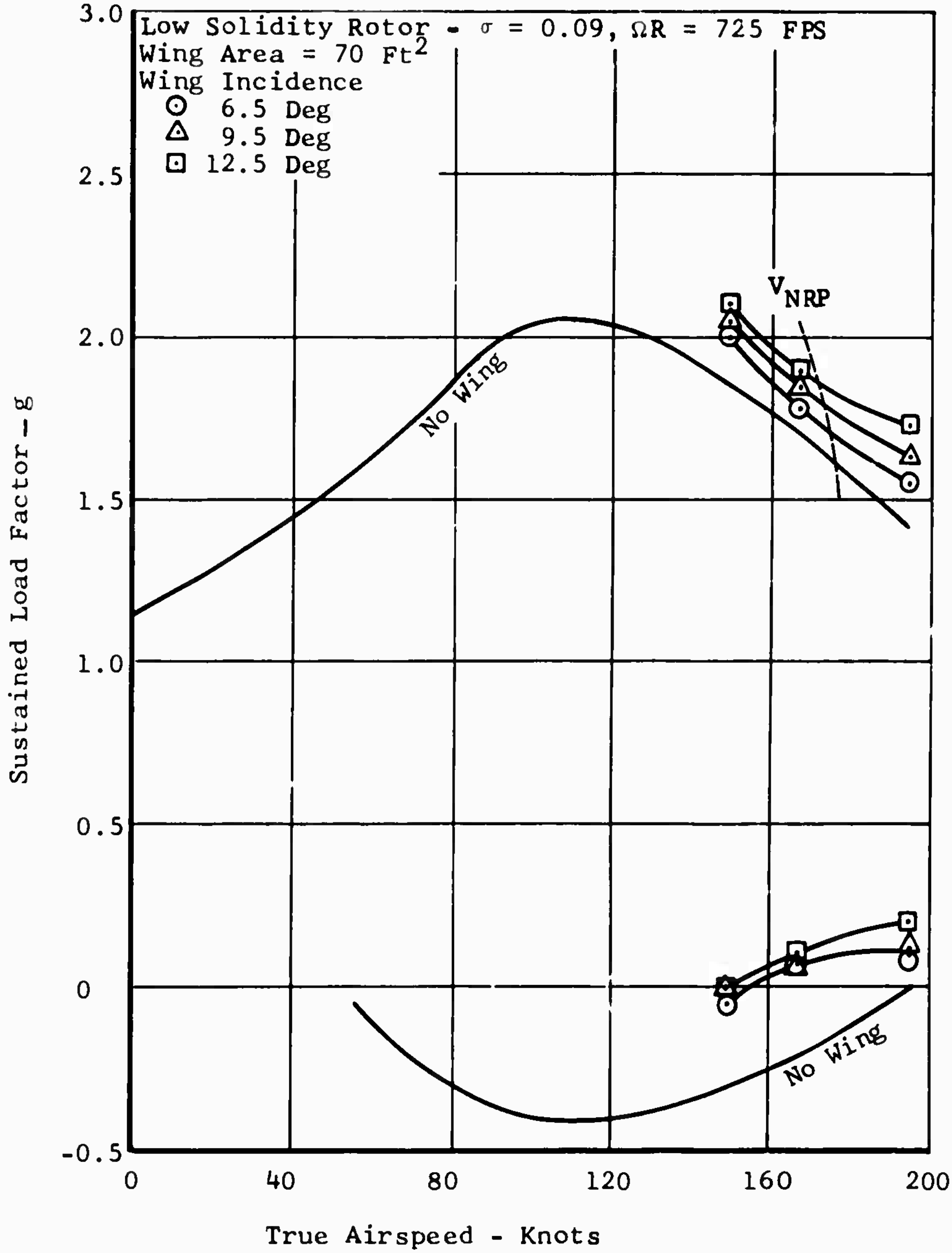

Figure 39. Task II - Maneuver Results,
Low Solidity Rotor, Small Wing.

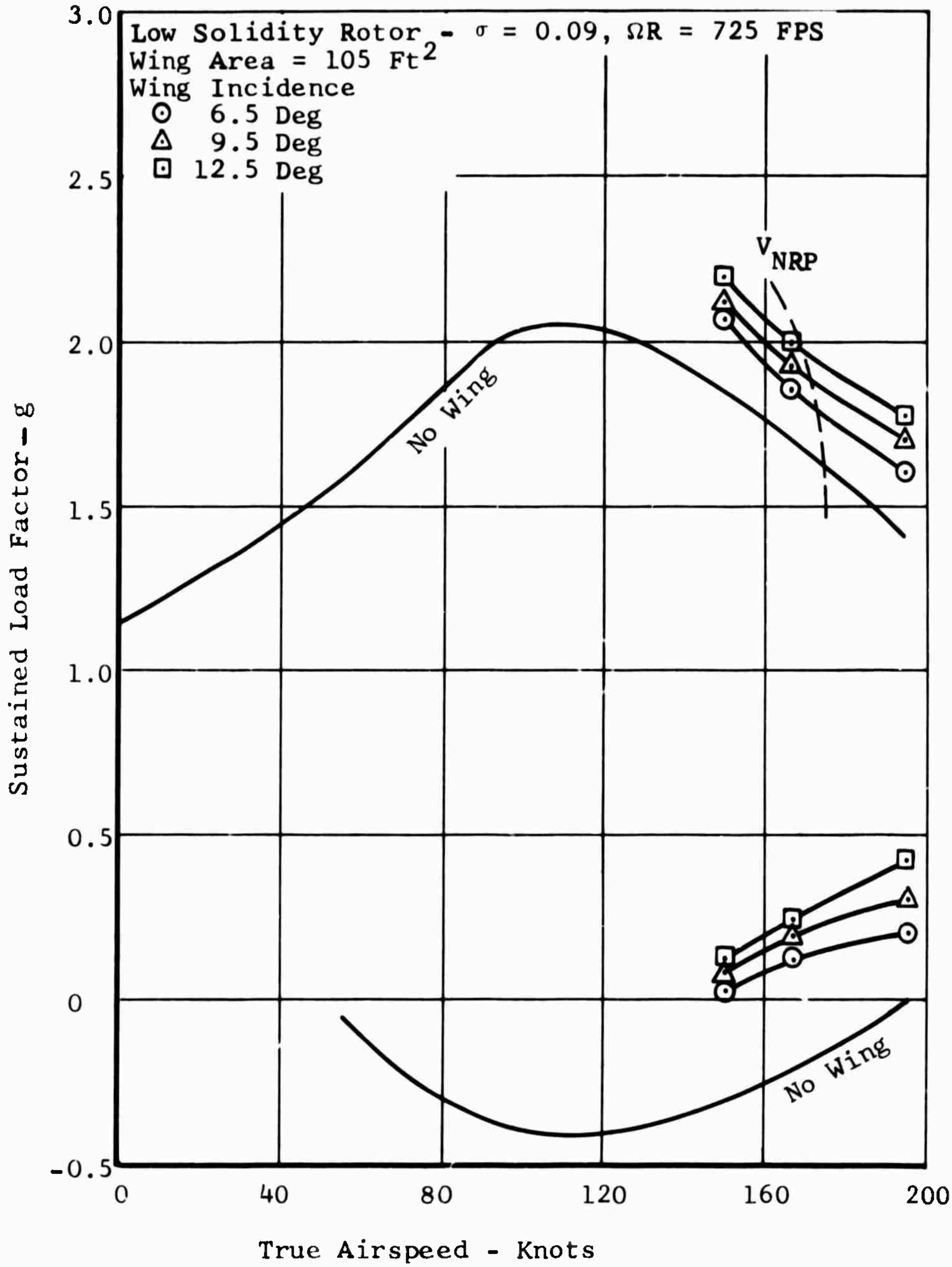

Figure 40. Task II - Maneuver Results,
Low Solidity Rotor, Large Wing.

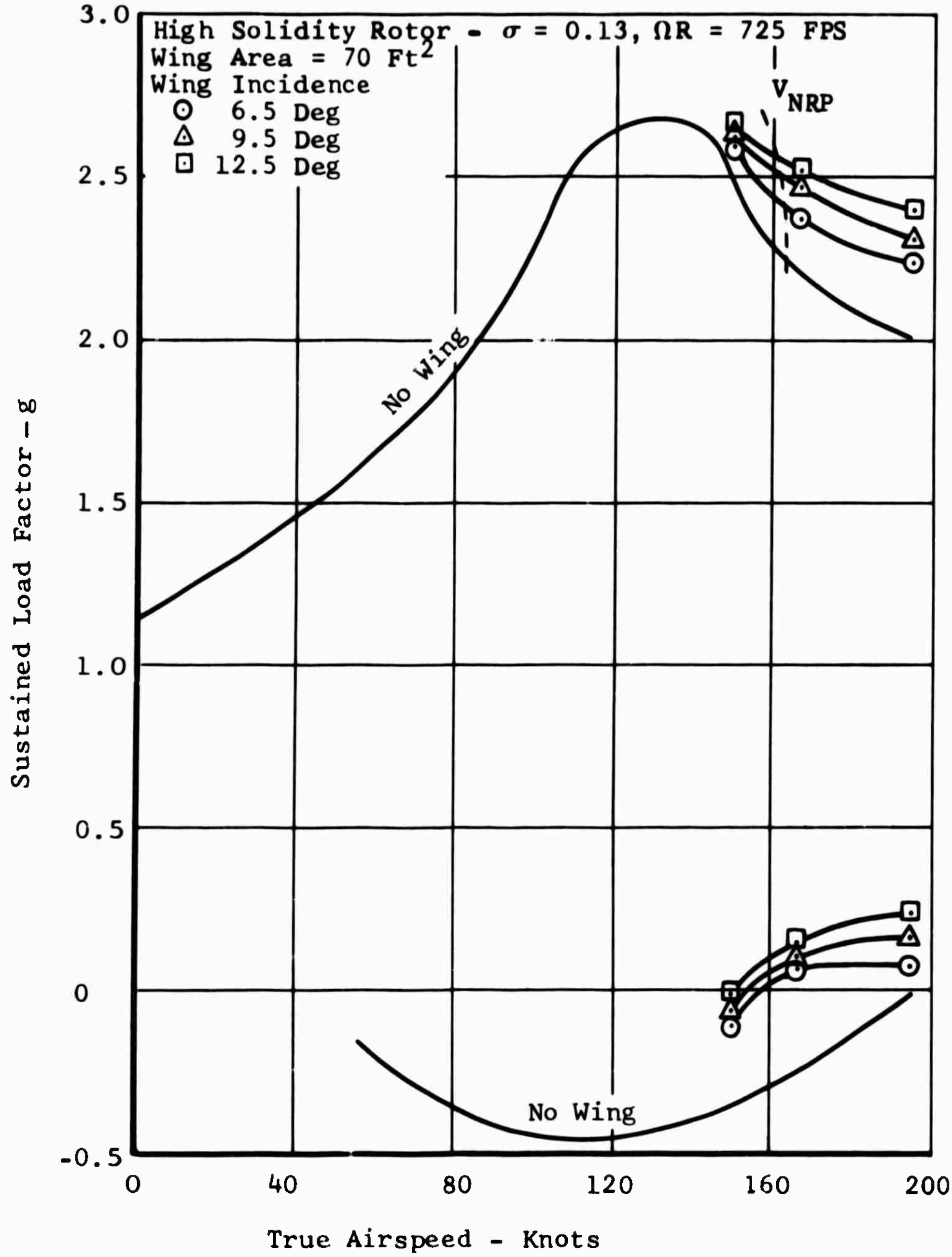

Figure 41. Task II - Maneuver Results, High Solidity Rotor, Small Wing.

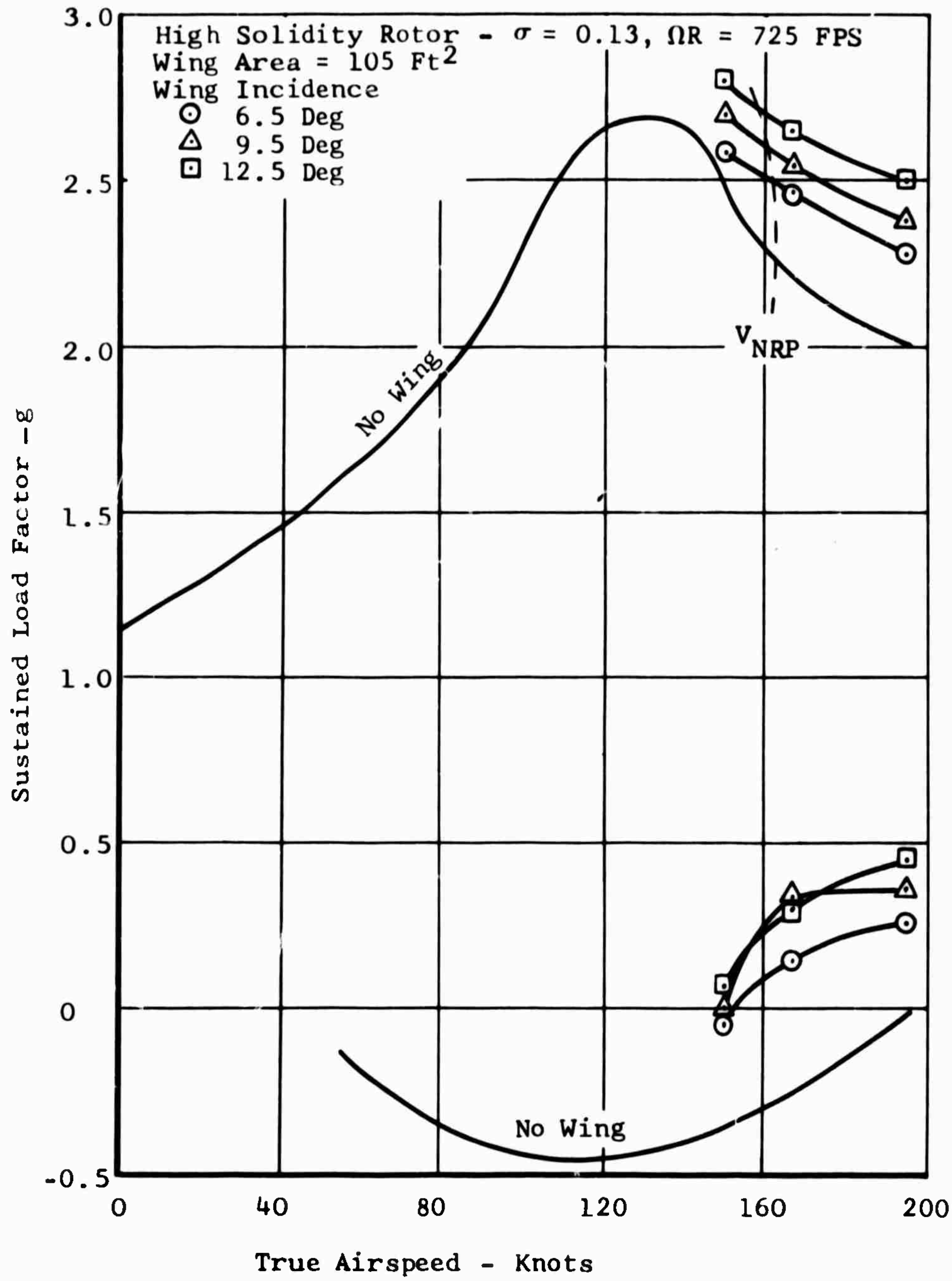

Figure 42. Task II - Maneuver Results, High Solidity Rotor, Large Wing.

Figure 43	Baseline Rotor $\sigma = 0.11$ $\Omega R = 725$ fps	No Wing	
Figure 44	Baseline Rotor $\sigma = 0.11$ $\Omega R = 725$ fps	Small Wing 70 Ft^2	Low Incidence 6.5 Deg
Figure 45	Baseline Rotor $\sigma = 0.11$ $\Omega R = 725$ fps	Large Wing 105 Ft^2	High Incidence 12.5 Deg

The three maneuvers shown were all limited by the rotor flapping criterion, and because all had the same rotor, differences in the load factors achieved should relate directly to the wing differences.

Considering first the wingless configuration, Figure 43, the peak load factor attained in the maneuver was 2.10 g's, the sustained load factor being 2.05 g's. At the time of peak g's, the rotor thrust was 32,500 pounds. For the small wing configuration, Figure 44, a peak load factor of 2.20 g's was achieved, the sustained capability being 2.15 g's. Both of these load factors represent 0.10g increases over the wingless configuration. At the peak load factor, the rotor thrust was again 32,500 pounds. Therefore, the increase in load factor correlates well with the wing lift at peak g's, 1800 pounds, which converts to 0.11 g. Similar comparisons exist for the large wing configuration, Figure 45. The rotor thrust at the peak load factor was again 32,500 pounds, the peak load factor being 2.40 g's, an increase of 0.30 g. This increase correlates well with the peak wing lift at peak g's--4350 pounds, 0.28g.

Effects of Wings on Pushover Capability

Although the addition of wings improved the pullup load factor capability, the pushover capability was significantly penalized. Whereas all the wingless configurations had zero-g capability at airspeeds up to 195 KTAS, none of the winged configurations achieved zero-g's beyond 160 KTAS. Furthermore, those winged configurations which produced the most improvement in pullup maneuvers produced the highest penalties in pushover capability.

The pushover g-penalties arise from the fact that the wing does not unload significantly in a pushover maneuver. The wing lift remains substantial because as the aircraft begins to lose altitude, the rate of descent maintains a significant angle of attack on the wing. This is illustrated by Figures 46 and 47 which give cyclic pushover maneuvers at 167 KTAS,

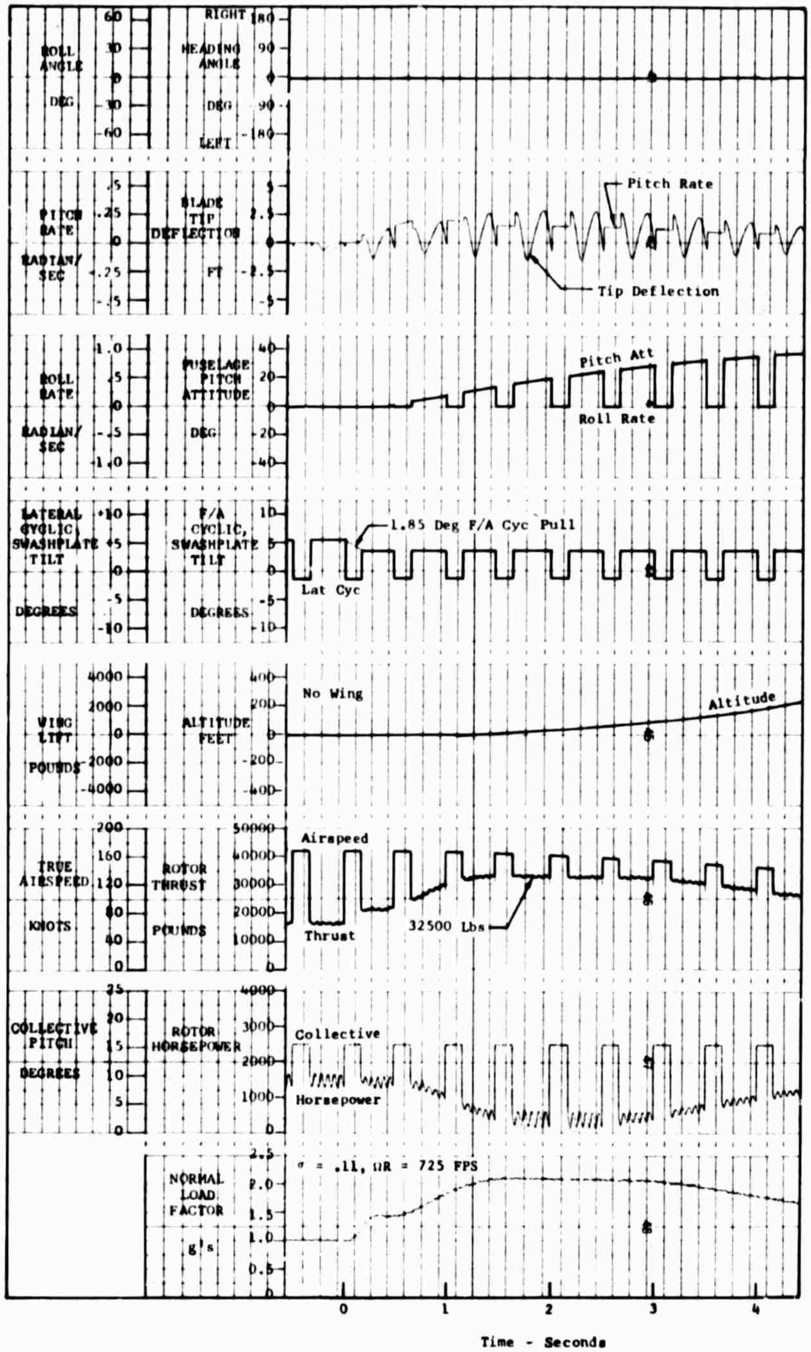

Figure 43. Maneuver Time History, F/A Cyclic Pullup, Baseline Rotor, No Wing, Maneuver Limited by Flapping.

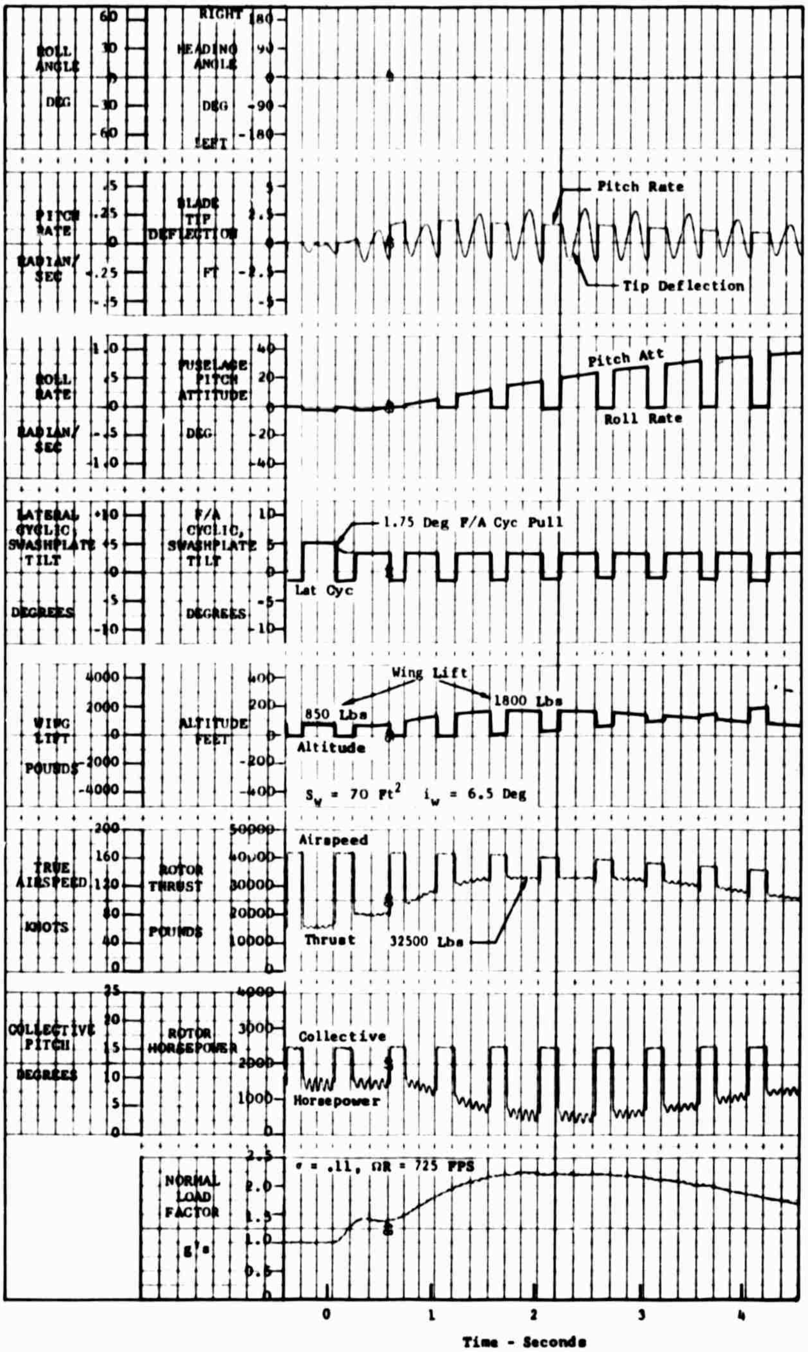

Figure 44. Maneuver Time History, F/A Cyclic Pullup, Baseline Rotor, Small Wing, Maneuver Limited by Flapping.

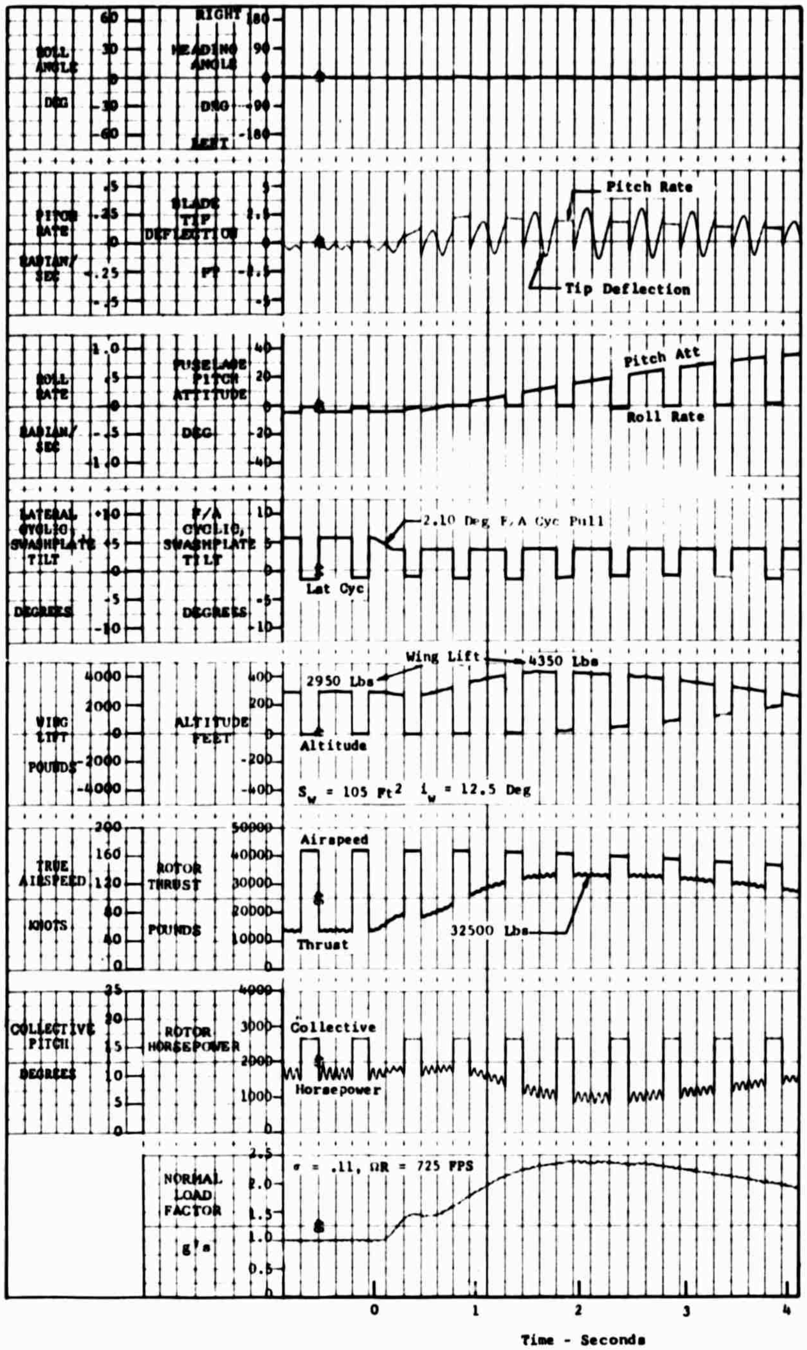

Figure 45. Maneuver Time History, F/A Cyclic Pullup, Baseline Rotor, Large Wing, Maneuver Limited by Flapping.

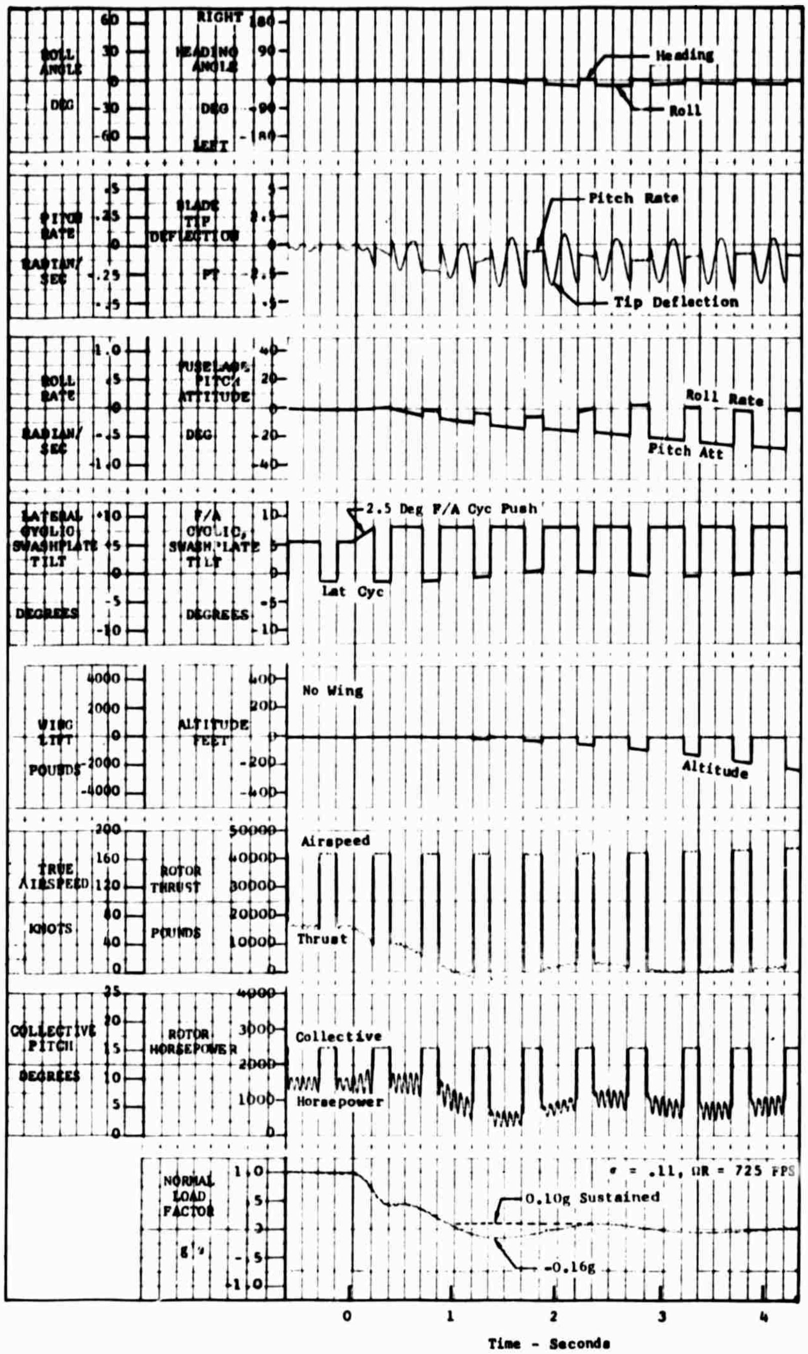

Figure 46. Maneuver Time History, F/A Cyclic Pushover, Baseline Rotor, No Wing, Maneuver Limited by Flapping.

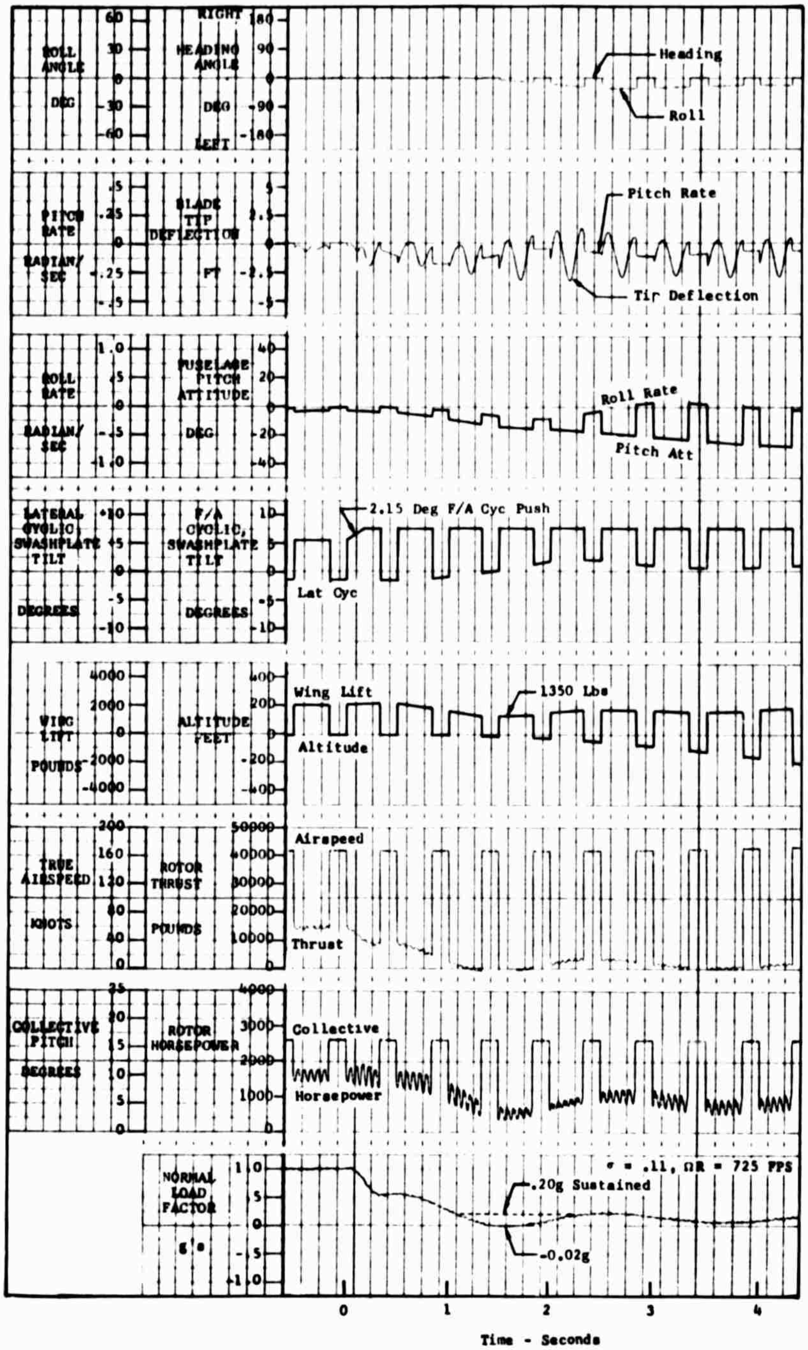

Figure 47. Maneuver Time History, F/A Cyclic Pushover, Baseline Rotor, Small Wing, Maneuver Limited by Flapping.

with and without a wing. The wingless configuration, Figure 46, achieved a minimum load factor of -0.16g, and 0.10g was sustained. For the winged case, Figure 47, the minimum and sustained load factors were -0.02 and 0.20g, respectively. The minimum wing lift was 1350 pounds, which converts to 0.09g and relates directly to the 0.10g net pushover penalty.

Wing Lift Characteristics in Trimmed and Maneuvering Flight

To establish the relationships between the wing lift in trimmed flight and the wing lift in maneuvering flight, the wing lift data was expressed in terms of wing lift coefficient, C_L. Table XVI gives a listing of the wing lift coefficients in trimmed and maneuvering flight for all 18 winged configurations. The maneuvering flight C_L's were based on the wing lift at peak g's, using the cyclic-only pullups at 167 and 195 KTAS, and the collective plus cyclic pullups at 150 KTAS.

Figure 48 summarizes the trimmed flight C_L's for all the winged configurations in combination with the baseline rotor. As would be expected, as wing incidence increased, the trimmed flight C_L increased. For the same wing incidence and at the same airspeed, the small wing had slightly higher C_L's than the large wing. However, the percentage increase in C_L was less than the percentage increase in wing area. Therefore, the large wing carried more lift in terms of pounds. As airspeed increased, the wing lift coefficient decreased because the aircraft was trimming at progressively lower angles of attack. However, above maximum airspeed for level flight, V_H, the trend reverses and C_L increased with airspeed. This results from the fact that above V_H, trimmed flight is maintained in a dive condition which increases the wing angle of attack.

To relate the trimmed flight wing lift coefficients to those in maneuvering flight, Figure 49 was constructed by plotting the wing lift coefficient in trim, C_{L_t}, versus the peak maneuvering wing lift coefficient, C_{L_m}, at 167 KTAS (data from Table XVI). Because C_L is nondimensional, thereby including effects of wing area and incidence, only the differences in rotor solidity were identified. Two important conclusions are drawn from Figure 49. First, the relationship between trimmed flight and maneuvering flight wing lift coefficients is independent of rotor solidity. That is, for any rotor solidity, when the trimmed flight C_L is defined by the wing area and incidence, the maneuvering flight C_L is also defined, and the increase in load factor which results from adding the wing can be predicted with reasonable accuracy.

TABLE XVI. WING LIFT COEFFICIENT IN TRIMMED FLIGHT AND IN PULLUP MANEUVER

Rotor Solidity	Airspeed (KTAS)	Wing Area (Ft^2)	Wing Incidence (Deg)	Wing C_L Trim	Wing C_L @ Peak g's in Maneuver*
0.09	150	70	6.5	0.22	0.32
			9.5	0.33	0.46
			12.5	0.45	0.56
		105	6.5	0.21	0.35
			9.5	0.32	0.43
			12.5	0.42	0.54
	167	70	6.5	0.18	0.32
			9.5	0.31	0.45
			12.5	0.42	0.56
		105	6.5	0.17	0.32
			9.5	0.28	0.44
			12.5	0.38	0.57
	195	70	6.5	0.19	0.27
			9.5	0.32	0.41
			12.5	0.45	0.55
		105	6.5	0.18	0.26
			9.5	0.30	0.39
			12.5	0.41	0.51
0.11	150	70	6.5	0.19	0.33
			9.5	0.32	0.42
			12.5	0.44	0.56
		105	6.5	0.19	0.29
			9.5	0.30	0.40
			12.5	0.41	0.53

* Collective + Cyclic Pullups @ 150 KTAS,
Cyclic-Only Pullups @ 167 and 195 KTAS

TABLE XVI. CONTINUED

Rotor Solidity	Airspeed (KTAS)	Wing Area (Ft^2)	Wing Incidence (Deg)	Wing C_L Trim	Wing C_L @ Peak g's in Maneuver
0.11	167	70	6.5	0.16	0.34
			9.5	0.29	0.45
			12.5	0.40	0.56
		105	6.5	0.15	0.31
			9.5	0.26	0.43
			12.5	0.36	0.55
	195	70	6.5	0.21	0.29
			9.5	0.33	0.41
			12.5	0.46	0.55
		105	6.5	0.19	0.28
			9.5	0.32	0.41
			12.5	0.43	0.53
0.13	150	70	6.5	0.19	0.28
			9.5	0.31	0.39
			12.5	0.43	0.50
		105	6.5	0.17	0.28
			9.5	0.29	0.38
			12.5	0.40	0.49
	167	70	6.5	0.16	0.33
			9.5	0.28	0.45
			12.5	0.38	0.56
		105	6.5	0.14	0.32
			9.5	0.25	0.44
			12.5	0.35	0.55
	195	70	6.5	0.22	0.33
			9.5	0.34	0.47
			12.5	0.47	0.60
		105	6.5	0.21	0.33
			9.5	0.32	0.46
			12.5	0.43	0.53

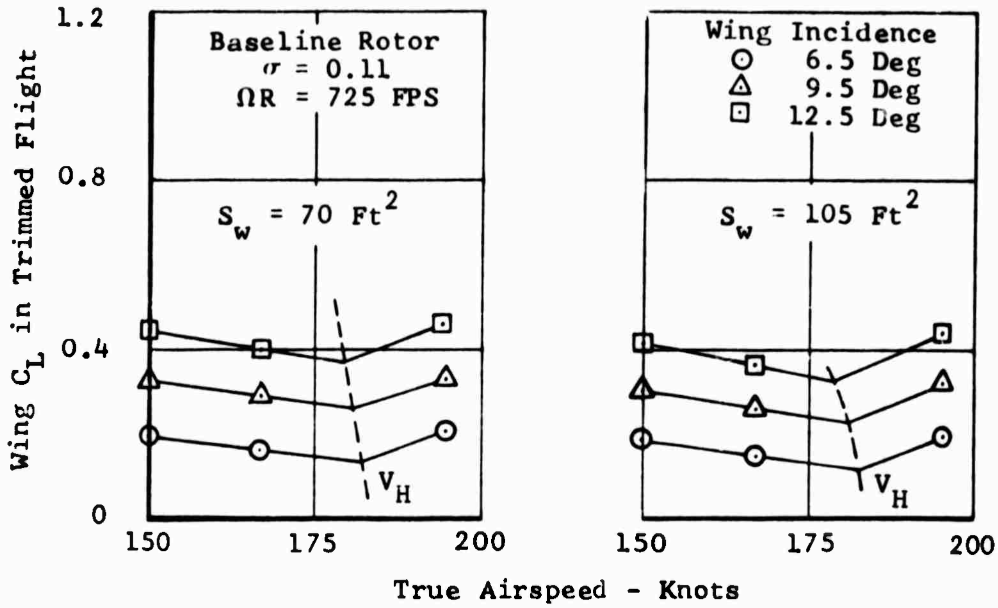

Figure 48. Wing Lift Coefficient in Trimmed Flight, Baseline Rotor, Six Wing Configurations.

The second important aspect of Figure 49 is that the increase in wing C_L from trimmed flight to maneuvering flight was the same for all values of C_{L_t}. For the airspeed shown, 167 KTAS, the increase in C_L was equal to 0.16. In effect, this means that the wing angle of attack change from trimmed to maneuvering flight was the same for all winged configurations. Consequently, it is the difference between C_{L_m} and C_{L_t} that is important, not the ratio of C_{L_m} to C_{L_t}.

The conclusions drawn from Figure 49 are similarly true at the other airspeeds considered. At 150 KTAS, the increase in C_L from trimmed to maneuvering flight was 0.12, and at 195 KTAS, 0.10. The trend with airspeed was not consistent because collective plus cyclic pullup data was used at 150 KTAS, and cyclic-only pullup data was used at 167 KTAS and 195 KTAS.

The effect of the control system on wing loading in maneuvering flight should not be ignored. If a more complicated control system were used which allowed pitching the fuselage significantly faster than the rotor, the wing loading in pullup maneuvers could be increased above the loadings discussed herein.

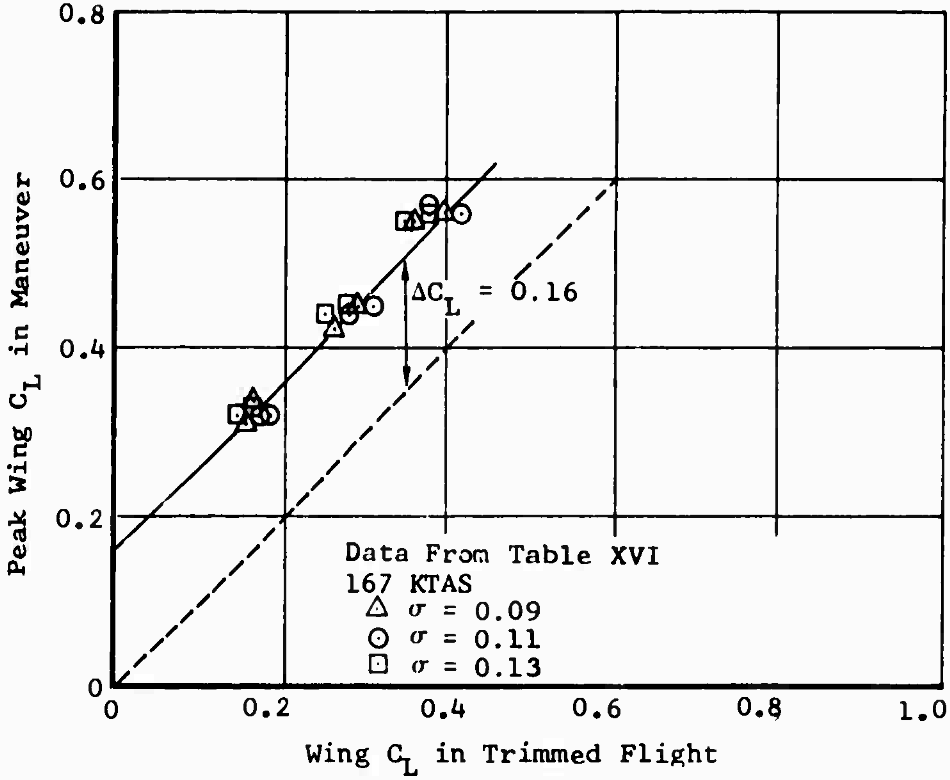

Figure 49. Relationship of Wing C_L in Trimmed Flight to Peak Wing C_L in Pullup Maneuver.

Configuration g-capability

The definition of g-capability for the winged configurations was the same as that used for the wingless configurations--the maximum load factor which was achieved and sustained at the normal rated power airspeed, V_{NRP}, of the configuration. Referring to Table XI for V_{NRP} and Figures 37 through 42 for the maneuver results, the maneuver capability of the 18 winged configurations was determined as given in Table XVII.

The data of Table XVII can be used to pinpoint the effects of wing incidence and wing area on configuration g-capability. Figure 50 isolates the effects of wing incidence by plotting g-capability at V_{NRP} versus wing incidence for the three rotor configurations and two wing areas. The effects of wing incidence are well defined, g-capability increasing linearly with incidence for all the solidities and areas considered. The range of incidences considered was not sufficient to define the optimum incidence.

TABLE XVII. MANEUVER CAPABILITY - WINGED CONFIGURATIONS

Rotor Solidity	Wing Area (Ft^2)	Wing Incidence (Deg)	V_{NRP} (KTAS)	Load Factor @ V_{NRP} (g)
0.09	70	6.5	173	1.73
		9.5	173	1.80
		12.5	171	1.87
	105	6.5	173	1.78
		9.5	172	1.88
		12.5	170	1.97
0.11	70	6.5	168	2.14
		9.5	167	2.20
		12.5	164	2.28
	105	6.5	168	2.22
		9.5	166	2.33
		12.5	163	2.41
0.13	70	6.5	163	2.41
		9.5	162	2.50
		12.5	160	2.57
	105	6.5	163	2.50
		9.5	160	2.60
		12.5	158	2.71

The effects of wing area on g-capability are given on Figure 51. The wing area is given in terms of exposed area rather than total area to reflect the fact that 45 square feet of total area is fuselage carry-through area and would actually represent a wingless configuration. For all solidities and wing incidences, the g-capability increases with exposed wing area up to the maximum area considered, 60 square feet (105 square feet total area).

The effects of rotor solidity and wing area on load factor capability at V_{NRP} are presented in carpet-plot form on Figure 52. Only the 12.5-degree incidence wings are presented because the lower incidence configurations had less maneuver capability, and only slightly better performance characteristics in terms of normal rated power airspeed and payload capability. As previously discussed, as either rotor solidity or wing area increased, the g-capability also increased. The maximum maneuver capability was 2.71 g's, achieved with the high solidity-large wing configuration ($\sigma = 0.13$, 60 square

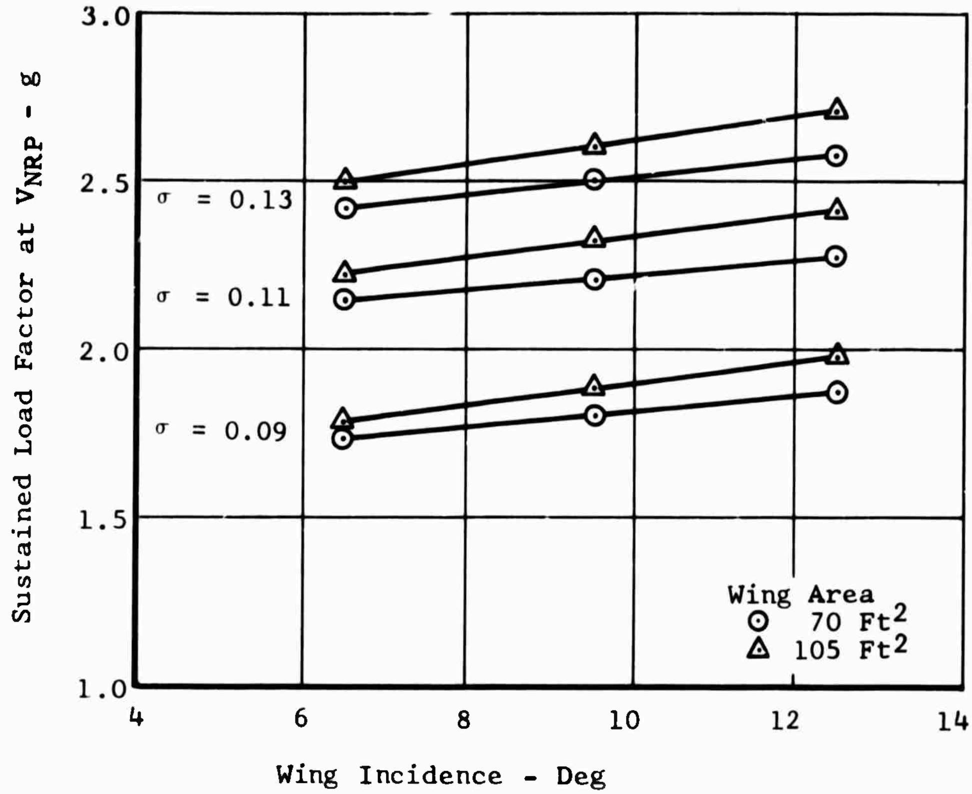

Figure 50. Effects of Wing Incidence on Load Factor Capability at V_{NRP}.

feet exposed area). The lowest capability configuration was the wingless-low solidity configuration (σ = 0.09), achieving only 1.63 g's at V_{NRP}. As in Task I, the range of capabilities was exaggerated by the fact that V_{NRP} is decreasing as rotor solidity and wing area are increasing.

The important aspect of Figure 52 is that there are many combinations of rotor solidity and wing area which together define a given level of maneuverability. For example, a 2.00g configuration could consist of a wingless configuration, the rotor solidity being 0.109, or at the other extreme, a configuration with an exposed wing area of 60 square feet and a rotor solidity of 0.091. Therefore, Figure 52 defines a locus of configurations which satisfy the load factor capabilities of interest in this study--2.00 and 1.75. A design requirement of 1.5 g's is not defined by Figure 52 because all of the configurations which were investigated had better than 1.5g

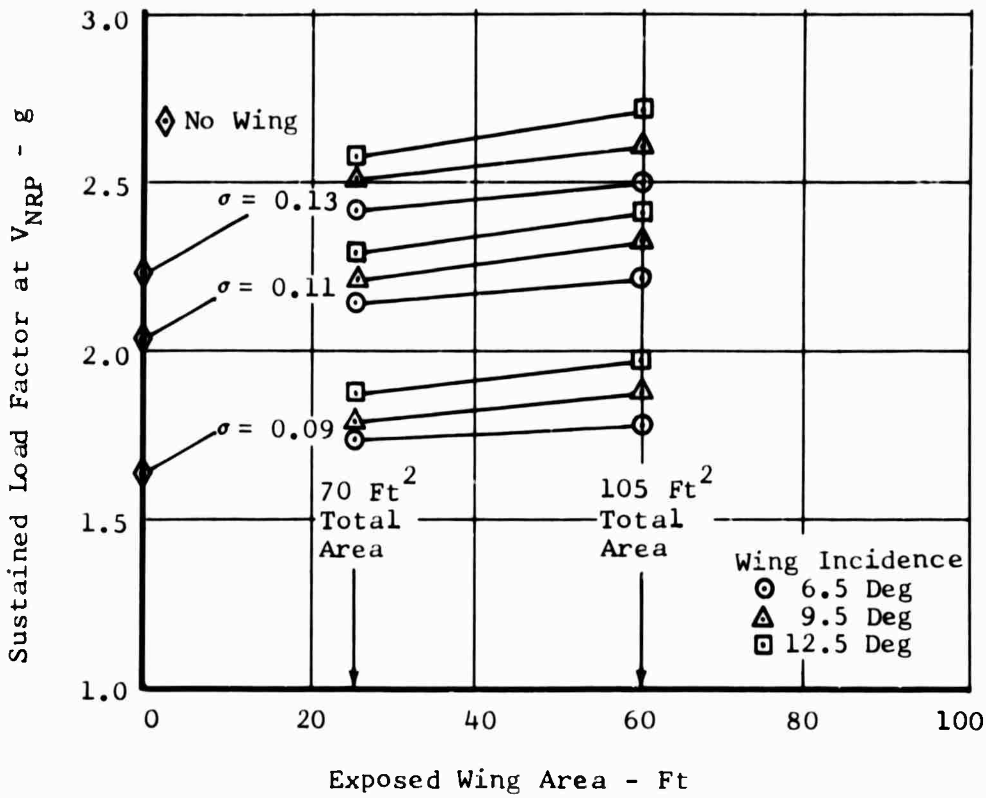

Figure 51. Effects of Wing Area on Load Factor Capability at V_{NRP}.

capability at V_{NRP}. If a design requirement of 1.5 g's were necessary, and if a wing were desirable, the configuration would consist of rotor solidities less than 0.09, or tip speeds less than 725 feet per second.

RELATIONSHIP OF MANEUVER CAPABILITY TO PERFORMANCE - TASK II

With the maneuver capability of the winged configurations defined in the previous discussion, attention is now turned to relating maneuver capability to the performance capability of the winged configurations. Also, the performance of the winged configurations is compared to that of the wingless configurations which have equal maneuver capability.

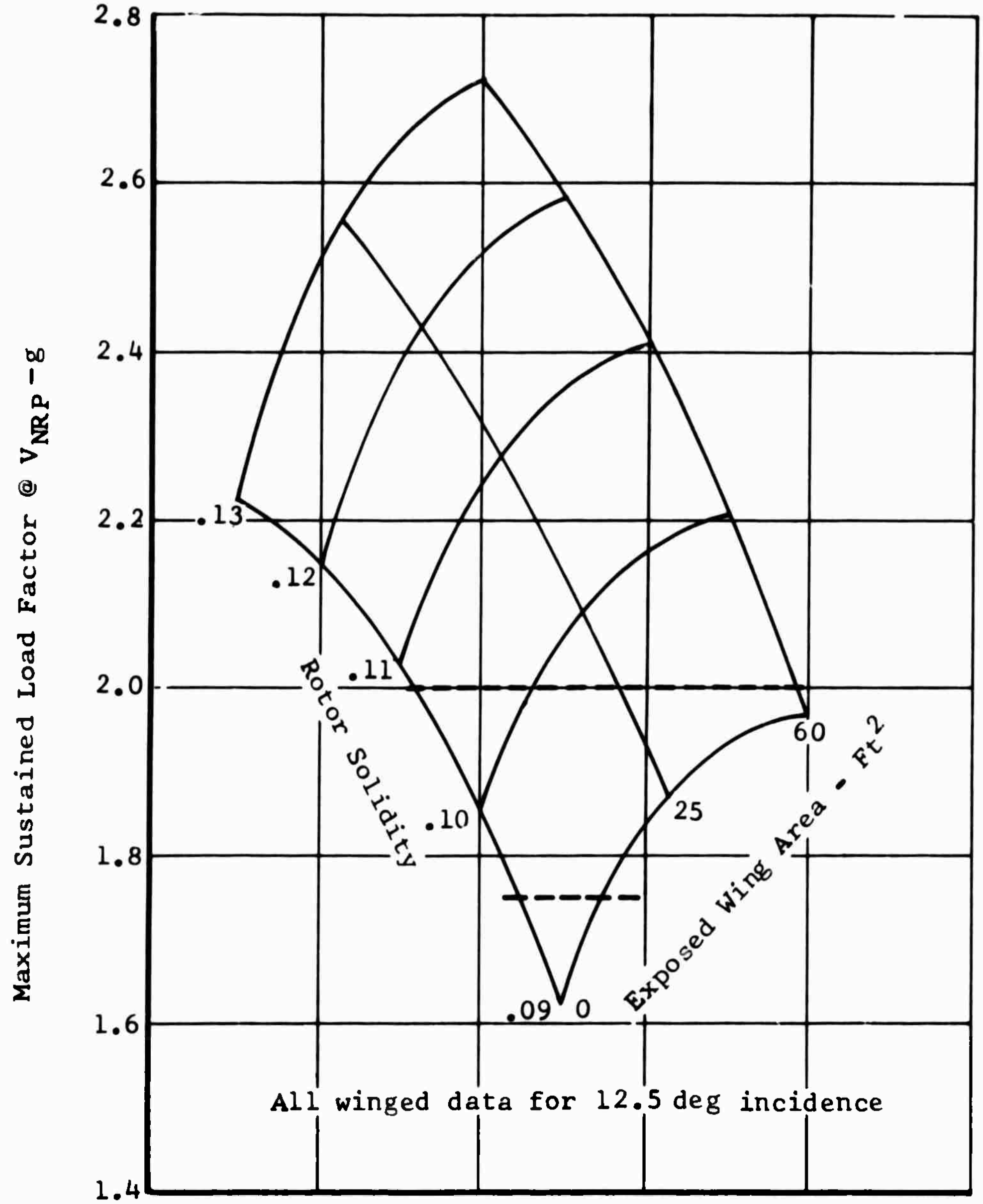

Figure 52. Effects of Rotor Solidity and Wing Area on g-Capability at V_{NRP}.

Relationship of g-Capability to V_{NRP}

The effects of rotor solidity and wing area on normal rated power airspeed are presented on Figure 53. As solidity and wing area were increased, the airspeed capability was reduced. However, as previously discussed, all the configurations exceeded the 150-KTAS cruise requirement. Also given on Figure 53 are the locus of configurations which satisfy 1.75g and 2.00g maneuverability levels.

With respect to the relationship of g-capability to V_{NRP}, there are two conclusions to be drawn from Figure 53. First, for a given level of maneuverability, V_{NRP} was the same for all configurations--winged or wingless--which satisfy the given g-level requirement. That is to say, within the framework of configurations investigated in Task II, all those configurations which were 2.00g configurations had the same V_{NRP} capability, and the same was true for other design g-levels. Therefore, when the g-capability is defined, the airspeed capability is also defined by the ground rules used in this study.

The second conclusion to be drawn from Figure 53 is that a requirement for high levels of maneuver ability penalizes the airspeed capability. If the design g-level was increased from 1.75 to 2.00 g's, V_{NRP} was reduced from 174 to 169 KTAS.

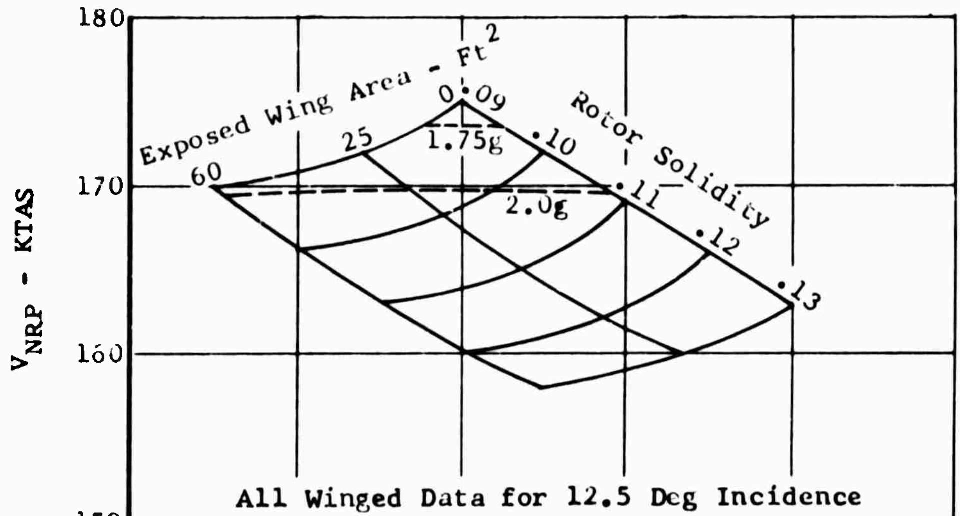

Figure 53. Effects of Rotor Solidity and Wing Area on V_{NRP} and Design g-Capability.

Relationship of g-Capability to Payload

From Table XV, payload as a function of rotor solidity and wing area is given on Figure 54 along with the locus of configurations which satisfy 1.75g and 2.00g levels of maneuverability. As solidity, wing area, or design g-level increased, the payload capability was decreased, emphasizing again that the design requirements for high levels of maneuverability are not compatible with the requirements for good performance.

The important aspect of Figure 54 is that all configurations which had equal maneuvering capability also had essentially the same payload capability. This is important because it means that the payload tradeoff between wingless and winged configurations is even. Consequently, when choosing between a winged or wingless configuration, payload requirements will not influence the decision. Considerations other than performance will dictate the choice, as will be discussed in Task III where particular configurations which satisfy 1.50g, 1.75g, and 2.00g maneuver levels are described.

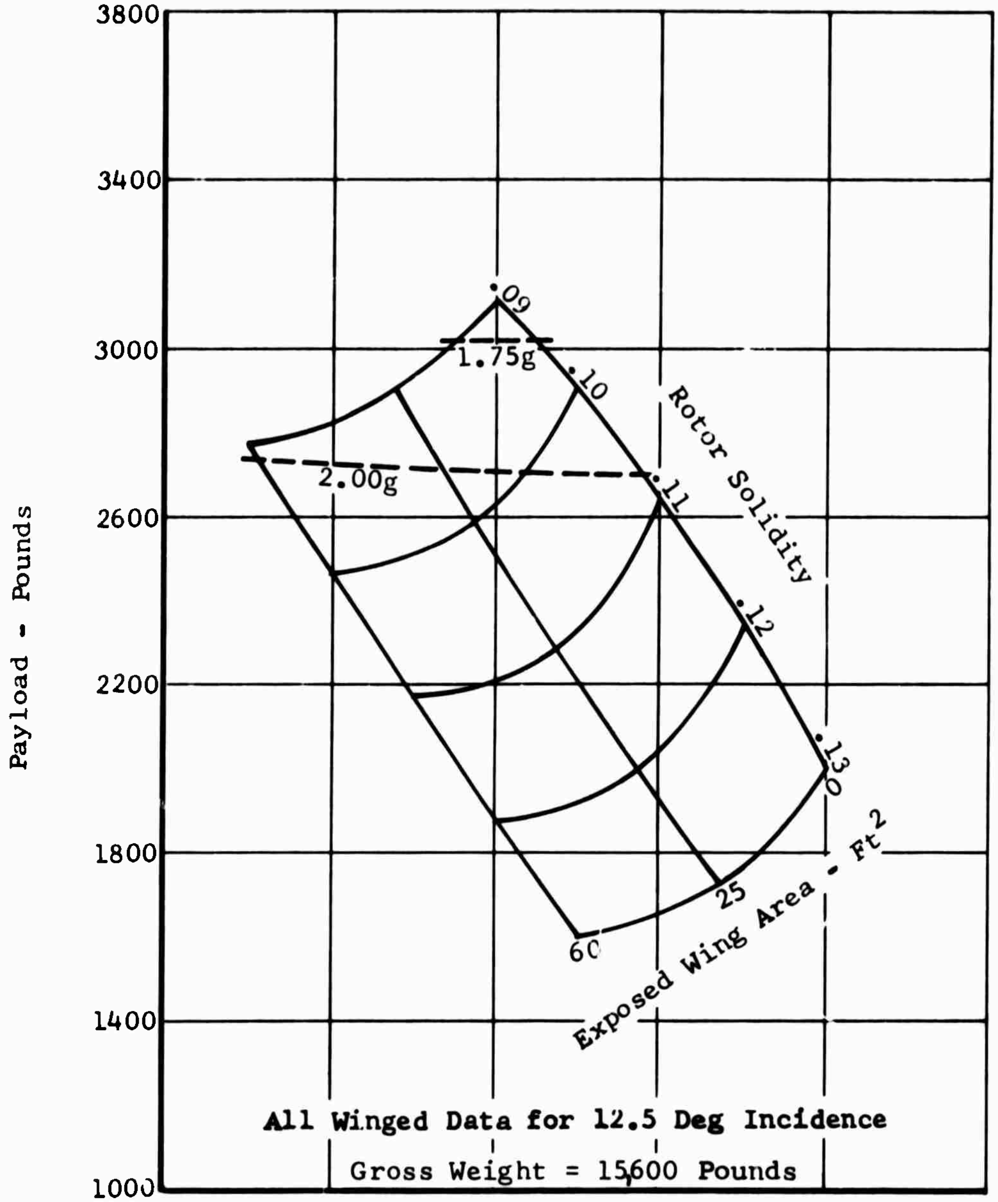

Figure 54. Effects of Rotor Solidity and Wing Area on Payload and Design g-Capability.

TASK III - OPTIMUM DESIGNS FOR THREE MANEUVERABILITY LEVELS

DESIGN CHOICE CRITERIA

At the conclusion of Tasks I and II, the results of the study efforts and objectives were reviewed to formulate a rationale for the synthesis of optimum configurations to meet three levels of maneuvering capability--1.50, 1.75, and 2.00 g's. These maneuverability levels were associated with cyclic-only turns and pullups at the normal rated power speed of each design. At the completion of the review, the conclusion was to synthesize a pure helicopter configuration to meet each required level of maneuverability. The factors which led to that conclusion are explained in the following paragraphs.

From the results of Tasks I and II, it was evident that both winged and pure helicopters designed for equal maneuvering capability have equal payload capability, or conversely, the same design gross weight. This situation is influenced, of course, by the application of other typical UTTAS study requirements to each configuration. The conclusion to be drawn is that between winged or pure helicopter, for equal maneuvering capability, there is no discernable difference in weight or overall size of a typical UTTAS vehicle.

The UTTAS air transportability requirements preclude wing disassembly considerations for some situations. Folding is questionable, since the result is an unavoidable increase in fuselage width, an increase in complexity, and probably a compromise in cabin accessibility.

Typical UTTAS design layouts result in wing locations that place the lower surface of the wing just above the inside roof line of the troop compartment. The wing is normally only 2 to 2.5 feet above the most logical position for the pivot point of a pintle-mounted machine gun. Some aspects of the upward field of fire are necessarily restricted by the wing. While no criterion is available for allowable field of fire, any unnecessary restriction is considered to be unacceptable.

Some of the problems associated with wings on helicopters that are well documented by earlier studies and flight tests can be alleviated by the use of variable geometry devices such as spoilers, flaps, ailerons or variable incidence controls. These devices are considered to be out of context in the overall UTTAS program because of emphasis on decreased complexity, reduced cost, improved maintainability and reliability, and the development of the smallest possible vehicle. For these reasons, a fixed geometry wing was considered to be the only configuration suitable for a UTTAS application.

Typical UTTAS design configurations with fixed geometry wings require high incidence settings (>10°) and the logical wing spar locations occur in areas that conflict with engine and transmission supporting structure. Access to the engine and transmission for maintenance is made more difficult by the presence of a wing.

Task II results revealed that winged configurations were more limited in their capability to achieve low (i.e., near zero) g, high-speed, maneuvering flight. This problem is the result of difficulty of reducing wing lift sufficiently during low g maneuvers. Wing stall in maneuvering flight is not a problem, especially at low speeds. This is because the increased induced velocity from the main rotor in accelerated flight tends to reduce the wing angle of attack. In fact, elementary momentum theory shows that the wing contribution to lift is multiplied by $(1 - \sigma a/4\mu)$. Thus, when $\mu = \sigma a/4$ (about 60 knots), then there is no wing lift change with angle of attack.

Finally, the results of Task I revealed that the maneuvering g range of interest (i.e., 0 to 2.0) could be satisfactorily attained by pure helicopter configurations.

SCOPE AND GROUND RULES - TASK III

At the beginning of Task III, the study ground rules were revised. Weights and performance estimations were reviewed. The objectives of these changes were to take advantage of the work already completed and to provide the most accurate definition of three UTTAS type vehicles designed for the three maneuvering requirements. The most important ground rule change was the decision to maintain a constant payload and allow other physical parameters to vary. This technique provides the most graphic illustrations of the effect of maneuverability requirements on overall UTTAS characteristics. A disc loading of 6.0 psf was maintained to make the results directly comparable to the earlier sections of the study. A rotational rotor tip speed of 725 fps was selected as the best compromise between μ, Mach, and noise effects in a 4000-foot, 95°F atmosphere. Rotor solidities were chosen based on the results of Task I.

Using the above ground rules, the following three configurations were chosen for further study:

1.50g Configuration	$\sigma = 0.085$	D = 55.3 Ft	GW = 14450 lb
1.75g Configuration	$\sigma = 0.095$	D = 56.4 Ft	GW = 15020 lb
2.00g Configuration	$\sigma = 0.110$	D = 58.2 Ft	GW = 15980 lb

STABILITY AND CONTROL ANALYSIS - TASK III

Three wingless helicopter configurations were selected for more detailed study from the initial group of configurations studied in Tasks I and II. Each of the three final configurations was designed to a different maneuvering g-level capability. The design g-levels investigated were 1.5g, 1.75g, and 2.0g. Longitudinal stability characteristics of the final three configurations are discussed below.

Longitudinal cyclic stick position gradients with respect to speed, forward stick margin at high speed (aft cg), and longitudinal dynamic stability were considered during and after the determination of an acceptable stick rigging and an adequate horizontal stabilizer size. Three horizontal stabilizer areas were considered: 35 square feet, 45 square feet, and 55 square feet. Limitation of main rotor flapping to less than one degree in trimmed level flight at a mid cg was the primary criterion used to determine an acceptable horizontal stabilizer incidence variation with longitudinal cyclic stick position.

The hybrid computer version of Bell Helicopter Company computer program C81 was used to calculate main rotor flapping as a function of horizontal stabilizer incidence. The flapping data was calculated for each of the three final configurations in combination with the three horizontal stabilizer areas investigated.

Figure 55 illustrates the relationship between stick position, stabilizer incidence, speed, and flapping with the unstable boundary of the long period oscillation also indicated. The requirement for forward stick with increasing speed and nose down stabilizer incidence is clearly shown on the figure. The lines of zero flapping and the design maximum continuous flapping are drawn by interpolation of the static trim data. In order to determine the elevator synchronization required, this graph is made for all cg, weight, and normal accelerations within the flight envelope. When all of these graphs are overlayed, a fairly narrow band remains within which the design maximum flapping limits are acceptable. A mechanical linkage is then designed to properly gear the stabilizer to the longitudinal cyclic stick.

After forward flight synchronization is determined, the slope of the synchronization must usually be reversed for acceptable rearward flight characteristics. Linear gearing would result in very nose down incidences for the aft stick positions required in rearward flight. The resulting upload requires more aft cyclic to trim pitching moment and rapidly narrows the aft stick margin. To improve this margin the stabilizer

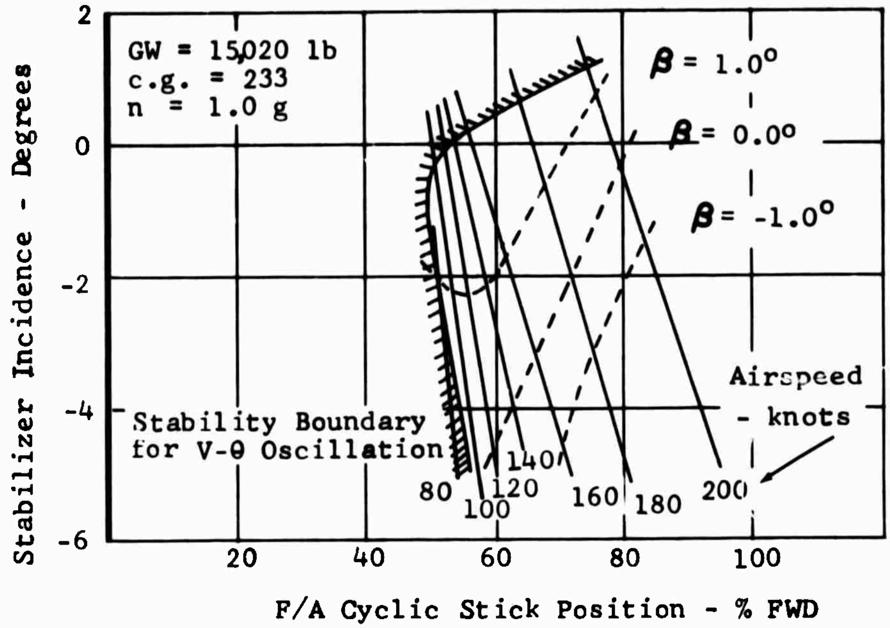

Figure 55. Sample Chart Used for Determination of Stabilizer Rigging

incidence must increase with aft stick, which is opposite to Figure 55. A parabolic-shaped gearing is the usual result and is used in all UH-1 series helicopters.

These stabilizer incidence riggings were then used in the digital computer version of program C81, and stability data was calculated. Main rotor flapping for the three configurations with a 45-square-foot stabilizer area is shown in Figure 56.

Figure 57 is a root locus plot of the phugoid mode of the 1.50g configuration. Root locus plots of the phugoid mode for the 1.75g and 2.00g configurations are given on Figures 58 and 59. The 35-square-foot stabilizer was not adequate to stabilize the phugoid mode. Short period response determined by the hybrid computer was acceptable for all elevator sizes. The dynamic stability criterion used to choose stabilizer area was that the VFR stability requirements of MIL-H-8501A (3.2.11) be met or exceeded at 30 KTAS without electronic stabilization. It was determined that a minimum stabilizer area of 45 square feet was necessary to satisfy this stability criterion. The 45-square-foot stabilizer was chosen because larger stabilizers might provide excessive angle-of-attack stability. This means that the pilot would have to trim larger pitching moments as power is varied from autorotation (large positive angle of attack) to full-power climb (large negative angle of attack). This pitch trim requirement results in greater than the 3-inch maximum stick travel allowed in MIL-H-8501A (3.2.10.2) for helicopters with large stabilizers. Root locus plots for the three final configurations with a 45-square-foot stabilizer are given on Figure 60. Since short period response does not enter into stabilizer sizing or gearing, data is not shown for this mode.

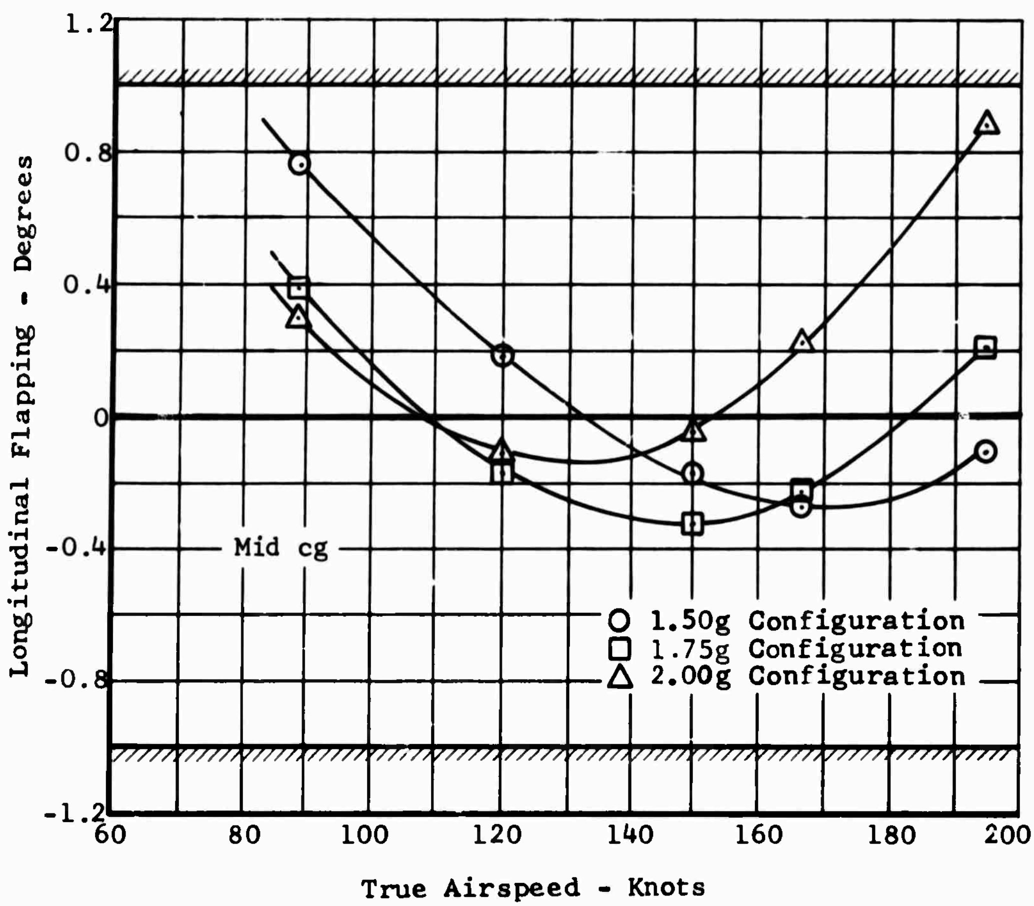

Figure 56. Task III Configurations - Longitudinal Flapping Versus Airspeed.

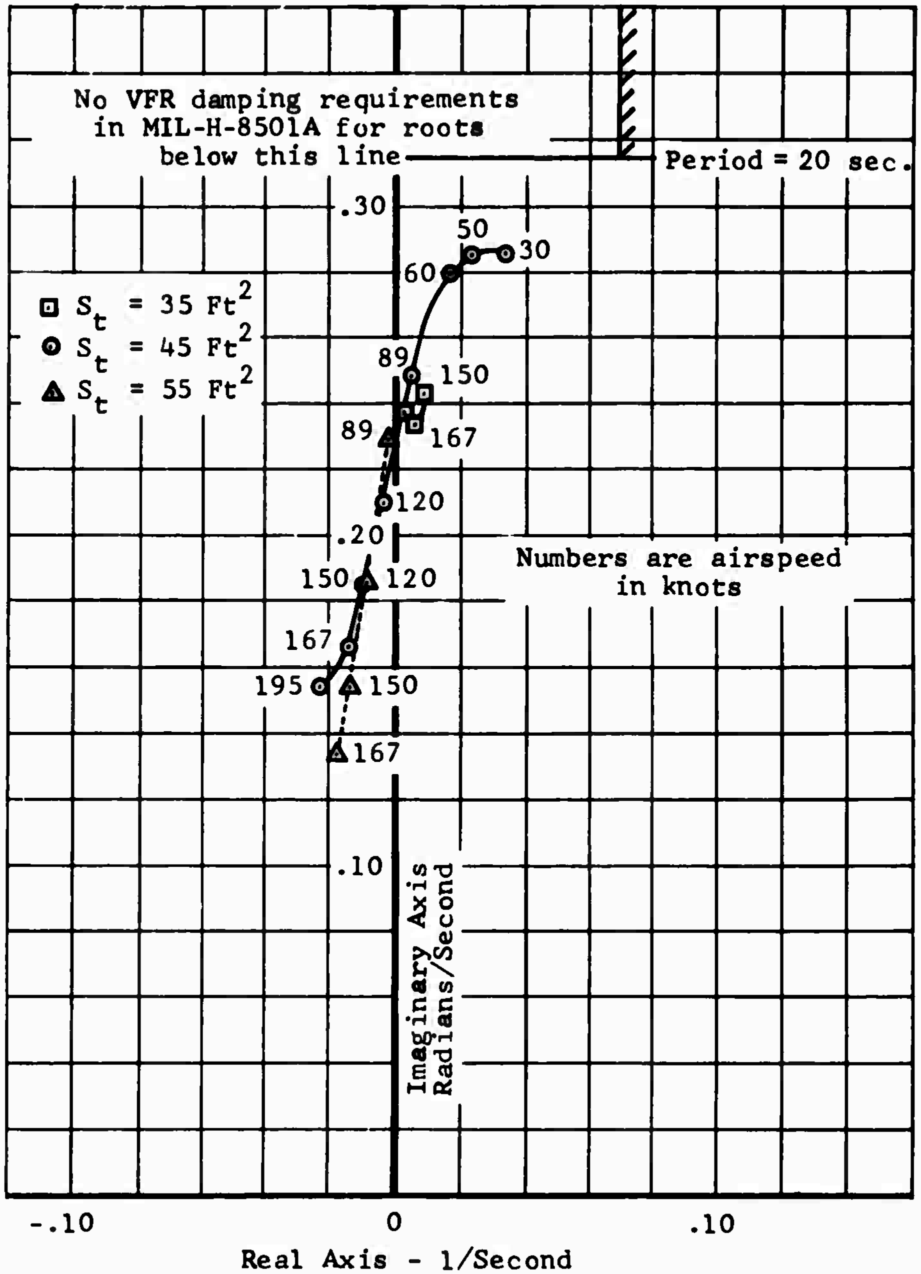

Figure 57. Phugoid Mode Root Locus Plot for
1.5g Configuration, aft cg.

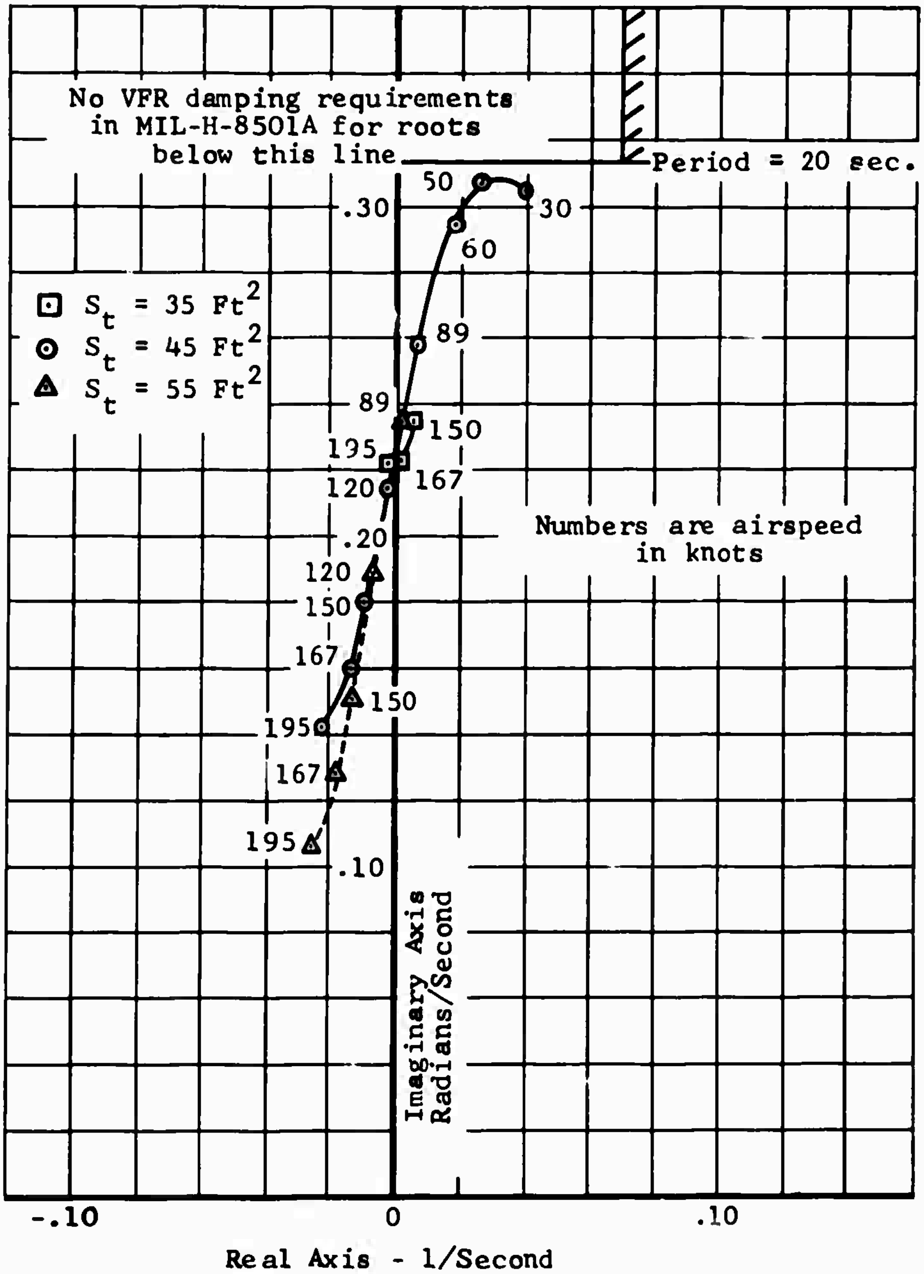

Figure 58. Phugoid Mode Root Locus Plot for 1.75g Configuration, aft cg.

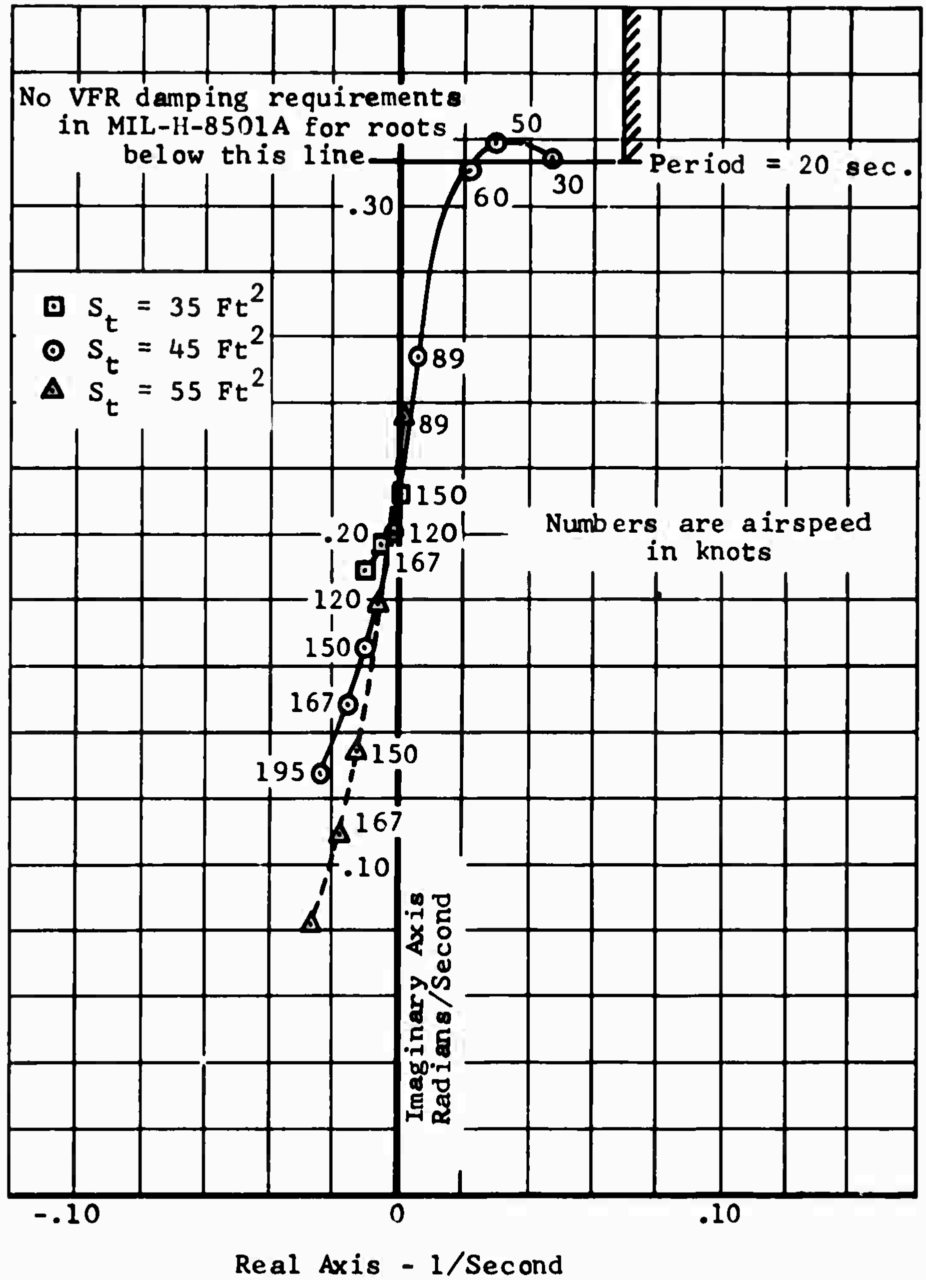

Figure 59. Phugoid Mode Root Locus Plot for 2.0g Configuration, aft cg.

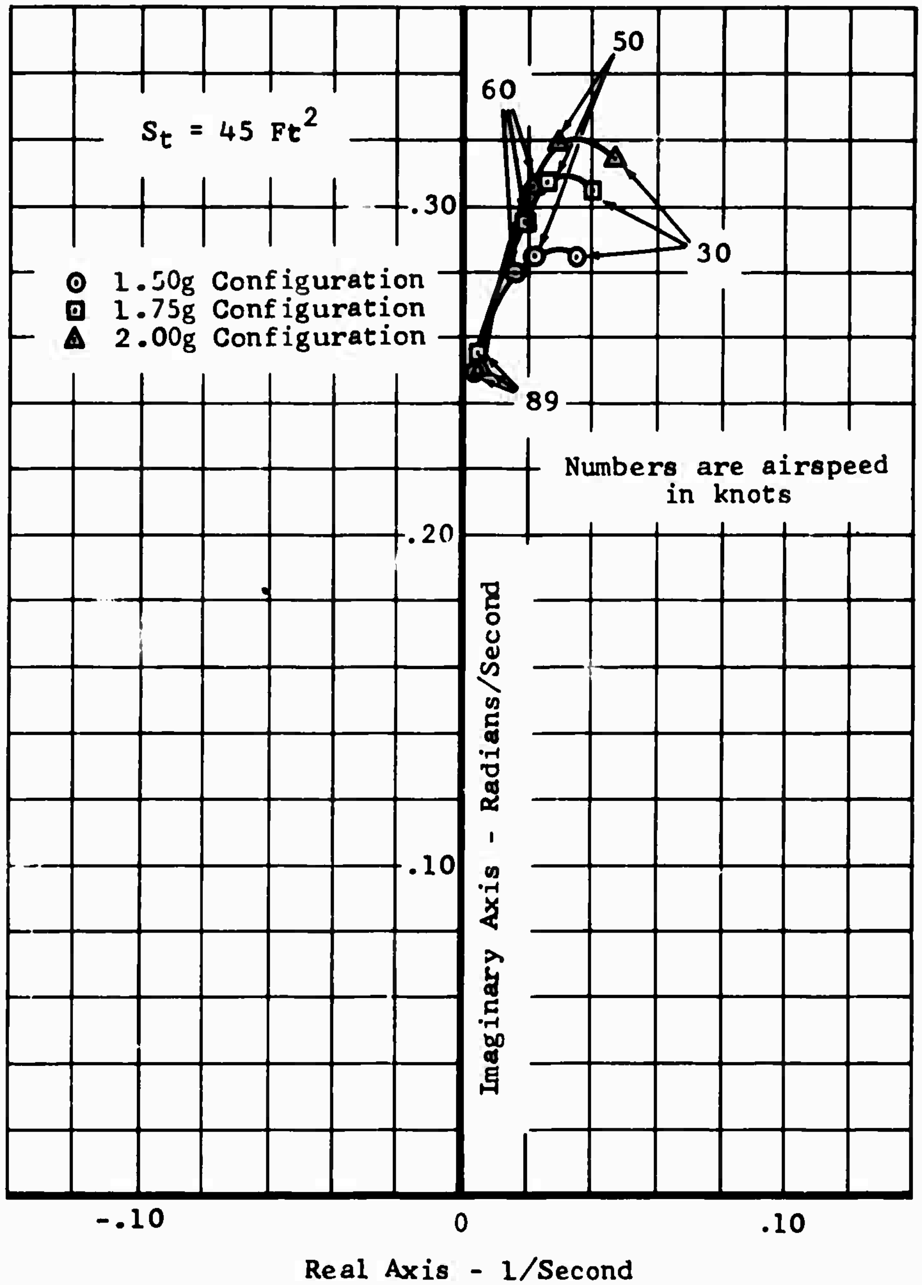

Figure 60. Task III Configuration—Phugoid Mode Root Locus Plot, aft cg.

As shown on Figure 61, the horizontal cyclic stick position gradient with respect to airspeed is positive for each of the three final configurations with a 45-square-foot stabilizer area. The stick margins in high speed forward flight were within MIL-H-8501A (3.2.1) requirements.

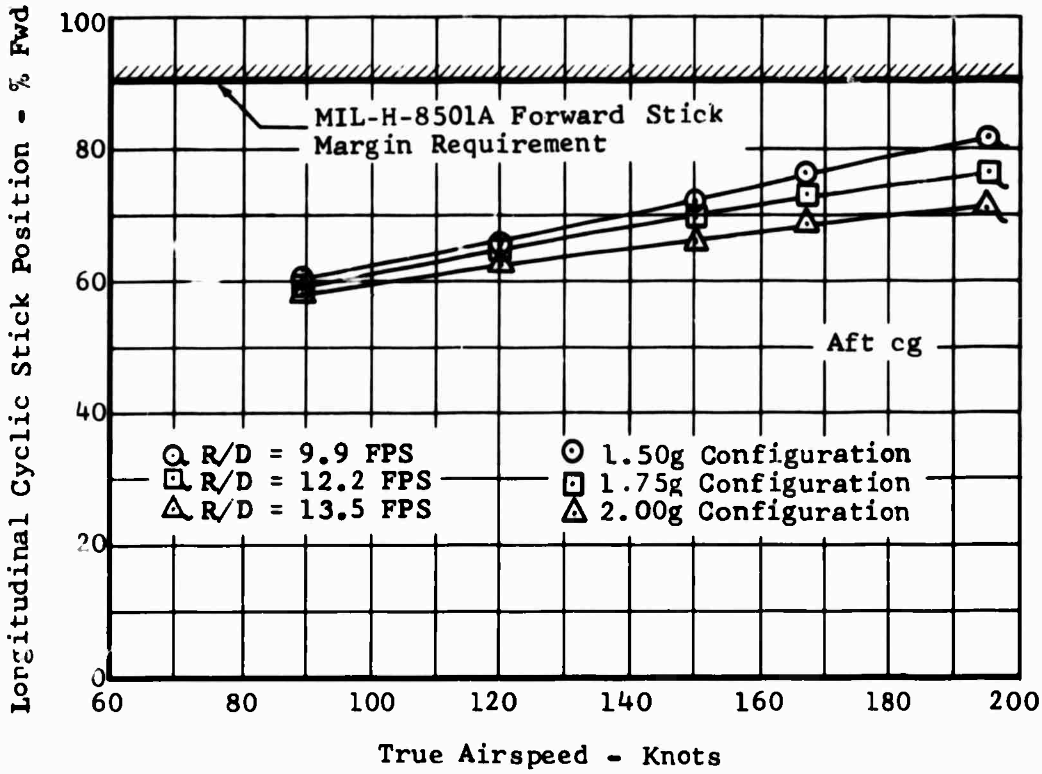

Figure 61. Task III Configurations—Longitudinal Cyclic Stick Position Versus Airspeed.

PERFORMANCE - TASK III

Power Available

The power available was based on an advanced technology engine with the installation losses and allowances as specified in Task I.

Hover

The hovering power required for the three Task III helicopters was calculated on the Bell Helicopter Computer program F35 as explained in Task I. The hover power required is shown on Figure 62. The installation losses and tail rotor power required were the same as discussed in Task I. The excess power necessary for climb and the uninstalled power available were also determined as in Task I. The uninstalled power required is shown in Table XVIII.

TABLE XVIII. TASK III - ENGINE POWER REQUIRED

Design Maneuver Level, g	σ	D (Ft)	Uninstalled Engine HP Rating S.L. Std Day
1.50	0.085	55.3	2555
1.75	0.095	56.4	2710
2.00	0.110	58.2	2970

Forward Flight

The forward flight power required was also calculated on F35 for the three Task III configurations. The equivalent flat plate drag area of all three configurations was taken to be 11.43 square feet, since the basic fuselage was the same size with the only difference being in the rotor. This drag value has been verified by wind-tunnel tests as pointed out in Task I. The swept tip improvement and tail rotor, transmission, and accessory losses were the same as explained in Task I. Speed power polars for the three Task III designs are shown on Figures 63 through 65. The military and normal rated power available are also shown on these figures. The maximum speeds are found from Figures 63 through 65 and are shown on Table XIX. Normal-rated power speeds were greater than 150 Knots for all cases.

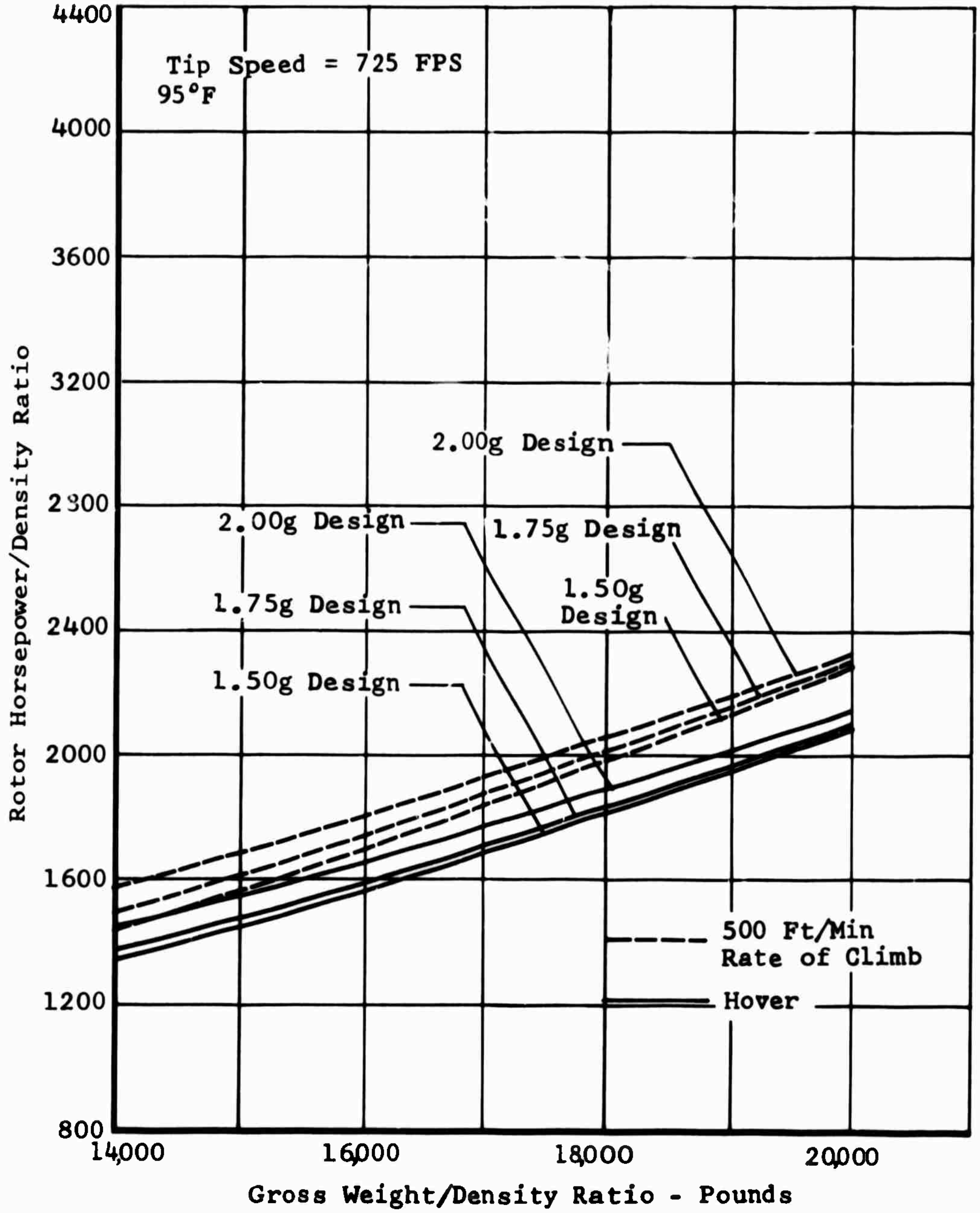

Figure 62. Task III - Wingless Helicopter Hover Power Required.

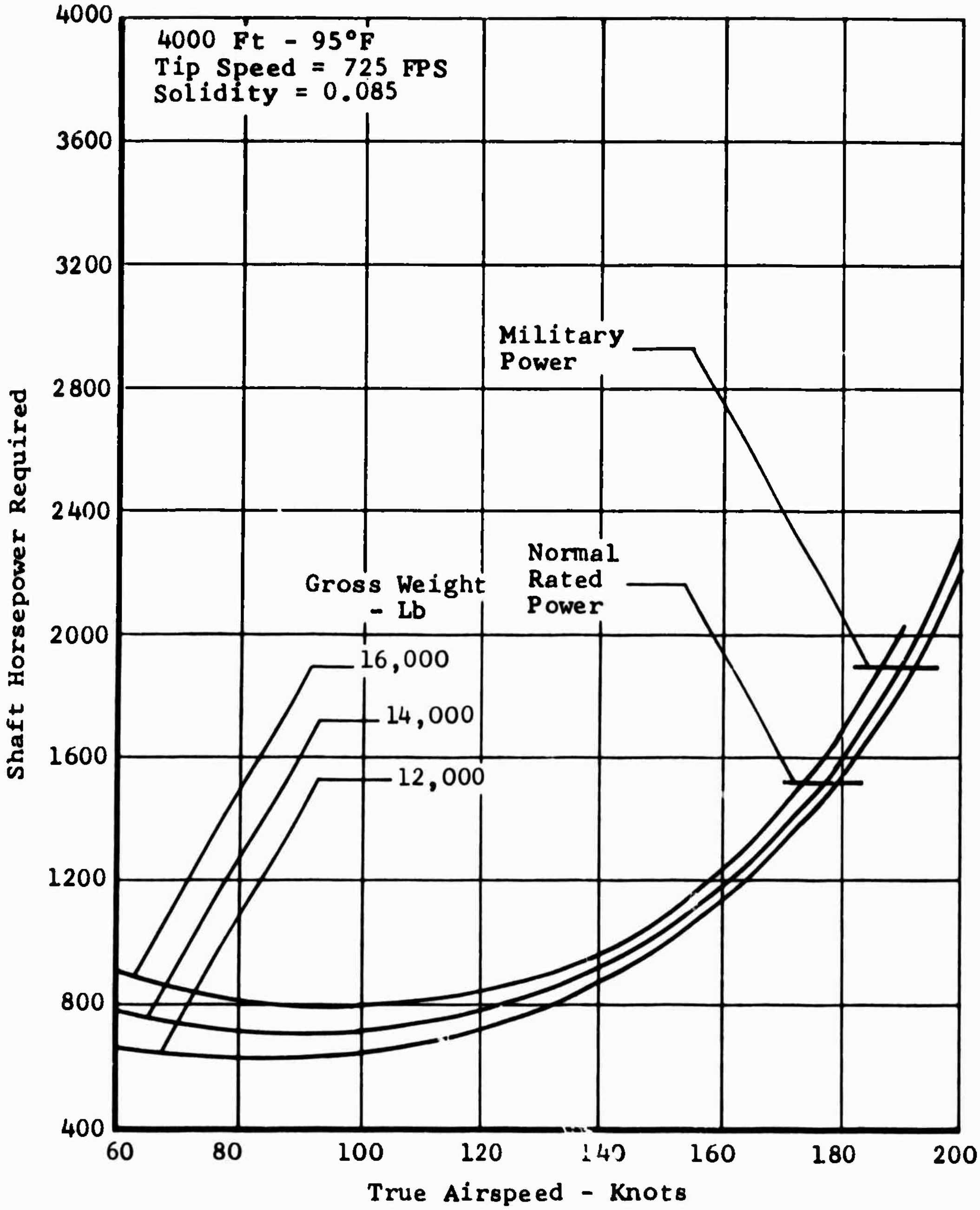

Figure 63. Task III - Wingless Helicopter, Speed Power Polar, 1.50g Design.

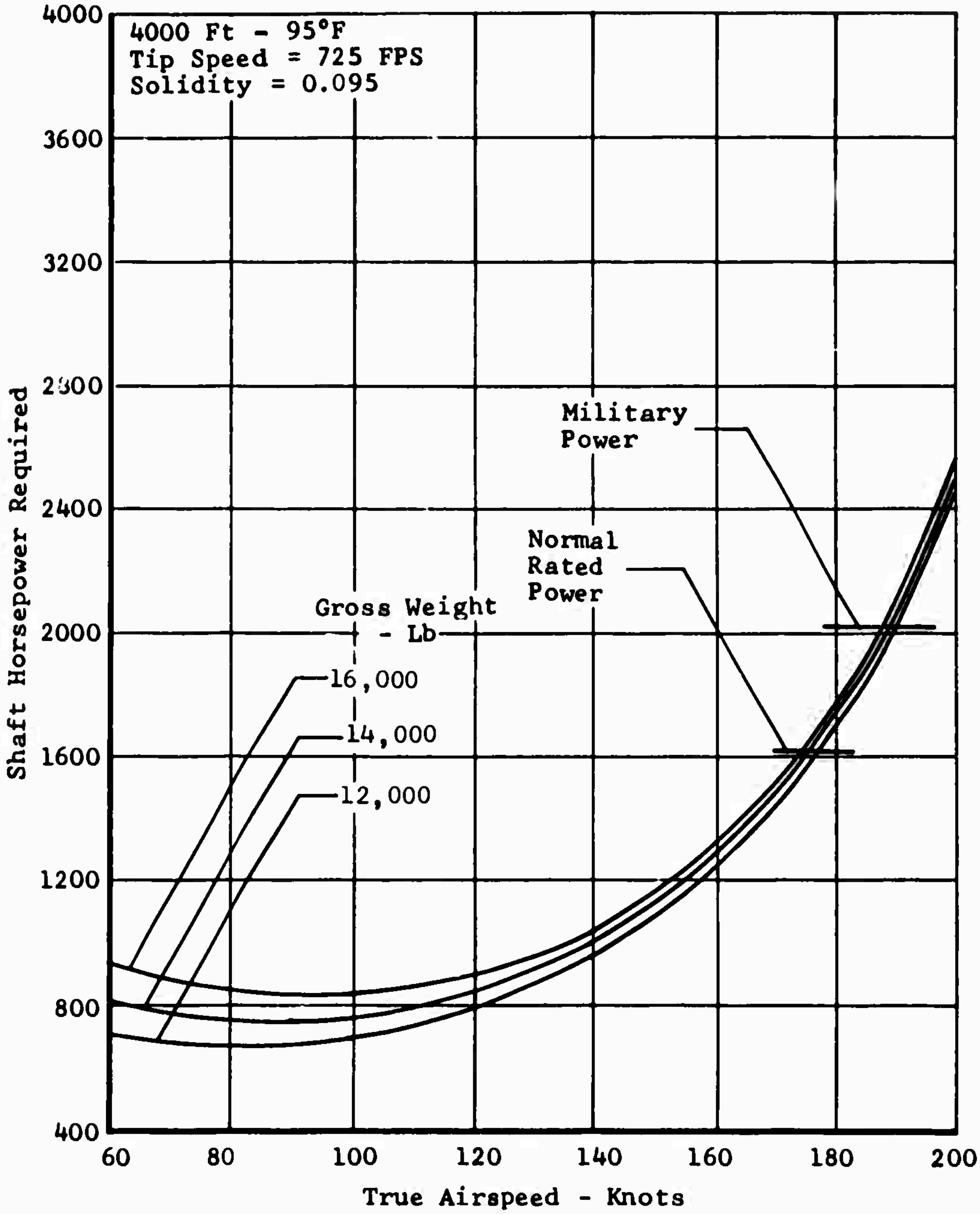

Figure 64. Task III - Wingless Helicopter, Speed Power Polar, 1.75g Design.

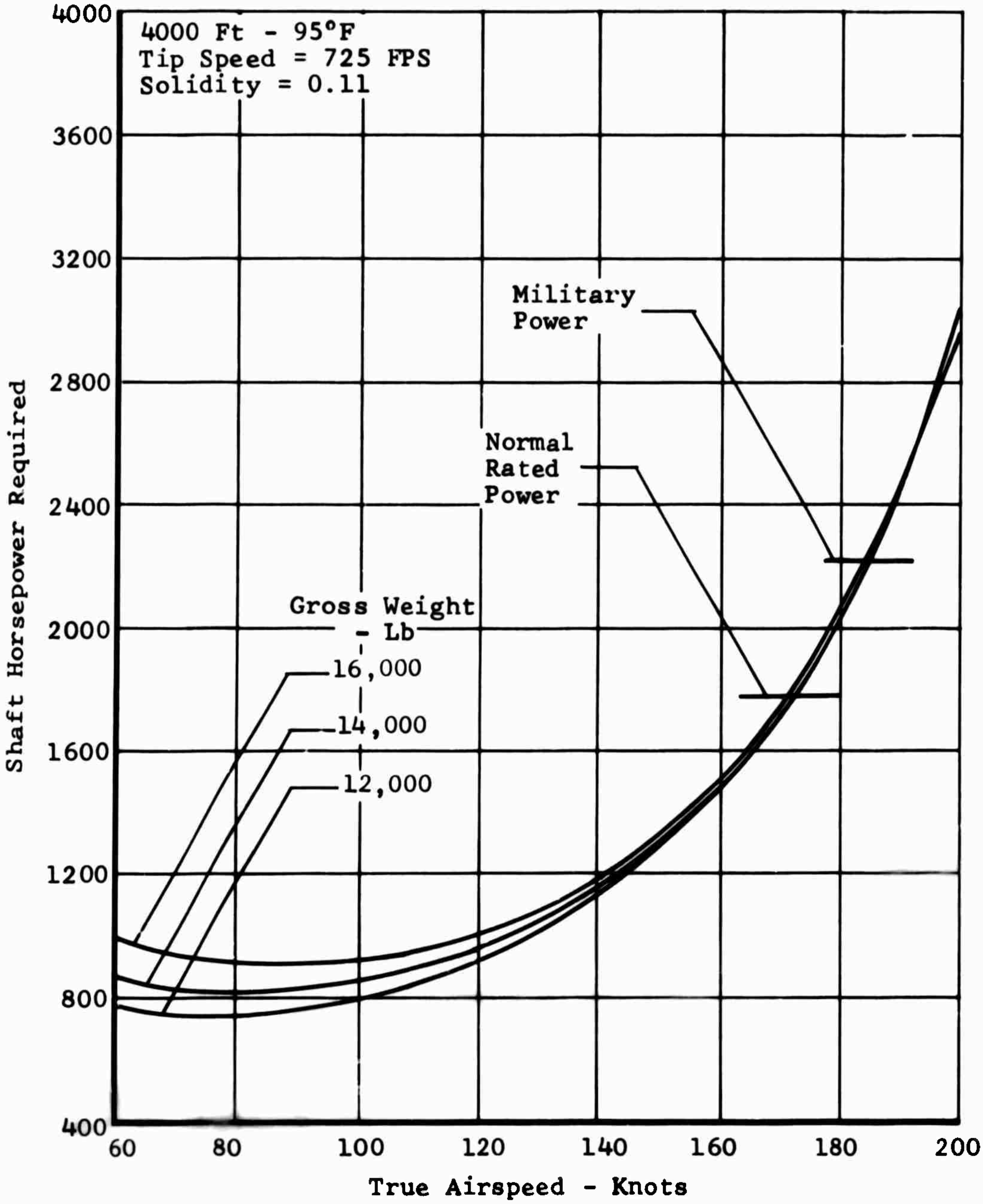

Figure 65. Task III - Wingless Helicopter, Speed Power Polar, 2.00g Design.

TABLE XIX. TASK III - MAXIMUM TRUE AIRSPEED, 4000 FT, 95°F					
Design Maneuver Level (g)	GW (Lb)	σ	D (Ft)	V_{NRP} KTAS	V_H KTAS
1.50	14,450	0.085	55.3	177	189
1.75	15,020	0.095	56.4	175	188
2.00	15,980	0.110	58.2	170	185

The specific ranges were calculated and are shown on Figures 66 through 68. The military rated power, normal rated power, and long-range cruise speed are also shown on these plots.

Weights

The weights for the Task III designs were estimated as in Task I and a summary weight statement is shown in Table XX.

Mission Analysis

Mission data for the Task III helicopters were calculated for the mission described in Task I. Since the Task III helicopters all carried the designed UTTAS payload of 2640 pounds, the variables for the mission were gross weight and fuel load. Table XXI shows the effects of the maneuver capability on the gross weight and fuel load.

TABLE XXI. TASK III - MISSION SUMMARY				
Design Maneuver Level (g)	GW (Lb)	σ	D (Ft)	Fuel (Lb)
1.50	14,450	0.085	55.3	1526
1.75	15,020	0.095	56.4	1646
2.00	15,980	0.110	58.2	1864

TABLE XX. TASK III - POINT DESIGN HELICOPTERS, SUMMARY WEIGHT STATEMENT

Design Maneuver Load Factor, g	1.50		1.75		2.00	
Design Gross Weight, Pounds		14,450		15,020		15,980
Engines (No. and Type)		2 ADV.		2 ADV.		2 ADV.
SHP - Uninstalled		2555		2710		2970
Main Rotor(s) Diameter, Feet		55.3		56.4		58.2
Solidity		0.085		0.095		0.110
Tip Speed, FPS		725		725		725
Weights, Pounds						
Rotor Group		1990		2242		2661
Wing Group		-		-		-
Tail Group		166		179		193
Body Group		1908		1923		1970
Alighting Gear		434		450		479
Flight Controls		695		706		724
Fixed	411		415		421	
Rotating	284		291		303	
Eng. Section/Nacelles		163		170		181
Propulsion		2167		2300		2500
Engine Install	545		568		601	
Induction System	60		62		66	
Exhaust	68		72		79	
Fuel System	329		356		400	
Controls	32		32		32	
Starting	37		38		40	
Rotor Brake	45		47		49	
Trans and Drive System	1051		1125		1233	
Passive Defense		200		200		200
Instruments		73		73		73
Hydraulics		88		91		95
Electrical		281		281		281
Avionics (inc nav)		411		411		411
Furnishings and Equipment		658		658		658
Air Conditioning		121		121		121
APU		93		93		93
Armament		175		175		175
Weight Empty		9623		10,073		10,815
Crew	600		600		600	
Payload (Pass or Cargo)	2640		2640		2640	
Fluids	61		61		61	
Survival Equipment	-		-		-	
Passive Defense	-		-		-	
Armament	-		-		-	
Fuel	1526		1646		1864	
Miscellaneous	-		-		-	
Useful Load		4827		4947		5165
Mission Weight		14,450		15,020		15,980

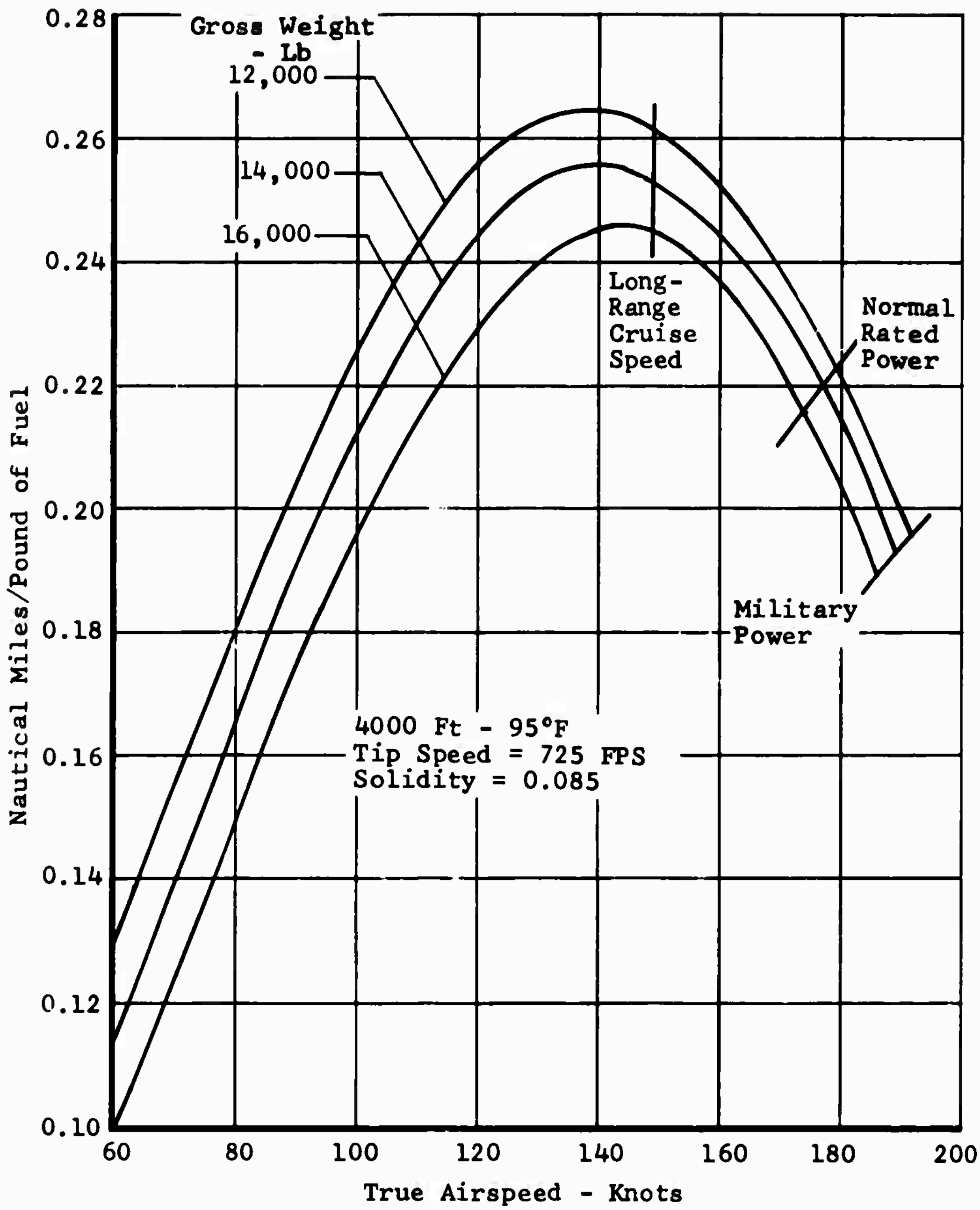

Figure 66. Task III - Wingless Helicopter, Specific Range, 1.50g Design.

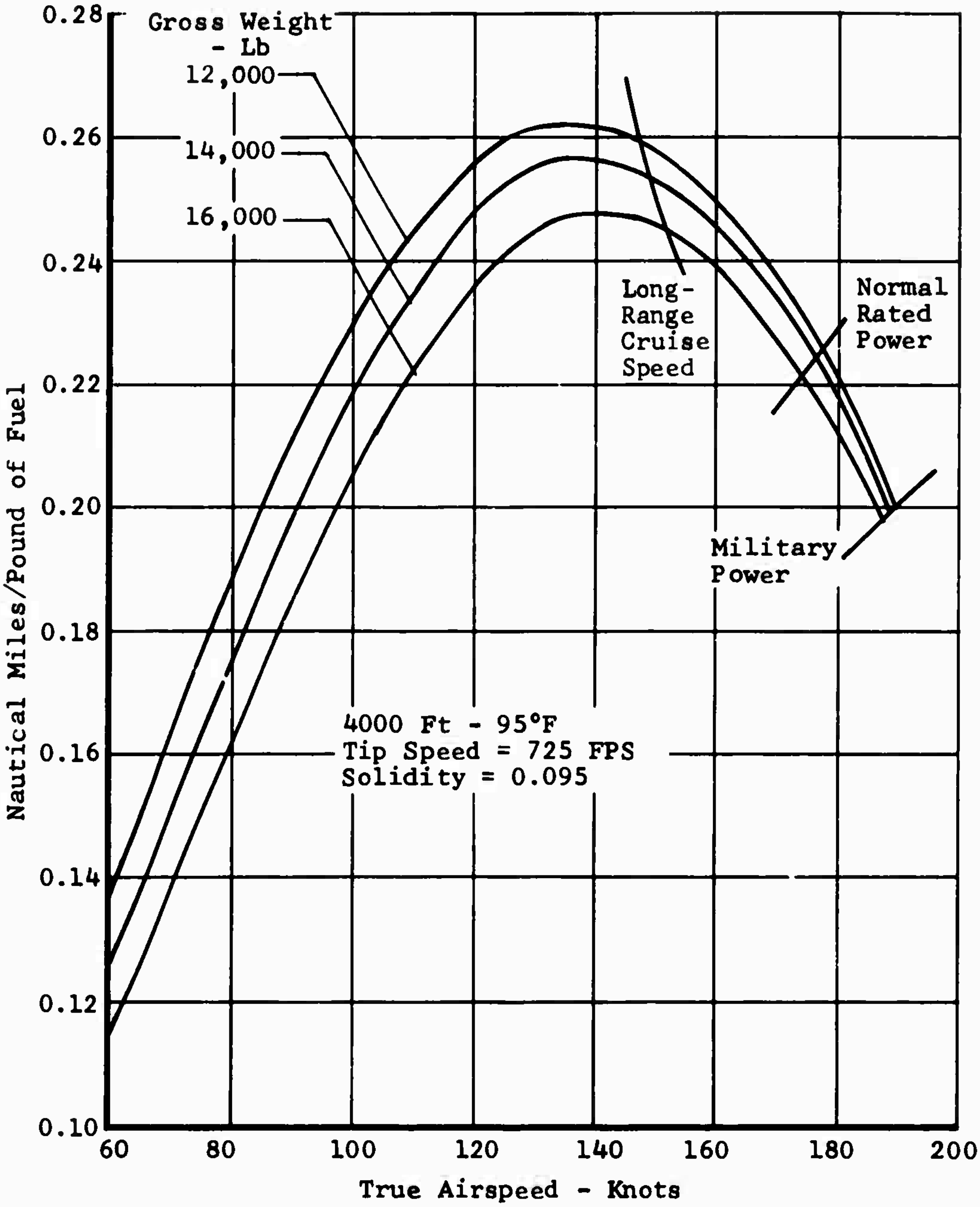

Figure 67. Task III - Wingless Helicopter, Specific Range, 1.75g Design.

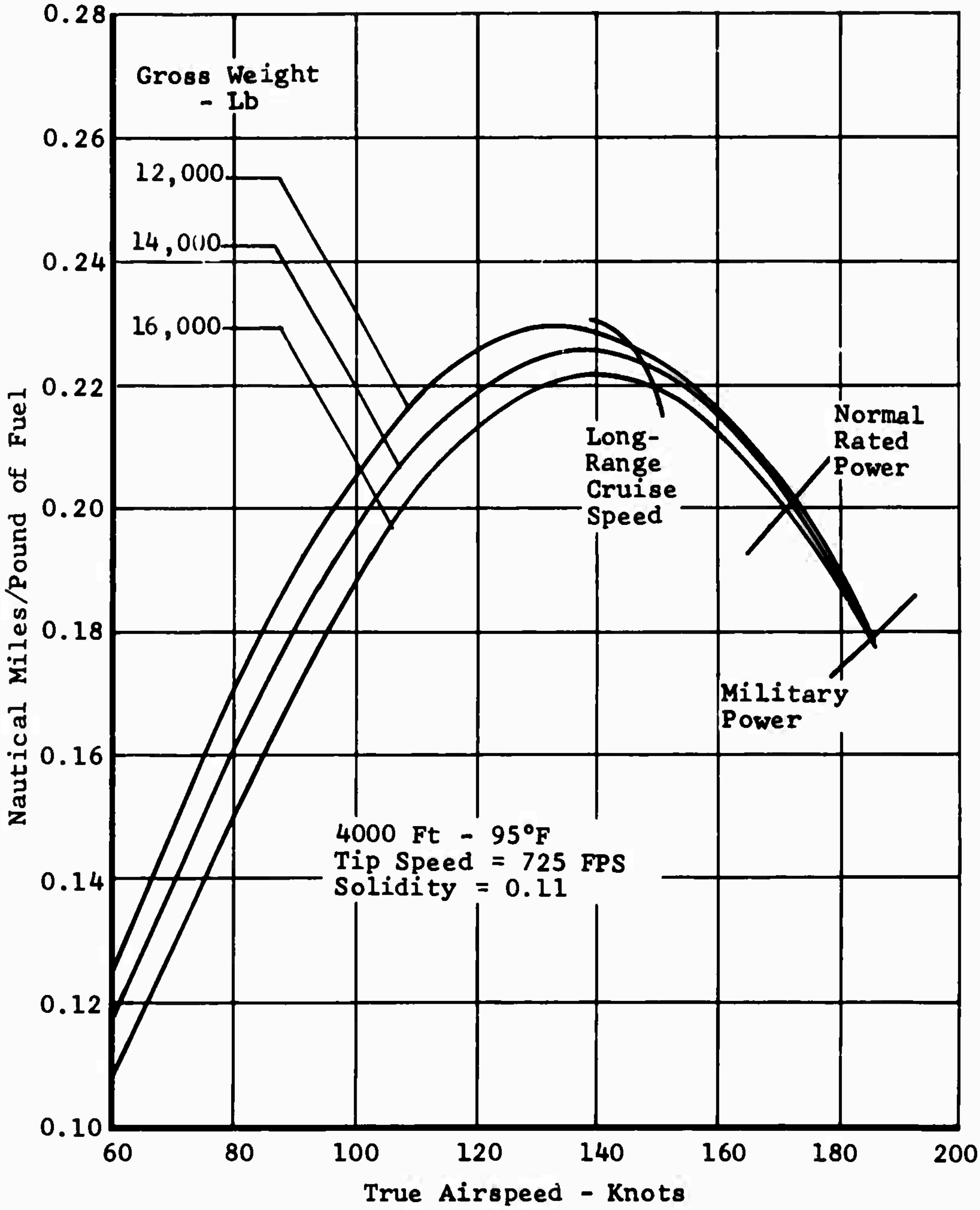

Figure 68. Task III - Wingless Helicopter, Specific Range, 2.00g Design.

SCOPE OF MANEUVERS INVESTIGATED - TASK III

The three configurations of Task III were investigated in 44 different maneuvers which are described in Table XXII. When compared to the maneuvers investigated in Tasks I and II, the scope of Table XXII includes one additional airspeed, 120 KTAS, and at the high end of the speed range, the maneuvers were run at the normal rated power airspeed of each configuration rather than at 167 KTAS. Additionally, the collective + cyclic pullup range was extended from 150 KTAS to V_{NRP}. The addition of 120 KTAS was necessary to accurately define the maneuver capability in the mid-airspeed range. The criteria used to limit the maneuvers were the same as those used in Tasks I and II, given on Table VII.

MANEUVER RESULTS - TASK III

Results of Pullup and Pushover Maneuvers

The sustained load factors attainable in the pullup and push-over maneuvers for the Task III configurations are given on Figures 69 through 71. The maneuvers are more fully described in Appendix V, which gives the magnitude of the control inputs and the limiting criteria as well as the load factors achieved.

Inspection of Figures 69 and 70 show that the 1.50g and 1.75g configurations did not achieve their design capability at V_{NRP}; however, the 2.00g configuration slightly exceeded its design capability as follows.

1.50g Configuration	1.45g's @ V_{NRP} (177 KTAS)
1.75g Configuration	1.70g's @ V_{NRP} (175 KTAS)
2.00g Configuration	2.03g's @ V_{NRP} (170 KTAS)

Other key factors concerning the g-capability of Task III configurations as presented in Figures 69 through 71 are:

1. Although the g-capability at V_{NRP} was defined by the choice of rotor solidities, at lower airspeeds all three configurations had significantly higher capability as follows:

Configuration	g's @ 150 KTAS	g's @ 120 KTAS
1.50g	1.76	2.14
1.75g	1.97	2.40
2.00g	2.30	2.43

TABLE XXII. SUMMARY OF MANEUVERS INVESTIGATED - TASK III

Maneuver	Control Input	True Airspeed - Knots						
Pullups	Cyclic			89	120	150	V_{NRP}	195
	Collective+Cyclic		56	89	120	150	V_{NRP}	
	Collective	0	56	89	120	150		
Pushovers	Cyclic			89	120	150	V_{NRP}	195
	Collective+Cyclic		56	89	120	150		
	Collective		56	89	120	150		
Coordinated Turns-Constant Altitude	Cyclic				120	150	V_{NRP}	195
	Collective+Cyclic		56	89	120	150		
Coordinated Turns-Constant Airspeed	Cyclic				120	150	V_{NRP}	195
	Collective+Cyclic		56	89	120	150		

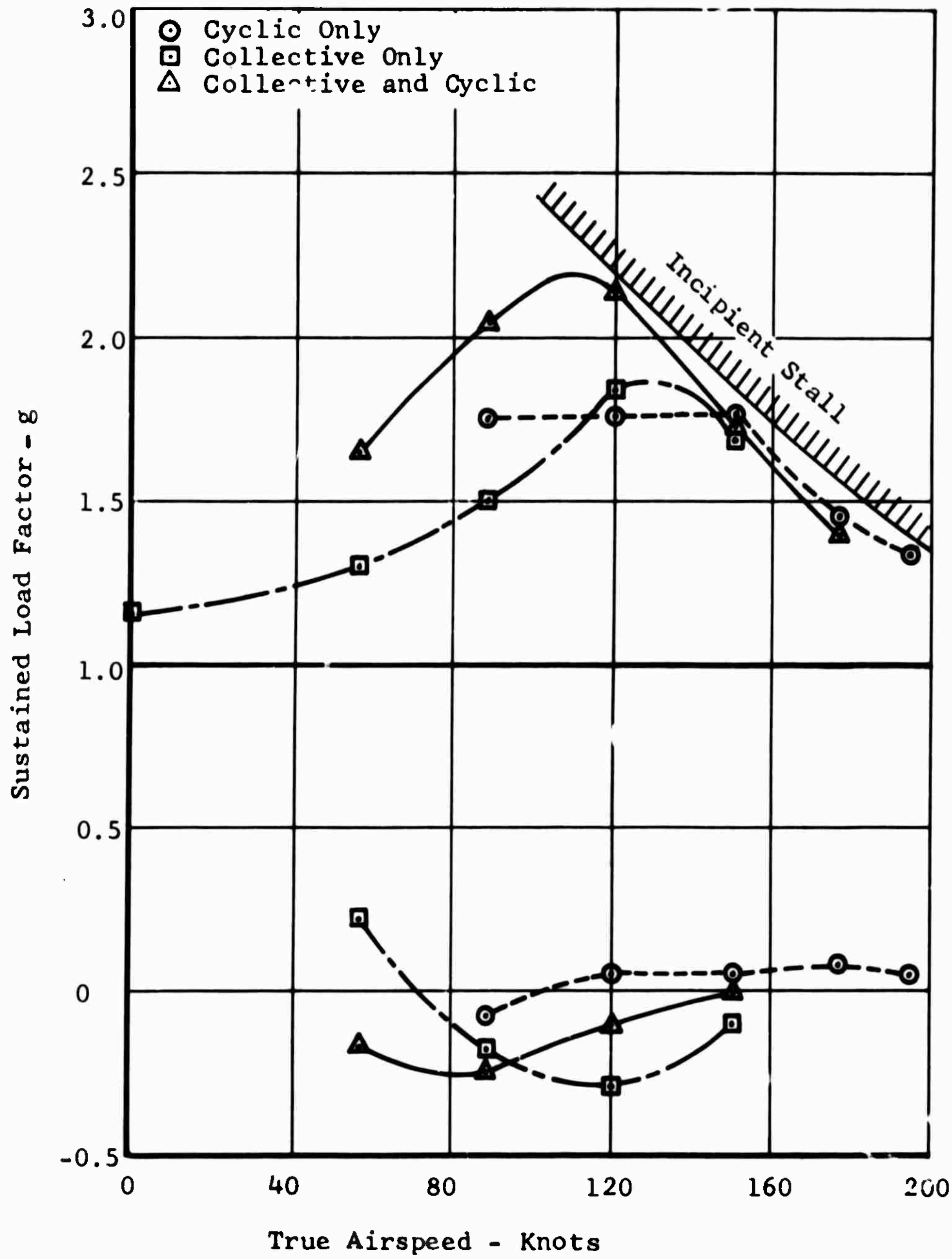

Figure 69. Task III - Maneuver Results, 1.5g Design.

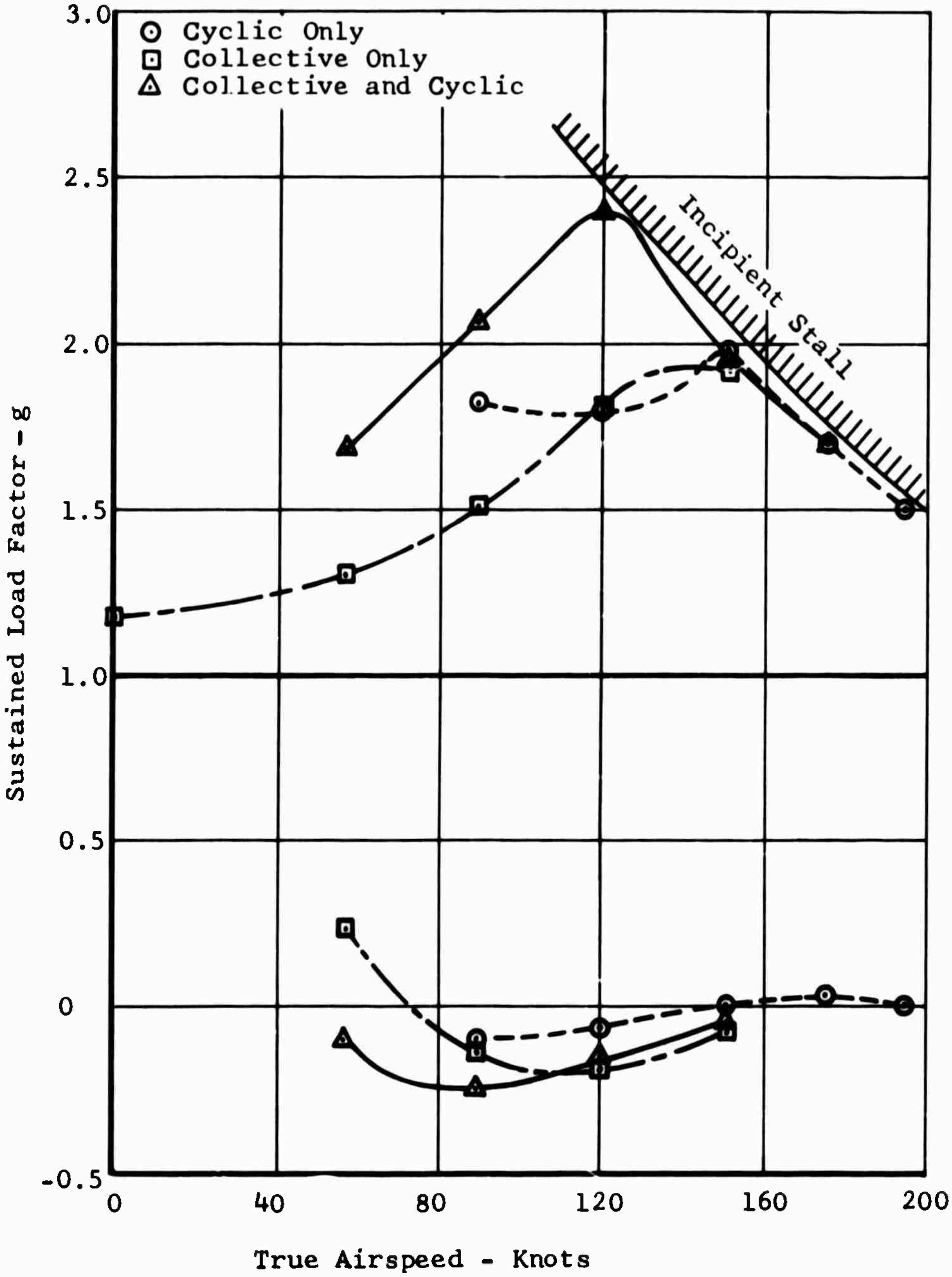

Figure 70. Task III - Maneuver Results, 1.75g Design.

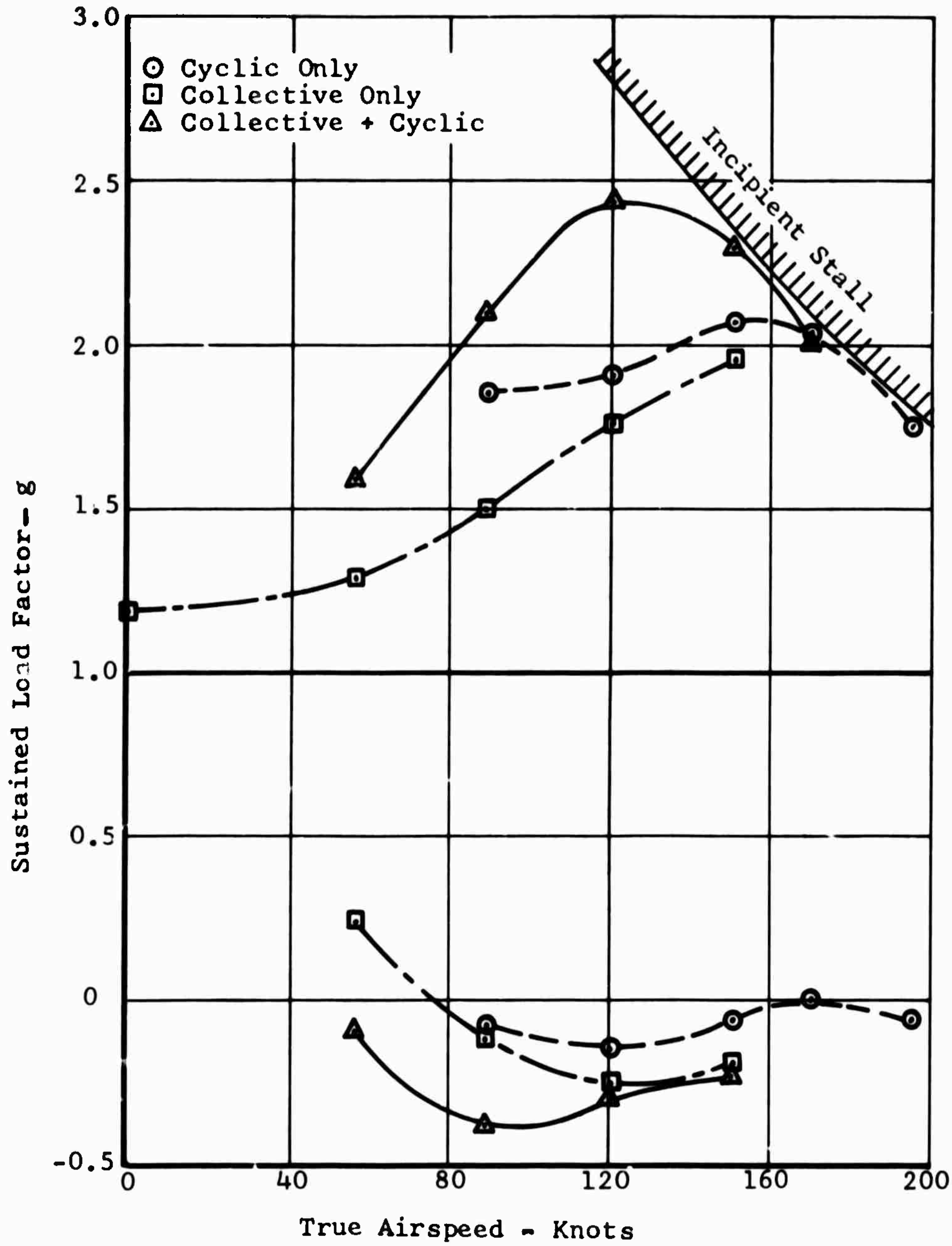

Figure 71. Task III - Maneuver Results, 2.00g Design.

2. At airspeeds less than the minimum power speed, all three configurations had about the same capability in both pullup and pushover maneuvers. For example, at 56 KTAS:

Configuration	Pullup g's	Pushover g's
1.50g	1.65	-0.17
1.75g	1.68	-0.10
2.00g	1.58	-0.10

3. All three configurations had zero or near zero g-capability throughout the airspeed range investigated.

The maneuver time histories of the limiting cyclic pullups at V_{NRP} are presented in Figures 72 through 74 for the Task III configurations. These are the maneuvers which define the g-capability of the three configurations.

Figure 72 gives the limiting cyclic pullup for the 1.50g configuration at V_{NRP} (177 KTAS). The magnitude of the pull was 0.85 degree, the maneuver being limited by a stall induced power rise at a load factor of 1.45 g's. The rapid power increase and increased oscillation in the thrust traces indicated the presence of blade stall about 3.0 seconds into the maneuver. A larger pull of 0.90 degree of cyclic was attempted, but the stall effects were increased to the point that both maximum horsepower and flapping limits were exceeded.

The time history of the limiting cyclic pullup for the 1.75g configuration at V_{NRP} (175 KTAS) is given on Figure 73. The maneuver was limited at 1.70 g's by stall effects, the cyclic input being a 1.00-degree pull. As for the 1.50g configuration, a larger pull was attempted, but the maximum horsepower and flapping limits were exceeded because of increased stall effects. The 2.00g configuration was limited by flapping at V_{NRP} without evidence of stall as shown on Figure 74. The sustained load factor was 2.03 g's achieved with a 1.05-degree cyclic pull.

The effects of the limiting criteria on the load factors achieved with the Task III configurations were consistent with results of Tasks I and II. At high airspeeds, both the pullup and pushover maneuvers were exclusively limited by the rotor criteria--maximum or zero horsepower and flapping. At low airspeeds, 89 KTAS and below, the maneuvers were commonly limited by the flight path criteria, with the exception of the collective pullup maneuvers which were limited by maximum horsepower at all airspeeds. Detailed information concerning the limiting criteria is given in Appendix V.

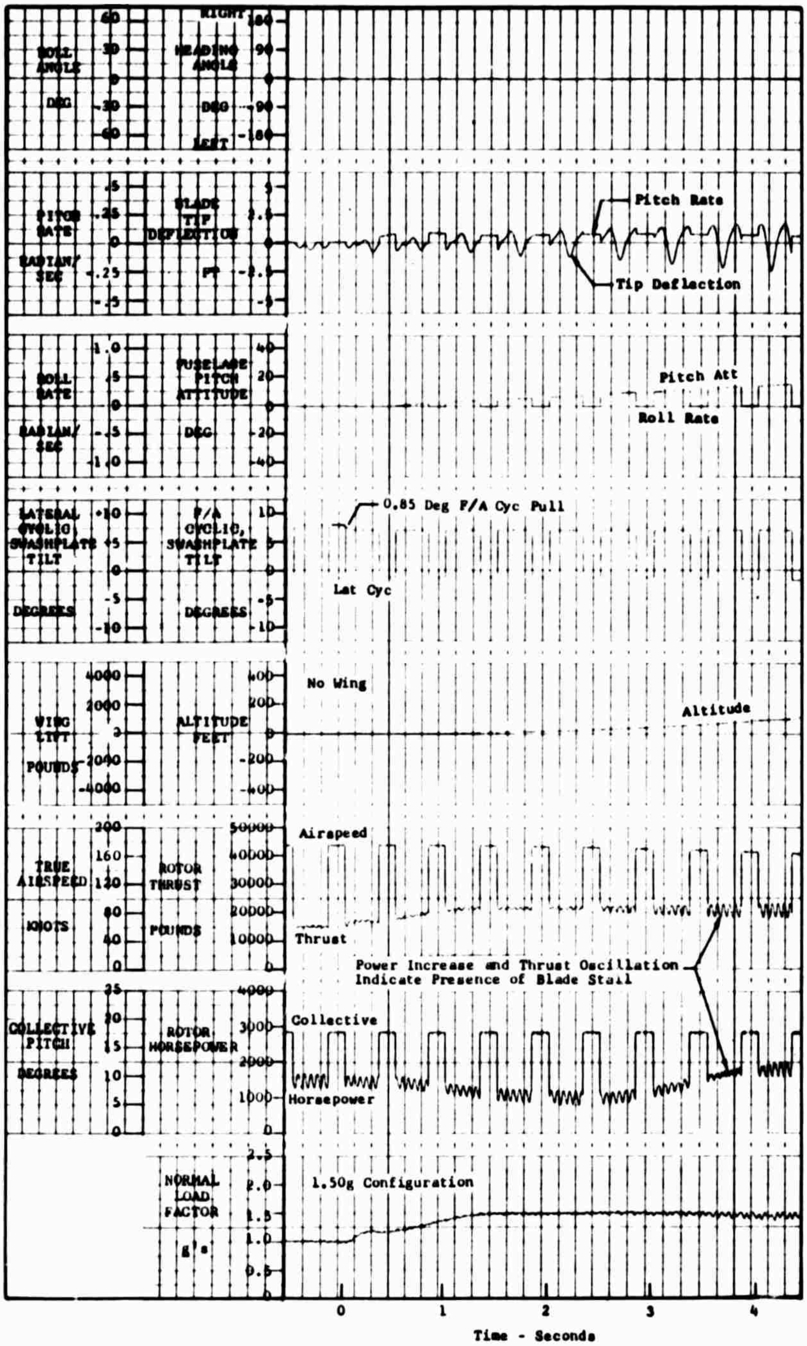

Figure 72. Maneuver Time History, 1.50g Configuration, Limiting Cyclic Pullup at V_{NRP}, Maneuver Limited by Maximum Horsepower.

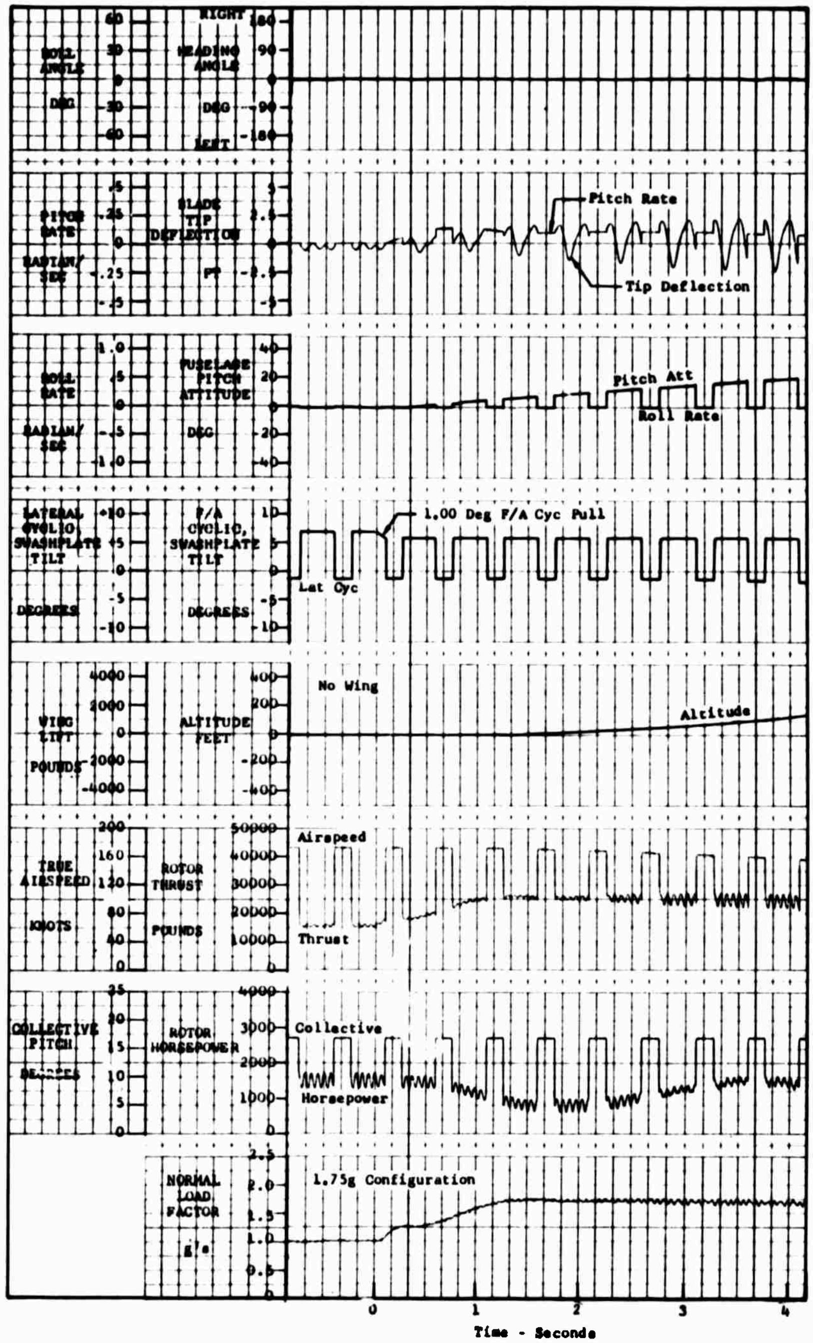

Figure 73. Maneuver Time History, 1.75g Configuration, Limiting Cyclic Pullup at V_{NRP}, Maneuver Limited by Flapping.

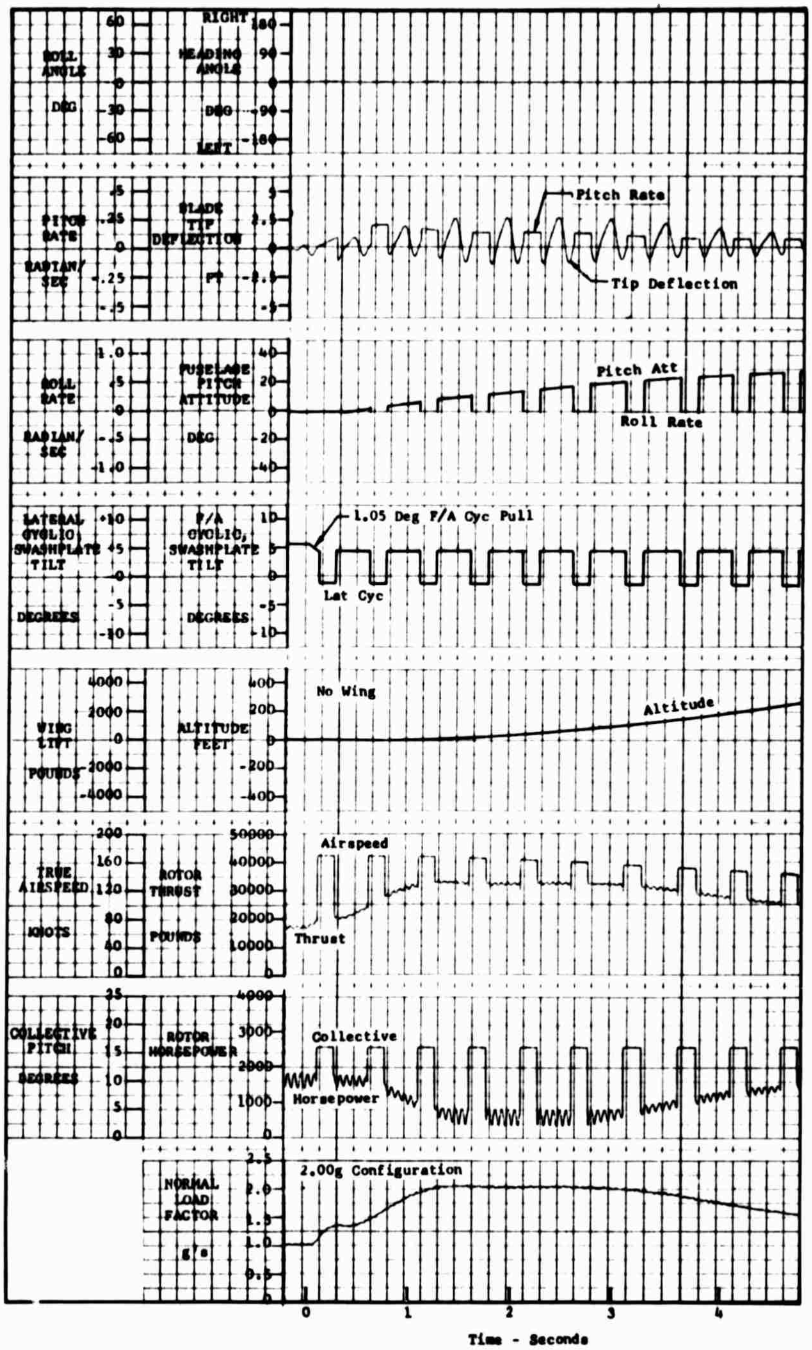

Figure 74. Maneuver Time History, 2.00g Configuration, Limiting Cyclic Pullup at V_{NRP}, Maneuver Limited by Flapping.

A key aspect of the maneuver results presented in Figures 69 through 71 is the variation of load factors achieved with different types of control inputs--cyclic-only, collective-only, and collective + cyclic. Of particular interest are the pullup maneuvers at the airspeeds at which all three types of control inputs were applied--89, 120, and 150 KTAS. To illustrate the impact of control input type, the three limiting pullup maneuvers for the 2.00g configuration at 150 KTAS are presented as follows:

Figure 75. Limiting Cyclic Pullup
Figure 76. Limiting Collective Pullup
Figure 77. Limiting Collective + Cyclic Pullup

These three maneuvers, though for the same configuration and airspeed, had three different limiting criteria and achieved three different load factors.

The limiting cyclic pullup, Figure 75, achieved a load factor capability of 2.07 g's, the maneuver being limited by the zero horsepower criterion. This result was typical for all cyclic pullup maneuvers in the mid-airspeed range--89 to 150 KTAS. These maneuvers were limited by zero horsepower for two reasons:

1. The early stages of a cyclic pullup maneuver are similar to an autorotational flight condition in which the rotor is "flared" to achieve powerless flight by extracting energy from the air.

2. In cyclic pullup maneuvers, a high pitch rate is established which alleviates stall by redistribution of the loading.

The characteristics of a collective pullup maneuver are much different from those of cyclic pullups. For the 2.00g configuration at 150 KTAS, Figure 76 gives the limiting collective pullup maneuver. The maneuver was limited by maximum horsepower at a sustained load factor of 1.95 g's. The increase in horsepower results from the fact that the thrust is increased by increasing the blade pitch, not by increasing the rotor angle of attack as in the flare maneuver. Additionally, in collective pullup maneuvers, the pitch rates are much less than in cyclic pullups and are not sufficient to significantly reduce stall effects. For further discussion of the effect of pitch rate on rotor stall see Reference 7.

Figure 77 presents the limiting collective + cyclic pullup for the 2.00g configuration at 150 KTAS. As would be expected, the characteristics of this maneuver were a compromise between those of cyclic-only and collective-only pullups.

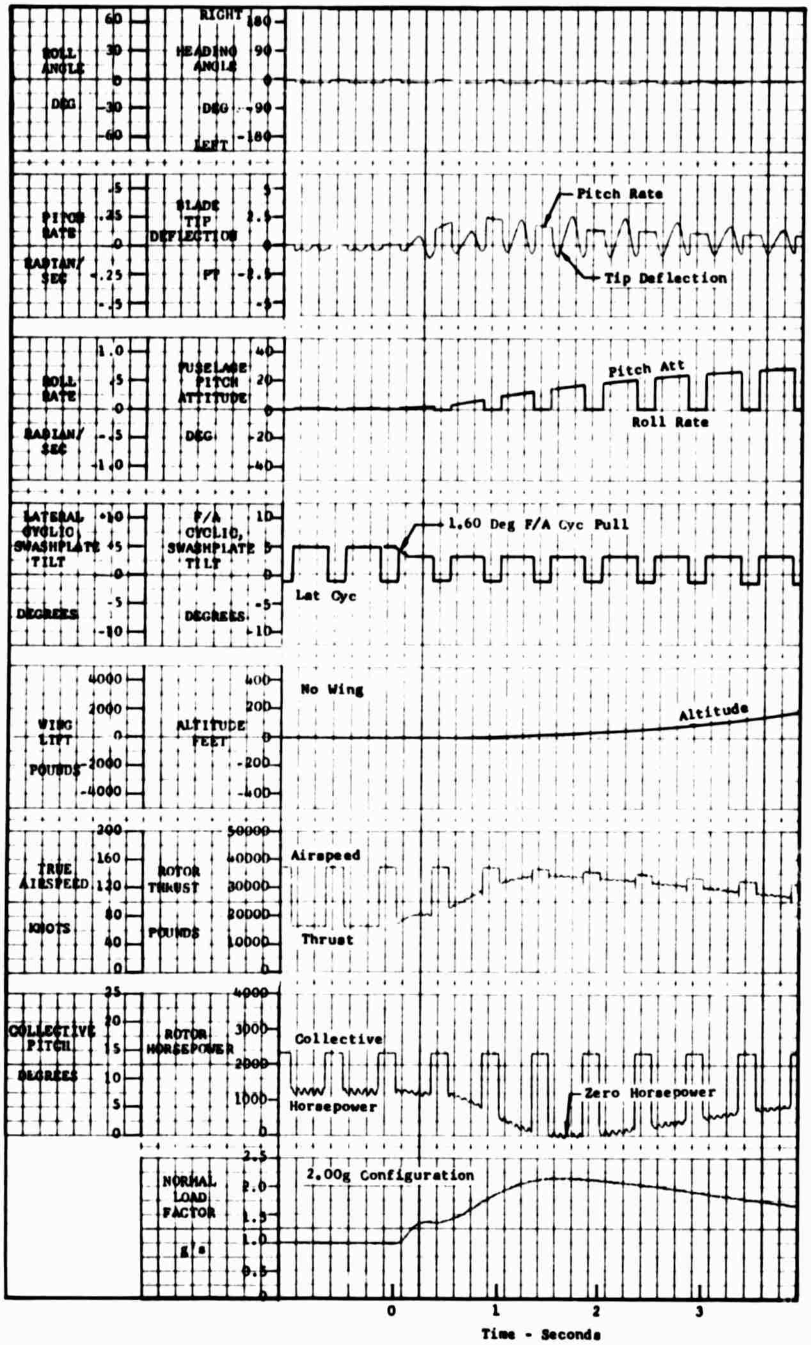

Figure 75. Maneuver Time History, 2.00g Configuration, Limiting Cyclic Pullup at 150 KTAS.

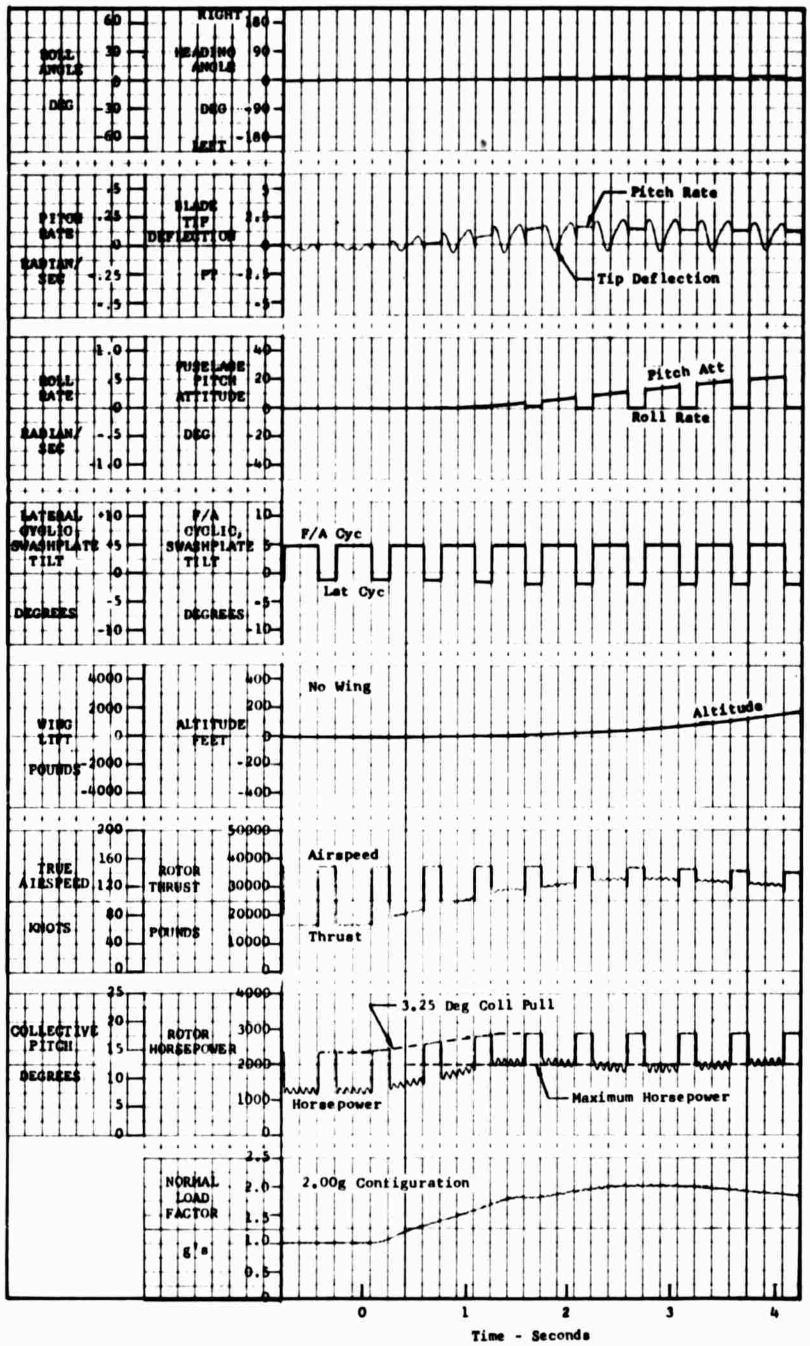

Figure 76. Maneuver Time History, 2.00g Configuration, Limiting Collective Pullup at 150 KTAS.

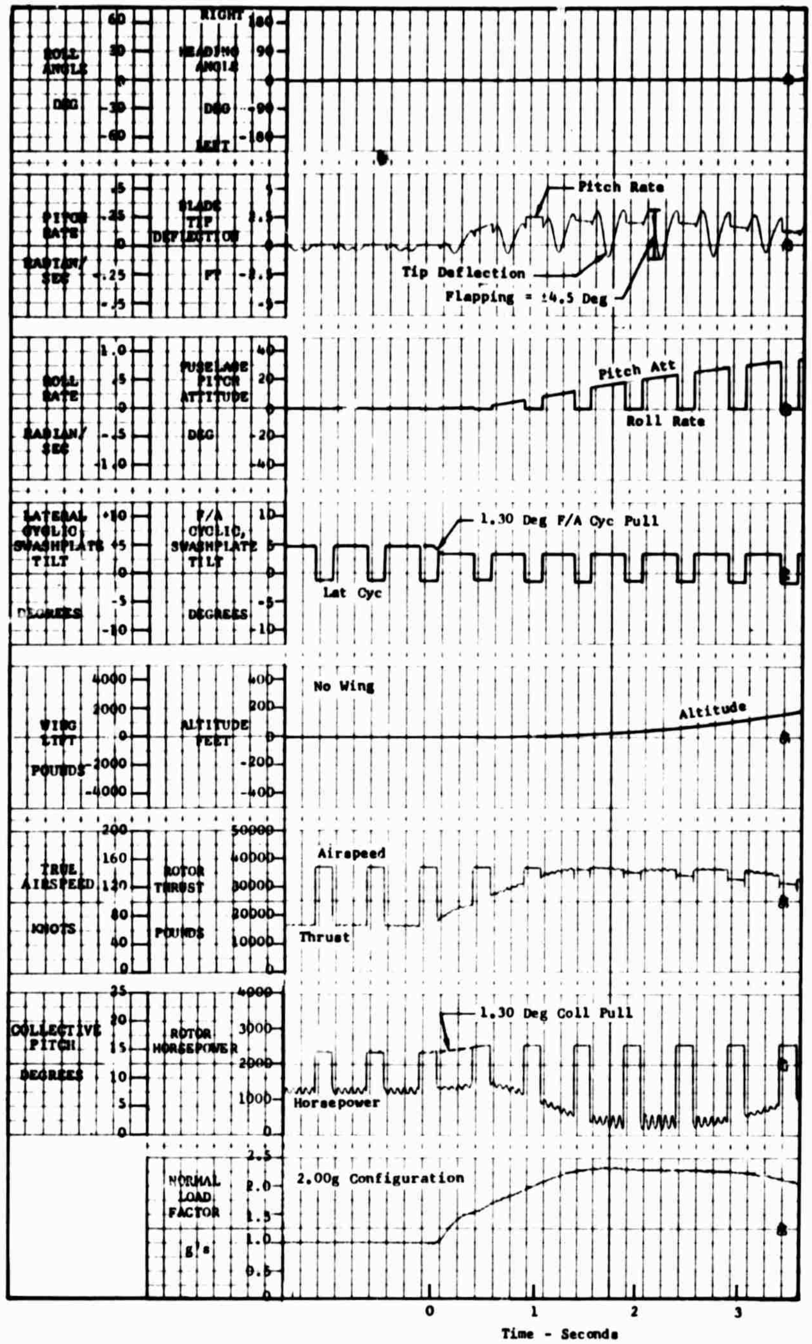

Figure 77. Maneuver Time History, 2.00g Configuration, Limiting Collective + Cyclic Pullup at 150 KTAS.

However, inspecting the pitch rate and horsepower traces of Figure 77 would indicate that the cyclic pullup characteristics predominate. The pitch rate was relatively high and the horsepower tended toward zero, but it was prevented from actually reaching zero by the collective pull. Consequently, a much higher load factor (2.30 g's) was achieved, and the maneuver was ultimately limited by the flapping criterion.

Flight Path Changes in Pullup Maneuvers

Tables XXIII and XXIV present the changes in airspeed and altitude which were noted in the pullup and pushover maneuver for the Task III configurations at airspeeds of 120 and 150 KTAS, and at V_{NRP}. Also given are the horizontal distances required to clear 200-foot vertical obstacles in the limiting pullup and pushover maneuvers. These distances include a 0.7-second pilot response time. Only the pullup maneuvers will be discussed herein.

As purely physical reasoning would indicate, the amount of altitude gained per unit of time in a pullup maneuver is only a function of the load factor, i.e., is independent of the configuration and airspeed considered. These facts can be illustrated by using the data of Table XXIII. Figure 78 presents the altitude gained in pullup maneuvers after 3.0 seconds as a function of load factor. The data was taken from Table XXIII, using the collective + cyclic pullup results at 120 and 150 KTAS and at V_{NRP}. Only the differences in configuration are identified on the curve. Independent of airspeed or configuration, a 1.50g pullup maneuver gained about 40 feet after 3.0 seconds, and a 2.00g maneuver resulted in a 90-foot gain of altitude. Also, the altitude gain was essentially independent of the type of control input used. The cyclic-only and collective-only data could be added to Figure 78 without significantly changing the curve. The conclusions drawn from Figure 78 are valid because the load factor time histories had essentially the same shape for the three configurations investigated. Within the 3.0 second time interval evaluated, if the shape of the load factor curve had varied significantly, even if the peak and sustained load factors were the same, the altitude gained could have been different.

The airspeed loss in a pullup maneuver shown on Figure 79 results from the aft tilt of the thrust vector. Therefore, the airspeed loss is independent of the entry airspeed, but it is slightly a function of the configuration and is strongly influenced by the type of control input. To achieve the same load factor, a cyclic-only pullup would require more aft-tilt of the rotor than either a collective + cyclic or collective-only pullup. A collective pullup would require the least amount of aft rotor tilt. Therefore, cyclic-only maneuvers should result in

TABLE XXIII. FLIGHT PATH CHANGES IN PULLUP MANEUVERS-TASK III CONFIGURATIONS

Design g-Level	Airspeed (KTAS)	Control Type	Sustained Load Factor (g)	Flight Path Changes After 3.0 Seconds Airspeed (KTAS)	Flight Path Changes After 3.0 Seconds Altitude (Feet)	Obstacle Clearance Distance* (Feet)
1.50g	177-V_{NRP}	Cyclic	1.45	-5	+45	1854
		Collective + Cyclic	1.40	-3	+40	1989
	150	Cyclic	1.76	-12	+65	1284
		Collective + Cyclic	1.73	-8	+60	1298
		Collective	1.68	-4	+55	1412
	120	Cyclic	1.76	-14	+55	1028
		Collective + Cyclic	2.14	-20	+100	886
		Collective	1.84	-2	+50	1077
1.75g	175-V_{NRP}	Cyclic	1.70	-10	+65	[illegible]
		Collective + Cyclic	1.70	-7	+65	[illegible]
	150	Cyclic	1.97	-16	+80	1225
		Collective + Cyclic	1.96	-14	+70	1209
		Collective	1.92	-4	+60	1292
	120	Cyclic	1.79	-14	+65	1012
		Collective + Cyclic	2.40	-28	+110	820
		Collective	1.80	-2	+65	1067
2.00g	170-V_{NRP}	Cyclic	2.03	-12	+90	1329
		Collective + Cyclic	2.00	-10	+90	1361
	150	Cyclic	2.07	-15	+90	1150
		Collective + Cyclic	2.30	-18	+110	1049
		Collective	1.95	-4	+70	1282
	120	Cyclic	1.90	-20	+70	968
		Collective + Cyclic	2.43	-24	+110	816
		Collective	1.76	-2	+60	1077

*Horizontal Distance Required to Clear 200-Ft Vertical Obstacle, 0.7 Sec Pilot Response Time.

TABLE XXIV. FLIGHT PATH CHANGES IN PUSHOVER MANEUVERS - TASK III CONFIGURATIONS

Design g-Level	Airspeed (KTAS)	Control Type	Sustained Load Factor (g)	Flight Path Changes After 3.0 Seconds: Airspeed (KTAS)	Flight Path Changes After 3.0 Seconds: Altitude (Feet)	Obstacle Clearance Distance* (Feet)
1.50g	177-V_{NRP}	Cyclic	0.08	+[illegible]	-90	1491
	150	Cyclic	0.05	+5	-85	1292
		Collective + Cyclic	0	+4	-90	1251
		Collective	-0.10	+3	-50	1384
	120	Cyclic	0.05	+7	-70	1092
		Collective + Cyclic	-0.10	+7	-100	1010
		Collective	-0.29	+3	-45	1172
1.75g	175-V_{NRP}	Cyclic	0.03	+2	-100	1406
	150	Cyclic	0	+5	-90	1254
		Collective + Cyclic	-0.05	+4	-110	1189
		Collective	-0.07	+2	-60	1344
	120	Cyclic	-0.07	+8	-90	1027
		Collective + Cyclic	-0.15	+8	-110	975
		Collective	-0.20	+4	-45	1160
2.00g	170-V_{NRP}	Cyclic	0	+2	-100	1369
	150	Cyclic	-0.06	+4	-100	1197
		Collective + Cyclic	-0.23	+4	-120	1137
		Collective	-0.19	+2	-60	1332
	120	Cyclic	-0.15	+7	-110	976
		Collective + Cyclic	-0.30	+7	-120	928
		Collective	-0.26	+4	-60	1124

*Horizontal Distance Required to Clear 200-Ft Vertical Obstacle, 0.7 Sec Pilot Response Time.

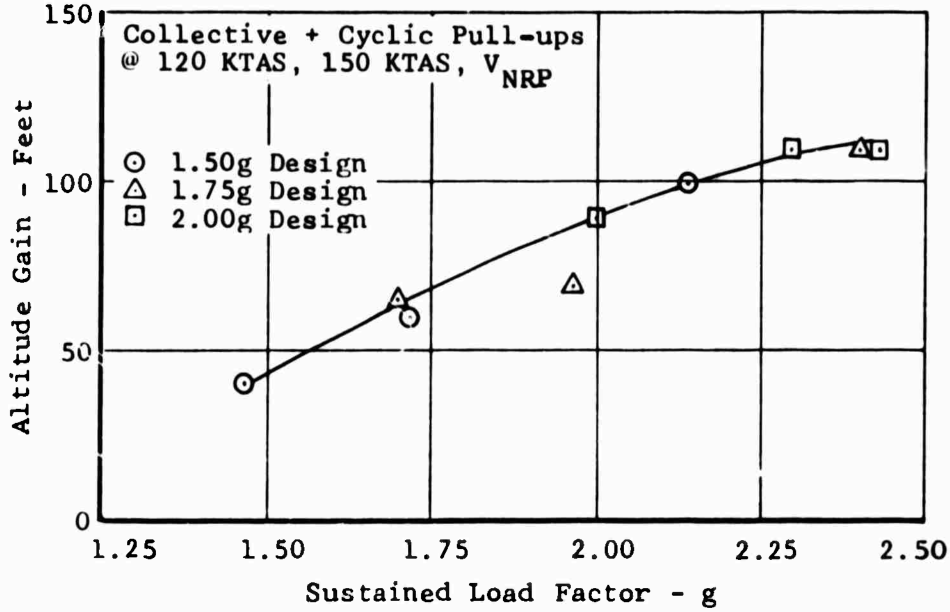

Figure 78. Task III Configurations,
Altitude Gain in Pullup Maneuvers
After Three Seconds.

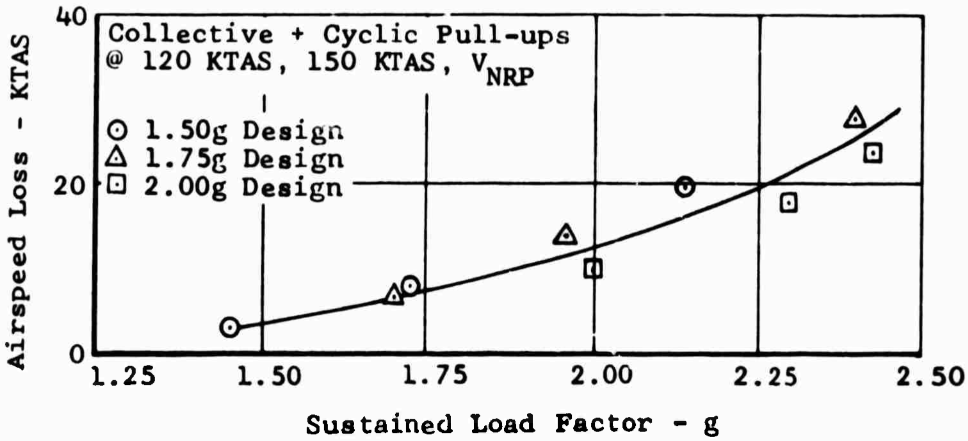

Figure 79. Task III Configurations,
Airspeed Loss in Pullup Maneuvers
After Three Seconds.

the largest airspeed loss, and collective-only maneuvers, the least. The collective + cyclic pullups result in an airspeed loss somewhere between the cyclic-only and collective-only pullups. Figure 79 presents the airspeed loss after 3.0 seconds for the Task III configurations in collective + cyclic pullup maneuvers at 120 and 150 KTAS and at V_{NRP}. As on Figure 78, only the configuration differences are identified. The data shows that the airspeed loss after 3.0 seconds ranged from 4 KTAS for a 1.50g collective + cyclic pullup to 12 KTAS for a 2.00g maneuver.

Figure 80 relates the design g-capability to the horizontal distance required to clear a 200-foot vertical obstacle in a pullup maneuver. The data was taken from Table XXIII, using the control type which resulted in the minimum distance required. The data includes a 0.7-second time allowance for the pilot response delay. As would be expected, at high airspeeds, the distance required was influenced by the design g-capability. For example, at 150 KTAS, the distance required was 1049 feet for the 2.00g configuration, but 1209 and 1284 feet were required for the 1.75g and 1.50g configurations respectively. However, at lower airspeeds, the distance required was much the same for all three configurations because the load factor capability was more nearly the same.

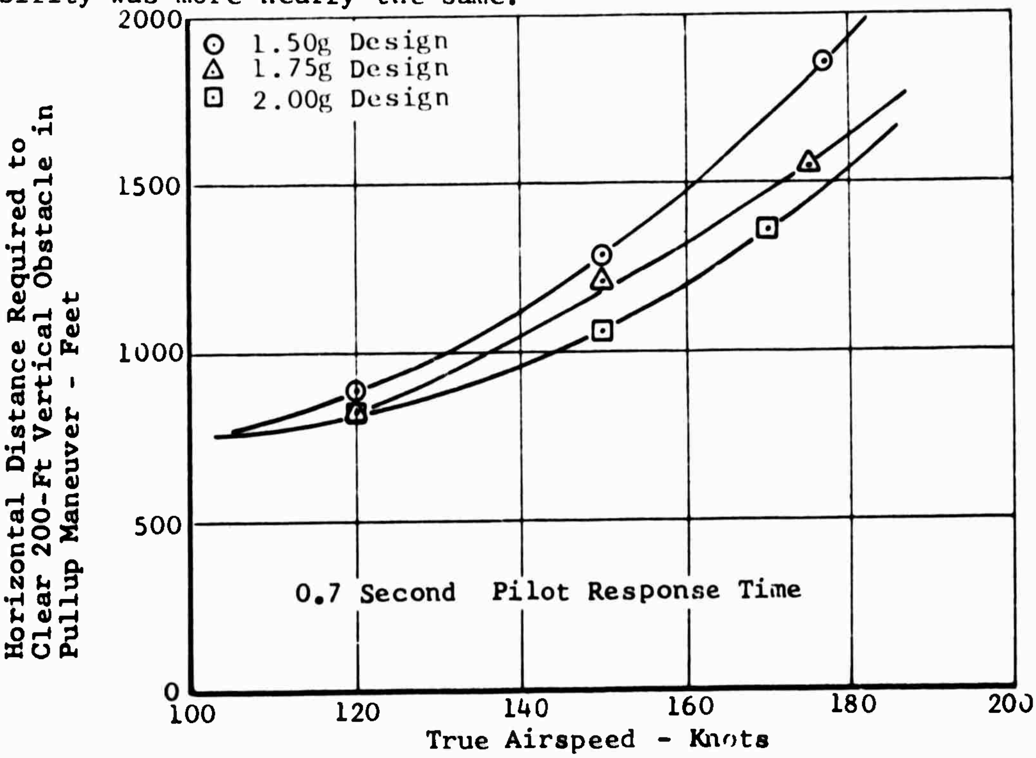

Figure 80. Effect of Design g-Capability on Distance Required to Clear 200-Foot Obstacle.

Coordinated Turns

The turning-flight load-factor capability of the Task III configurations was equal to the pullup maneuver capability. However, the important characteristic of the turn maneuvers was found to be the "bleeding" of airspeed or altitude which was necessary to satisfy the flight path constraints of constant altitude or airspeed.

To illustrate the flight path changes which occur in cyclic-only coordinated turns, Figure 81 gives the airspeed-loss in constant altitude turns, and Figure 82 shows the altitude-loss in constant airspeed turns. Both figures are for the 2.00g configuration, and the turn entry airspeed was 150 KTAS. The figures are summarized as follows:

Load Factor	Airspeed-Loss, Constant Altitude	Altitude-Loss, Constant Airspeed
1.50g	15 KTAS	350 Feet
1.75g	23 KTAS	450 Feet
2.00g	31 KTAS	550 Feet

If collective pitch was used in combination with cyclic to accomplish the turn, both airspeed and altitude were maintained throughout the turn. These turns were run to the maximum horsepower available limit. The results are summarized in Table XXV for the Task III configurations at airspeeds from 56 KTAS to 150 KTAS. The table shows that at 150 KTAS, only the 2.00g configuration had 2.00g constant airspeed and altitude turning capability. However, at 120 KTAS, all three configurations had 2.00g capability. At lower airspeeds, the capability remained roughly constant for all three designs, although less than 2.00 g's.

TABLE XXV. TURN CAPABILITY, CONSTANT AIRSPEED AND ALTITUDE, COLLECTIVE + CYCLIC TURNS, TASK III CONFIGURATIONS

Airspeed (KTAS)	Maximum Sustained Load Factor in Turning Flight Maintaining Altitude and Airspeed* 1.5g Design	1.75g Design	2.00g Design
150	1.75g	1.85g	2.00g
120	2.00g	2.00g	2.00g
89	1.90g	1.90g	1.96g
56	1.70g	1.65g	1.60g

* All turns limited by rotor horsepower available.

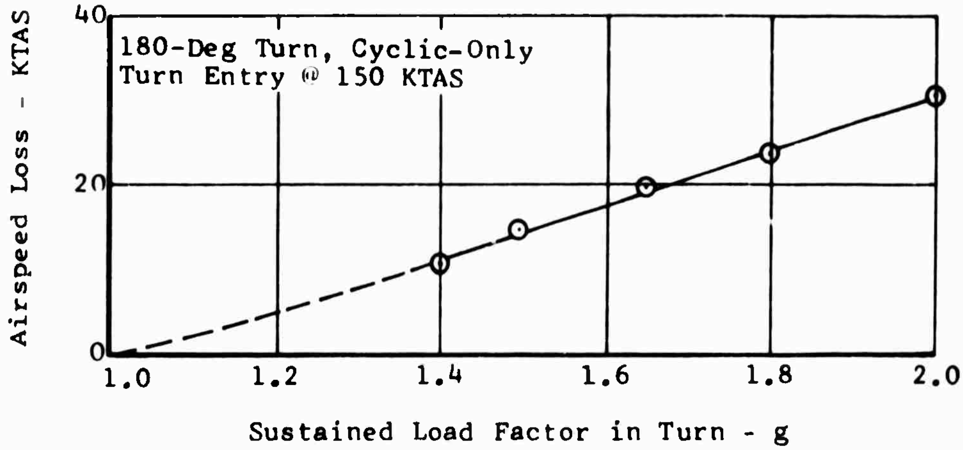

Figure 81. Task III - 2.00g Configuration, Airspeed Loss in Constant Altitude Turn.

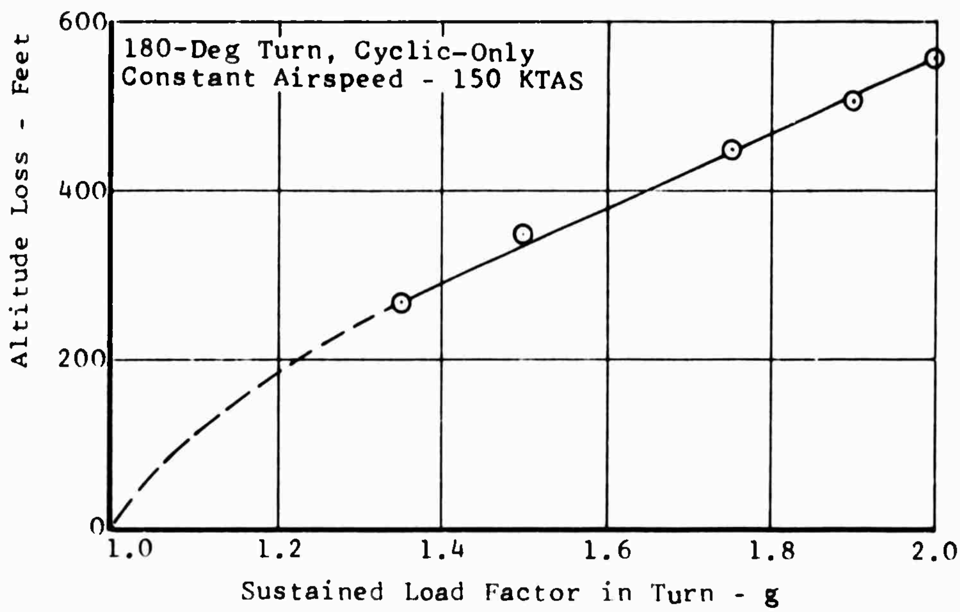

Figure 82. Task III - 2.00g Configuration, Altitude Loss in Constant Airspeed Turn.

ROTOR NOISE CHARACTERISTICS

The external noise produced by an aircraft and the resulting possibility of aural detection are characteristics of primary importance to low-level, nap-of-the-earth flight. Two aspects of detection are: the propagated noise which makes an observer aware that a new object has appeared or is about to appear on the horizon; and the aural signature which enables the observer to identify the object as an aircraft and, with experience, the type of aircraft. In the following paragraphs, the noise reduction features incorporated in the UTTAS design are described, and the flyover noise levels are estimated. The factors affecting aural detection are discussed, and the detection distance and arrival-interval are given, taking these factors into account.

Noise Reduction Features

The UTTAS design, as compared to that of the UH-1H, incorporates several noise reduction features. The main rotor tip speed is reduced approximately 11 percent. The number of rotor blades is increased from two to four for the main rotor and from two to three for the tail rotor. This not only reduces the noise level but, in the case of the main rotor, alters its aural signature by increasing the pulsing rate or blade passage frequency. An additional feature is the incorporation of advanced blade tips designed to mitigate high-speed noise due to compressibility effects. Still another feature is the partial unloading of the tail rotor by the vertical tail fin during forward flight conditions.

Estimated Levels

Rotor noise sources are classified as discrete-frequency and broadband. Discrete-frequency sources are associated with the blade pressure pattern and the blade thickness, and the broadband sources are associated with vortex shedding and the boundary layer. Asymmetrical aerodynamic loading produced by induced turbulence, wake interaction, compressibility, stall and interference affects both types of noise sources, and along with modulation and distortion effects, determines the acoustical signature of a helicopter rotor.

Calculation of the discrete-frequency noise components was based on the rotor noise theory developed by Lowson and Ollerhead (Reference 8). The calculation of the peak sound-pressure level of the broadband noise component, which is important only for main rotors, was based on an empirical equation given by Schlegel et al (Reference 9). The broadband component's center frequency, spectral distribution,and directivity were calculated using the formulas derived by Lowson (Reference 10).

The computational procedure consisted of the following: the individual noise components of the main and tail rotors were calculated separately for the hover condition, the sound-pressure levels of both rotors were added to obtain the combined spectrum, and then the perceived noise level was calculated.

Correlation studies show that the prediction technique is adequate for the hover condition but underestimates rotor noise at forward airspeeds, particularly at speeds where the advancing-tip Mach number exceeds 0.85. To account for this discrepancy, the incremental increase in noise, from hover to design cruise speed, was assumed to be the same as that measured for the UH-1H during flyovers, and verified by noise measurements of UH-1 main rotors in a wind tunnel (Reference 11). This delta increase was based on equivalent advancing tip Mach numbers. The noise mitigating effects on tip shapes were based on flyover test data and measured data from full-scale and model rotors in wind tunnels (Reference 12).

Estimated noise levels for the UTTAS vehicle are shown in Figure 83 and compared with measured data of the UH-1H during level-flight flyovers. The maximum benefits from the noise reduction features were realized at airspeeds above 100 knots. The lower main rotor tip speed permitted the UTTAS vehicle to fly at its design cruise speed (150 KTAS) at approximately the same advancing tip Mach number as the UH-1H at 100 knots. In fact, at airspeeds up to 190 knots, the flyover noise of the UTTAS vehicle was less than that of the UH-1H at 130 knots. At design cruise speed of 150 knots, the UTTAS vehicle was quieter by 7 PNdb than the UH-1H at 130 knots. At airspeeds below 100 knots the UTTAS was slightly louder, by approximately 2 PNdb, than the UH-1H.

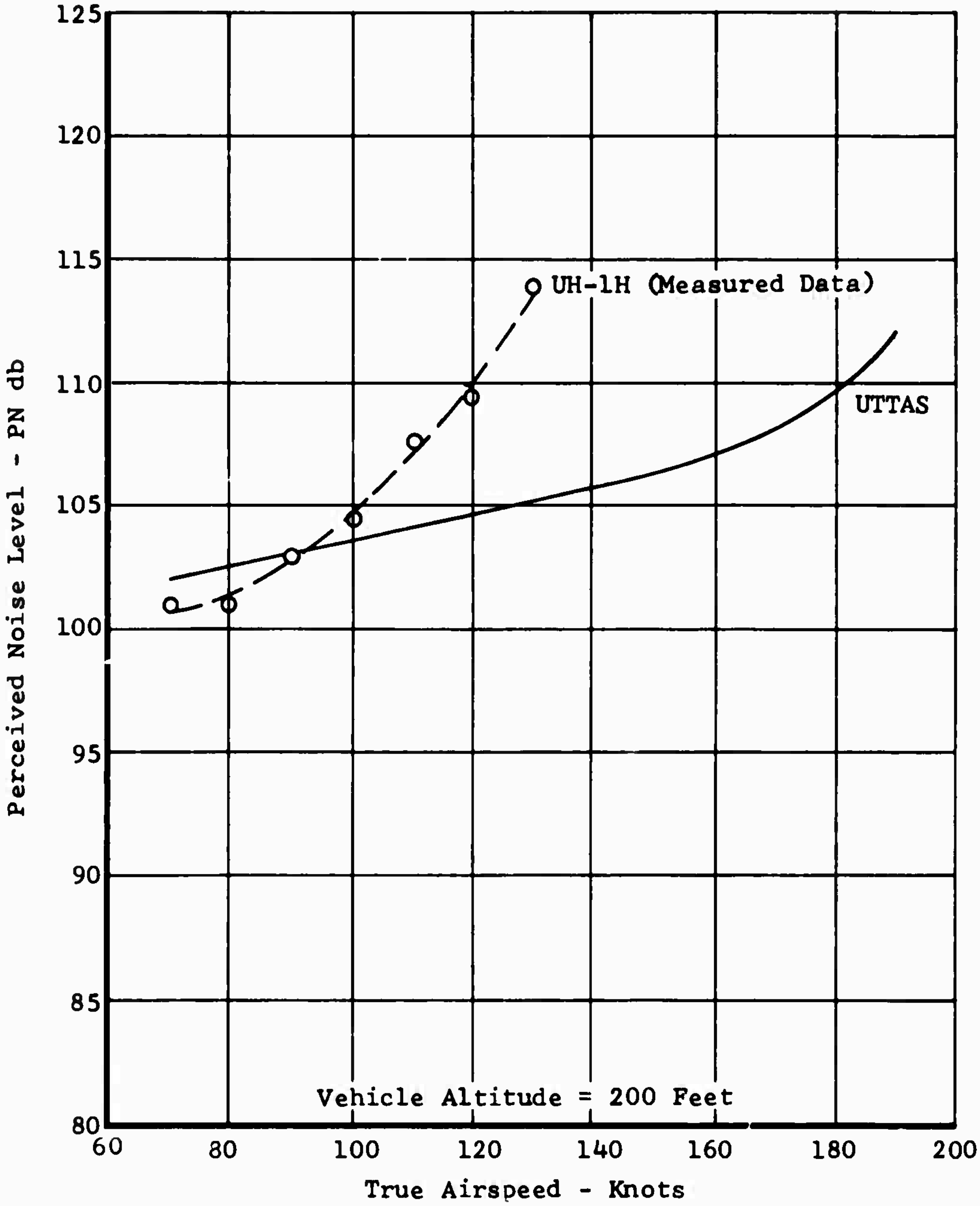

Figure 83. Estimated External Noise Level During Flyover.

Aural Detection Distance and Arrival-Interval

Factors which influence the propagation of a vehicle's noise are the spherical spreading of sound, atmospheric absorption, refraction by wind and temperature gradients, and attenuation of the terrain. In addition, the background noise at the observer determines the level at which the propagated sound can be detected.

The UTTAS vehicle's sound-pressure level and frequency spectrum, calculated for a range of 200 feet, were used as a basis in estimating the aural detection distance. To account for the spherical spreading of sound, six decibels per doubling of distance were subtracted from the spectral distribution. The attenuation of sound over open and partially wooded terrain was considered, and no beneficial or adverse effects of wind and temperature gradients were considered, although they can become significant factors. Background noise levels measured in remote areas were used to establish an aural detection criterion. Detection occurs when the vehicle's propagated noise is seven to nine decibels below the background noise.

The spectral distribution of the UTTAS vehicle is such that the critical source frequencies, the frequencies propagated the fartherest, occur in the 150-to 300-Hertz frequency range. The average background noise levels in this frequency range are approximately 28 decibels. Hence, detection is assumed to occur when the vehicle's propagated noise reaches a level of 20 decibels at the observer's position. This level corresponds to the average human ear's audibility threshold; therefore, the detection criterion chosen is considered to be conservative.

Considering the factors above, the aural detection distances of the UTTAS vehicle are given in Table XXVI for hover and for several level-flight approach speeds at an altitude of 200 feet. Calculated data for the UH-1H are presented also for comparison purposes.

It was estimated that the UTTAS vehicle will be aurally detected at a distance of 8700 feet during hover over partially wooded terrain, approximately 4 percent less than that estimated for the UH-1H. At cruise and higher maneuvering speeds, the detection range is correspondingly less for the UTTAS vehicle than for the UH-1H

The arrival-interval, defined as the time required for the aircraft to reach the observer after being aurally detected is often of more significance than the detection distance. Arrival-intervals for the UTTAS vehicle and UH-1H are estimated in Figure 84. As can be seen, the element of tactical surprise

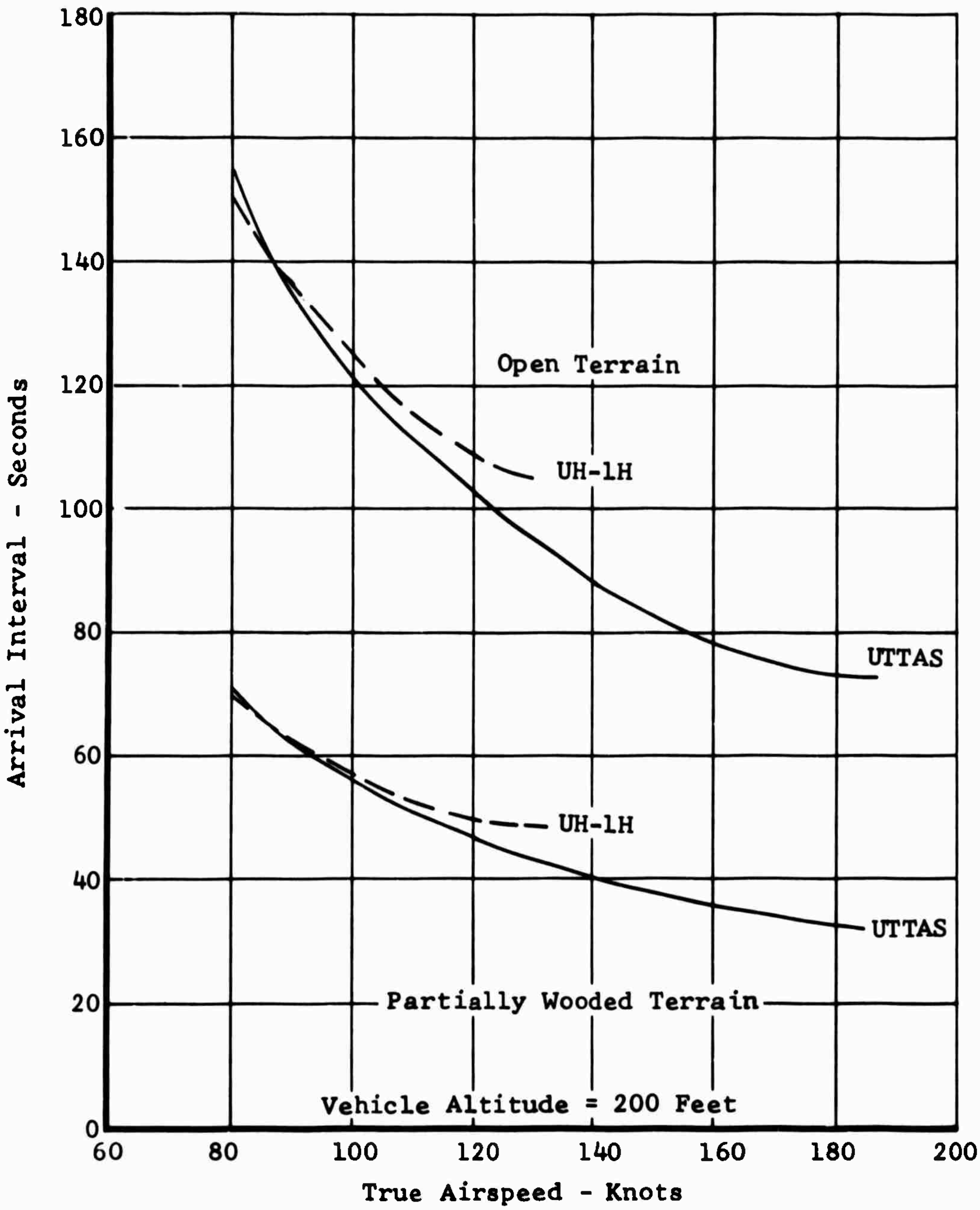

Figure 84. Estimated Arrival-Interval After Aural Detection.

TABLE XXVI. AURAL DETECTION DISTANCE		
	Detection Distance, Feet	
	Partially Wooded Terrain	Open Terrain
Hover		
UTTAS	8,700	18,200
UH-1H	9,100	20,100
Forward Flight		
UTTAS		
100 Kt	9,500	20,500
150 Kt	9,700	21,100
180 Kt	10,100	22,300
UH-1H		
100 Kt	9,700	21,100
130 Kt	10,600	23,000

is enhanced in the design of the UTTAS vehicle. At cruise speed and above, arrival-intervals are reduced by as much as 33 percent. Hence, in the use of the UTTAS vehicle in place of the UH-1N, a ground observer has one-third less time to take counter or evasive action.

ROTOR DESIGN AND FATIGUE EVALUATION

Objective

Parametric distributions of weight and stiffness were established for two separate rotor systems by an analytical design cycle that emphasized rotor fatigue life as the major criterion. The initial objective was to incur zero fatigue damage for the entire spectrum of normal flight conditions. The objective was later revised to specify a rotor fatigue life of 5000 hours, which still may be conservative with regard to other limiting factors such as leading-edge erosion and accidental physical damage.

Design Cycle

The analytical design cycle used in the study is illustrated in functional form in Figure 85. The status of each design was evaluated after each of three major operations, and a decision was made either to proceed with the evaluation of the current parameters or to revise the parameters and begin a new evaluation. For the baseline 2.0g configuration, twenty variations of rotor structural parameters were studied. Seven variations were studied for the alternate 1.5g configuration. Evaluations of the final rotor designs are given below, following a description of the analytical procedures and design rules that were used in the design cycle.

1. Selection of Initial Structural Parameters. An experimental 33-inch chord blade section, currently under development at BHC, was selected as the physical model for this study. This choice assured that the weight and stiffness values of the basic blade section would reflect current construction techniques. The weight and stiffness values were scaled to reflect the required chord lengths. The root-retention system was represented by the addition of doublers, tapering from 0.10R to 0.30R. The hub region (0.0R to 0.10R) was represented as a titanium flexure designed to locate the first inplane-cantilever natural frequency at 1.5 per rev and to incur no fatigue damage at ±4.5 degrees of rotor flapping.

2. Location of Natural Frequencies. BHC Computer Program C02 (Reference 2) was used to calculate natural frequencies for the selected parameters at specified values of rotor rpm and collective pitch. Both coupled and uncoupled natural frequencies are plotted automatically as a function of rotor speed. A fan of excitation frequencies is also plotted to aid in the evaluation of the frequency placement.

3. Rotor bending-moment distributions were computed for conditions at 4000 feet altitude, 95°F temperature by BHC Computer Program C81 (AGAJ68, Reference 13). The flight spectrum, established by BHC personnel in the Fatigue Evaluation Group, is presented in Table XXVII. Rotor loads were computed only for stabilized forward flight, turns, and pullups. Fatigue damage for the balance of the flight spectrum is nil or insignificant if reasonable life is shown for the high-speed level and maneuvering flight conditions. Oscillatory stress levels were calculated with the conservative assumption that the oscillatory beamwise and chordwise bending moments are adversely phased for the critical point at each radial location on the blade.

4. Revision of Structural Parameters. When revisions to the rotor structural parameters were required, manufacturing complexity and cost were considered by retaining a constant

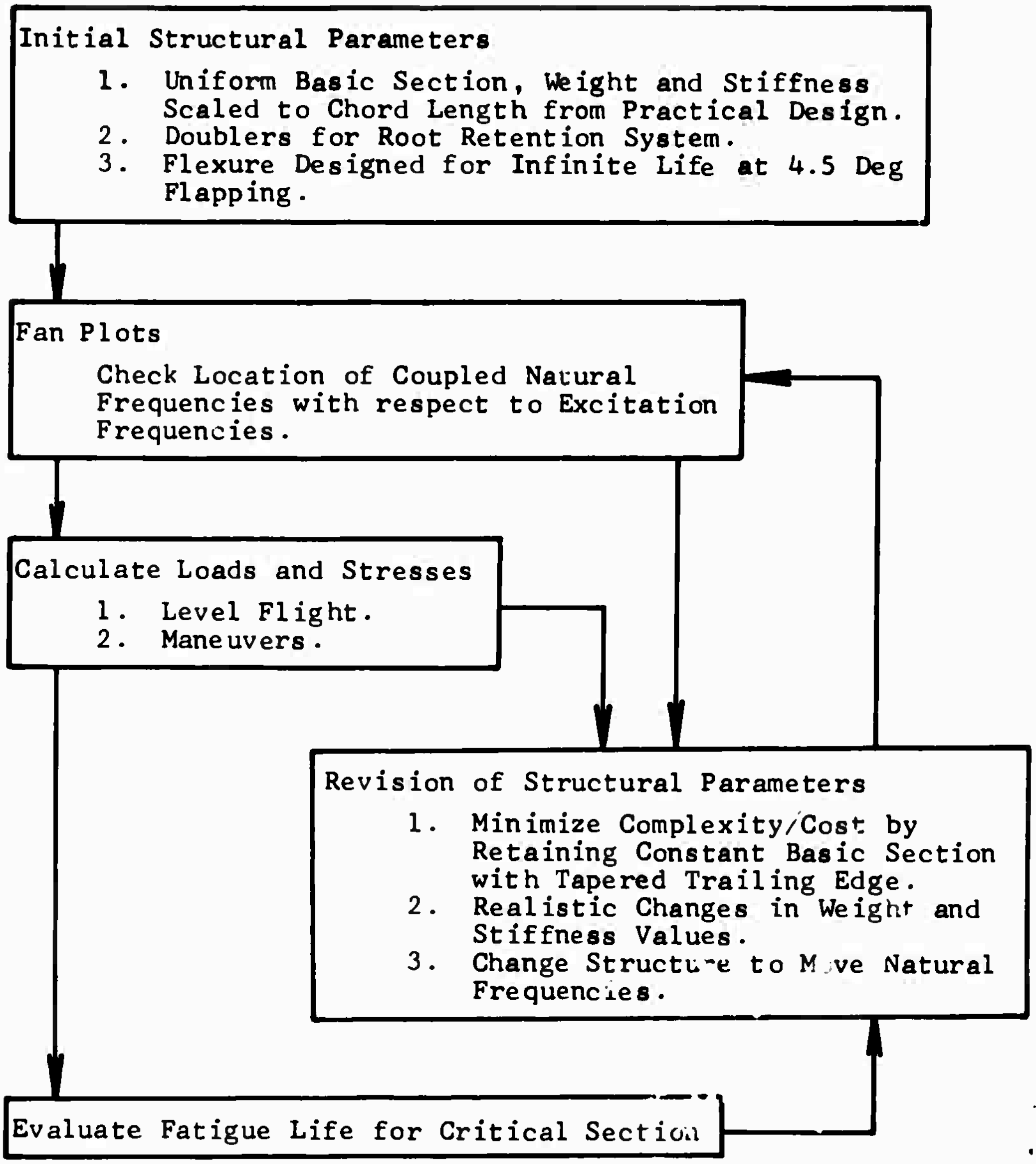

Figure 85. Rotor Design Cycle for Fatigue Evaluation.

TABLE XXVII. FLIGHT SPECTRUM - FREQUENCY OF OCCURRENCE

Flight Condition		% Time
I. Ground Conditions		2.50
II. IGE Maneuvers		7.07
III. OGE Flight		
A. Stabilized Forward Flight		80.0
0.2 V_H	1.0	
0.3 V_H	1.0	
0.4 V_H	2.0	
0.5 V_H	7.0	
0.6 V_H	6.0	
0.7 V_H	8.0	
0.8 V_H	15.0	
0.9 V_H	25.0	
V_H	12.0	
V_L	3.0	
B. Full-Power Climbs		2.00
C. Turns at 1.25 g's		1.20
0.5 V_H	.30	
0.7 V_H	.60	
0.9 V_H	.30	
D. Turns at 1.75 g's		2.00
0.5 V_H	.50	
0.7 V_H	1.00	
0.9 V_H	.50	

TABLE XXVII. - Continued			
Flight Condition			% Time
E.	Turns at 2.00 g's		.80
	0.5 V_H	.20	
	0.7 V_H	.40	
	0.9 V_H	.20	
F.	Cyclic Pullup at 1.25 g's		.075
	0.5 V_H	.03	
	0.9 V_H	.045	
G.	Cyclic Pullup at 1.75 g's		.125
	0.5 V_H	.05	
	0.9 V_H	.075	
H.	Cyclic Pullup at 2.00 g's		.050
	0.5 V_H	.02	
	0.9 V_H	.03	
I.	Steady Hover		1.00
J.	Control Reversals		.18
K.	Normal Acceleration		1.00
L.	Normal Deceleration		1.00
M.	Partial Power Descent		1.00

basic-blade section with the exception of a tapered trailing edge. Changes in weight and stiffness values were made in a manner consistent with the restraint imposed by an external airfoil shape of fixed dimensions.

An iteration cycle for the selection of rotor structural parameters was outlined in the study proposal (Reference 14, pages 8, 9). According to that proposal, section properties at local spanwise stations would be altered to eliminate both overstressed and understressed regions, resulting in a non-uniform beam. If a rotor natural frequency is located closely below an excitation frequency, stiffening the overstressed region of the blade will drive the natural frequency higher, and, ultimately, an unrealistic rotor design will result. The procedure used during the study, therefore, emphasized satisfactory location of the rotor natural frequencies before rotor loads were calculated for the flight spectrum.

5. Fatigue Life Evaluation. The rotor-blade fatigue life was calculated according to the cumulative-damage theory (Reference 15); the frequency-of-occurrence values shown in Table XXVII were used. The critical section for all rotors was at 0.55R, for which a mean stress level of 13,000 psi was assumed. No fatigue damage was calculated for oscillatory stress levels less then 4,000 psi.

Rotor Design for Baseline 2.0g Configuration

Weight and stiffness distributions for the baseline rotor (2.0g configuration) are given in Table XXVIII. Figures 86 and 87 are natural-frequency fan plots for the collective modes and cyclic modes, respectively. For rigid rotors, the only difference between the mode types is that the collective modes are pinned inplane (free to pivot about the mast axis) while the cyclic modes are cantilevered inplane (not free to pivot).

Oscillatory stress levels are plotted versus radial station in Figure 88 for the level flight conditions. The V_L flight condition was calculated at a 6-degree dive angle to correspond to the military-rated power limit of the baseline rotorcraft configuration. Loads and stresses for the low-speed and low-g flight conditions were not calculated because the absence of fatigue damage for these conditions was confirmed during prior fatigue evaluations. The critical section is at 0.55R for all flight conditions for which loads were computed.

The fatigue life calculated for the baseline rotor was 2800 hours, as shown in Table XXIX. The largest amount of damage was incurred for V_L in a 6-degree dive. If the frequency of occurrence for this flight condition were assigned a lower value,

TABLE XXVIII. STRUCTURAL PARAMETERS FOR BASELINE ROTOR

Diameter: 57.5 Feet | Blades: Four
Chord: 29.8 Inches | Hub Type: Rigid

Segment (Δr = 0.05R)	Beamwise EI/10^6 (lb-in.^{2})	Chordwise EI/10^6 (lb-in.^{2})	Weight/Inch (lb/in.)
1	15.30	10272.	7.000
2	11.10	2338.	4.000
3	1625.00	2800.	4.300
4	223.00	9425.	1.620
5	121.00	7950.	1.130
6	87.80	7783.	0.980
7	62.50	7666.	0.927
8	61.30	6975.	0.909
9	61.20	6275.	0.896
10	61.10	5565.	0.880
11	61.00	4850.	0.865
12	60.90	4215.	0.854
13	60.90	3997.	0.845
14	60.90	3853.	0.841
15	60.90	3693.	0.838
16	60.90	3571.	0.833
17	60.90	3571.	0.833
18	60.90	3571.	0.833
19	60.90	3571.	0.833
20	60.90	3571.	0.833
			(25 lb Tip Wt)

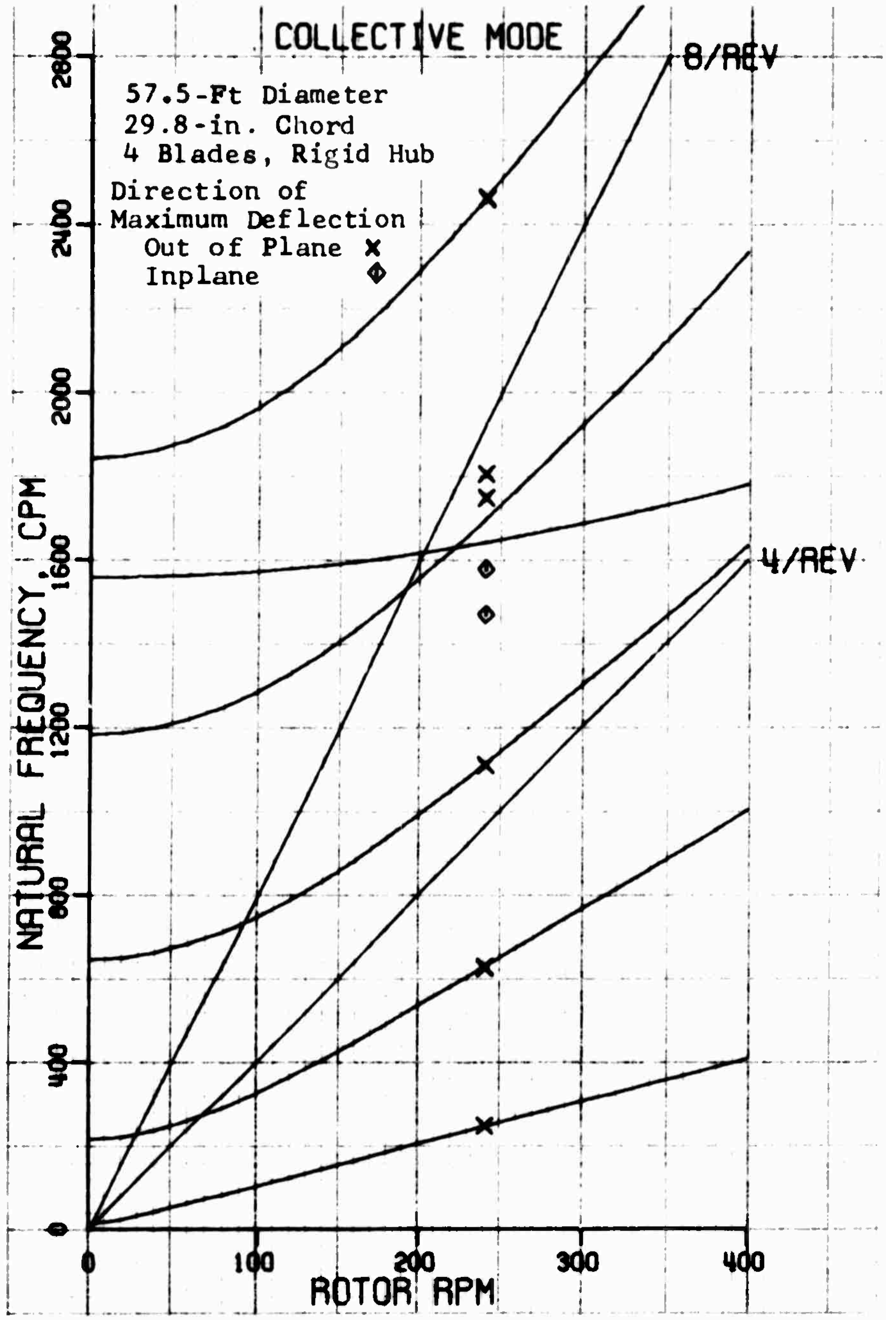

Figure 86. Collective Mode Frequencies for Baseline Rotor.

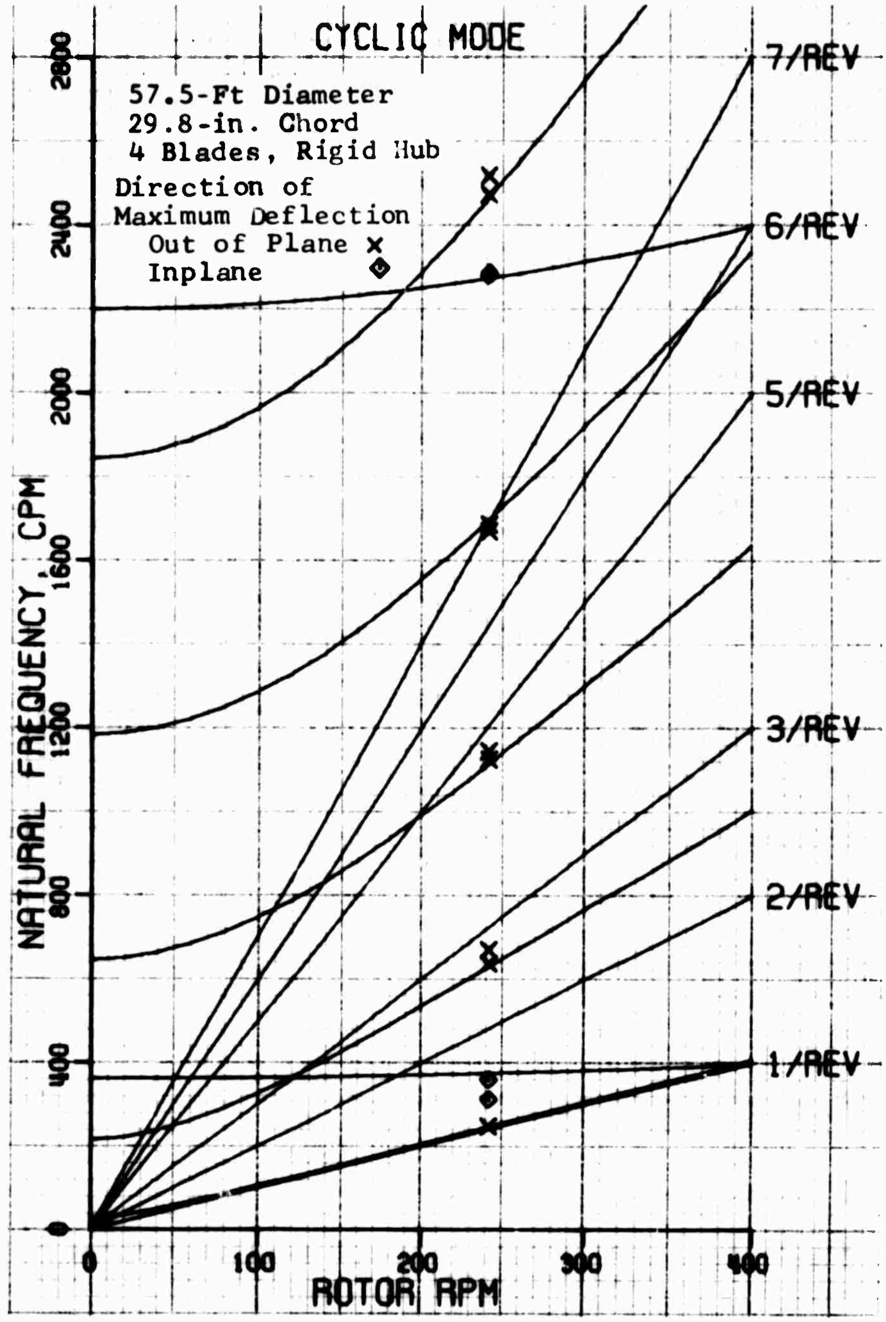

Figure 87. Cyclic Mode Frequencies for Baseline Rotor.

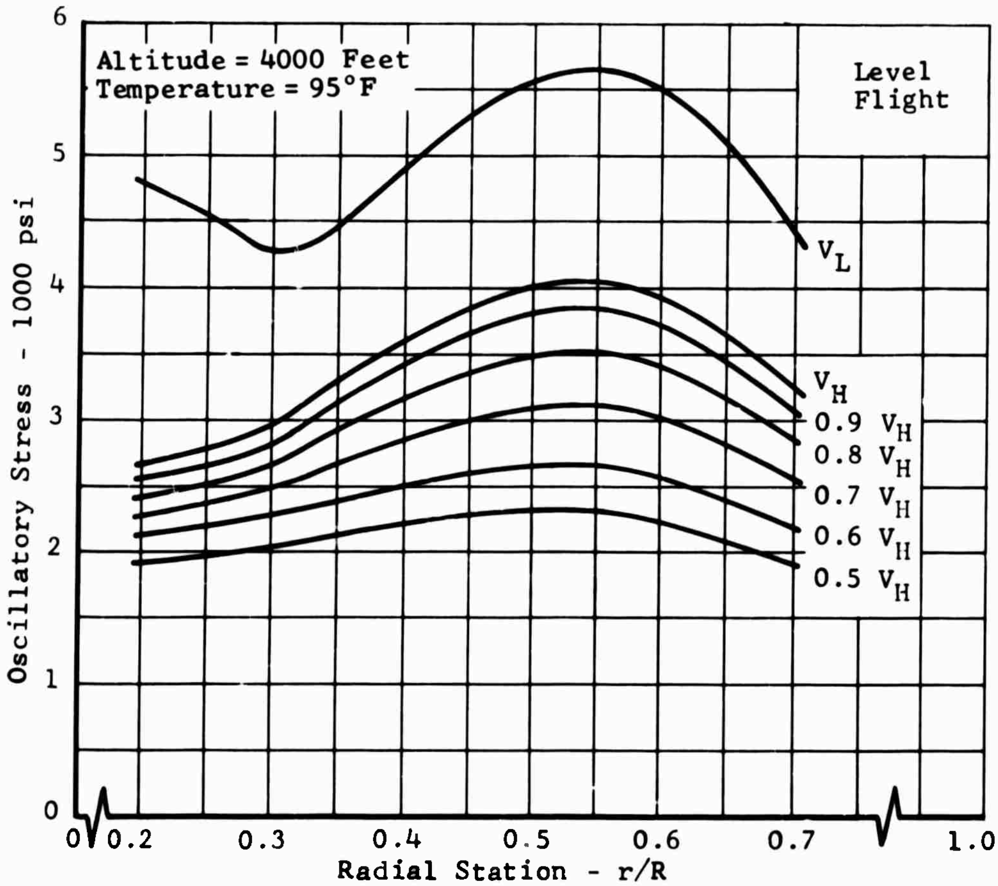

Figure 88. Oscillatory Stress Distributions for Baseline Rotor.

TABLE XXIX. FATIGUE EVALUATION, BASELINE ROTOR

Flight Condition	Flight Time (%)	Oscillatory Stress (psi)	Damage Fraction
Stabilized 1.0g Flight			
0.2 V_H	1.0		
0.3 V_H	1.0		
0.4 V_H	2.0		
0.5 V_H	7.0	2350	-
0.6 V_H	6.0	2670	-
0.7 V_H	8.0	3140	-
0.8 V_H	15.0	3530	-
0.9 V_H	25.0	3870	-
V_H	12.0	4080	.002381
V_L	3.0	5690	.018763
Turns at 1.25g			
0.5 V_H	0.3		
0.7 V_H	0.6		
0.9 V_H	0.3		
Turns at 1.75g			
0.5 V_H	0.5		
0.7 V_H	1.0	3970	-
0.9 V_H	0.5	5670	.003061

TABLE XXIX. - Continued			
Flight Condition	Flight Time (%)	Oscillatory Stress (psi)	Damage Fraction
Turns at 2.00g			
0.5 V_H	0.2		
0.7 V_H	0.4	3220	-
0.9 V_H	0.2	6100	.002087
Pullups at 1.25g			
0.5 V_H	0.03		
0.9 V_H	0.045		
Pullups at 1.75g			
0.5 V_H	0.05	2900	-
0.9 V_H	0.075	9140	.008535
Pullups at 2.00g			
0.5 V_H	0.02	3480	-
0.9 V_H	0.03	7110	.000830
		Total Damage Fraction =	.035653

$$\text{Fatigue Life} = \frac{100 \text{ Hours}}{.035653} = 2800 \text{ Hours}$$

the fatigue life would be increased. Reference 16 shows that the frequency of occurrence for limit-speed flight is a function of installed power.

Rotor Design for Alternate 1.5g Configuration

Weight and stiffness distributions for the alternate rotor (1.5g configuration) are given in Table XXX. Figures 89 and 90 are natural-frequency fan plots for the collective and cyclic modes, respectively.

The flight-spectrum specifications were changed to reflect the lower maneuvering requirement. In Table XXVII, 1.50g was substituted for 2.00g, 1.375g was substituted for 1.75g, etc. Similar to the baseline rotor, the critical section was at 0.55R for all flight conditions. The only flight condition incurring damage is at V_L. That condition was run for level flight, however, and required an excessive amount of power. Reducing the power required by diving would result in lower stresses and a longer fatigue life. As shown in Table XXXI, the fatigue life calculated for the alternate rotor was well in excess of 5000 hours.

TABLE XXX. STRUCTURAL PARAMETERS FOR ALTERNATE ROTOR

Diameter: 55.4 Feet Blades: Four
Chord: 22.2 Inches Hub Type: Rigid

Segment (Δr = 0.05R)	Beamwise EI/10^6 (lb-in.^{2})	Chordwise EI/10^6 (lb-in.^{2})	Weight/Inch (lb/in.)
1	11.40	9566.	6.340
2	8.27	2177.	3.620
3	1210.00	2086.	3.900
4	166.00	7022.	1.470
5	90.10	5920.	1.020
6	65.40	5800.	0.888
7	57.80	5710.	0.840
8	56.60	5200.	0.823
9	56.60	4670.	0.812
10	56.50	4150.	0.797
11	56.40	3610.	0.783
12	56.30	3140.	0.774
13	56.30	2980.	0.765
14	56.30	2870.	0.762
15	56.30	2750.	0.759
16	56.30	2660.	0.755
17	56.30	2660.	0.755
18	56.30	2660.	0.755
19	56.30	2660.	0.755
20	56.30	2660.	0.755
			(25 lb Tip Wt)

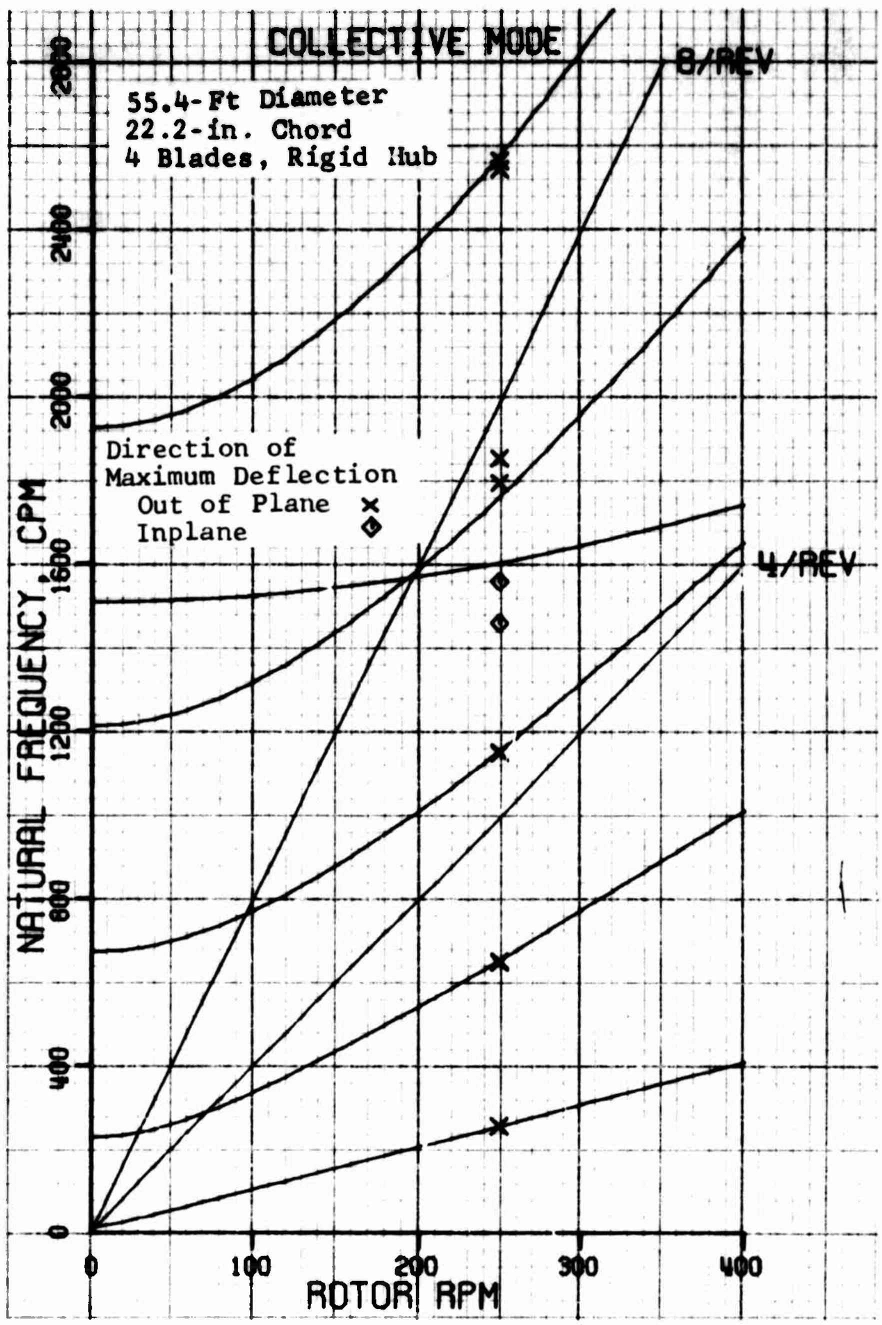

Figure 89. Collective Mode Frequencies for Alternate Rotor.

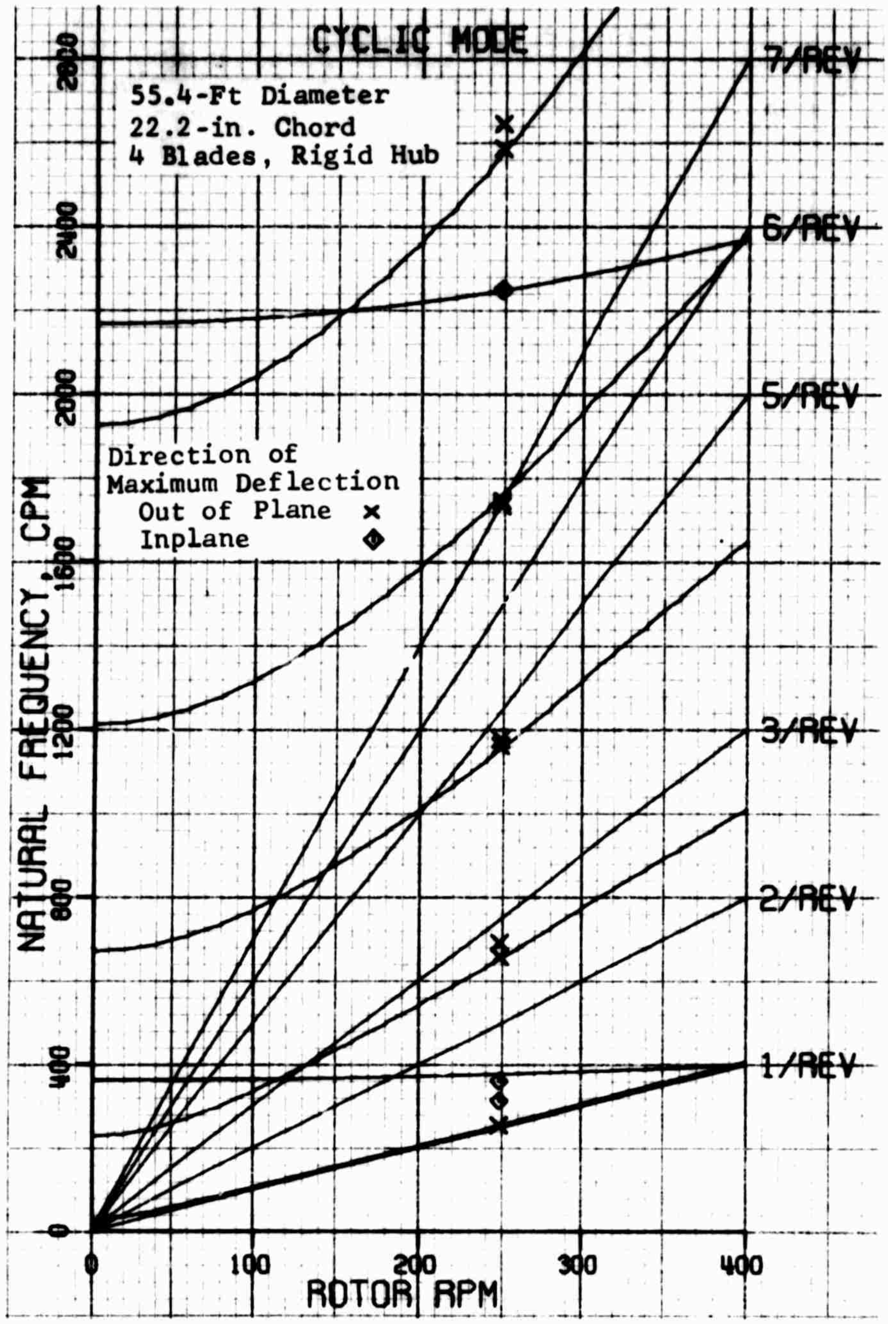

Figure 90. Cyclic Mode Frequencies for Alternate Rotor.

TABLE XXXI. FATIGUE EVALUATION, ALTERNATE ROTOR

Flight Condition	Flight Time (%)	Oscillatory Stress (psi)	Damage Fraction
Stabilized 1.0g Flight			
0.2 V_H	1.0		
0.3 V_H	1.0		
0.4 V_H	2.0		
0.5 V_H	7.0		
0.6 V_H	6.0		
0.7 V_H	8.0		
0.8 V_H	15.0		
0.9 V_H	25.0	2800	-
V_H	12.0	3280	-
V_L	3.0	5110	.008063
Turns at 1.125g			
0.5 V_H	0.3		
0.7 V_H	0.6		
0.9 V_H	0.3		
Turns at 1.375g			
0.5 V_H	0.5		
0.7 V_H	1.0	2650	-
0.9 V_H	0.5	3260	-

TABLE XXXI. - Continued			
Flight Condition	Flight Time (%)	Oscillatory Stress (psi)	Damage Fraction
Turns at 1.50g			
0.5 V_H	0.2		
0.7 V_H	0.4	2940	-
0.9 V_H	0.2	3940	-
Pullups at 1.125g			
0.5 V_H	0.03		
0.9 V_H	0.045		
Pullups at 1.375g			
0.5 V_H	0.05	2000	-
0.9 V_H	0.075	3440	-
Pullups at 1.50g			
0.5 V_H	0.02		
0.9 V_H	0.03	3670	-
		Total Damage Fraction =	.008063

$$\text{Fatigue Life} = \frac{100 \text{ Hours}}{.008063} = \text{Over 5000 Hours}$$

UTTAS MANEUVERING CONSIDERATIONS

The question of a recommended maneuvering requirement for UTTAS vehicles cannot be answered without consideration of additional factors that are subjective and beyond the scope of this study. Among these are turning radius and dive recovery.

Figure 91 presents the relationship of speed, maneuvering load factor, and turn radius. All UTTAS vehicles defined by the ground rules of this study had normal rated power level flight speeds that were 170 KTAS or greater. At 170 KTAS, a 1.50g capability results in a 2500-foot turn radius. During a 180-degree turn, the aircraft would describe a semicircle with a diameter of approximately one mile. With a 2.00g capability, the diameter is still greater than 3000 feet. In order to maintain reasonable turning radii without slowing the aircraft excessively, the higher maneuvering capability would certainly be indicated.

If the stringent MIL-S-8698 definition of Dive Speed (V_L) = 1.2 x V_H is used, UTTAS vehicles will characteristically have dive speeds in excess of 220 knots. At these speeds, rate of descent is necessarily high and dive recovery capability becomes an item of concern. Figure 92 shows representative dive conditions for the three helicopter configurations studied during Task III.

Figure 93 presents the altitude lost during dive recovery from these conditions for the pure helicopter configurations of Task III and a representative synthesized configuration with a small wing. From this comparison, it is apparent that pure helicopters sized for V_{NRP} maneuver capabilities of less than 2.0g have large altitude losses during dive recovery situations. At these high dynamic pressure conditions, the wing is very effective in the improvement of dive recovery characteristics. Both types of aircraft would appear to be adequate if they possess a 2.0g capability at V_{NRP}. This argument, coupled with the difficulty of attaining zero g maneuverability with winged configurations, would lead to the conclusion that a feasible configuration is a pure helicopter with a V_{NRP} capability of 2.00g's or greater.

The positive load factor requirement, however, is directly tied to the dive speed definition. If the UTTAS criterion results in dive speeds in the 200-210K range, it would be possible to provide adequate dive recovery capability with a smaller rotor system that was sized for less than 2.00g at V_{NRP}. The reduced size rotor would be reflected in reduced engine power requirements, less fuel required, and a generally smaller aircraft with a proportionate cost saving. For example,

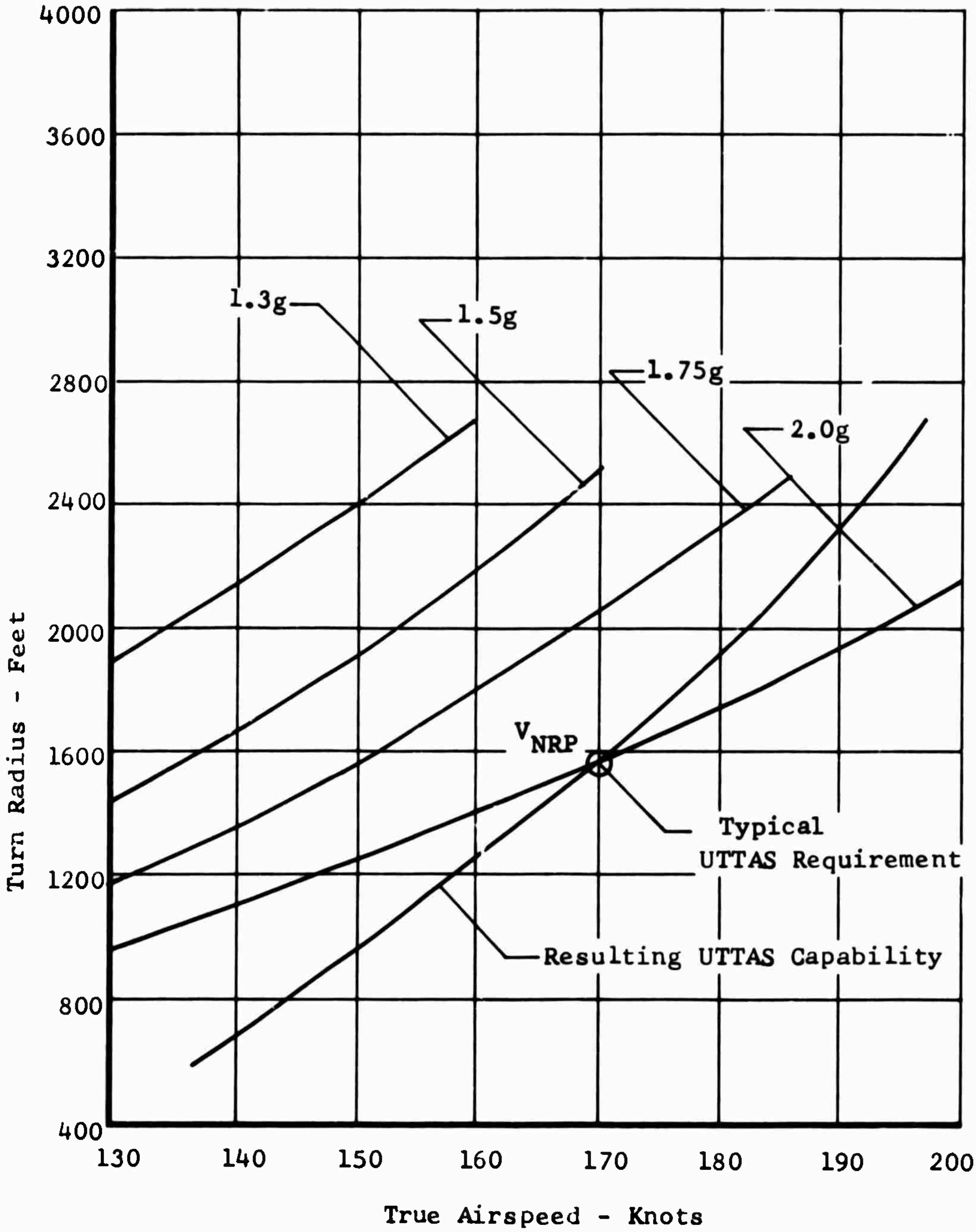

Figure 91. Turn Radius vs Speed.

the design that was sized for 1.75g capability at V_{NRP} has a 2.00g capability at 150 KTAS and offers a gross weight reduction of 960 pounds compared to the 2.00g configuration. Other factors which would support a recommendation in favor of a high maneuvering capability are: an aircraft with good maneuvering characteristics can be expected to maintain higher speed during nap-of-the-earth flight; and normal maneuvers will utilize less of the rotor's limit capability which will avoid high structural stresses and should reduce vibration.

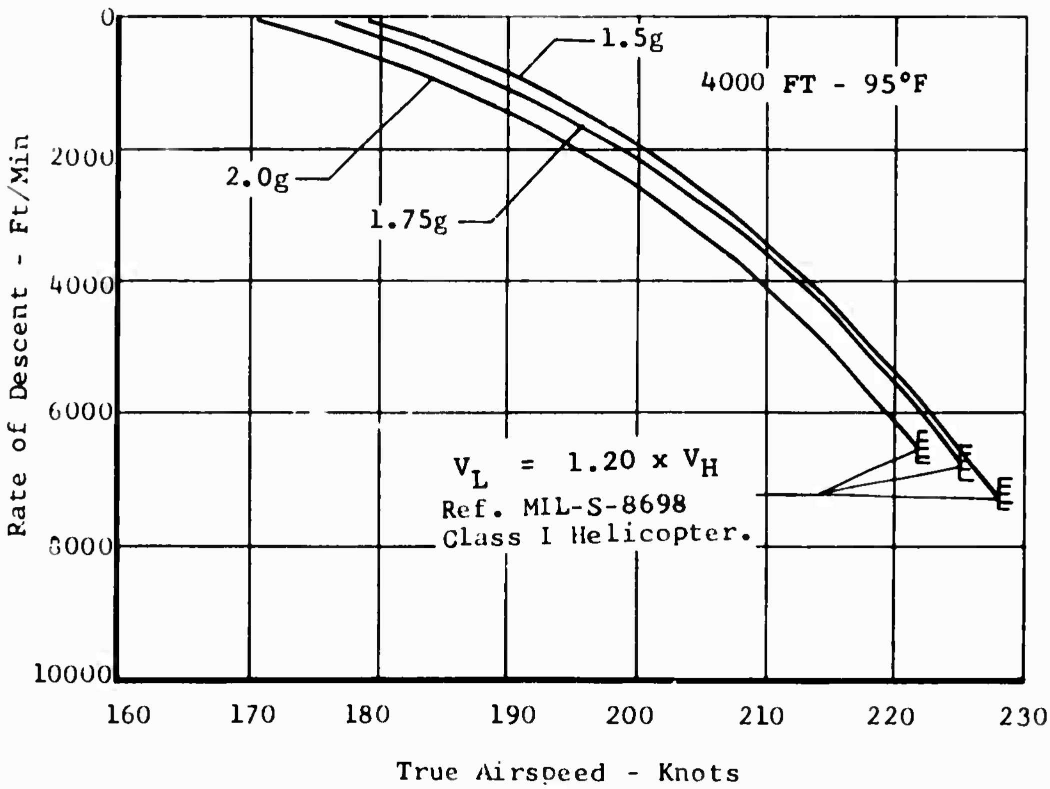

Figure 92. Rate of Descent at Normal Rated Power.

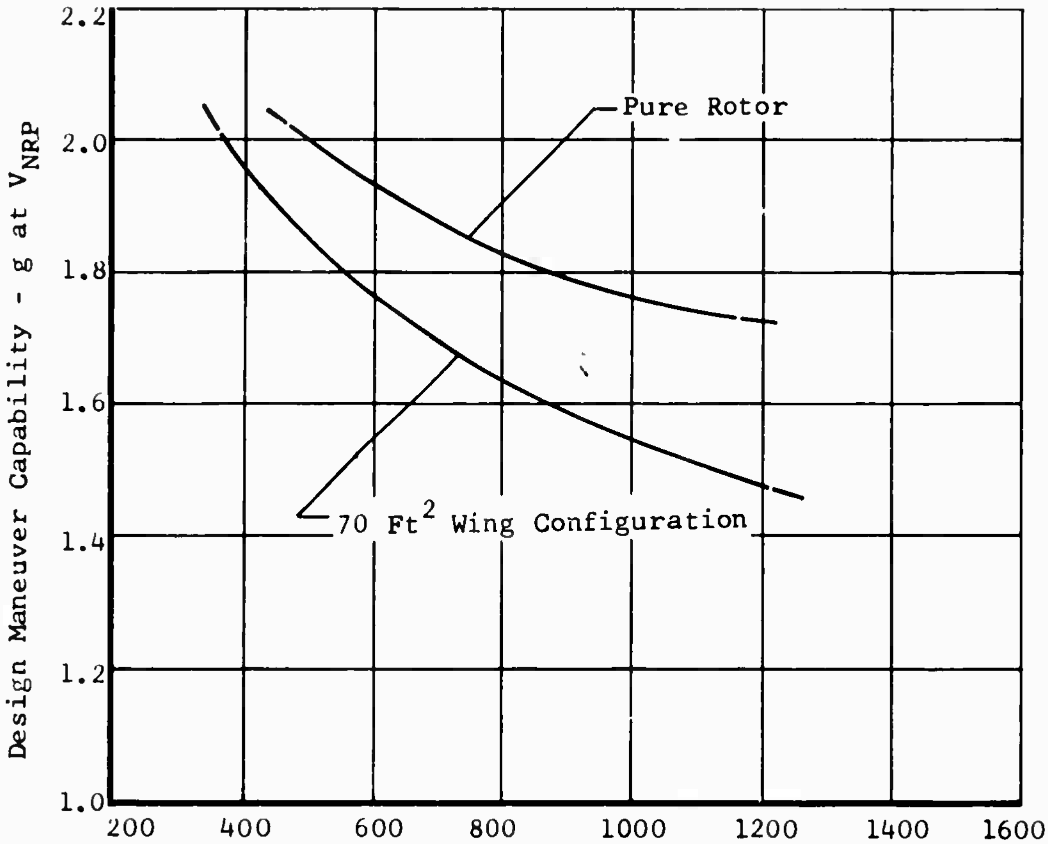

Δh_L = Altitude Lost During Pullout at V_L, Normal Rated Power

Figure 93. Dive Recovery at High Speed.

TASK IV - TECHNICAL RISK ANALYSIS

The problems that were defined and the conceptual considerations which became apparent during this study were reviewed to provide an assessment of technical risk. These were divided into three broad categories:

Category 1 - Those problems which can be expected to be solved during development of a vehicle or during its deployment by training.

Category 2 - Those areas which require additional study effort.

Category 3 - Those areas which would have definite and major impact on the design of a UTTAS vehicle.

Category 1. The identified problem area is the result of the limiting conditions for pullup and pushover maneuvers. In some cases, cyclic pullups were limited by rotor overspeed conditions, and pushovers by maximum power available. Failure to control rotor overspeed as the rotor shaft horsepower required goes to zero and then negative during pullup maneuvers could result in serious damage to the main and tail rotor components. Conversely, during pushovers, the rotor power required increases markedly, leading to underspeed conditions if maximum engine power available values are exceeded. Of the two possibilities, the pullup maneuver will probably be used most often, and avoidance of rotor overspeed conditions will be the most annoying piloting task. At this time, training would appear to be the most promising method of avoiding the problems inherent in pullups and pushovers. Under some conditions, rotor rpm is the limiting parameter during pullup and flare maneuvers in the AH-1 helicopters. Pilots have learned to monitor rotor rpm satisfactorily, although additional effort is definitely required. The alternative is a device capable of absorbing excess rotor energy such as rotor blade tip air brakes with their associated increase in complexity and cost of the rotor system.

Category 2. Two situations have been identified. The first concerns the problem of achieving zero g maneuvering flight with a winged helicopter configuration. The problem occurs in high-speed pushovers, and usually the rotor flapping limit (4.5 degrees) established for this study was the limiting parameter. Rotor systems other than those with a hingeless flexbeam hub (i.e., with flapping hinges of some type) may offer possibilities for achieving lower g-flight before a limit is reached. Additional study would be required to clarify this point.

As discussed in Task III, the dive recovery situation for vehicles with the speed range of typical UTTAS helicopters is of concern. If the dive speed definition ($1.2 \times V_L$) of MIL-S-8698 is applied, the resulting dive speeds will be in excess of 220 KTAS. The factor 1.2 may be too high for use with the newer generations of fast helicopters. Additional study is required to determine a dive speed definition for the UTTAS.

Category 3. Three major problems are defined in this category. The first concerns the maneuvering capability of UTTAS type helicopters under conditions of low-density altitude and light gross weight. A typical vehicle capable of 2.00 g's at V_{NRP} and design gross weight in a 4000-foot, 95°F atmosphere would be capable of over 4.00 g's at sea level at minimum flight weight. This is considerably in excess of the 3.00g structural load factor requirement. If the structural load factor requirement is increased, the result will be an increase in structural weight, overall size, power required, and cost. A g-limiting device in the control system may be considered but must represent an increase in complexity, weight and cost. Pilot monitoring of load factor will require proper instrumentation, increase pilot workload, and require additional pilot training.

As pointed out in the discussion of Task III, the high-speed level flight portion of the frequency of occurrence spectrum proved to be the condition imposing the most fatigue damage on the dynamic components. Even for the relatively severe maneuvering conditions used for this study, maneuvering flight was not the dominating condition for determining component life. Of course, this situation would be common to any new development program and is not peculiar to the UTTAS. It does point up, however, that the frequency of occurrence spectrum must be carefully considered in light of the mission requirements, and the desired fatigue life to avoid definition of conditions which would not be representative of operational usage and would adversely affect design of a vehicle.

Finally, the results of this study revealed that many maneuvers were limited by factors not readily apparent to a pilot. The flapping limits of the hingeless flexbeam rotor is a case in point. To define this limit for a pilot would require the invention of a monitoring device not presently available. The addition of parameters to monitor in the cockpit during maneuvering flight is certainly undesirable. The alternative is a rotor system comparable to present generation configurations which transmit indications of distress in the form of vibration and roughness when damaging loads are being applied. The approach is probably not feasible for all the attainable flight conditions of a UTTAS vehicle.

REFERENCES

1. Livingston, C.L., ROTOR AERODYNAMIC CHARACTERISTICS PROGRAM F35(J), Bell Helicopter Company Report 599-004 900, Bell Helicopter Company, Fort Worth, Texas, June, 1967.

2. Blankenship, B.L., and Harvey, K.W., A DIGITAL ANALYSIS FOR HELICOPTER PERFORMANCE AND ROTOR BLADE BENDING MOMENTS, Journal of the American Helicopter Society, Volume 7, Number 4, October 1962.

3. Duhon, J.M., Harvey, K.W., Blankenship, B.L., COMPUTER FLIGHT TESTING OF ROTORCRAFT, Journal of the American Helicopter Society, Volume 10, Number 4, October 1965.

4. Harvey, K.W., Blankenship, B.L., and Drees, J.M., ANALYTICAL STUDY OF HELICOPTER GUST RESPONSE AT HIGH FORWARD SPEEDS, USAAVLABS Technical Report 69-1, U. S. Army Aviation Materiel Laboratories, Fort Eustis, Virginia, September 1969, AD 862594.

5. Drees, J.M., and Wortmann, F.X., DESIGN OF AIRFOILS FOR ROTORS, Proceedings of Third CAL/AVLABS Symposium, Aerodynamics of Rotary Wing and V/STOL Aircraft, Volume I, June 1969.

6. Brown, E.L., and Schmidt, P.S., THE EFFECT OF HELICOPTER PITCHING VELOCITY ON ROTOR LIFT CAPABILITY, Journal of the American Helicopter Society, Volume 8, Number 4, October 1963.

7. Brown, E.L., and Red, J.A., RESULTS OF THE WIND TUNNEL TESTS OF THE QUARTER-SCALE SEMI-SPAN MODEL OF THE BELL XV-3 TILTING-ROTOR CONVERTIPLANE, Bell Helicopter Company Report 200-094-270, Bell Helicopter Company, Fort Worth, Texas, September 1958.

8. Lowson, M.V., and Ollerhead, J.B., STUDIES OF HELICOPTER ROTOR NOISE, Wyle Laboratories Inc.; USAAVLABS Technical Report 68-60, U.S. Army Aviation Materiel Laboratories, Fort Eustis, Virginia, May 1968, AD 684394.

9. Schlegel, R.G., King, R.J., and Mull, H.R., HELICOPTER ROTOR NOISE GENERATION AND PROPAGATION, Sikorsky Aircraft; USAAVLABS Technical Report 66-4, U.S. Army Aviation Materiel Laboratories, Fort Eustis, Virginia, October 1966, AD 645884.

10. Lowson, M.V., THOUGHTS ON BROADBAND NOISE RADIATION BY A HELICOPTER, Wyle Laboratories Research Staff WR 68-20, Wyle Laboratories, Inc., Huntsville, Alabama, December 1968.

11. Cox, C.R., FULL-SCALE HELICOPTER ROTOR NOISE MEASUREMENTS IN AMES 40- BY 80-FOOT WIND TUNNEL, Bell Helicopter Company Report 576-099-052, Bell Helicopter Company, Fort Worth, Texas, July 1967.

12. Cox, C.R., ROTOR NOISE MEASUREMENTS IN WIND TUNNELS, Proceedings, Third Cal/AVLABS Symposium, Aerodynamics of Rotary Wing and V/STOL Aircraft, Volume 1, June 1969.

13. Blankenship, B.L., and Bird, B.J., PROGRAM AGAJ68 ROTOR-CRAFT FLIGHT SIMULATION, Bell Helicopter Company Report 599-068-904, Bell Helicopter Company, Fort Worth, Texas, September 25, 1969.

14. Anon., STUDY PROPOSAL FOR ANALYSIS OF MANEUVERABILITY EFFECTS ON ROTOR/WING DESIGN CHARACTERISTICS, Bell Helicopter Company Report 299-099-602, Volume I - Technical Quotation, Bell Helicopter Company, Fort Worth, Texas, February 9, 1970

15. Minor, Milton A., CUMULATIVE DAMAGE IN FATIGUE, ASME Journal of Applied Mechanics, Volume 12, Number 3, 1945.

16. Graham, G.L., COMBAT OPERATIONAL FLIGHT PROFILES ON THE UH-1C, AH-1G AND UH-1H HELICOPTERS, Journal of the American Helicopter Society, Volume 15, Number 4, October 1970.

APPENDIX I

TASK I - PERFORMANCE DATA

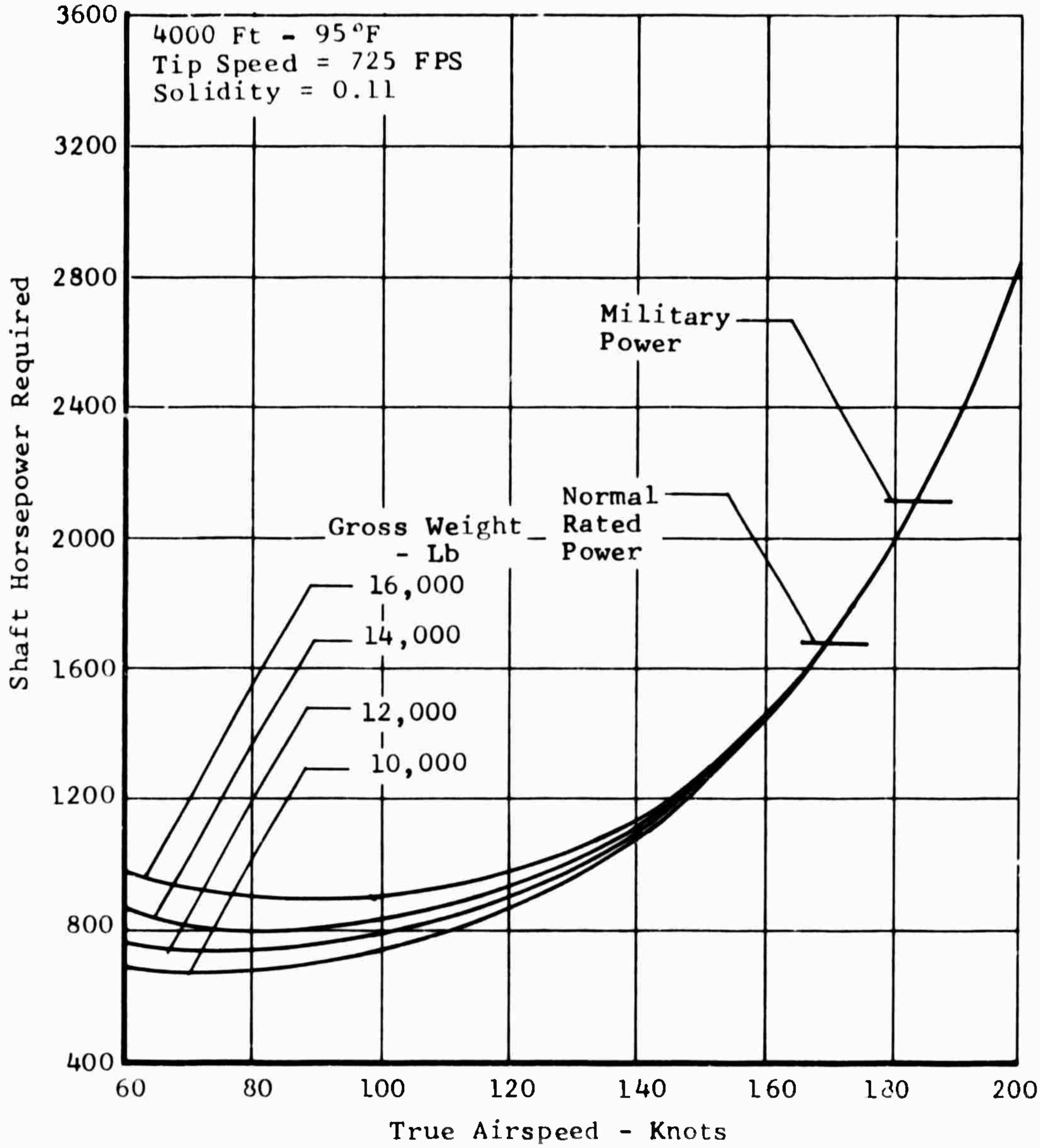

Figure 94. Task I - Wingless Helicopter, Speed Power Polar

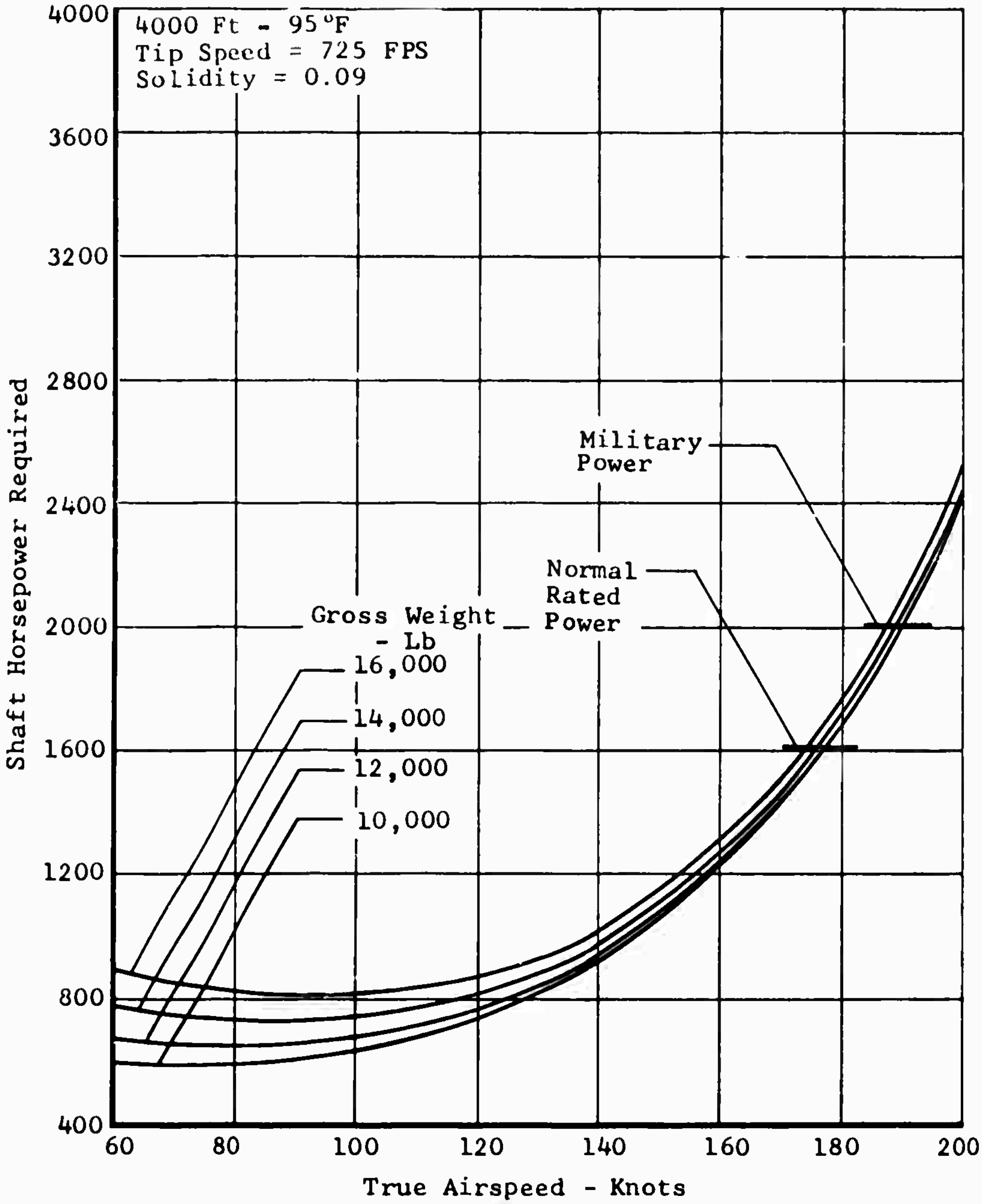

Figure 95. Task I - Wingless Helicopter, Speed Power Polar.

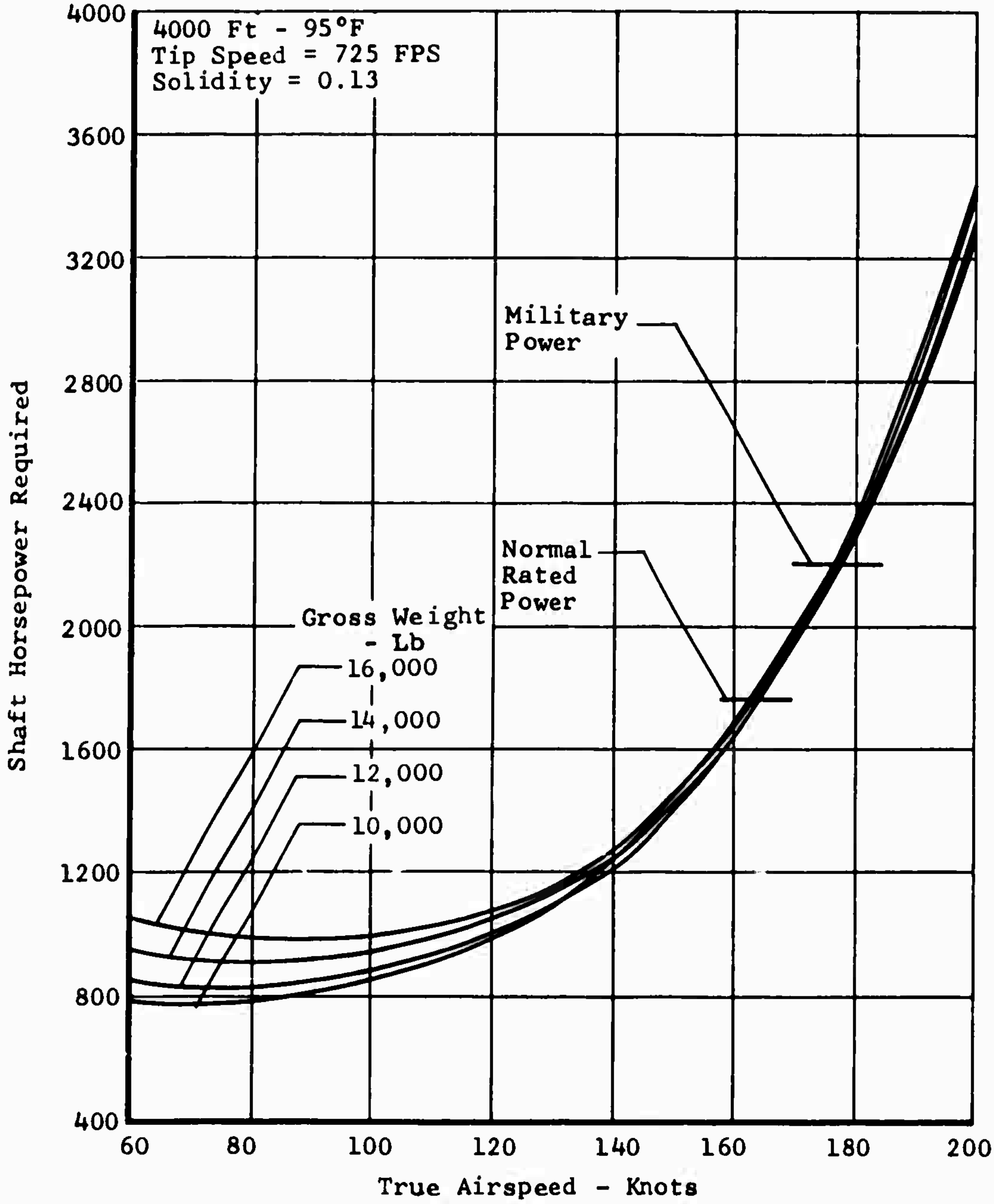

Figure 96. Task I - Wingless Helicopter, Speed Power Polar.

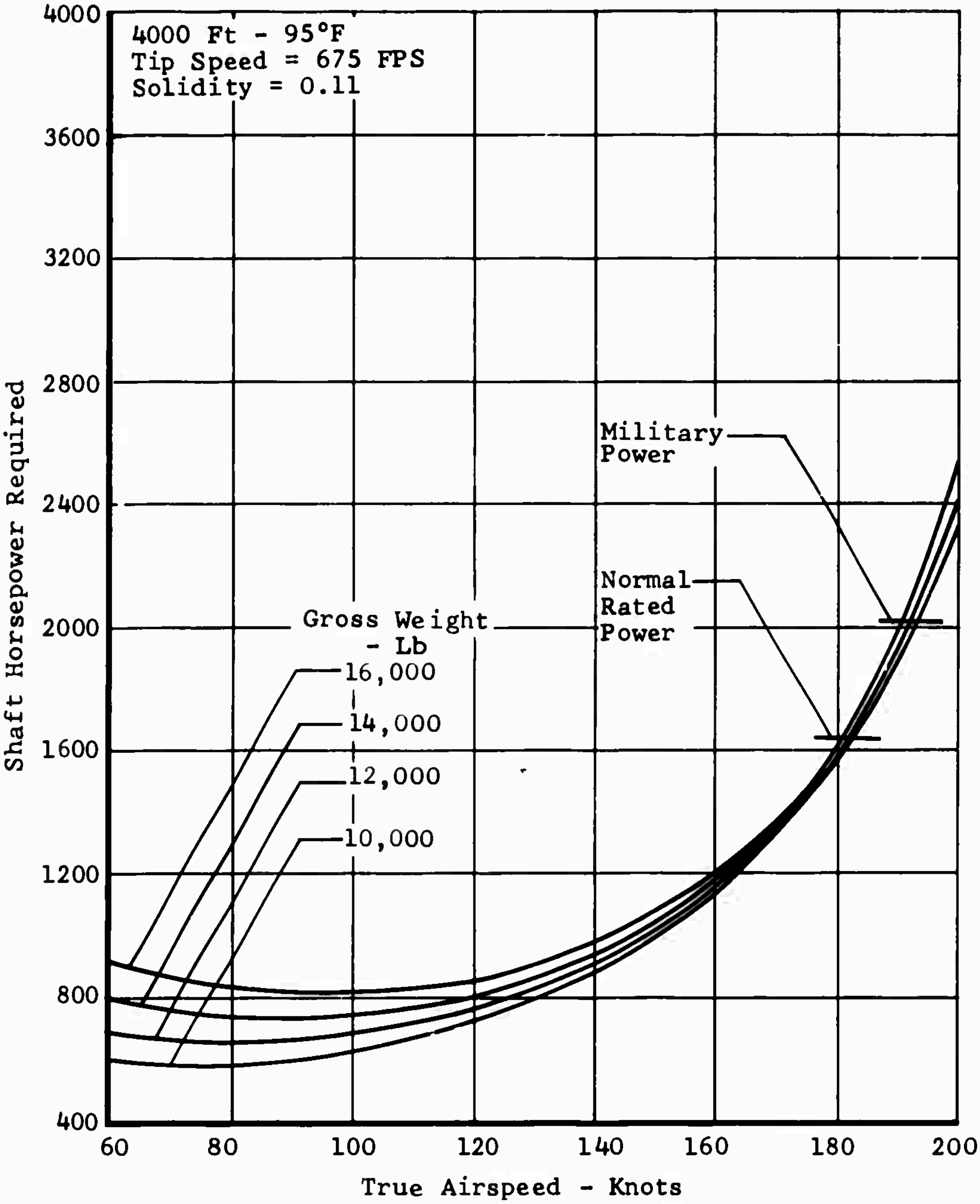

Figure 97. Task I - Wingless Helicopter, Speed Power Polar.

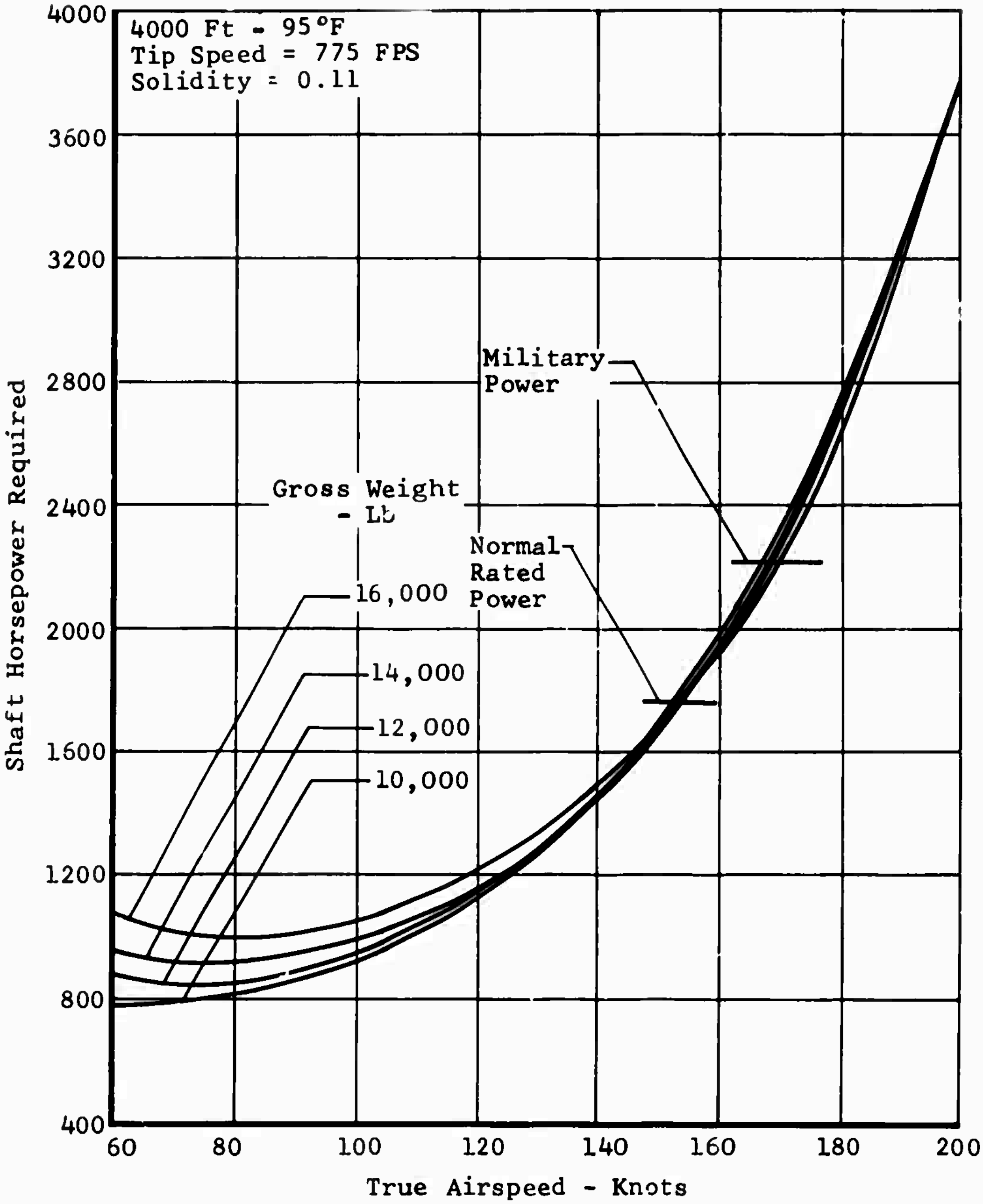

Figure 98. Task I - Wingless Helicopter, Speed Power Polar.

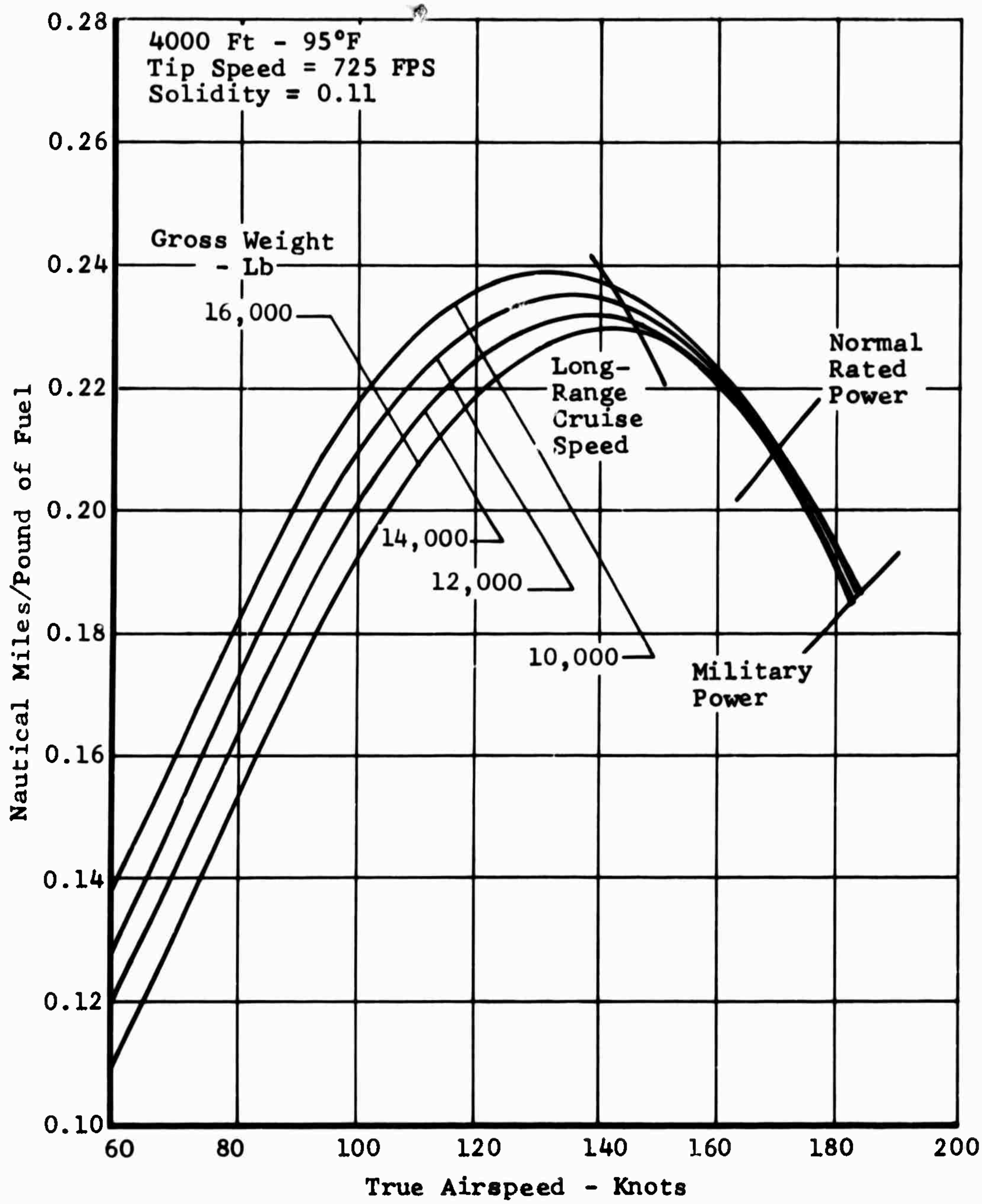

Figure 99. Task I - Wingless Helicopter, Specific Range.

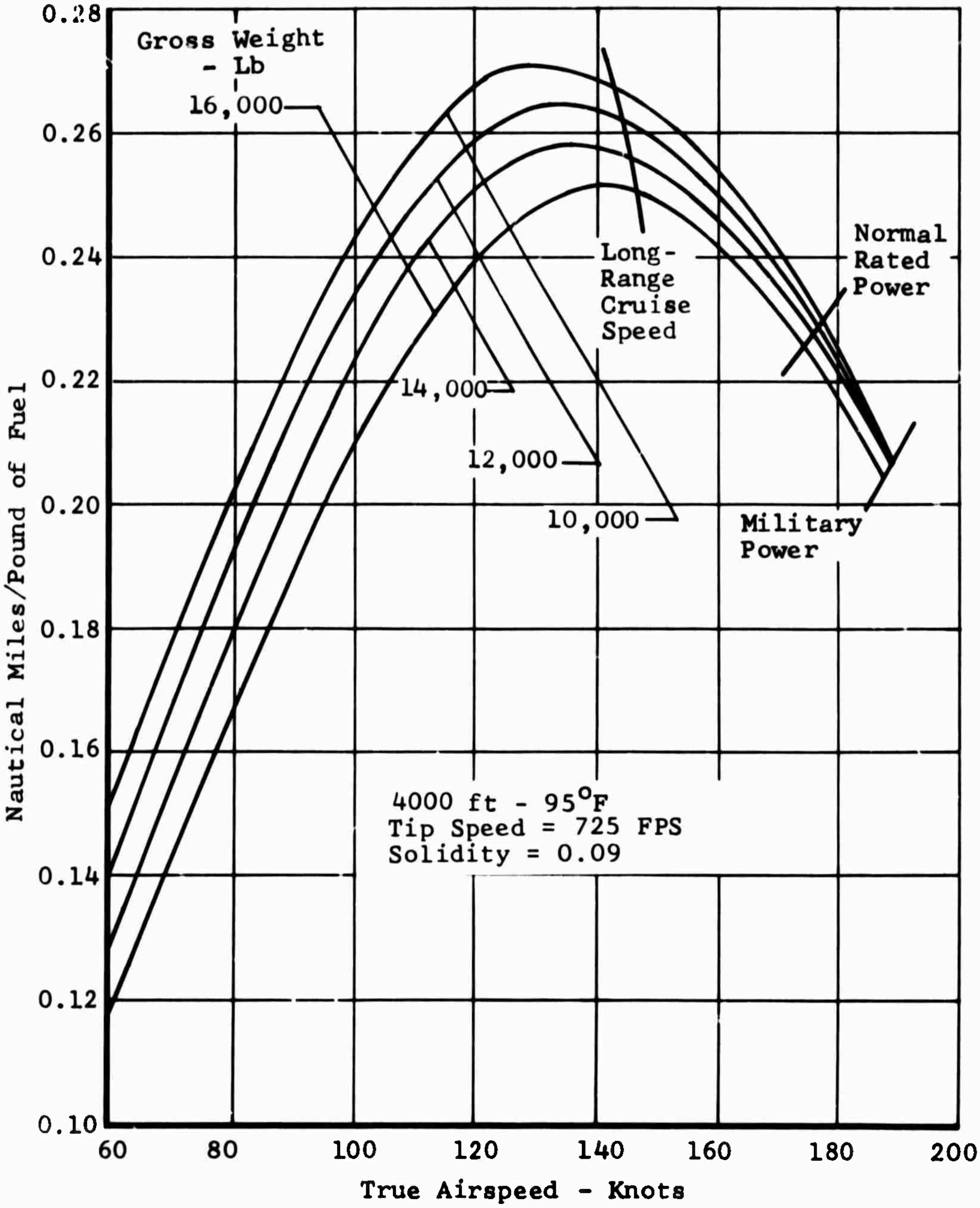

Figure 100. Task I - Wingless Helicopter, Specific Range.

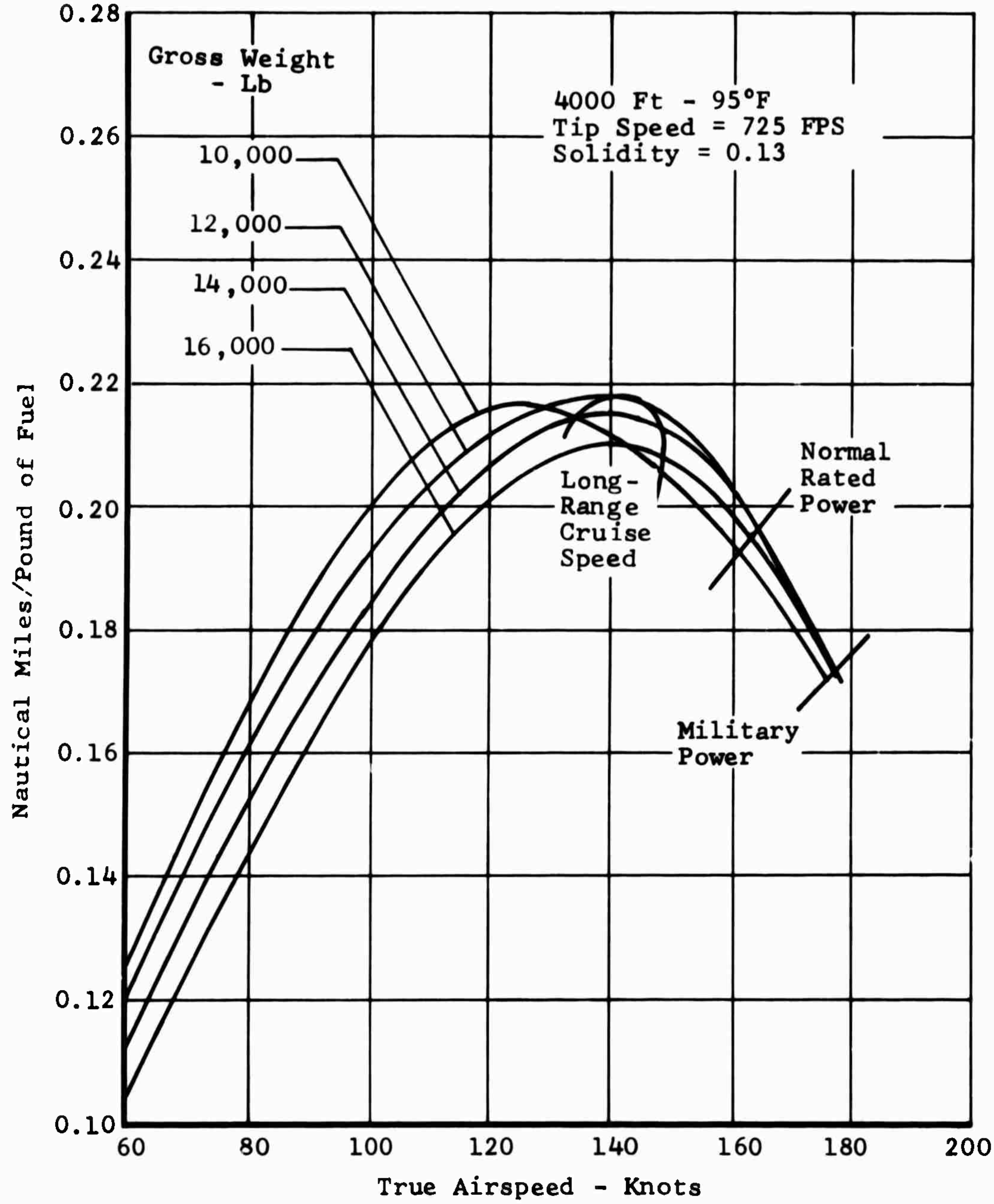

Figure 101. Task I - Wingless Helicopter, Specific Range.

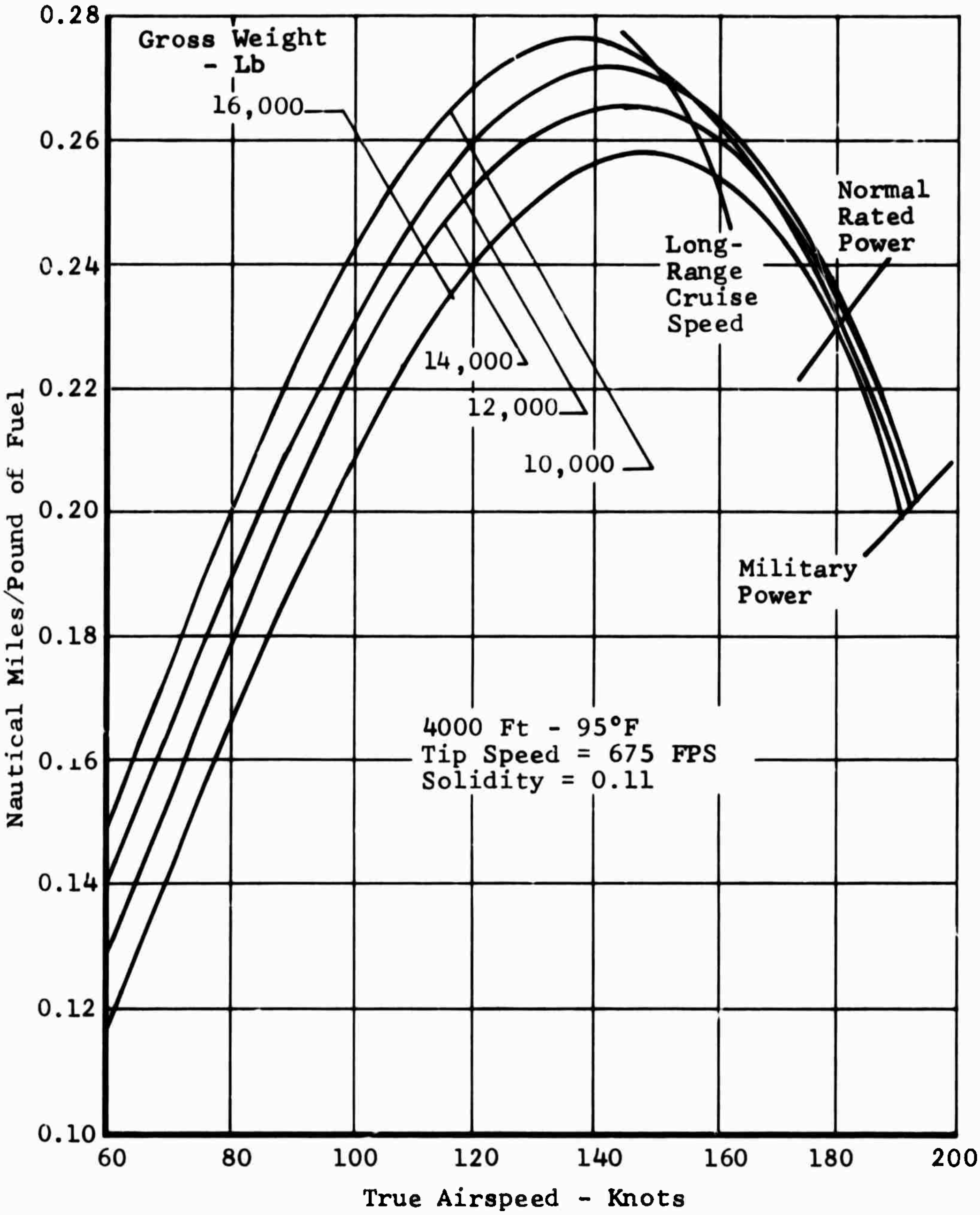

Figure 102. Task I - Wingless Helicopter, Specific Range.

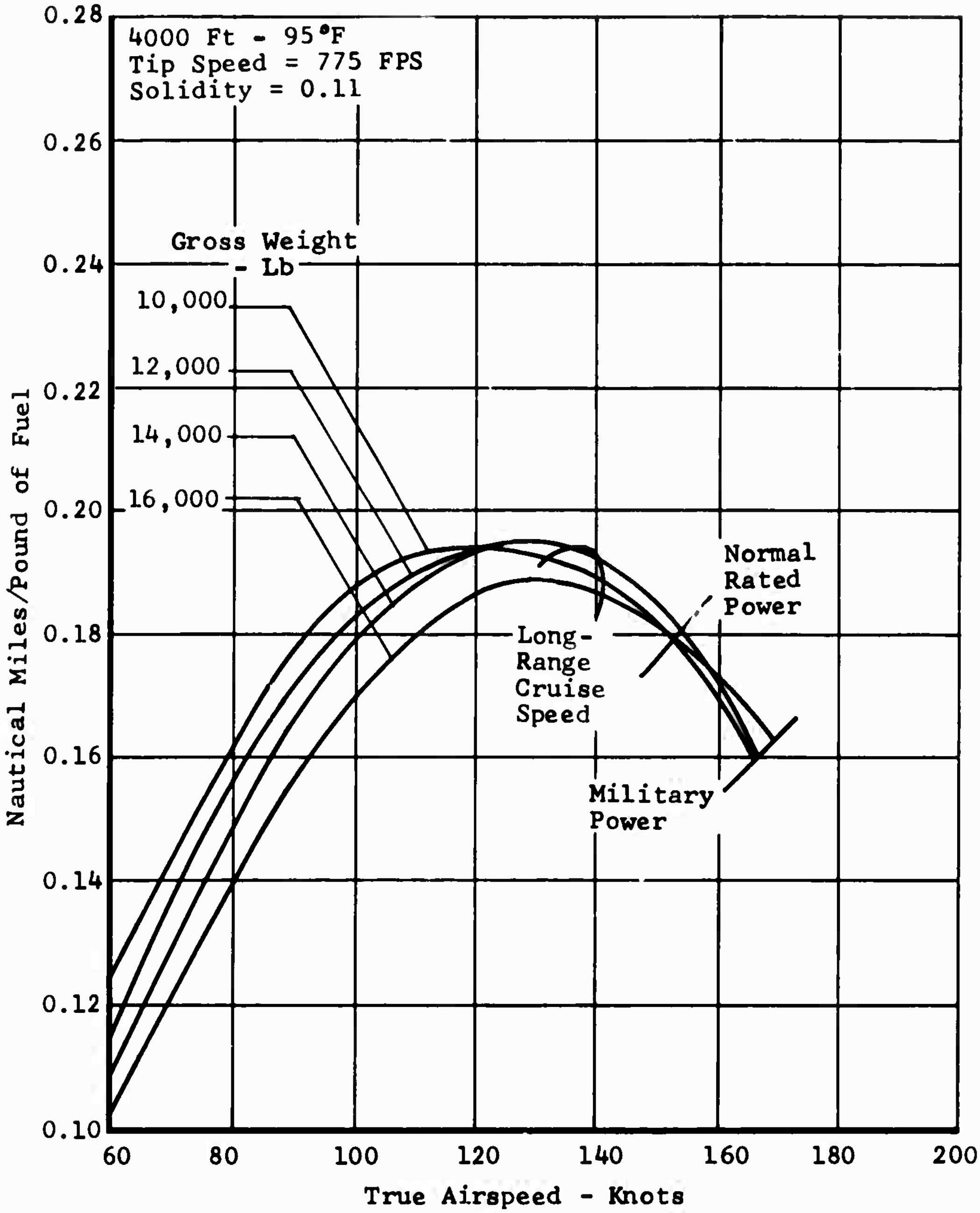

Figure 103. Task I - Wingless Helicopter, Specific Range.

APPENDIX II

TASK I - MANEUVER RESULTS, BASIC DATA

TABLE XXXII. INPUT RATE AND TIME PHASING DATA, TASK I - BASELINE CONFIGURATION

	Cyclic Input		Collective Input			Sustained
Airspeed (KTAS)	Rate (Inch/Sec)	Amount (Deg)	(Inch/Sec)	Time Delay (Sec)	Amount (Deg)	Load Factor (g)
56	4	3.40	–	–	–	1.41
	6	3.40	–	–	–	1.41
	8	3.40	–	–	–	1.41
	6	2.50	1.5	0	2.50	1.60
		2.80		.5	2.80	1.65
		2.90		1.0	2.90	1.65
		2.50	3.0	0	2.50	1.55
		2.60		.5	2.60	1.62
		2.80		1.0	2.80	1.65
		2.50	4.5	0	2.50	1.55
		2.55		.5	2.55	1.60
		2.70		1.0	2.70	1.65
89	4	3.60	–	–	–	1.86
	6	3.50	–	–	–	1.85
	8	3.60	–	–	–	1.86
	6	2.50	1.5	0	2.50	2.00
		2.75		.5	2.75	2.07
		3.40		1.0	3.40	2.14
		2.50	3.0	0	2.50	1.93
		2.70		.5	2.70	2.00
		3.10		1.0	3.10	2.15
		2.50	4.5	0	2.50	1.92
		2.65		.5	2.65	1.99
		3.00		1.0	3.00	2.13
150	4	2.40	–	–	–	2.12
	6	2.40	–	–	–	2.12
	8	2.40	–	–	–	2.10
	6	1.60	1.5	0	1.60	2.25
		1.70		.5	1.70	2.26
		1.75		1.0	1.75	2.24
		1.65	3.0	0	1.65	2.25
		1.65		.5	1.65	2.23
		1.65		1.0	1.65	2.18
		1.60	4.5	0	1.60	2.22
		1.65		.5	1.65	2.23
		1.70		1.0	1.70	2.20
167	4	2.00	–	–	–	2.05
	6	2.00	–	–	–	2.05
	8	2.00	–	–	–	2.05

TABLE XXXIII. RESULTS OF PULLUP AND PUSHOVER MANEUVERS, TASK I BASELINE CONFIGURATION - $\sigma = 0.11$, $\Omega R = 725$ FPS

Maneuver Description			Sustained Load Factor (g)	Limiting Criteria
Airspeed (KTAS)	Control Type	Amount (Deg)		
195	Cyclic Pull	1.00	1.70	Flapping
	Cyclic Push	2.00	0	Flapping
167	Cyclic Pull	1.85	2.05	Flapping
	Cyclic Push	2.50	0.02	Flapping, zero horsepower
150	Cyclic Pull	2.35	2.12	Zero horsepower
	Collective + Cyclic Pull	1.60	2.25	Flapping
	Collective Pull	3.25	1.95	Maximum horsepower
	Cyclic Push	2.85	0.04	Flapping
	Collective + Cyclic Push	2.30	-0.15	Flapping
	Collective Push	6.00	-0.23	Flapping
89	Cyclic Pull	3.50	1.85	Zero horsepower, pitch rate
	Collective + Cyclic Pull	2.50	2.00	Pitch rate
	Collective Pull	3.50	1.50	Maximum horsepower
	Cyclic Push	4.25	-0.05	Pitch rate
	Collective + Cyclic Push	3.50	-0.26	Flapping
	Collective Push	8.0	-0.15	Extreme flight condition
56	Collective + Cyclic Pull	2.50	1.60	Pitch rate
	Collective Pull	3.50	1.35	Maximum horsepower
	Collective + Cyclic Push	3.25	0.05	Extreme flight condition
	Collective Push	5.00	0.55	Zero horsepower
0	Collective Pull	1.50	1.20	Maximum horsepower

TABLE XXXIV. RESULTS OF PULLUP AND PUSHOVER MANEUVERS, TASK I
LOW TIP SPEED CONFIGURATION - $\sigma = 0.11$, $\Omega R = 675$ FPS

Maneuver Description			Sustained Load Factor (g)	Limiting Criteria
Airspeed (KTAS)	Control Type	Amount (Deg)		
195	Cyclic Pull	0.40	1.30	Flapping
	Cyclic Push	2.00	0	Flapping
167	Cyclic Pull	1.00	1.60	Flapping
	Cyclic Push	2.50	-0.03	Flapping, zero horsepower
150	Cyclic Pull	1.60	1.80	Incipient stall
	Collective + Cyclic Pull	1.00	1.80	Incipient stall
	Collective Pull	2.40	1.80	Incipient stall
	Cyclic Push	2.85	-0.02	Flapping, zero horsepower
	Collective + Cyclic Push	2.10	-0.15	Flapping, zero horsepower
	Collective Push	6.25	-0.25	Flapping
89	Cyclic Pull	3.60	1.85	Pitch rate, zero horsepower
	Collective + Cyclic Pull	2.65	2.00	Pitch rate
	Collective Pull	4.00	1.60	Maximum horsepower
	Cyclic Push	4.25	-0.05	Pitch rate
	Collective + Cyclic Push	4.00	-0.30	Flapping
	Collective Push	10.00	-0.25	Extreme flight conditions
56	Collective + Cyclic Pull	2.75	1.60	Flapping, pitch rate
	Collective Pull	3.50	1.30	Maximum horsepower
	Collective + Cyclic Push	4.25	-0.10	Pitch rate
	Collective Push	5.00	0.60	Zero horsepower
0	Collective Pull	1.50	1.10	Maximum horsepower

TABLE XXXV. RESULTS OF PULLUP AND PUSHOVER MANEUVERS, TASK I – HIGH TIP SPEED CONFIGURATION - $\sigma = 0.11$, $\Omega R = 775$ FPS

Maneuver Description			Sustained Load Factor (g)	Limiting Criteria
Airspeed (KTAS)	Control Type	Amount (Deg)		
195	Cyclic Pull	2.00	2.15	Flapping, zero horsepower
	Cyclic Push	2.00	0.15	Maximum horsepower
167	Cyclic Pull	2.50	2.25	Flapping
	Cyclic Push	2.50	0.15	Flapping
150	Cyclic Pull	2.75	2.25	Zero horsepower
	Collective + Cyclic Pull	2.00	2.50	Flapping
	Collective Pull	2.00	1.50	Maximum horsepower
	Cyclic Push	3.00	0.05	Flapping
	Collective + Cyclic Push	2.25	-0.10	Flapping
	Collective Push	7.00	-0.30	Flapping
89	Cyclic Pull	3.25	1.80	Pitch rate, flapping
	Collective + Cyclic Pull	2.50	2.05	Pitch rate
	Collective Pull	3.35	1.53	Maximum horsepower
	Cyclic Push	4.10	0.03	Pitch rate
	Collective + Cyclic Push	4.50	-0.40	Extreme flight conditions
	Collective Push	10.00	-0.30	Extreme flight conditions
56	Collective + Cyclic Pull	2.35	1.60	Pitch rate
	Collective Pull	3.30	1.35	Maximum horsepower
	Collective + Cyclic Push	4.25	-0.18	Pitch rate
	Collective Push	5.00	0.60	Extreme flight conditions
0	Collective Pull	1.50	1.15	Maximum horsepower

TABLE XXXVI. RESULTS OF PULLUP AND PUSHOVER MANEUVERS, TASK I - LOW SOLIDITY CONFIGURATION - $\sigma = 0.09$, $\Omega R = 725$ FPS

Maneuver Description			Sustained Load Factor (g)	Limiting Criteria
Airspeed (KTAS)	Control Type	Amount (Deg)		
195	Cyclic Pull	0.60	1.40	Incipient stall
	Cyclic Push	2.25	0	Flapping
167	Cyclic Pull	1.35	1.70	Incipient stall
	Cyclic Push	2.75	0	Flapping
150	Cyclic Pull	2.00	1.85	Flapping, zero horsepower
	Collective + Cyclic Pull	1.15	1.85	Incipient stall
	Collective Pull	2.75	1.80	Incipient stall
	Cyclic Push	3.00	0.03	Flapping
	Collective + Cyclic Push	2.25	-0.13	Flapping
	Collective Push	7.00	-0.30	Flapping
89	Cyclic Pull	3.75	1.75	Pitch rate, flapping
	Collective + Cyclic Pull	2.75	2.00	Pitch rate
	Collective Pull	4.00	1.55	Maximum horsepower
	Cyclic Push	4.35	0	Pitch rate
	Collective + Cyclic Push	4.25	-0.35	Flapping
	Collective Push	10.00	-0.20	Extreme flight condition
56	Collective + Cyclic Pull	2.75	1.60	Pitch rate
	Collective Pull	3.50	1.30	Maximum horsepower
	Collective + Cyclic Push	4.25	-0.05	Pitch rate
	Collective Push	5.00	0.63	Zero horsepower
0	Collective Pull	1.50	1.15	Maximum horsepower

TABLE XXXVII. RESULTS OF PULLUP AND PUSHOVER MANEUVERS, TASK I - HIGH SOLIDITY CONFIGURATION - $\sigma = 0.13$, $\Omega R = 725$ FPS

Maneuver Description			Sustained Load Factor (g)	Limiting Criteria
Airspeed (KTAS)	Control Type	Amount (Deg)		
195	Cyclic Pull	1.50	2.00	Incipient stall
	Cyclic Push	2.00	0	Flapping, zero horsepower
167	Cyclic Pull	2.25	2.20	Flapping
	Cyclic Push	2.50	0	Flapping
150	Cyclic Pull	2.65	2.30	Flapping, zero horsepower
	Collective + Cyclic Pull	1.90	2.50	Flapping
	Collective Pull	2.50	1.70	Maximum horsepower
	Cyclic Push	3.00	0	Flapping
	Collective + Cyclic Push	2.25	-0.15	Flapping
	Collective Push	7.00	-0.35	Flapping
89	Cyclic Pull	3.35	1.90	Pitch rate
	Collective + Cyclic Pull	2.50	2.05	Pitch rate
	Collective Pull	3.35	1.55	Maximum horsepower
	Cyclic Push	4.25	-0.05	Flapping
	Collective + Cyclic Push	4.00	-0.40	Flapping
	Collective Push	10.00	-0.30	Extreme flight conditions
56	Collective + Cyclic Pull	2.35	1.60	Pitch rate
	Collective Pull	3.50	1.35	Maximum horsepower
	Collective + Cyclic Push	4.25	-0.15	Pitch rate
	Collective Push	5.00	0.60	Zero horsepower
0	Collective Pull	1.50	1.15	Maximum horsepower

APPENDIX III

TASK II - PERFORMANCE DATA

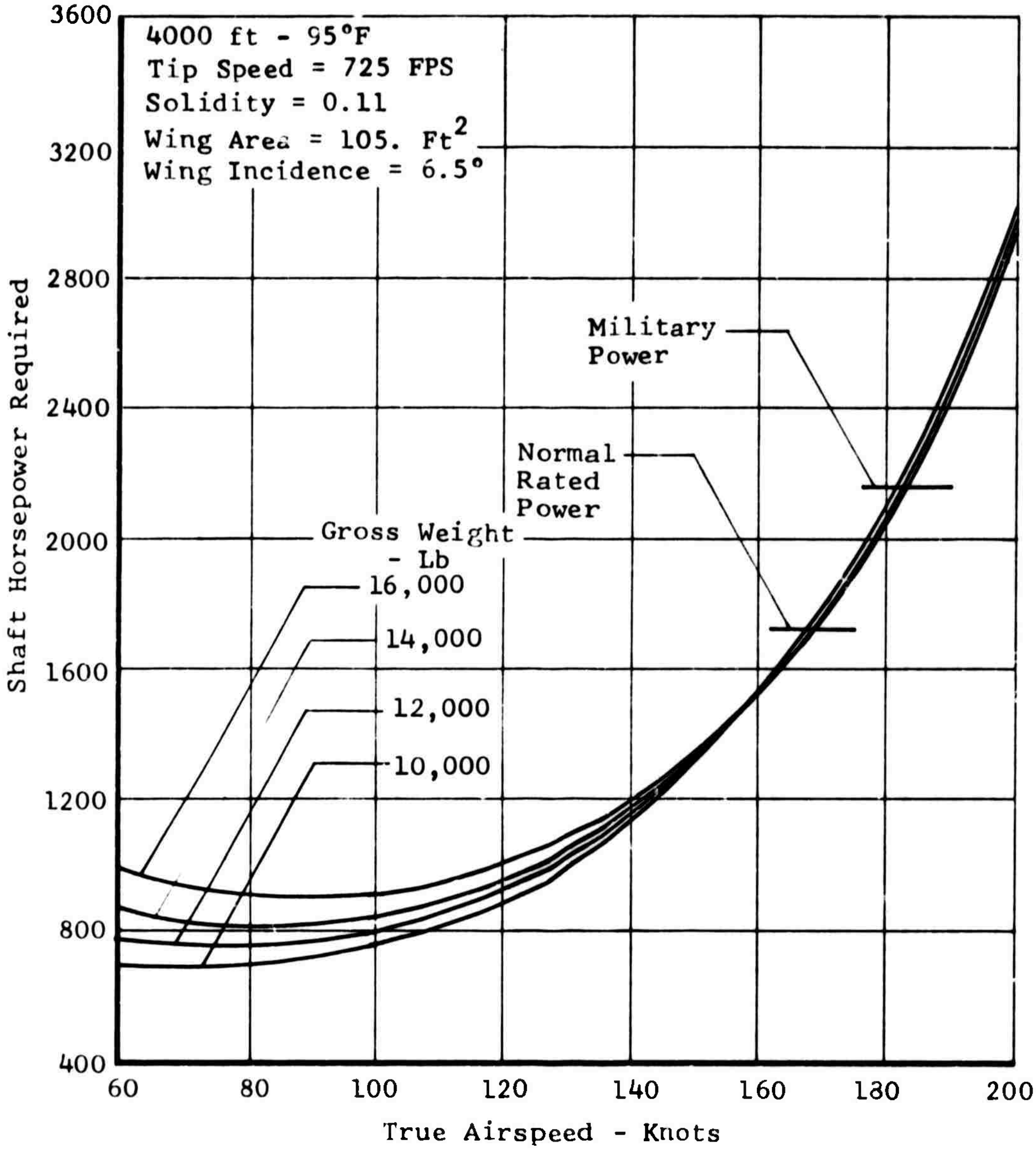

Figure 104. Task II - Winged Helicopter, Speed Power Polar.

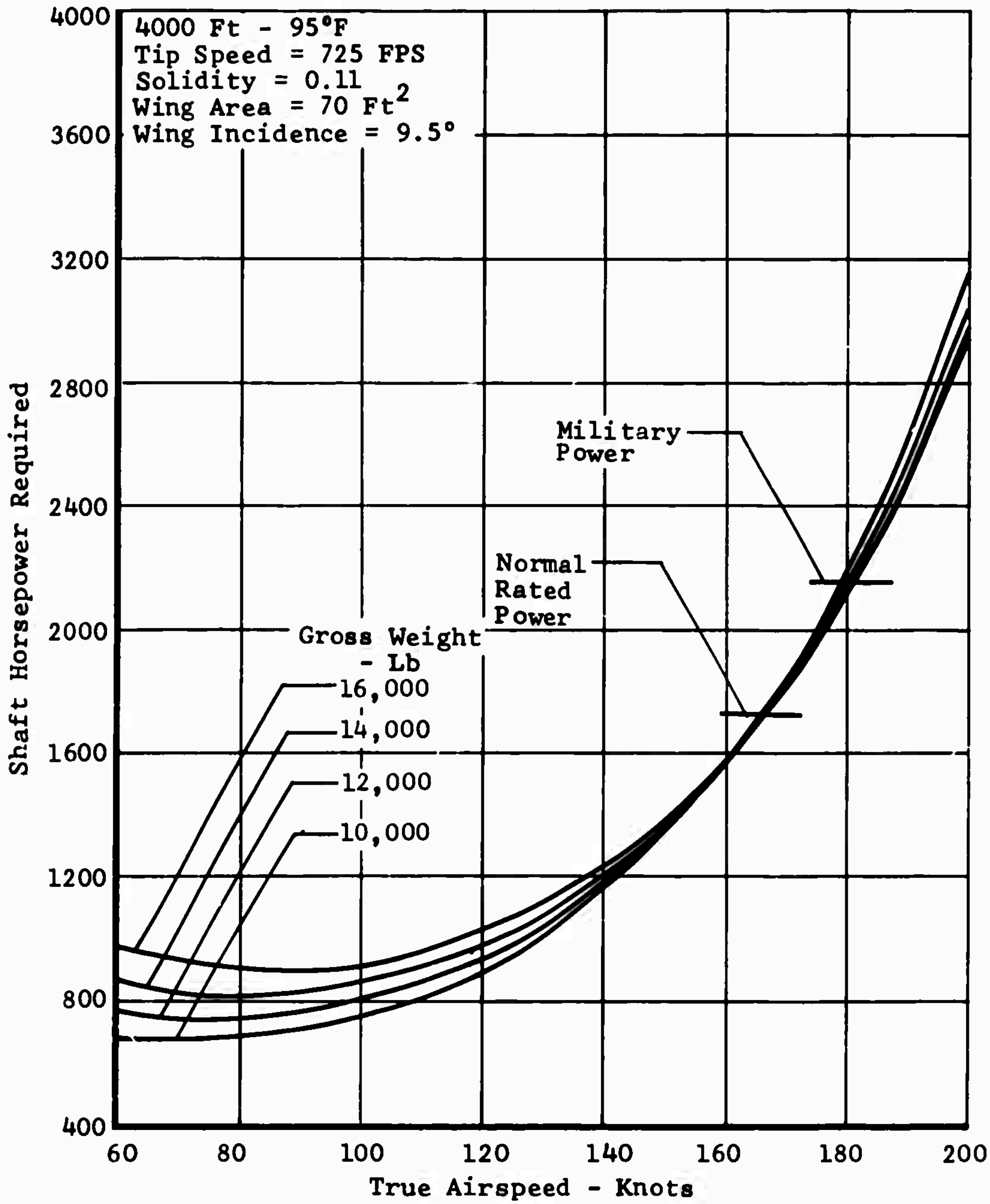

Figure 105. Task II - Winged Helicopter, Speed Power Polar.

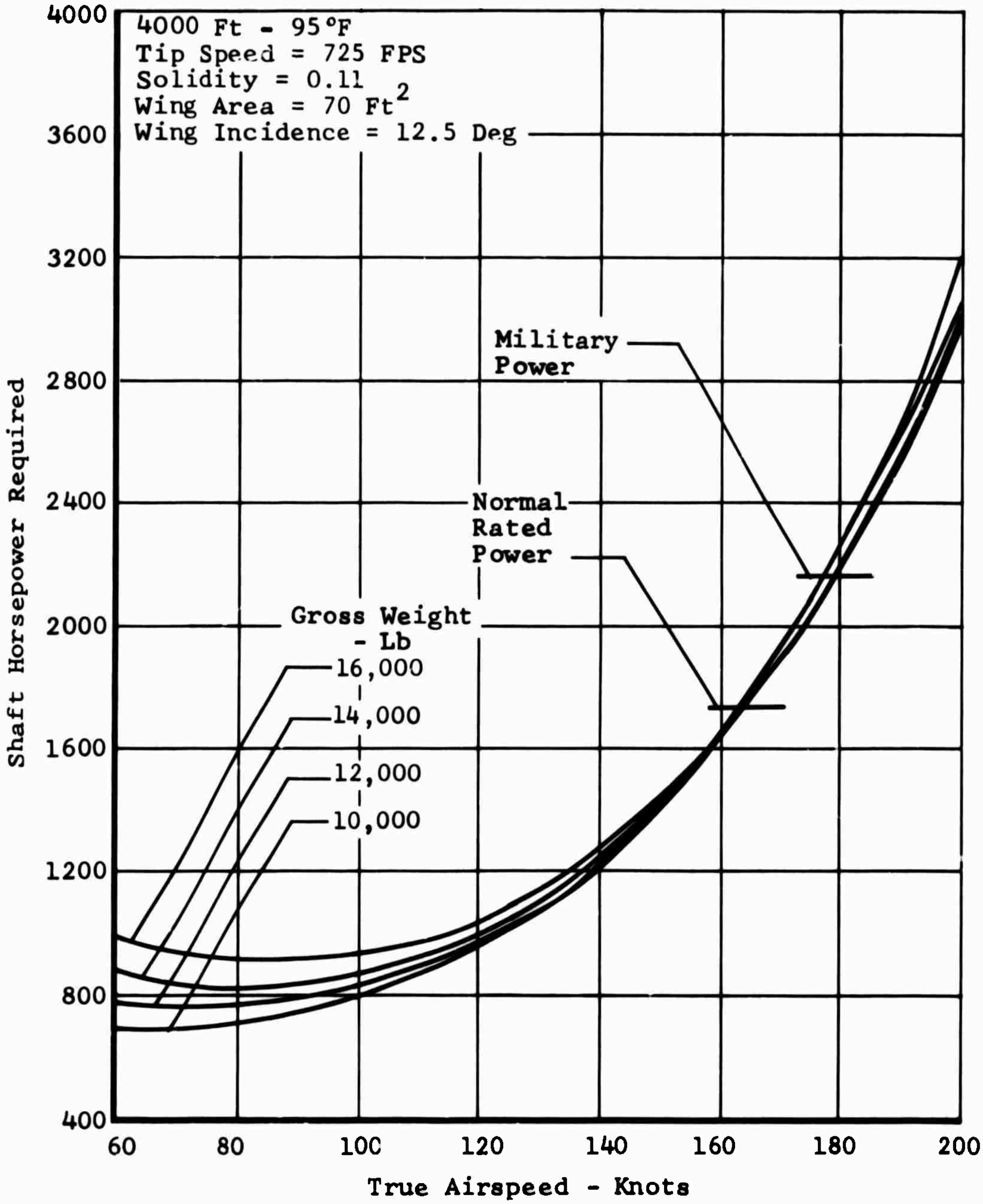

Figure 106. Task II - Winged Helicopter, Speed Power Polar.

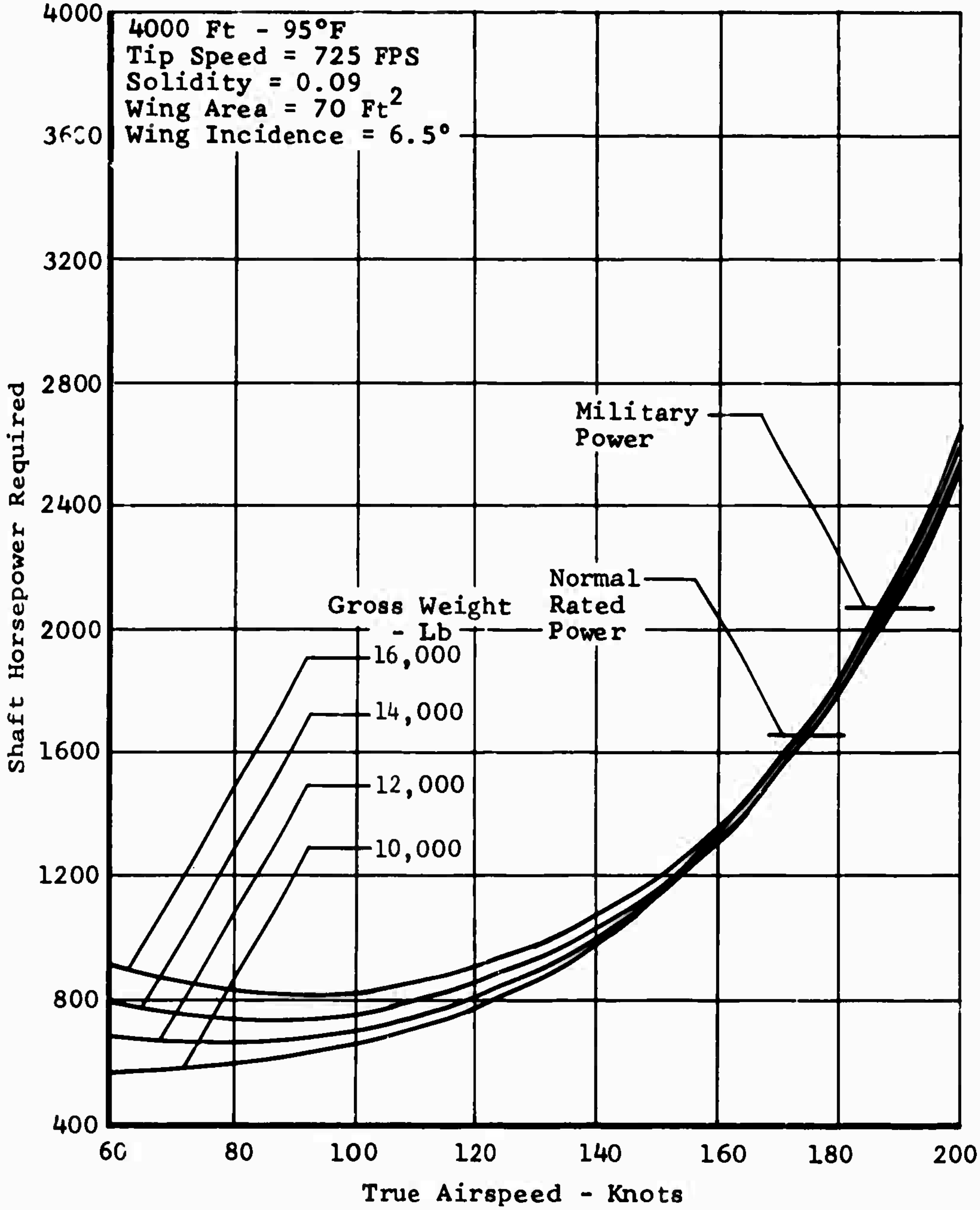

Figure 107. Task II - Winged Helicopter, Speed Power Polar.

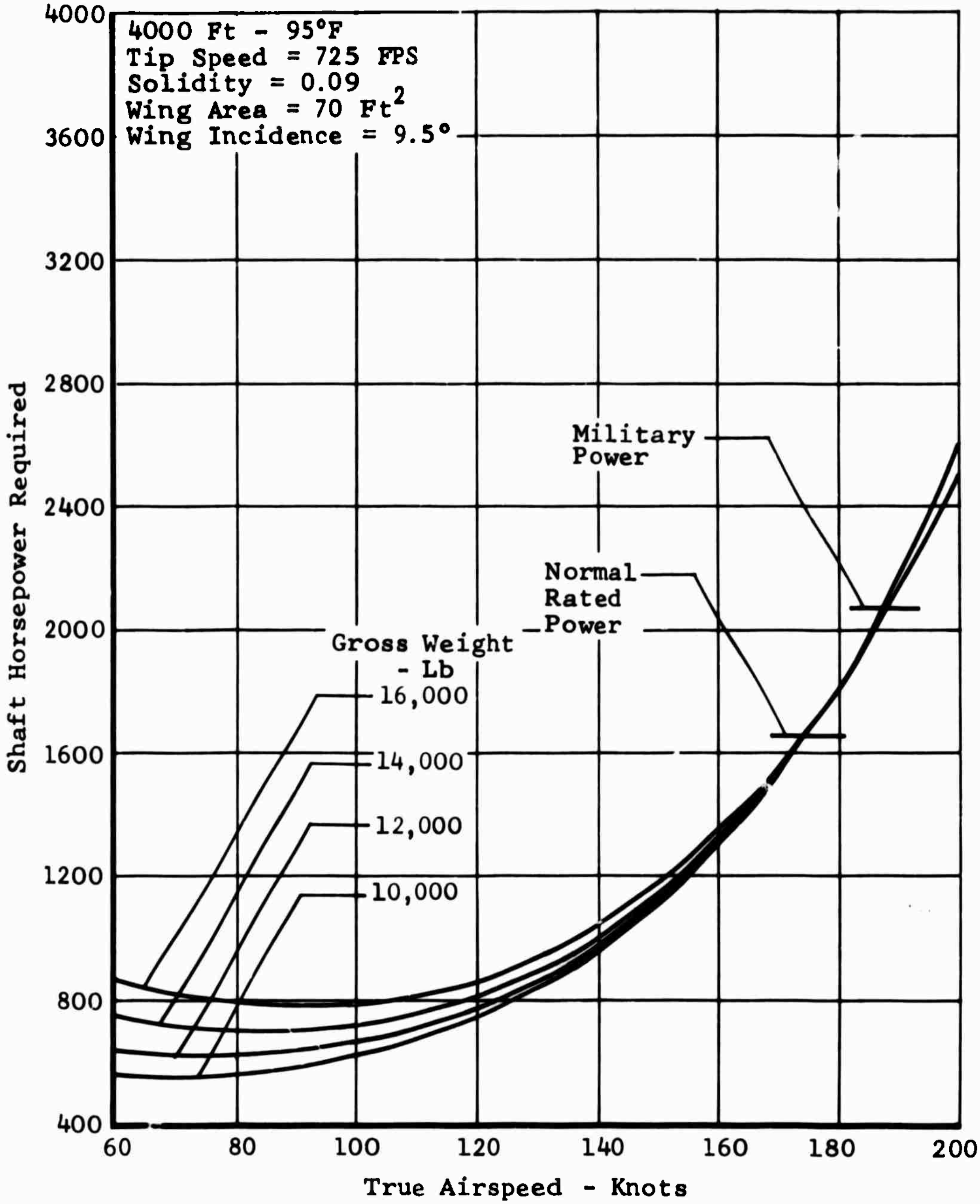

Figure 108. Task II - Winged Helicopter, Speed Power Polar.

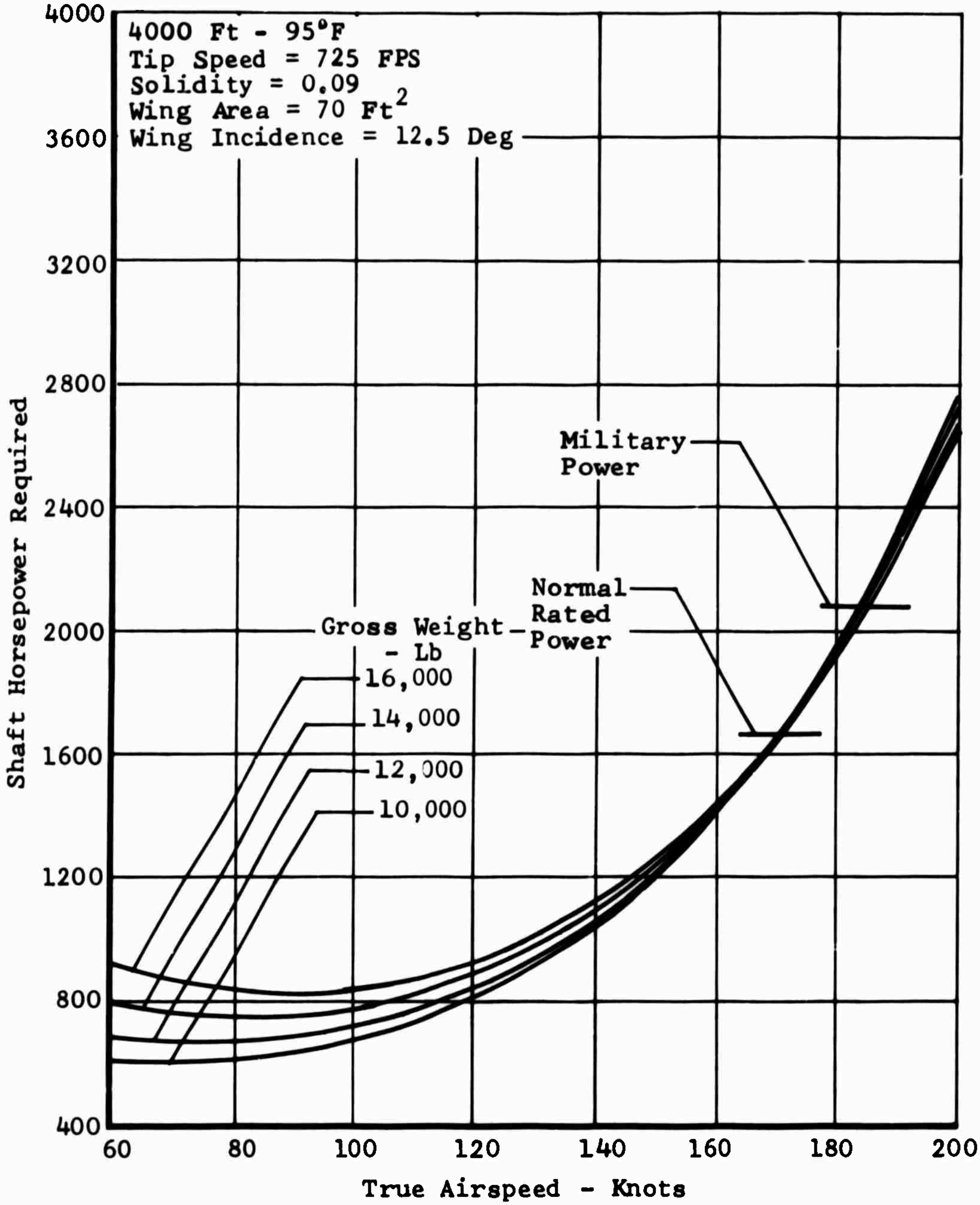

Figure 109. Task II - Winged Helicopter, Speed Power Polar.

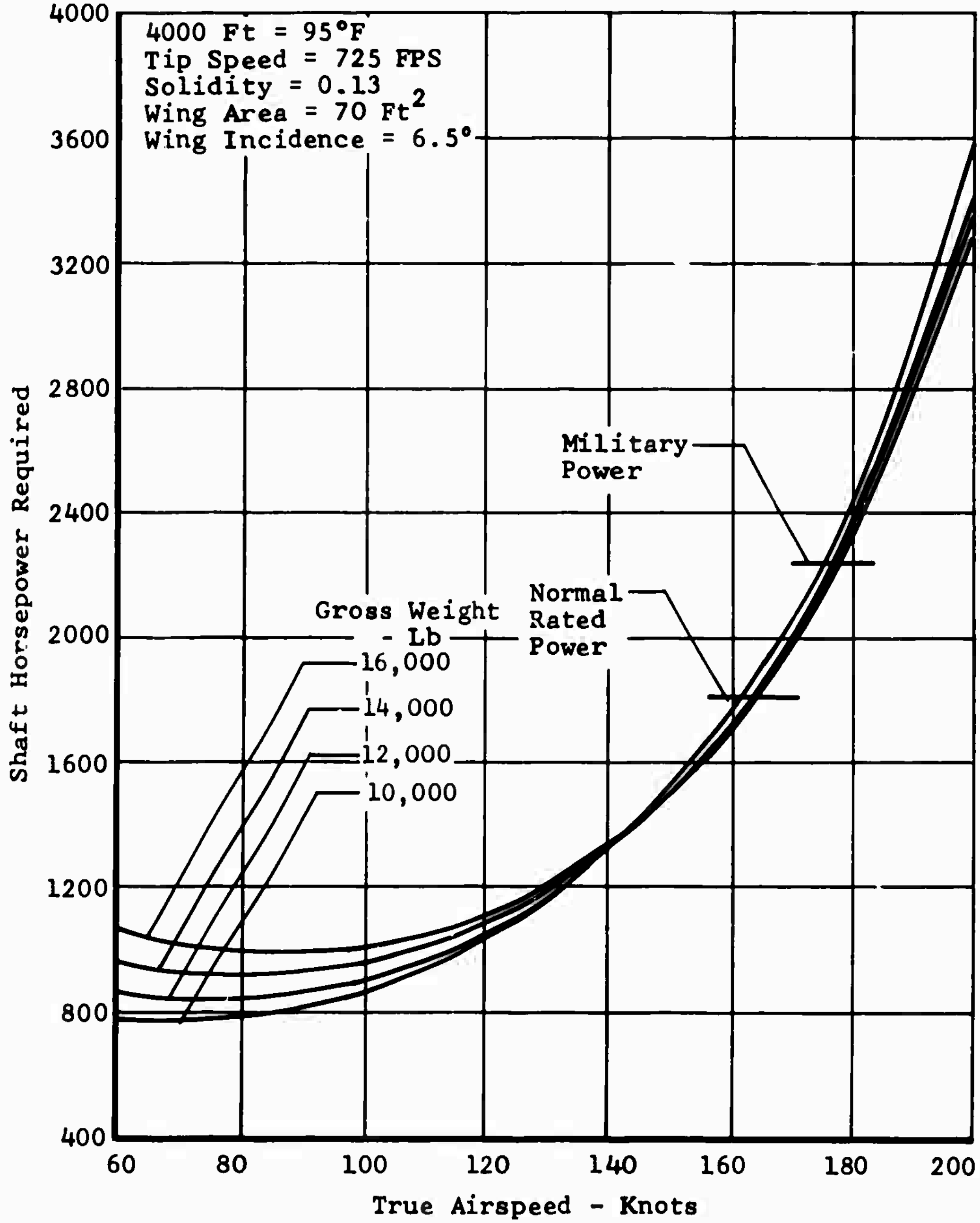

Figure 110. Task II - Winged Helicopter, Speed Power Polar.

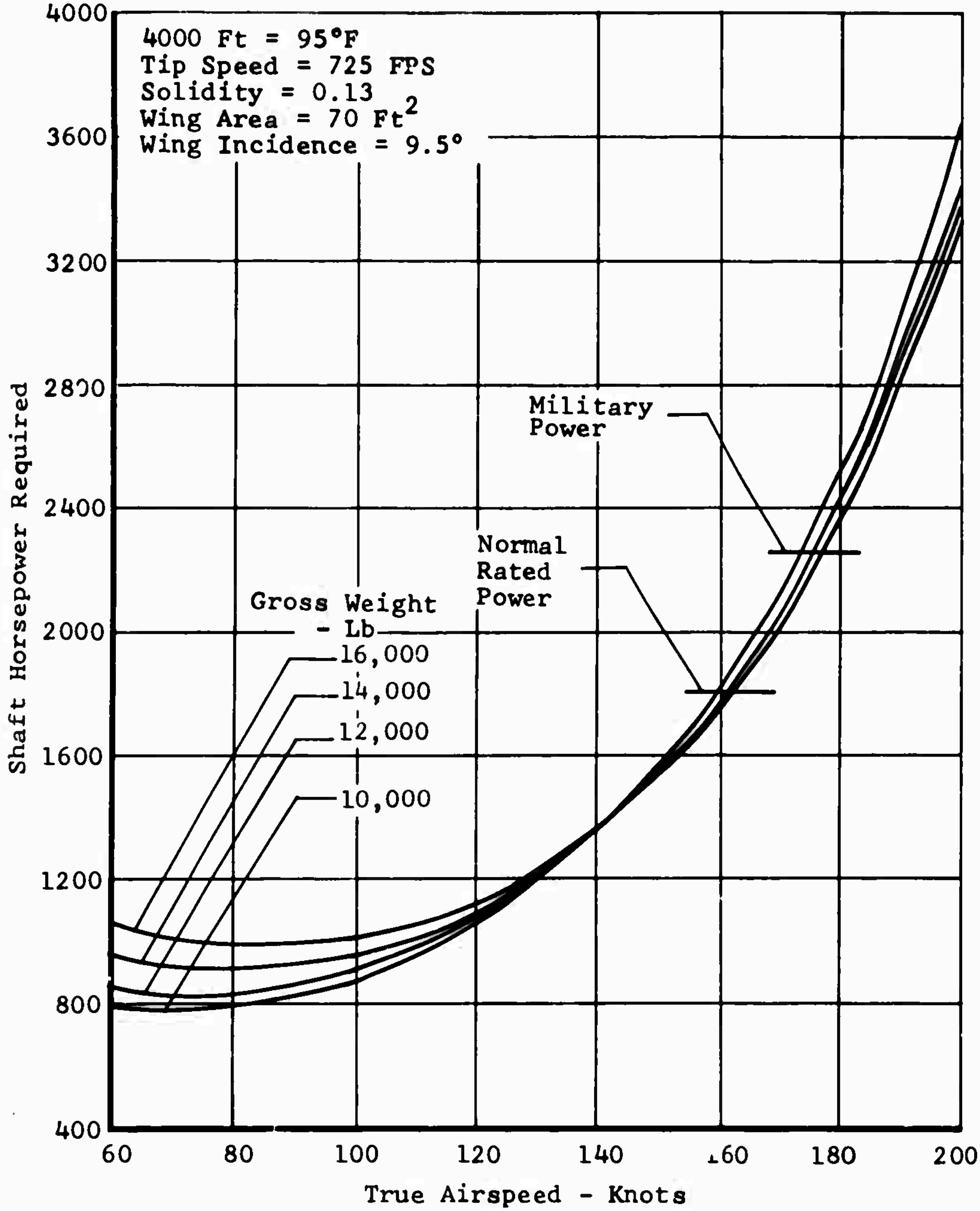

Figure 111. Task II - Winged Helicopter, Speed Power Polar.

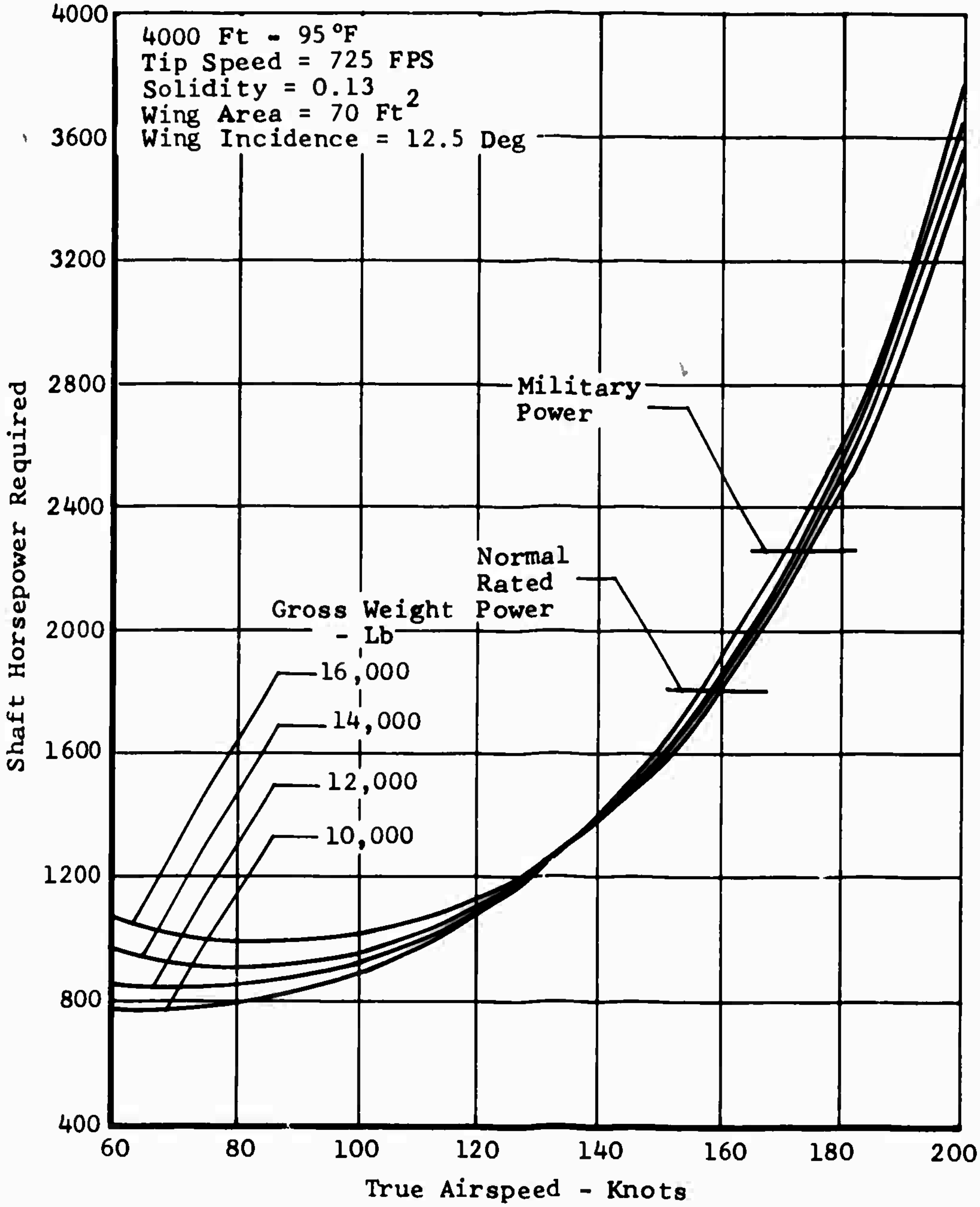

Figure 112. Task II - Winged Helicopter, Speed Power Polar.

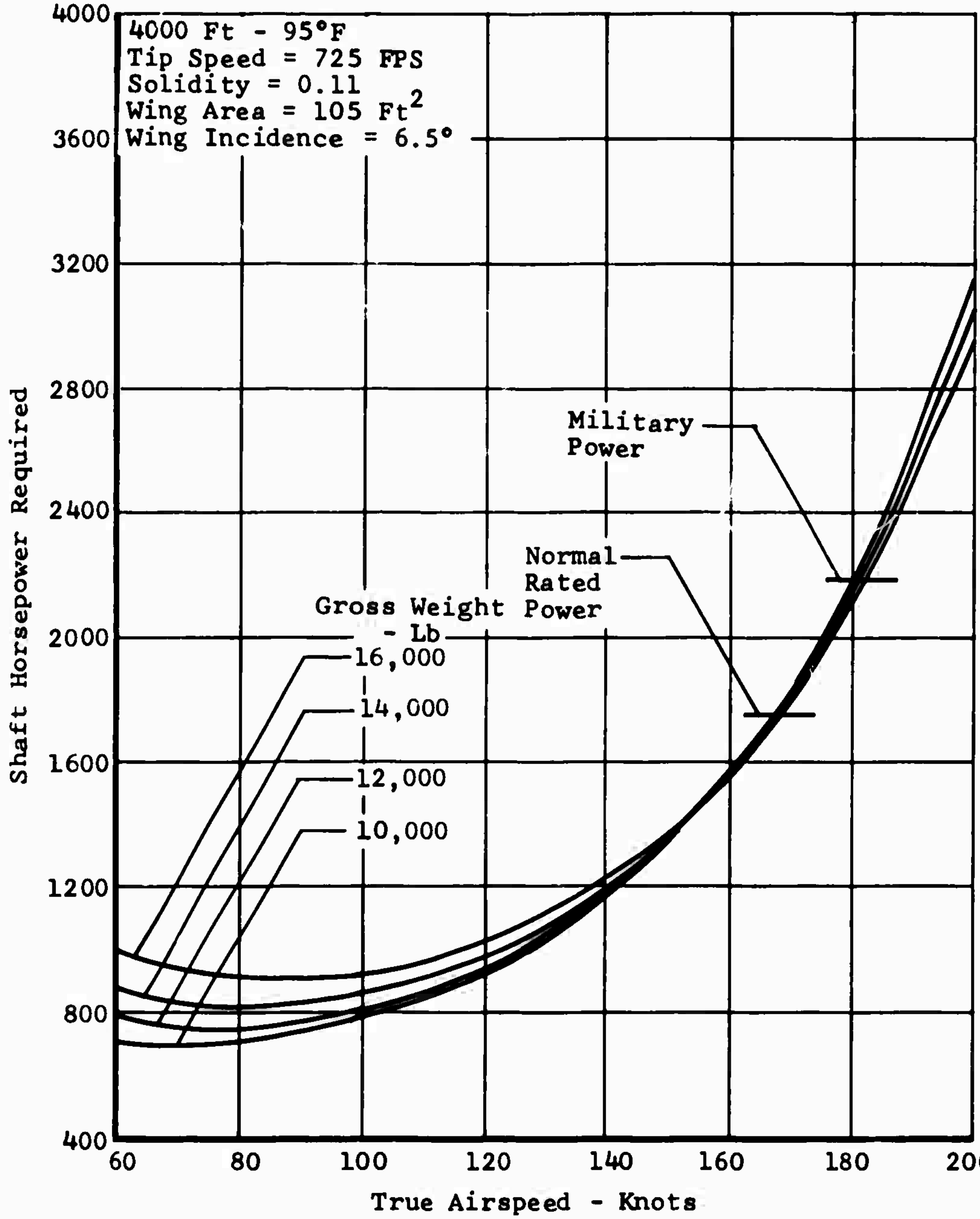

Figure 113. Task II - Winged Helicopter, Speed Power Polar.

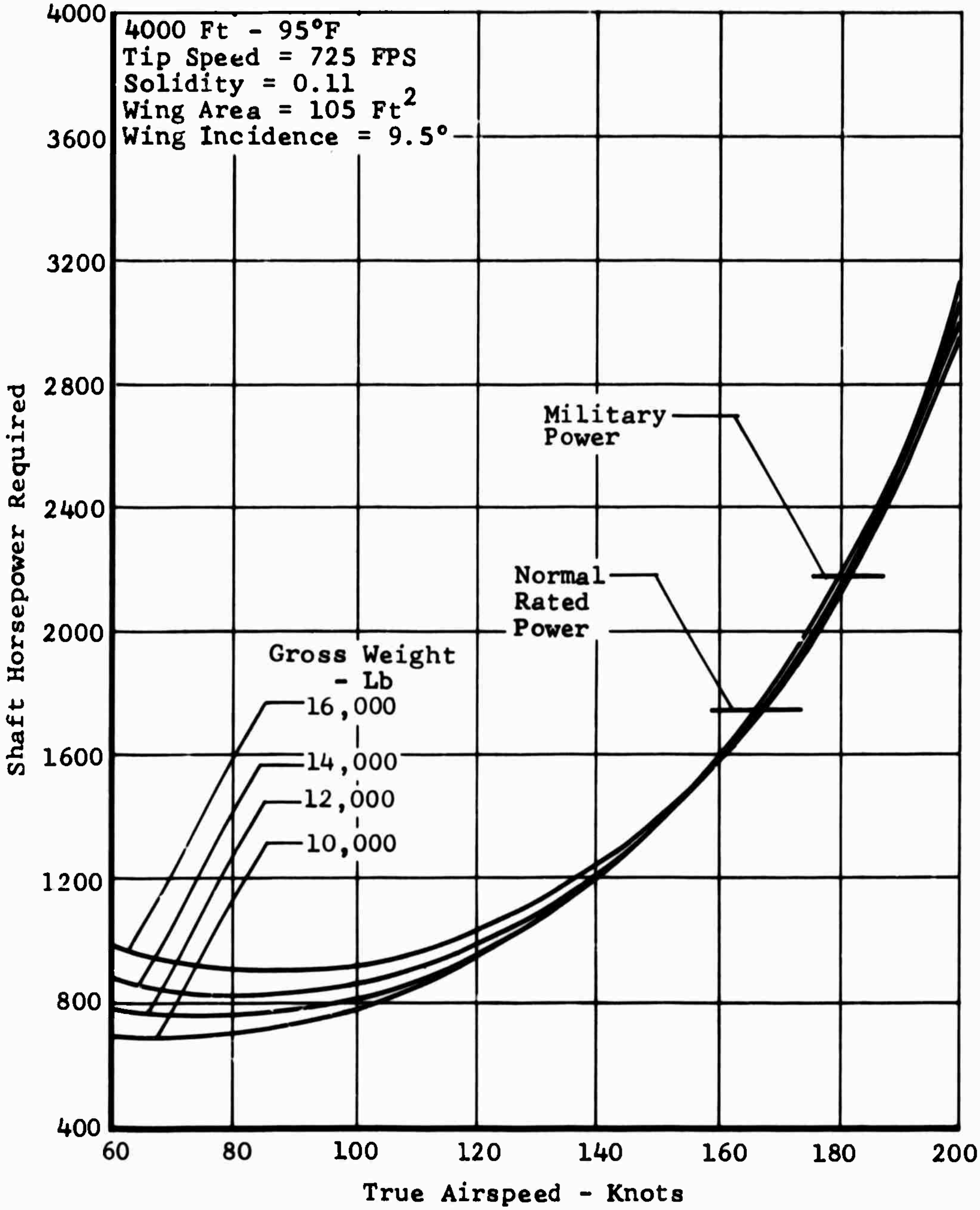

Figure 114. Task II - Winged Helicopter, Speed Power Polar.

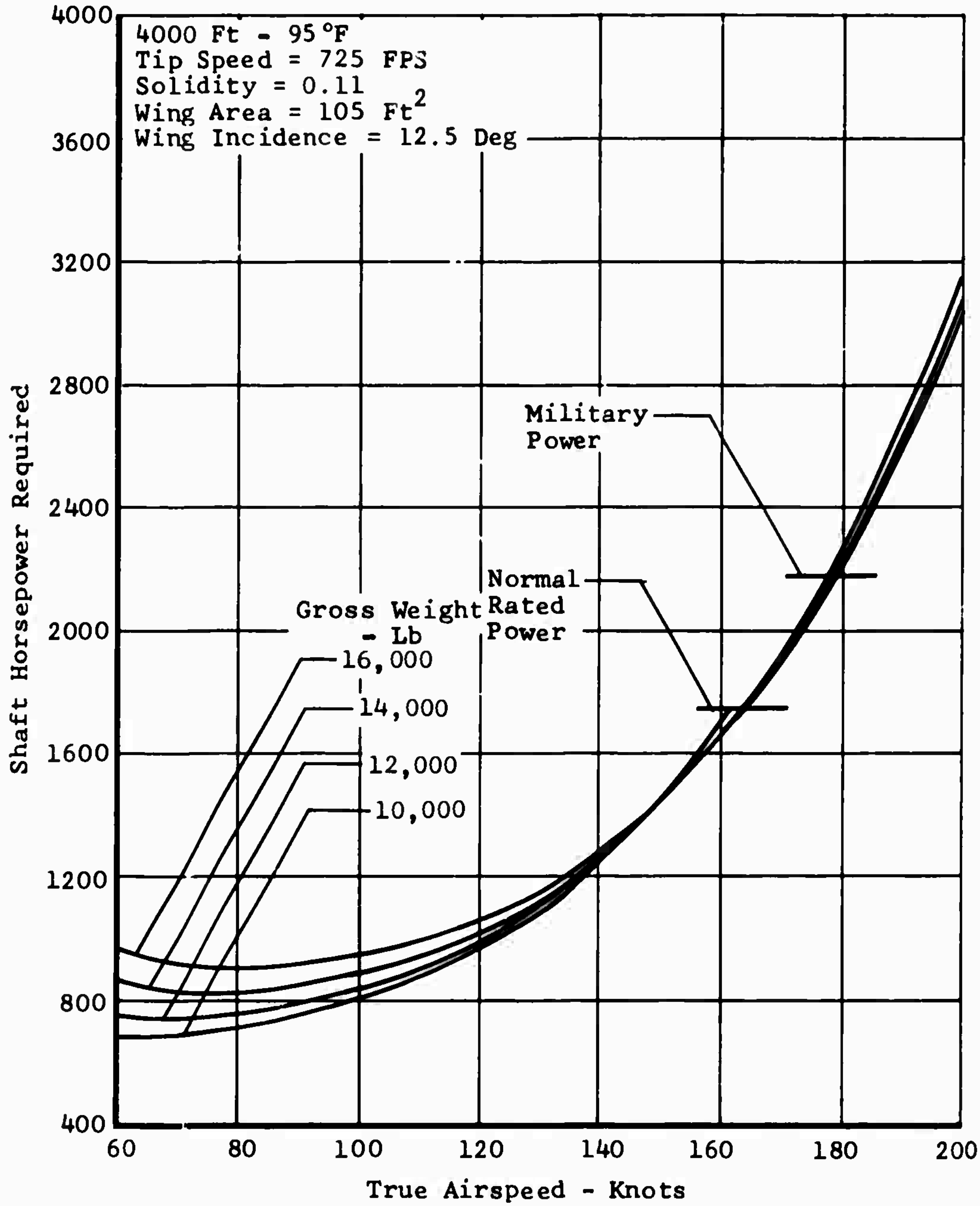

Figure 115. Task II - Winged Helicopter, Speed Power Polar.

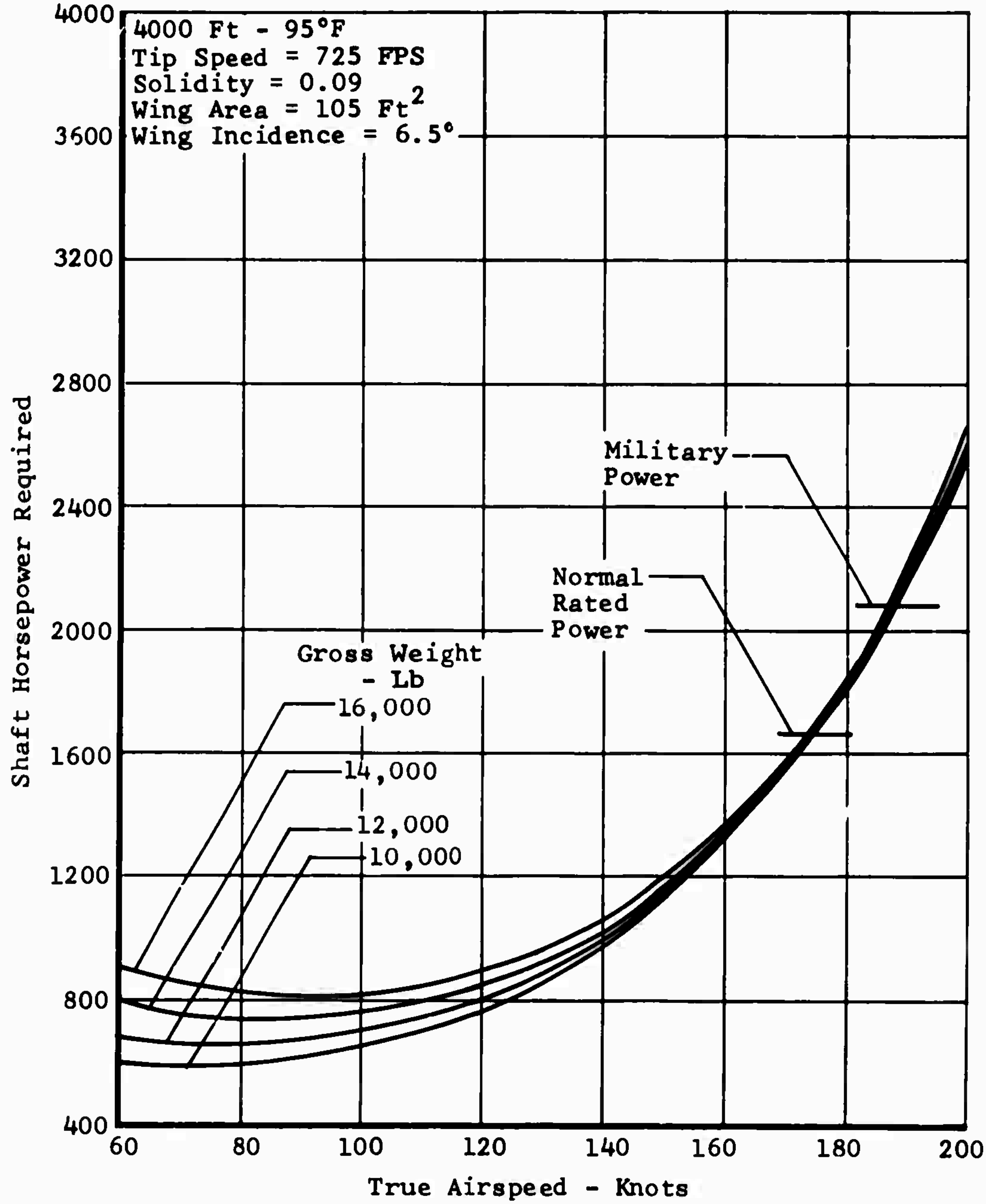

Figure 116. Task II - Winged Helicopter, Speed Power Polar.

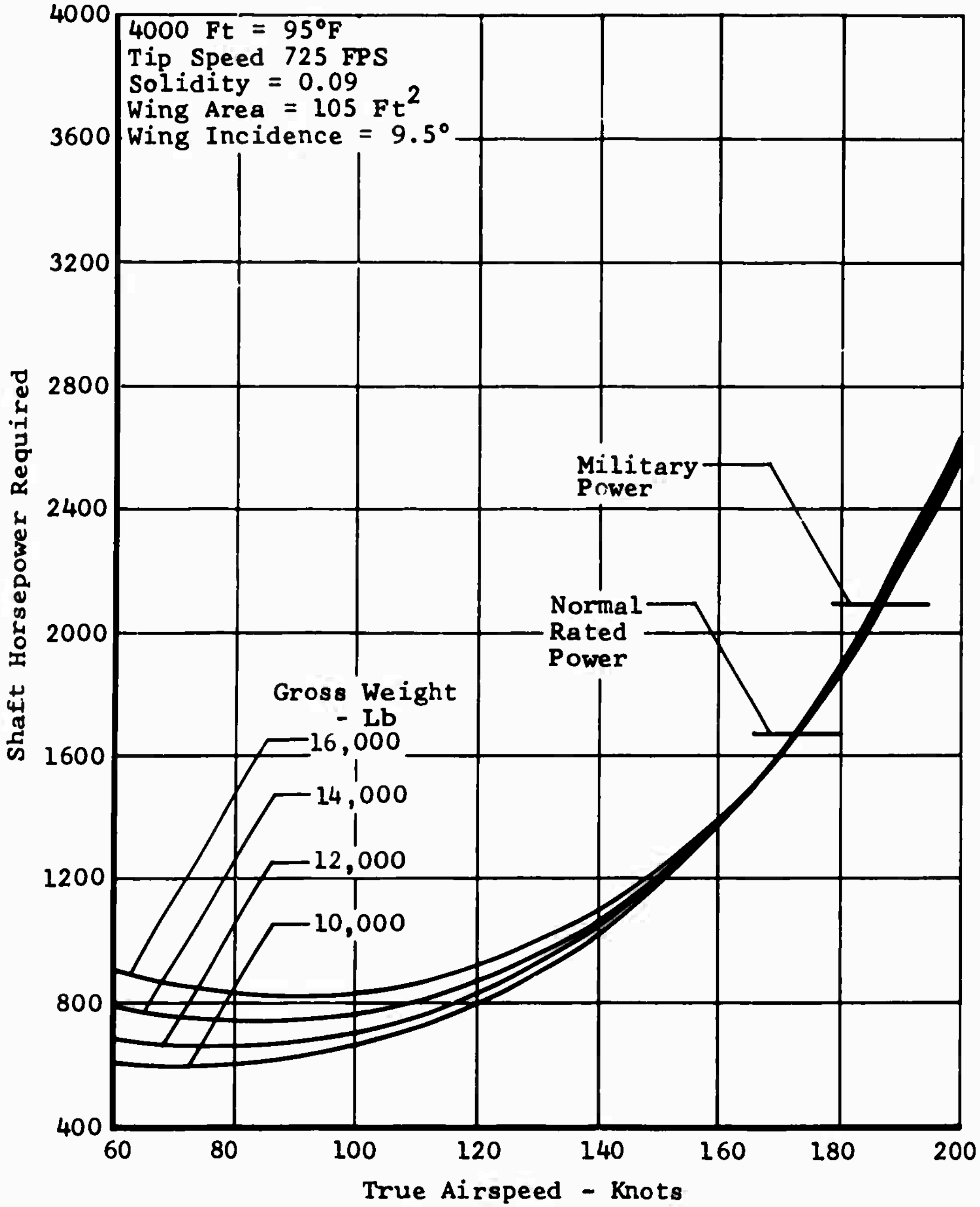

Figure 117. Task II - Winged Helicopter, Speed Power Polar.

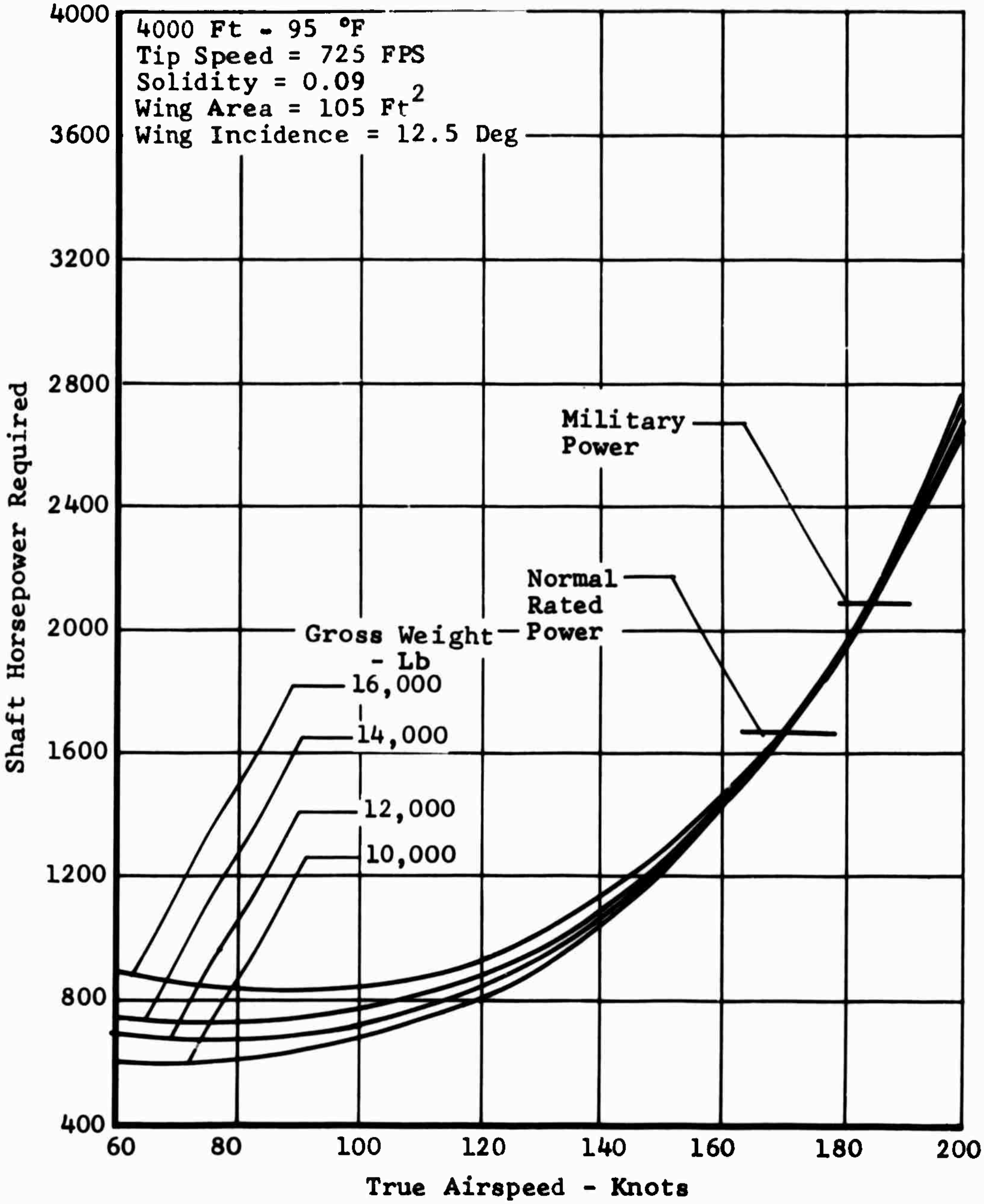

Figure 118. Task II - Winged Helicopter, Speed Power Polar.

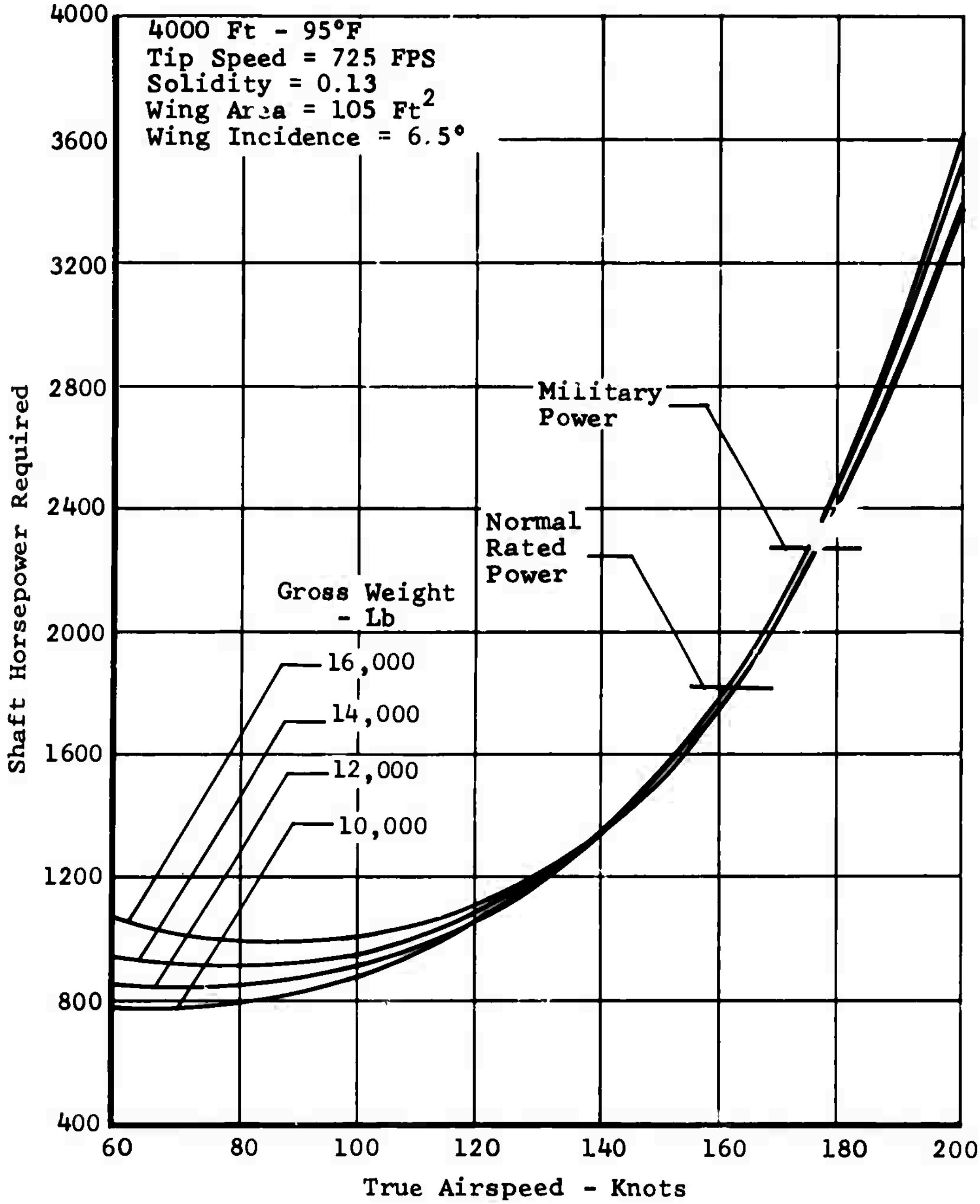

Figure 119. Task II - Winged Helicopter, Speed Power Polar.

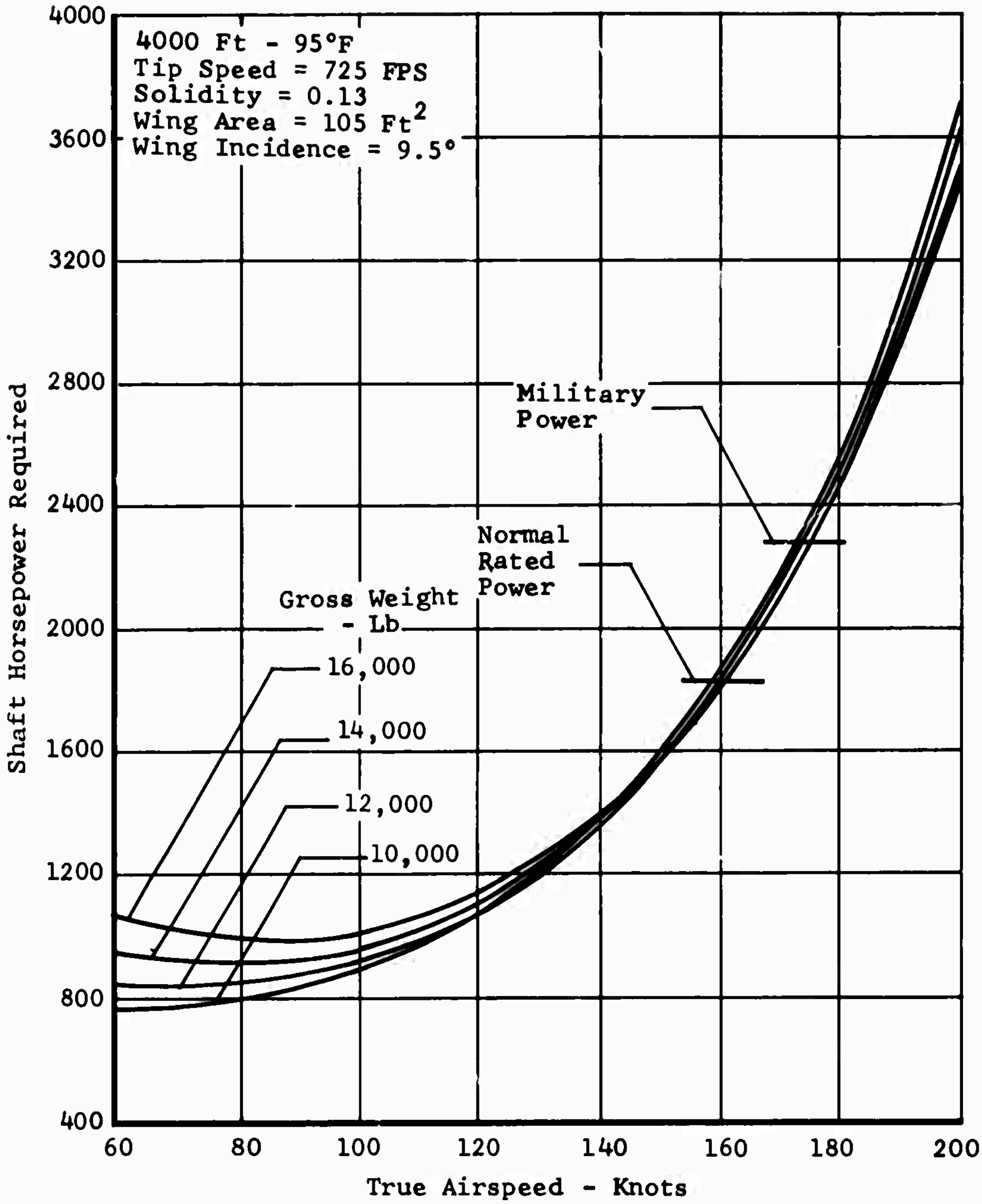

Figure 120. Task II - Winged Helicopter, Speed Power Polar.

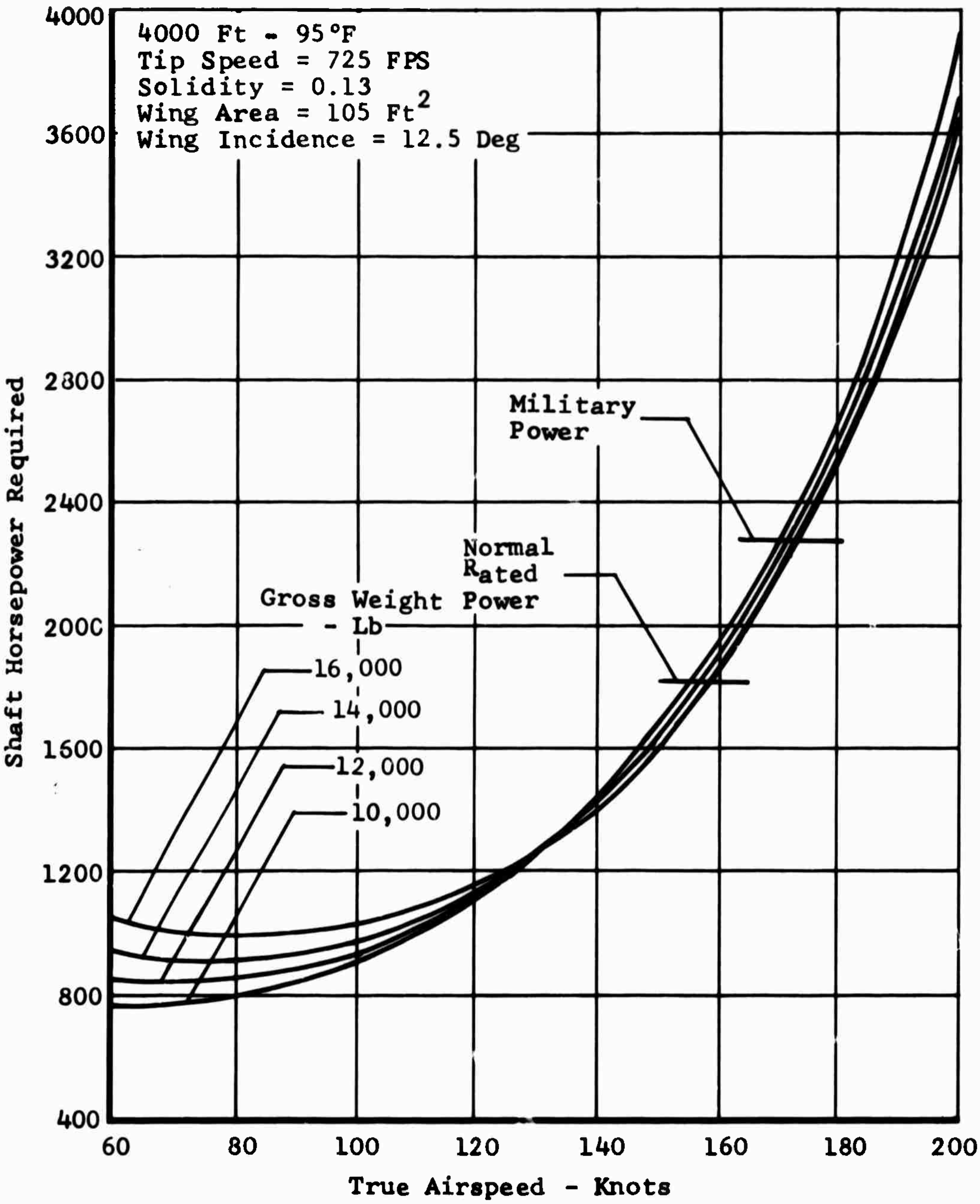

Figure 121. Task II - Winged Helicopter, Speed Power Polar.

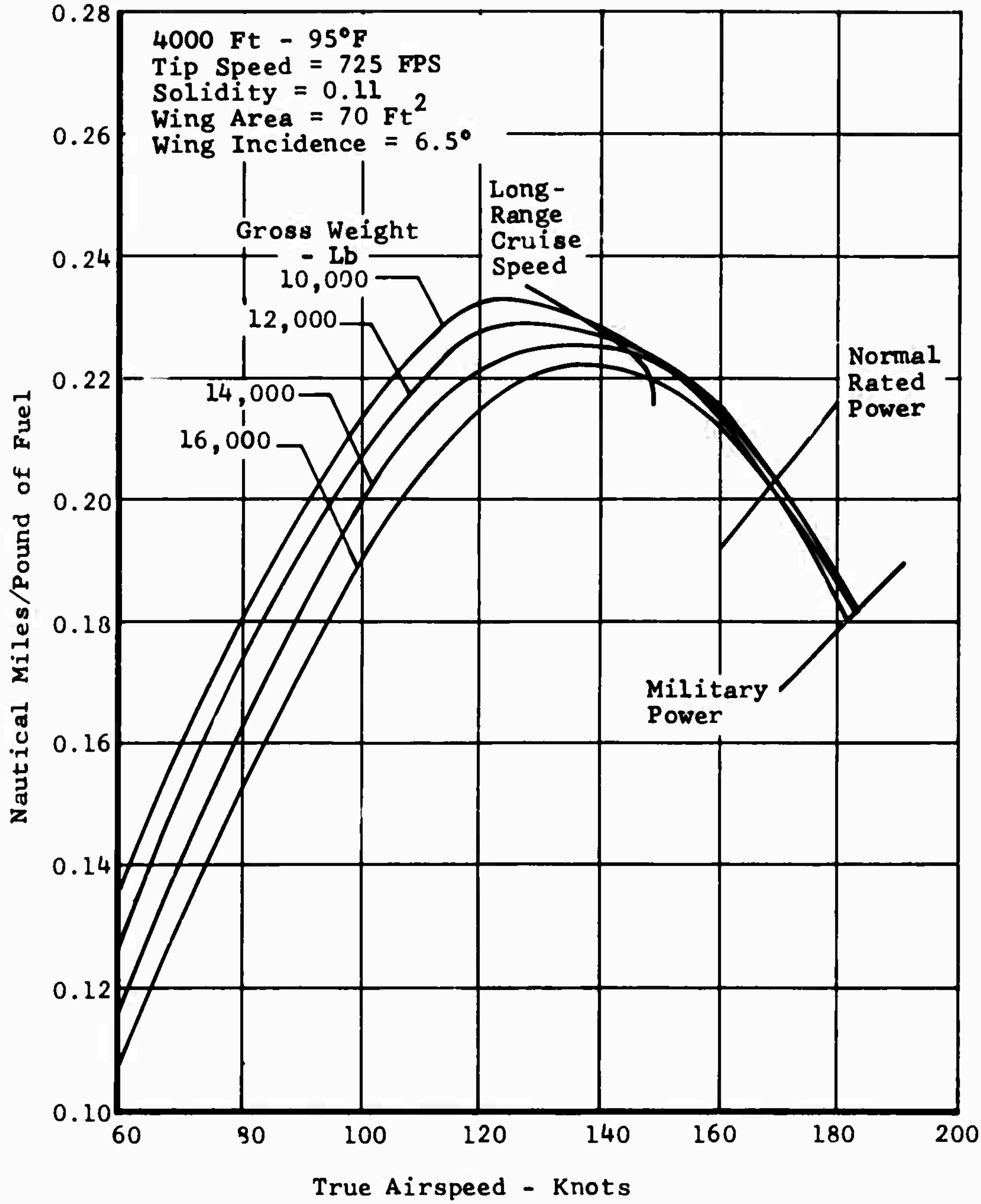

Figure 122. Task II - Winged Helicopter, Specific Range.

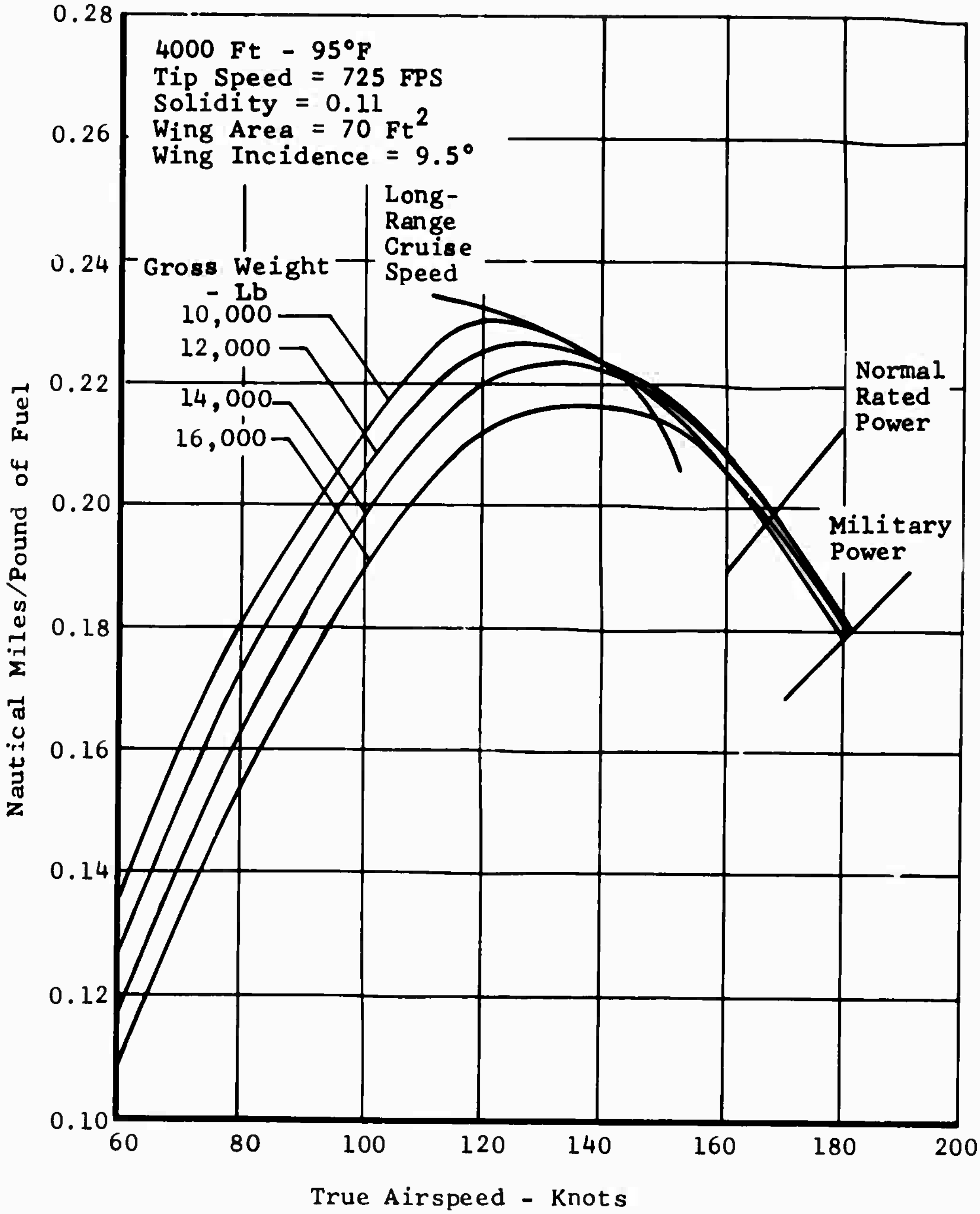

Figure 123. Task II - Winged Helicopter, Specific Range.

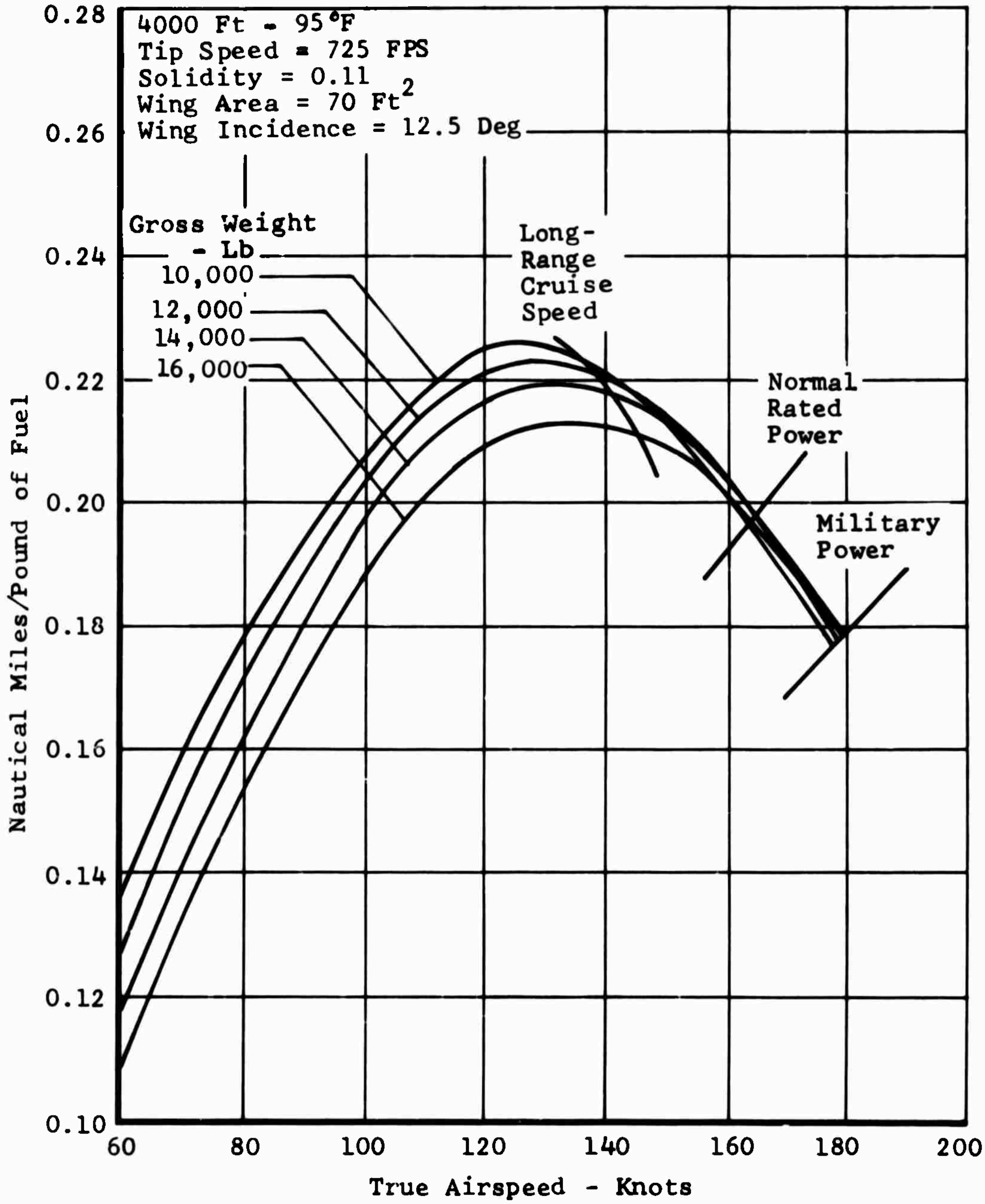

Figure 124. Task II - Winged Helicopter, Specific Range.

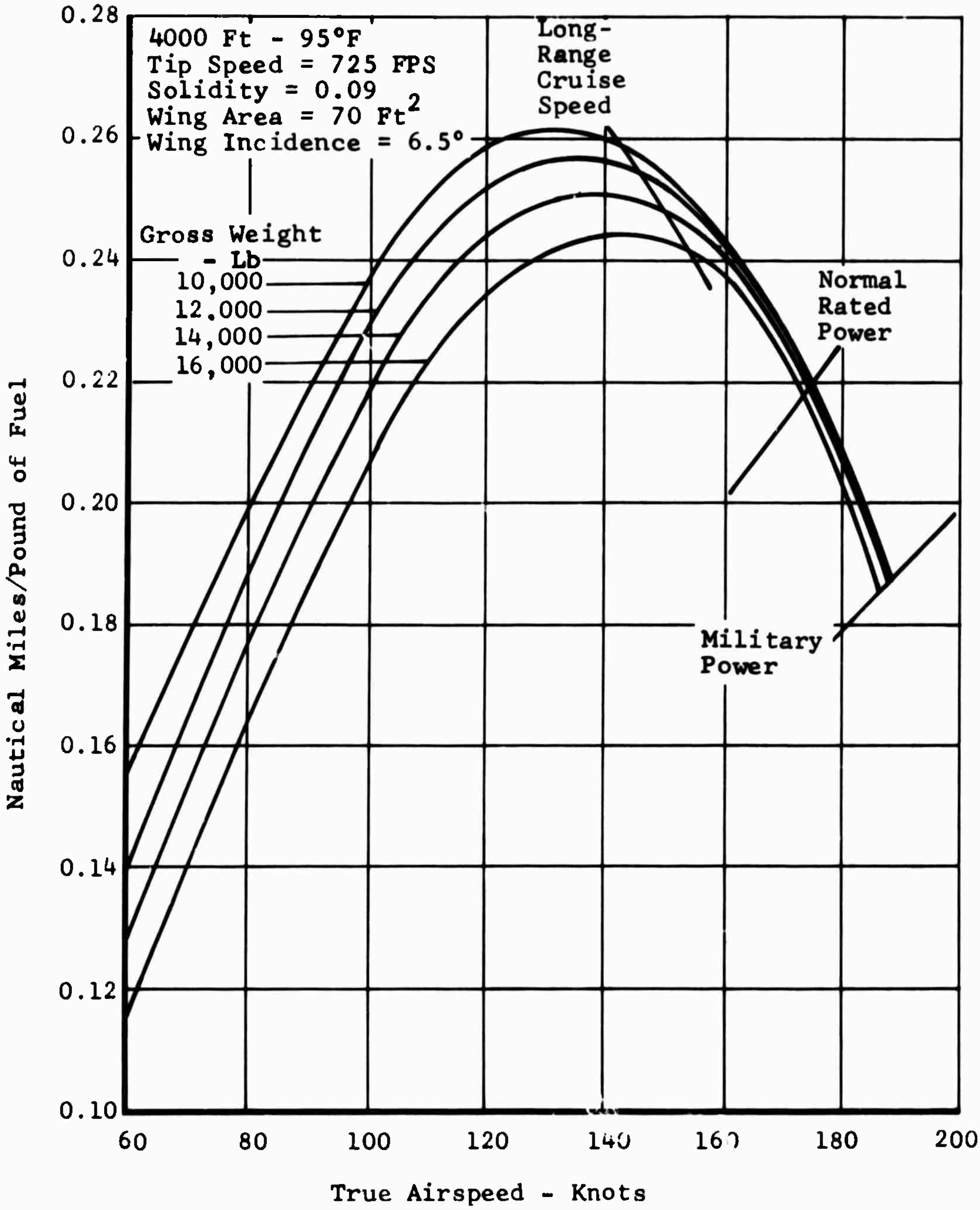

Figure 125. Task II - Winged Helicopter, Specific Range.

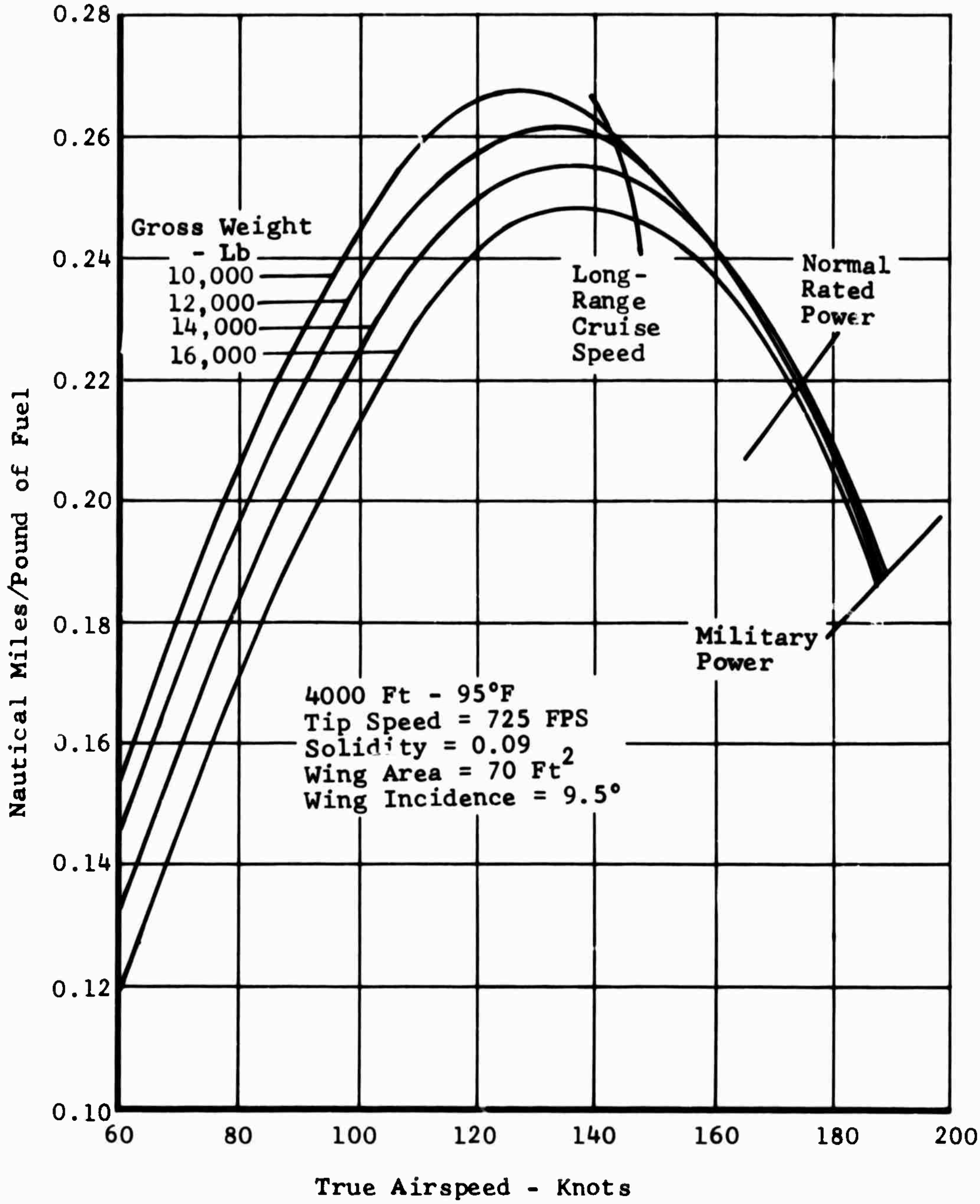

Figure 126. Task II - Winged Helicopter, Specific Range.

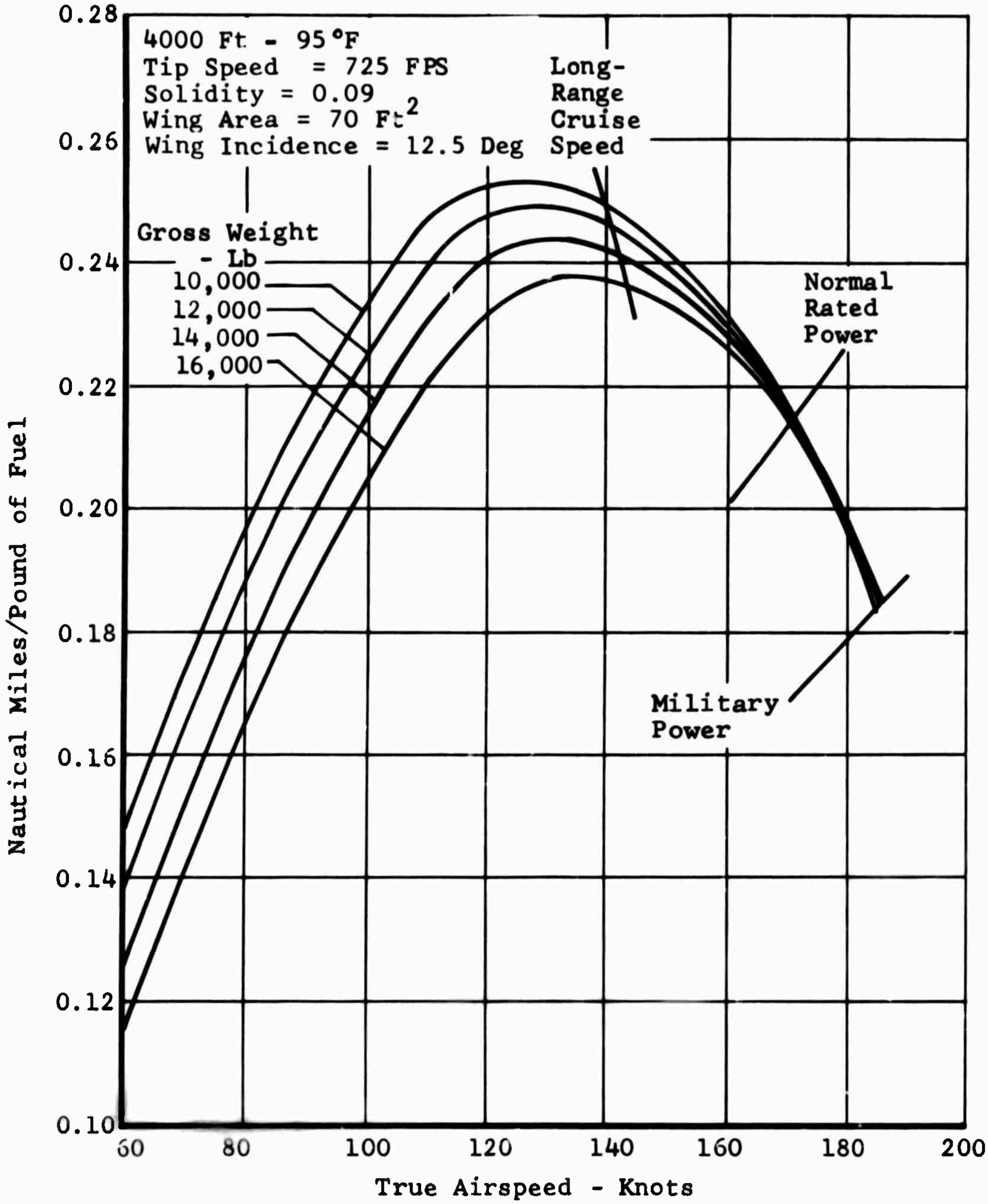

Figure 127. Task II - Winged Helicopter, Specific Range.

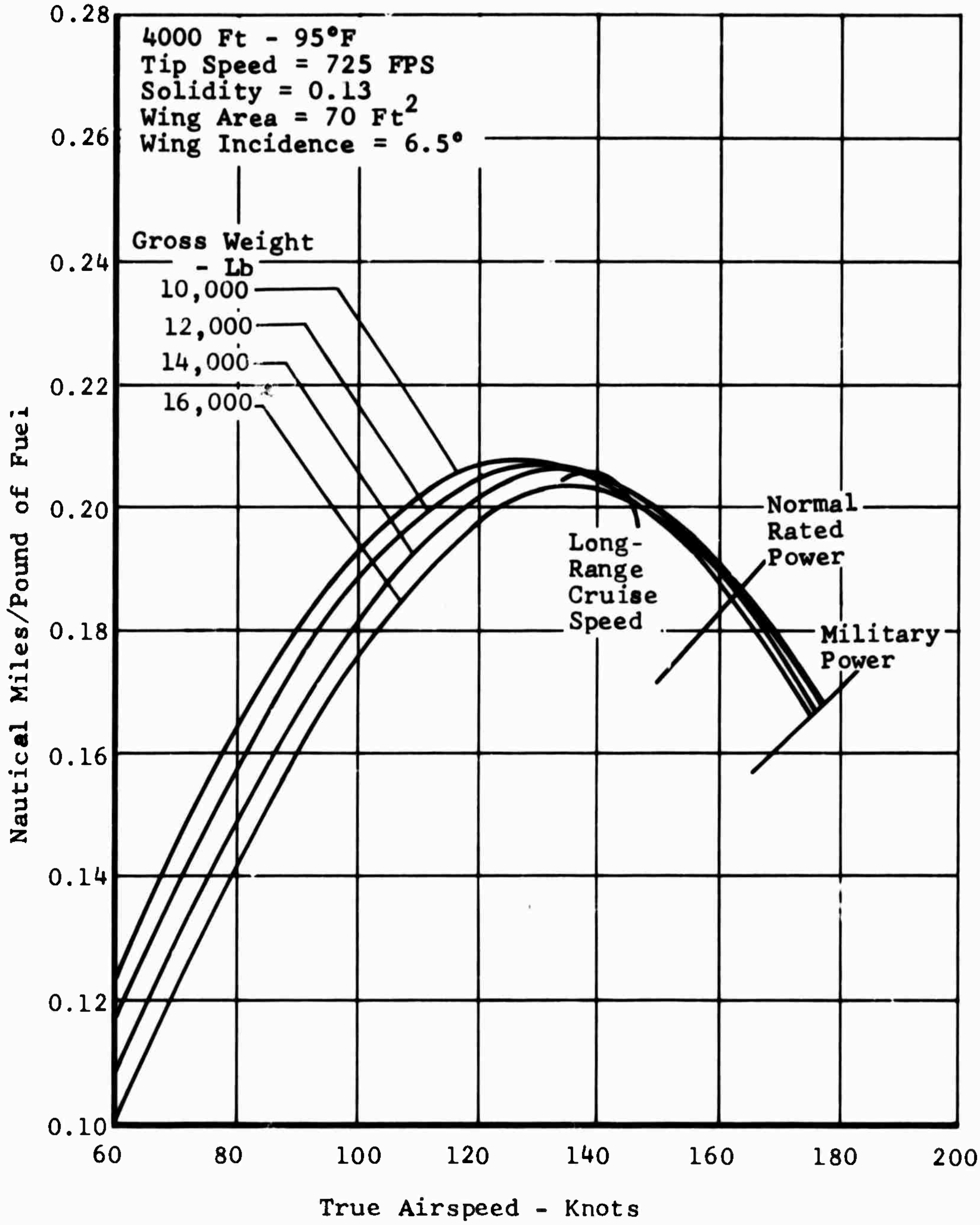

Figure 128. Task II - Winged Helicopter, Specific Range.

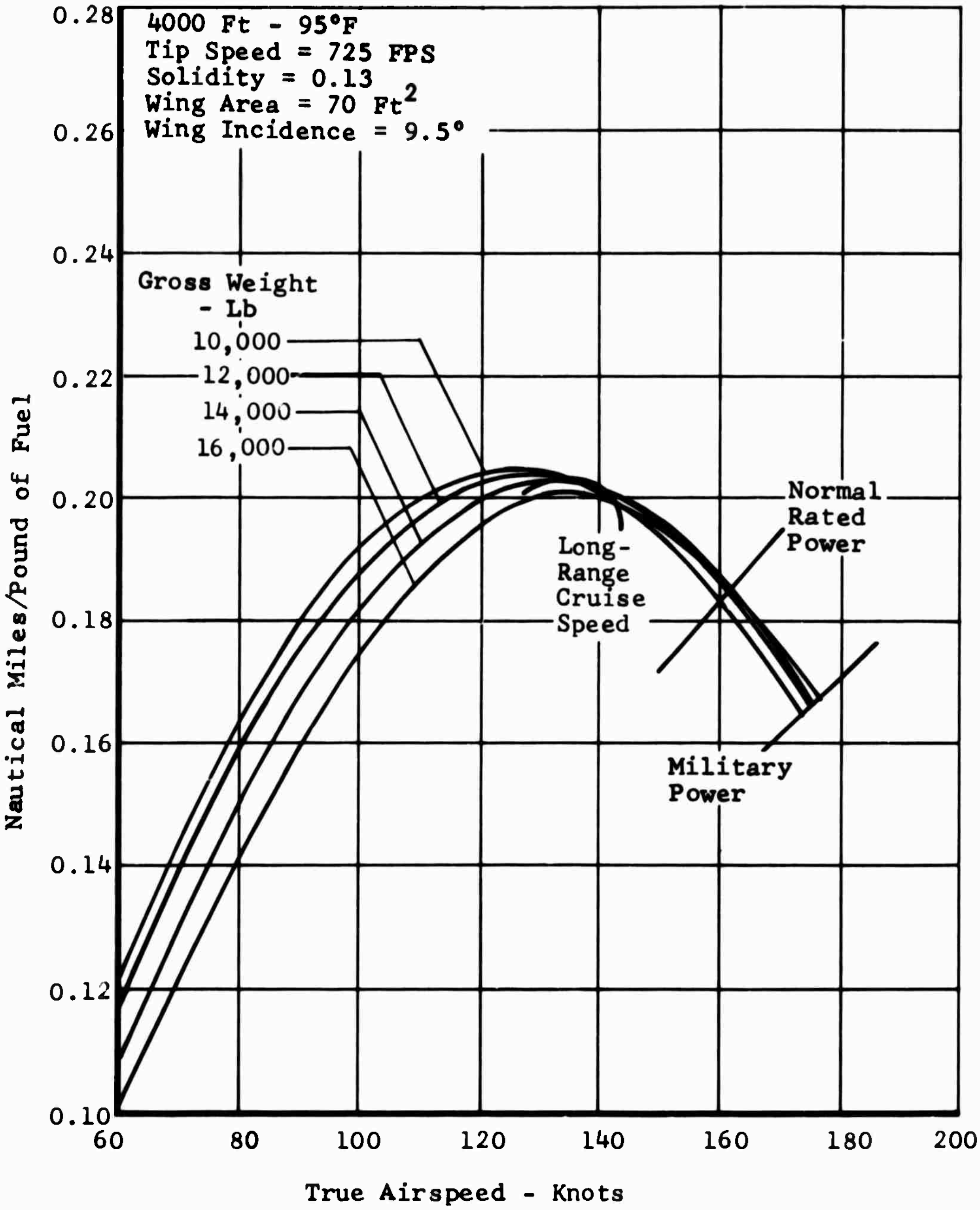

Figure 129. Task II - Winged Helicopter, Specific Range.

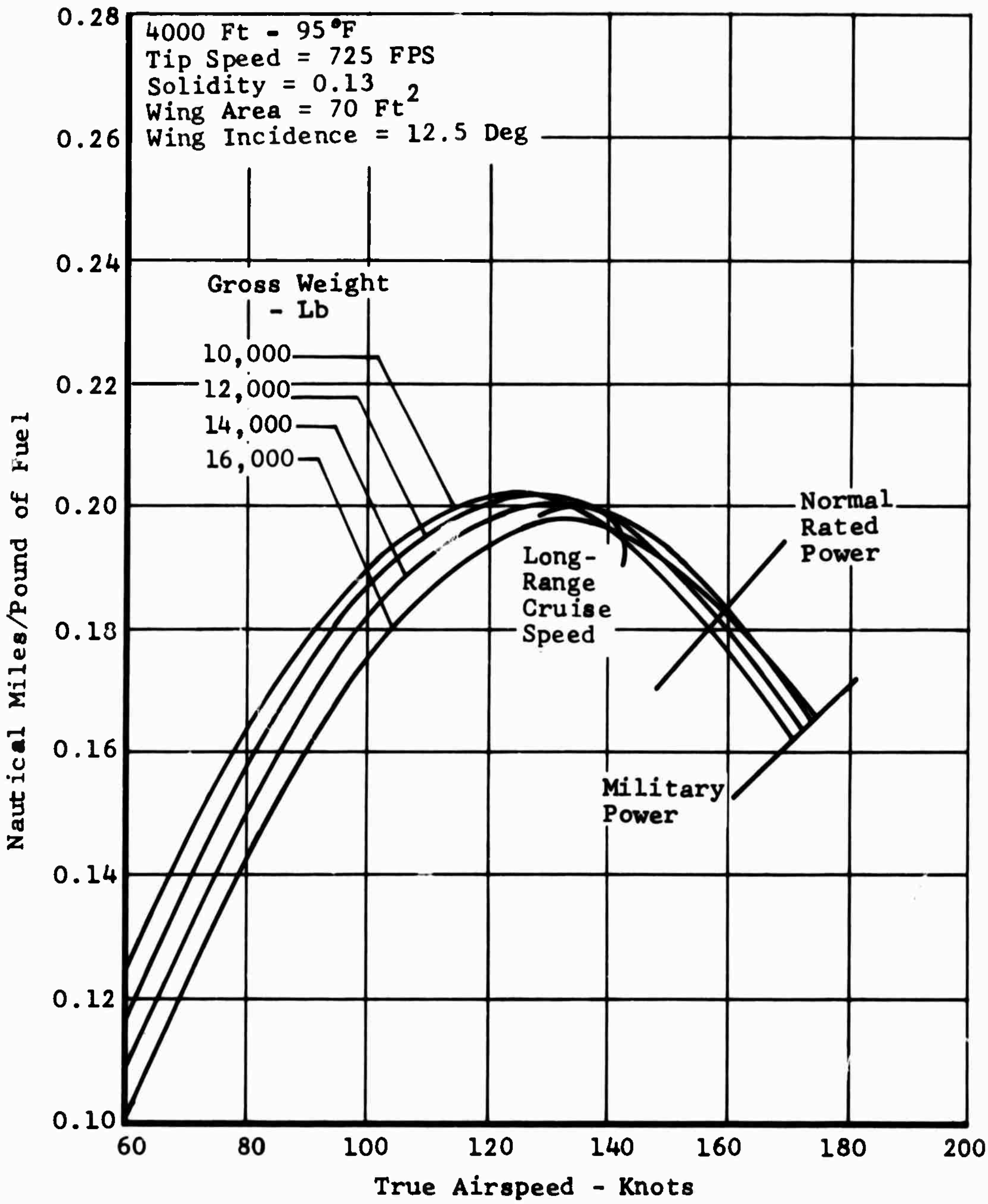

Figure 130. Task II - Winged Helicopter, Specific Range.

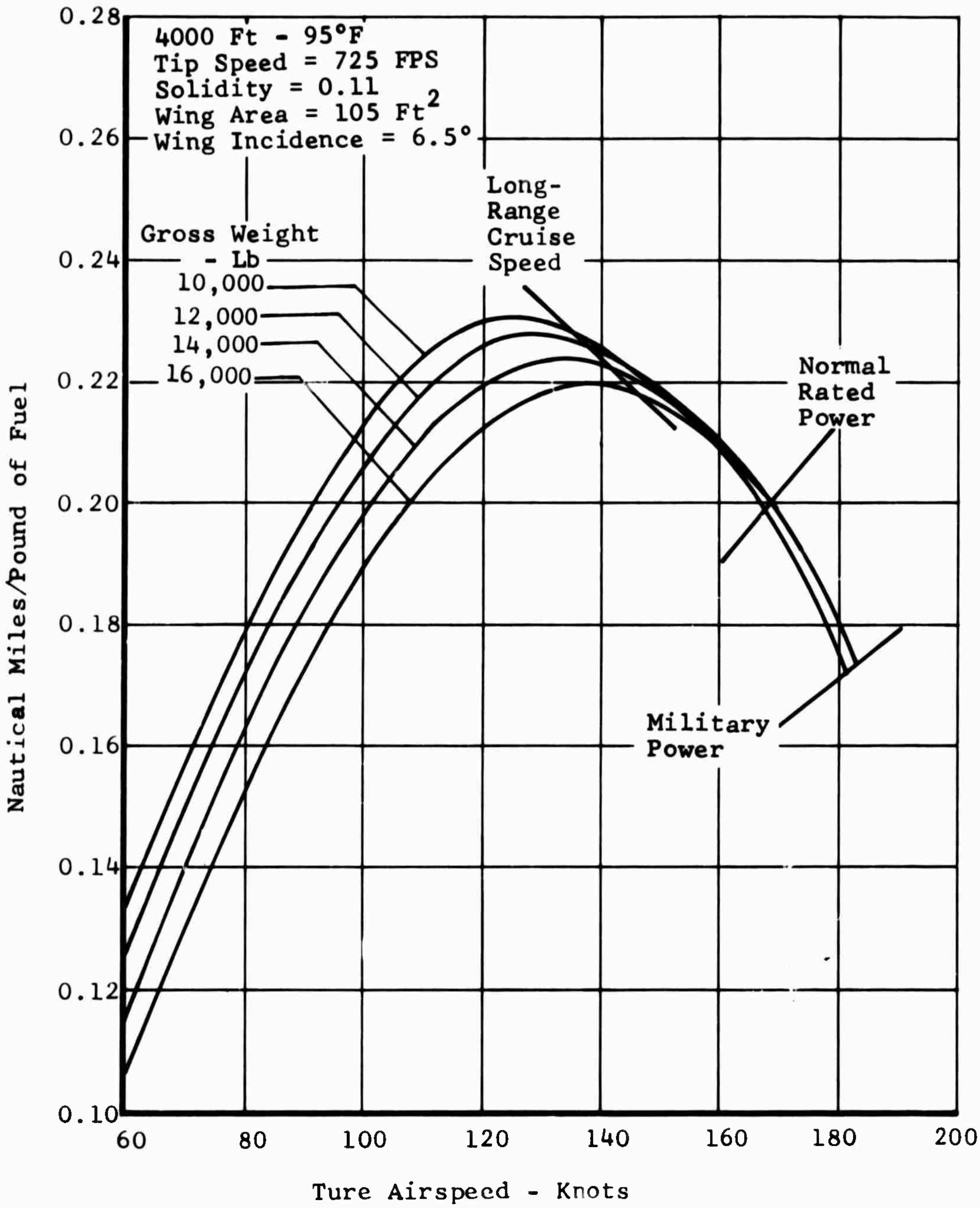

Figure 131. Task II - Winged Helicopter, Specific Range.

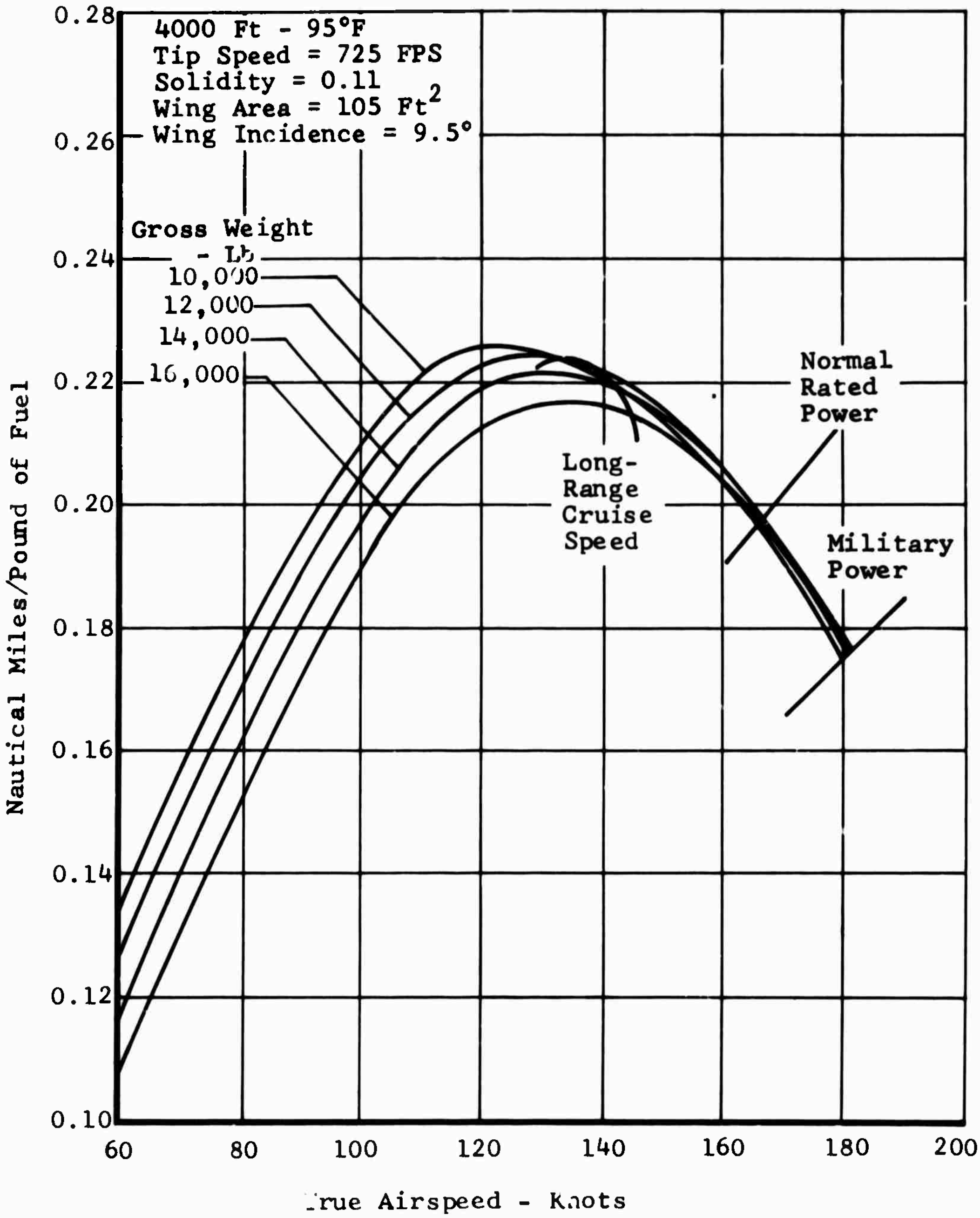

Figure 132. Task II - Winged Helicopter, Specific Range.

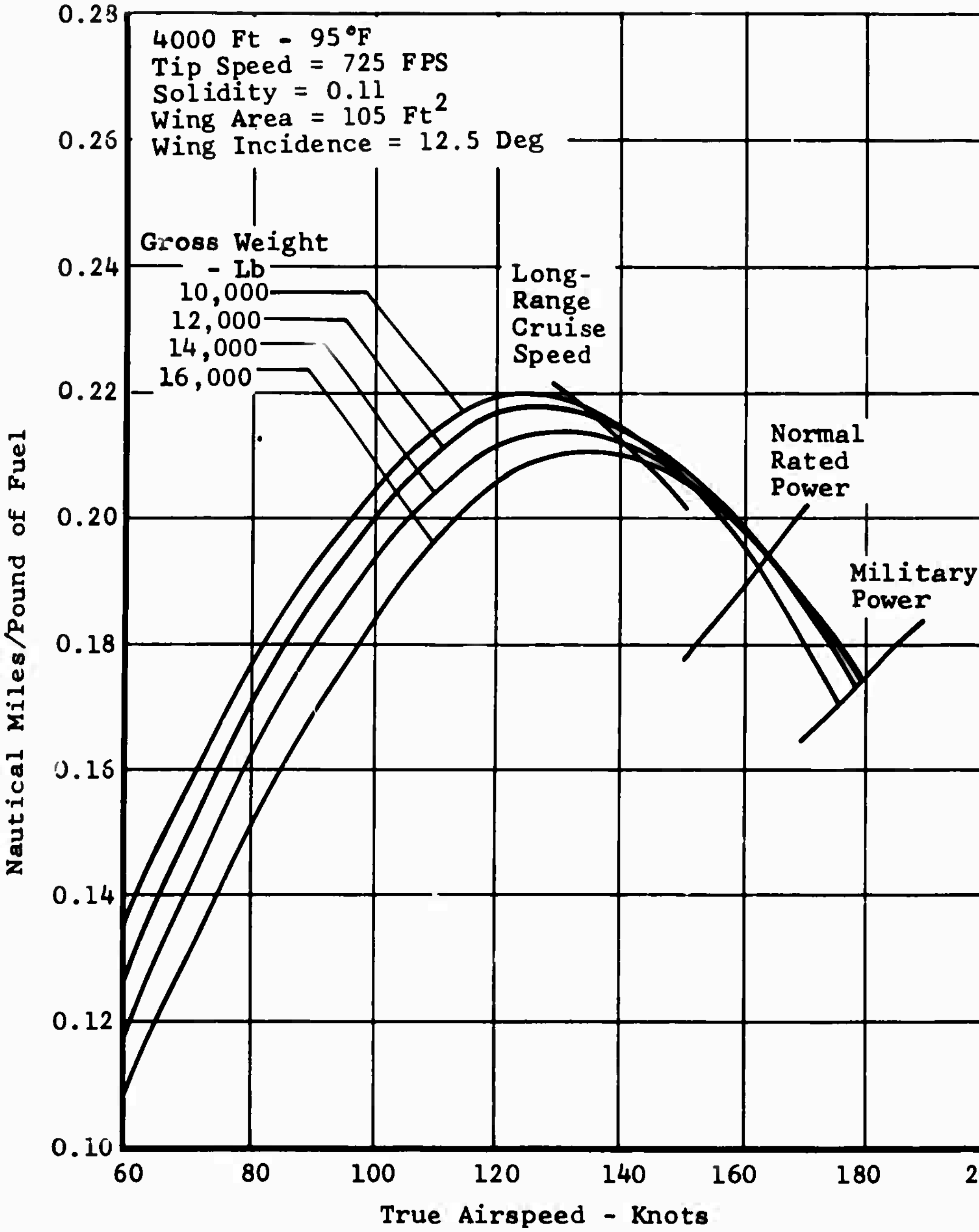

Figure 133. Task II - Winged Helicopter, Specific Range.

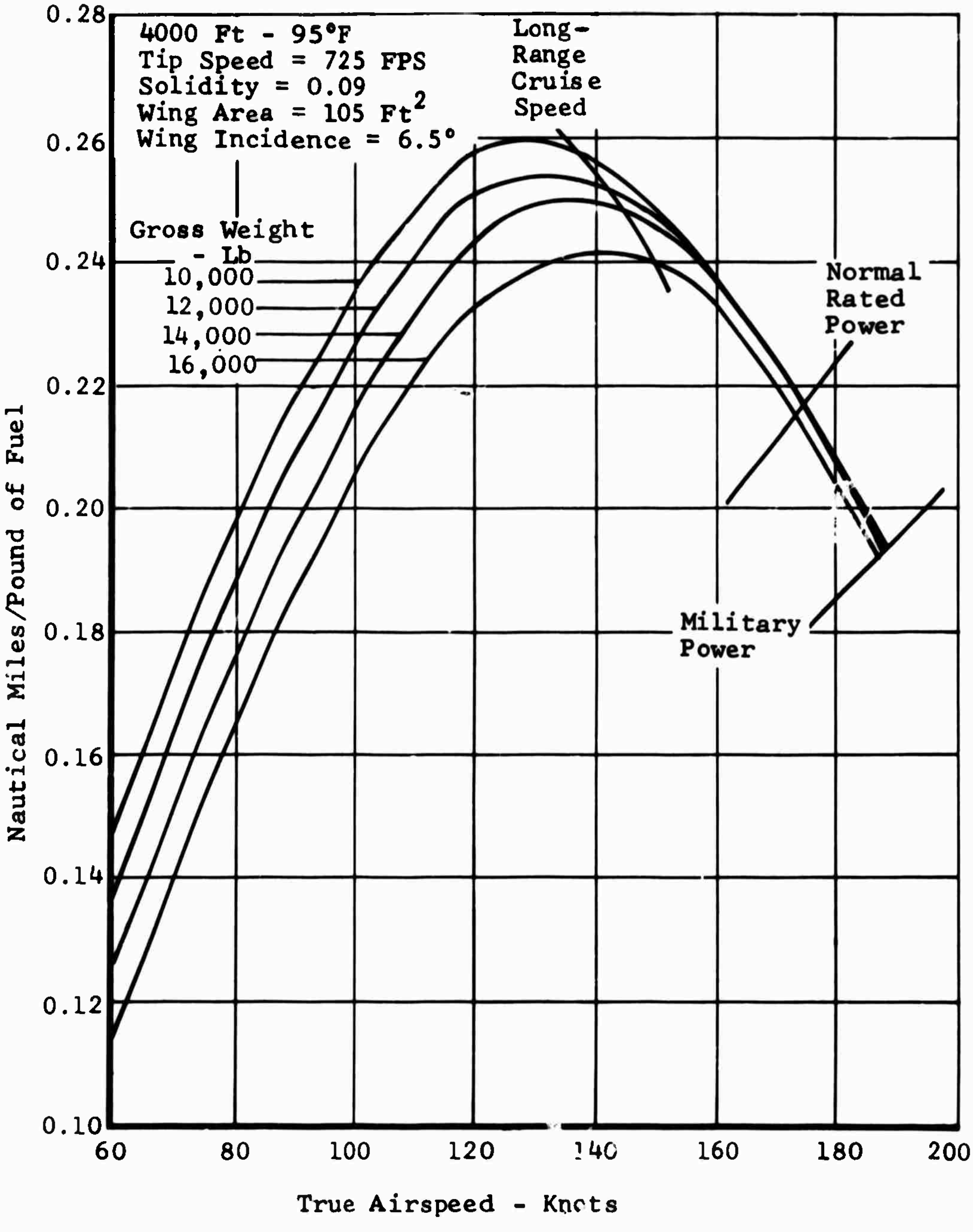

Figure 134. Task II - Winged Helicopter, Specific Range.

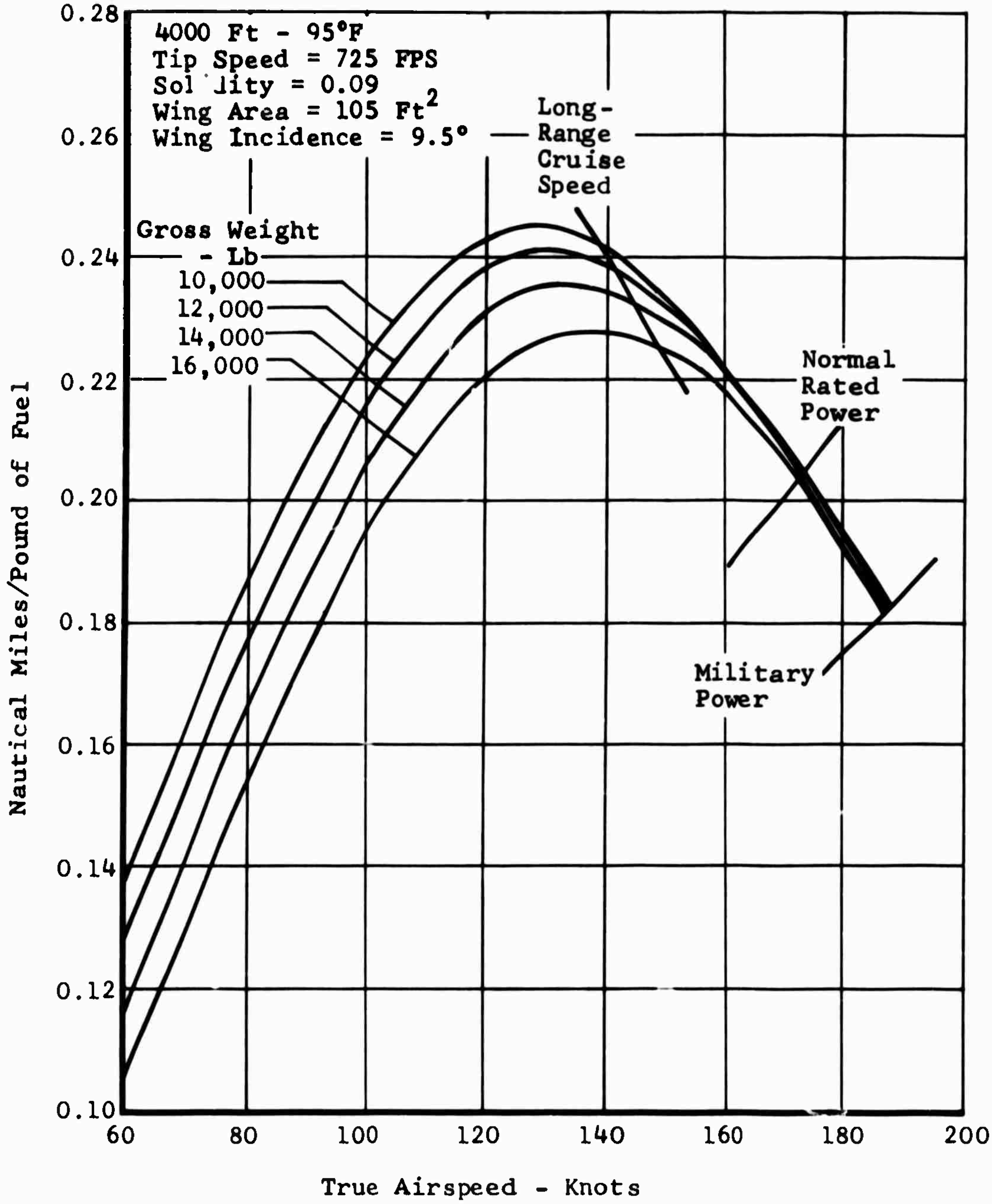

Figure 135. Task II - Winged Helicopter, Specific Range.

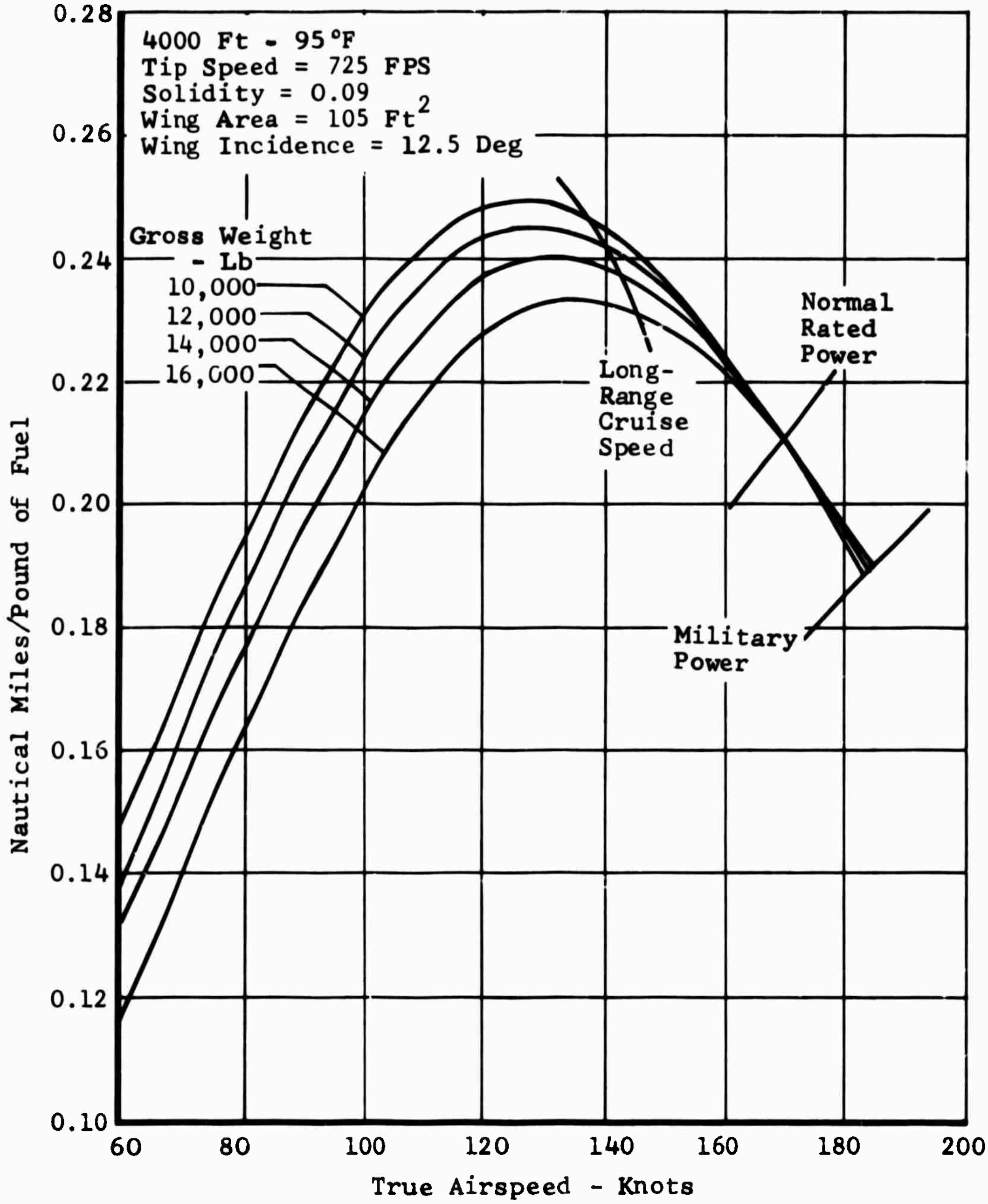

Figure 136. Task II - Winged Helicopter, Specific Range.

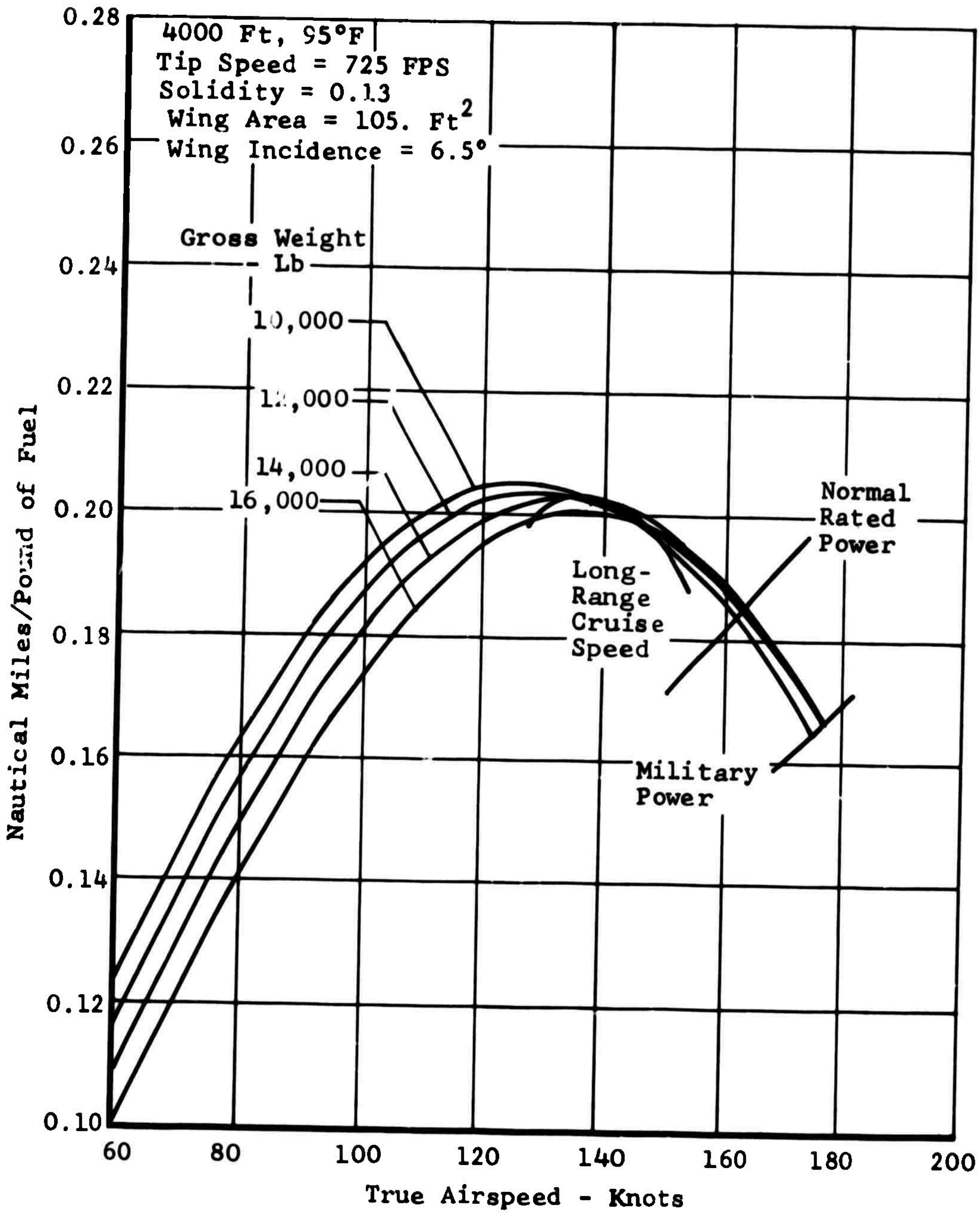

Figure 137. Task II - Winged Helicopter, Specific Range.

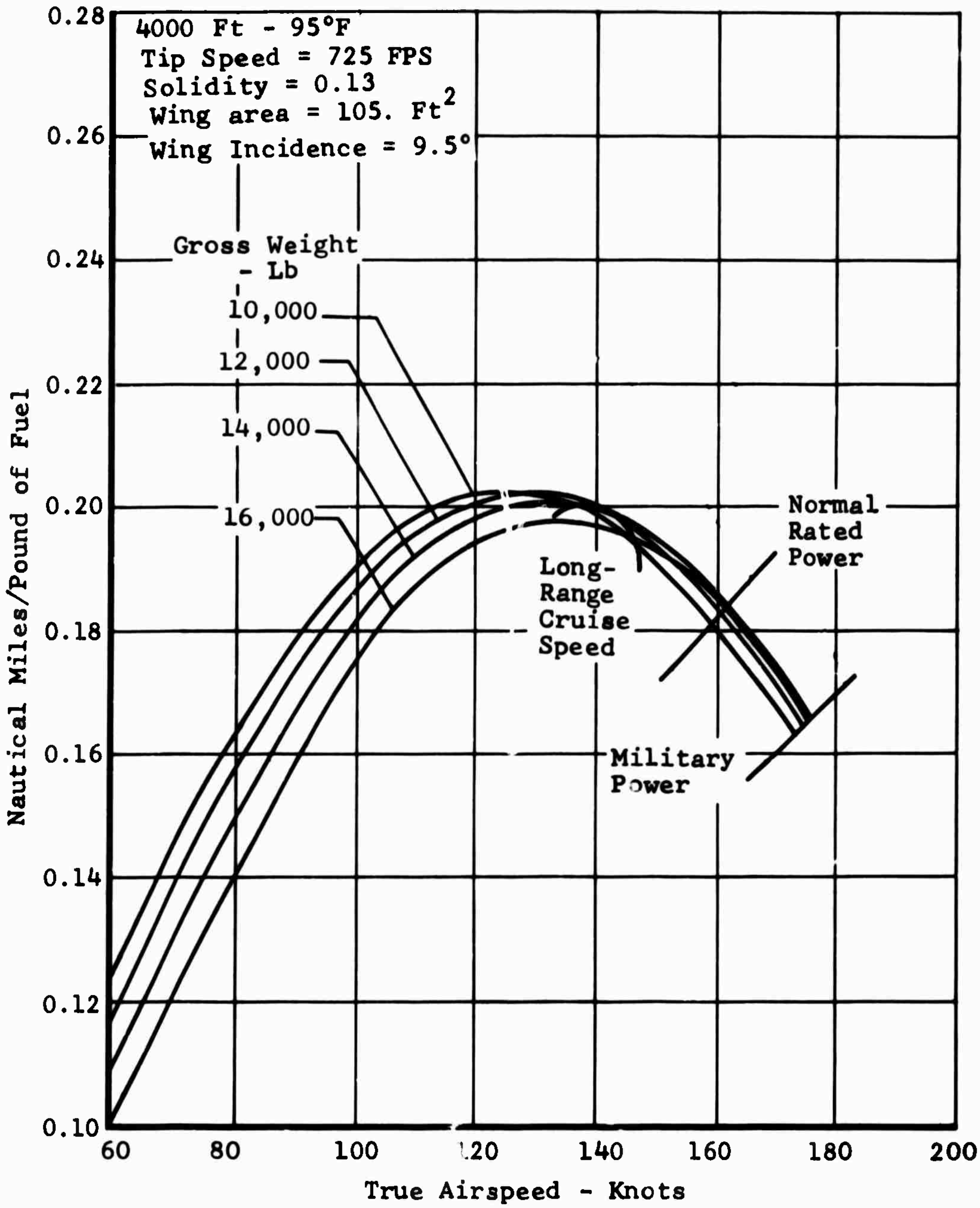

Figure 138. Task II - Winged Helicopter, Specific Range.

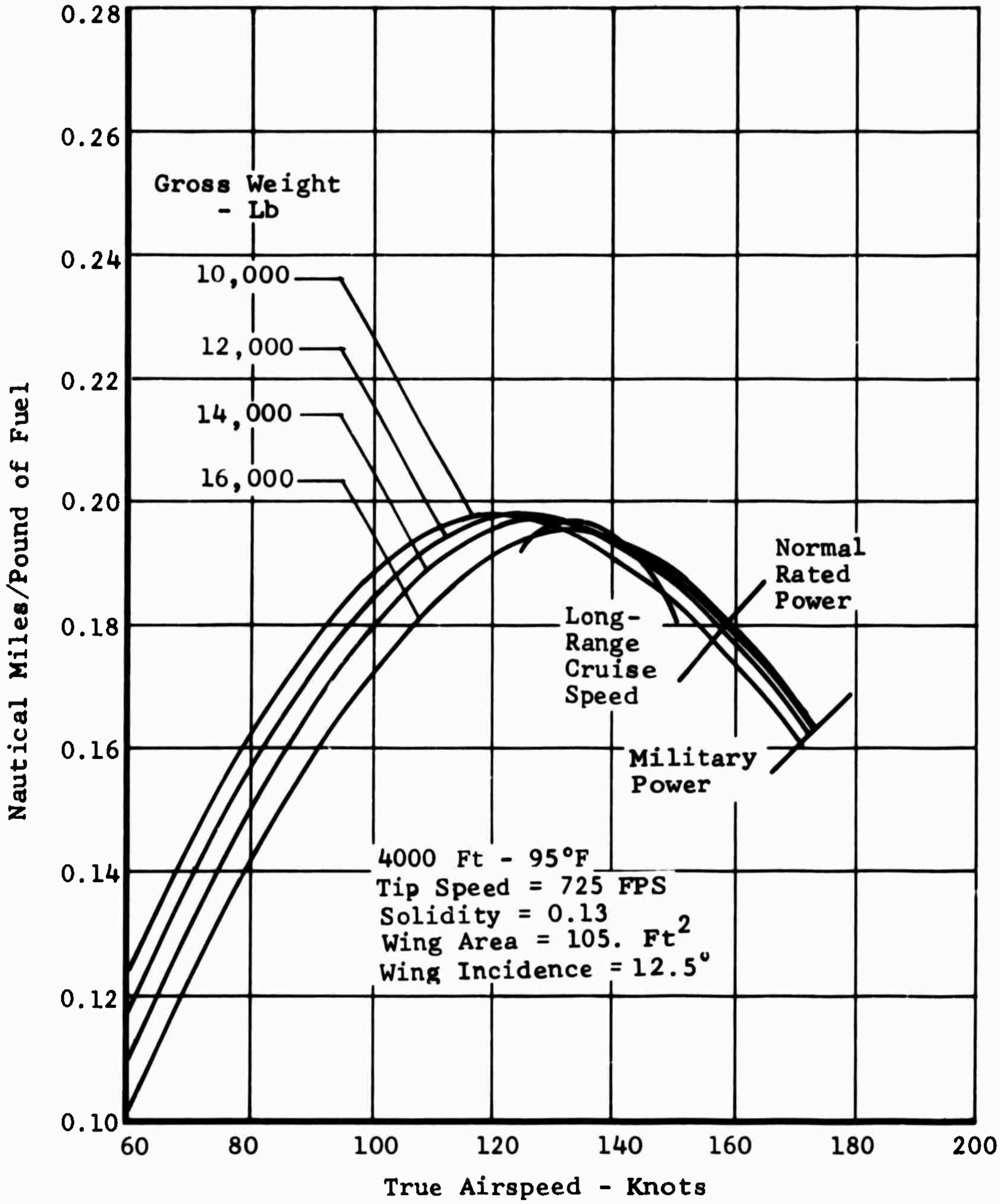

Figure 139. Task II - Winged Helicopter, Specific Range.

APPENDIX IV

TASK II - MANEUVER RESULTS, BASIC DATA

TABLE XXXVIII. RESULTS OF PULLUP AND PUSHOVER MANEUVERS, TASK II – WINGED CONFIGURATIONS, LOW SOLIDITY ROTOR

Wing Incidence (Deg)	Wing Area (Ft^2)	Maneuver Description			Sustained Load Factor (g)	Limiting Criteria
		Airspeed (KTAS)	Control Type	Amount (Deg)		
6.5	70	195	Cyclic Pull	0.70	1.55	Incipient Stall
			Cyclic Push	1.90	0.10	Flapping
		167	Cyclic Pull	1.30	1.78	Incipient Stall
			Cyclic Push	2.40	0.07	Flapping
		150	Cyclic Pull	2.00	2.00	Incipient Stall
			Collective + Cyclic Pull	1.20	1.95	Incipient Stall
			Collective Pull	3.05	1.85	Maximum Horsepower
			Cyclic Push	2.85	0.02	Flapping
			Collective + Cyclic Push	2.20	-0.05	Flapping
			Collective Push	6.75	0.02	Flapping
	105	195	Cyclic Pull	0.75	1.60	Incipient Stall
			Cyclic Push	1.60	0.20	Flapping
		167	Cyclic Pull	1.40	1.85	Incipient Stall
			Cyclic Push	2.25	0.12	Flapping
		150	Cyclic Pull	2.15	2.07	Flapping
			Collective + Cyclic Pull	1.25	2.00	Incipient Stall
			Collective Pull	3.05	1.83	Maximum Horsepower
			Cyclic Push	2.75	0.07	Flapping
			Collective + Cyclic Push	2.00	0.02	Flapping
			Collective Push	6.70	0.02	Flapping

TABLE XXXVIII - CONTINUED

Wing Incidence (Deg)	Wing Area (Ft^2)	Maneuver Description			Sustained Load Factor (g)	Limiting Criteria
		Airspeed (KTAS)	Control Type	Amount (Deg)		
9.5	70	195	Cyclic Pull	0.85	1.63	Incipient Stall
			Cyclic Push	1.90	0.12	Flapping
		167	Cyclic Pull	1.40	1.85	Incipient Stall
			Cyclic Push	2.40	0.07	Flapping
		150	Cyclic Pull	2.10	2.05	Flapping
			Collective + Cyclic Pull	1.25	2.00	Incipient Stall
			Collective Pull	3.10	1.85	Maximum Horsepower
			Cyclic Push	2.80	0.05	Flapping
			Collective + Cyclic Push	2.15	0	Flapping
			Collective Push	6.75	0.02	Flapping
	105	195	Cyclic Pull	0.95	1.70	Incipient Stall
			Cyclic Push	1.45	0.30	Flapping
		167	Cyclic Pull	1.55	1.92	Incipient Stall
			Cyclic Push	2.10	0.19	Flapping
		150	Cyclic Pull	2.25	2.12	Flapping
			Collective + Cyclic Pull	1.35	2.05	Incipient Stall
			Collective Pull	2.90	1.75	Maximum Horsepower
			Cyclic Push	2.60	0.15	Flapping
			Collective + Cyclic Push	1.90	0.08	Flapping
			Collective Push	6.70	0.07	Flapping

TABLE XXXVIII - CONTINUED

Wing Incidence (Deg)	Wing Area (Ft^2)	Maneuver Description			Sustained Load Factor (g)	Limiting Criteria
		Airspeed (KTAS)	Control Type	Amount (Deg)		
12.5	70	195	Cyclic Pull	0.95	1.73	Incipient Stall
			Cyclic Push	1.75	0.20	Flapping
		167	Cyclic Pull	1.55	1.90	Incipient Stall
			Cyclic Push	2.30	0.10	Flapping
		150	Cyclic Pull	2.20	2.10	Incipient Stall
			Collective + Cyclic Pull	1.30	2.00	Incipient Stall
			Collective Pull	2.95	1.70	Maximum Horsepower
			Cyclic Push	2.70	0.10	Flapping
			Collective + Cyclic Push	2.10	0	Flapping
			Collective Push	6.5	0.03	Flapping
	105	195	Cyclic Pull	1.10	1.77	Incipient Stall
			Cyclic Push	1.30	0.42	Flapping
		167	Cyclic Pull	1.65	1.99	Incipient Stall
			Cyclic Push	1.35	0.23	Flapping
		150	Cyclic Pull	2.43	2.19	Flapping
			Collective + Cyclic Pull	1.40	2.10	Incipient Stall
			Collective Pull	2.50	1.60	Maximum Horsepower
			Cyclic Push	2.45	0.15	Flapping
			Collective + Cyclic Push	1.30	0.12	Flapping
			Collective Push	6.25	0.15	Flapping

TABLE XXXIX. RESULTS OF PULLUP AND PUSHOVER MANEUVERS, TASK II – WINGED CONFIGURATIONS, BASELINE ROTOR

Wing Incidence (Deg)	Wing Area (Ft^2)	Maneuver Description			Sustained Load Factor (g)	Limiting Criteria
		Airspeed (KTAS)	Control Type	Amount (Deg)		
6.5	70	195	Cyclic Pull	1.10	1.90	Flapping
			Cyclic Push	1.75	0.15	Flapping
		167	Cyclic Pull	1.75	2.15	Flapping
			Cyclic Push	2.35	0.05	Flapping
		150	Cyclic Pull	2.15	2.20	Flapping
			Collective + Cyclic Pull	1.50	2.30	Flapping
			Collective Pull	3.00	1.90	Maximum Horsepower
			Cyclic Push	2.75	0.05	Flapping
			Collective + Cyclic Push	2.10	-0.03	Flapping
			Collective Push	7.00	-0.05	Flapping
	105	195	Cyclic Pull	1.10	1.95	Flapping
			Cyclic Push	1.40	0.30	Flapping
		167	Cyclic Pull	1.85	2.22	Flapping
			Cyclic Push	1.90	0.22	Flapping
		150	Cyclic Pull	2.00	2.10	Flapping
			Collective + Cyclic Pull	1.55	2.33	Flapping
			Collective Pull	2.80	1.72	Maximum Horsepower
			Cyclic Push	2.50	0.10	Flapping
			Collective + Cyclic Push	1.85	0.05	Flapping
			Collective Push	6.5	0.02	Flapping

TABLE XXXIX - CONTINUED

Wing Incidence (Deg)	Wing Area (Ft^2)	Maneuver Description: Airspeed (KTAS)	Maneuver Description: Control Type	Maneuver Description: Amount (Deg)	Sustained Load Factor (g)	Limiting Criteria
9.5	70	195	Cyclic Pull	1.20	1.98	Flapping
			Cyclic Push	1.75	0.20	Flapping
		167	Cyclic Pull	1.85	2.20	Flapping
			Cyclic Push	2.25	0.10	flapping
		150	Cyclic Pull	2.25	2.25	Flapping
			Collective + Cyclic Pull	1.50	2.35	Flapping
			Collective Pull	3.00	1.75	Maximum Horsepower
			Cyclic Push	2.65	0.03	Flapping
			Collective + Cyclic Push	2.10	-0.02	Flapping
			Collective Push	7.00	-0.05	Flapping
	105	195	Cyclic Pull	1.40	2.10	Flapping
			Cyclic Push	1.20	0.43	Flapping
		167	Cyclic Pull	2.05	2.33	Flapping
			Cyclic Push	1.85	0.25	Flapping
		150	Cyclic Pull	2.25	2.22	Flapping
			Collective + Cyclic Pull	1.65	2.38	Flapping
			Collective Pull	2.50	1.67	Maximum Horsepower
			Cyclic Push	2.35	0.17	Flapping
			Collective + Cyclic Push	1.75	0.12	Flapping
			Collective Push	6.00	0.10	Flapping

TABLE XXXIX - CONTINUED

Wing Incidence (Deg)	Wing Area (Ft^2)	Maneuver Description			Sustained Load Factor (g)	Limiting Criteria
		Airspeed (KTAS)	Control Type	Amount (Deg)		
12.5	70	195	Cyclic Pull	1.30	2.05	Flapping
			Cyclic Push	1.60	0.25	Flapping
		167	Cyclic Pull	1.90	2.25	Flapping
			Cyclic Push	2.15	0.20	Flapping
		150	Cyclic Pull	2.25	2.22	Flapping
			Collective + Cyclic Pull	1.60	2.40	Flapping
			Collective Pull	2.40	1.67	Maximum Horsepower
			Cyclic Push	2.50	0.10	Flapping
			Collective + Cyclic Push	2.00	0	Flapping
			Collective Push	6.50	0.03	Flapping
	105	195	Cyclic Pull	1.50	2.25	Flapping
			Cyclic Push	1.15	0.43	Flapping
		167	Cyclic Pull	2.10	2.38	Flapping
			Cyclic Push	1.85	0.23	Flapping
		150	Cyclic Pull	2.60	2.44	Flapping
			Collective Cyclic Pull	1.75	2.50	Flapping
			Collective Pull	2.00	1.52	Maximum Horsepower
			Cyclic Push	2.50	0.13	Flapping
			Collective + Cyclic Push	1.85	0.11	Flapping
			Collective Push	6.50	0.08	Flapping

TABLE XL. RESULTS OF PULLUP AND PUSHOVER MANEUVERS, TASK II - WINGED CONFIGURATIONS, HIGH SOLIDITY ROTOR

Wing Incidence (Deg)	Wing Area (Ft^2)	Maneuver Description			Sustained Load Factor (g)	Limiting Criteria
		Airspeed (KTAS)	Control Type	Amount (Deg)		
6.5	70	195	Cyclic Pull	1.55	2.24	Flapping
			Cyclic Push	1.95	0.08	Flapping
		167	Cyclic Pull	2.10	2.37	Flapping
			Cyclic Push	2.35	0.07	Flapping
		150	Cyclic Pull	2.55	2.44	Flapping
			Collective + Cyclic Pull	1.70	2.58	Flapping
			Collective Pull	2.25	1.62	Maximum Horsepower
			Cyclic Push	3.00	0.04	Flapping
			Collective + Cyclic Push	2.35	-0.12	Flapping
			Collective Push	7.50	-0.12	Flapping
	105	195	Cyclic Pull	1.65	2.28	Flapping
			Cyclic Push	1.50	0.27	Flapping
		167	Cyclic Pull	2.20	2.47	Flapping
			Cyclic Push	2.00	0.15	Flapping
		150	Cyclic Pull	2.65	2.48	Flapping
			Collective + Cyclic Pull	1.80	2.53	Flapping
			Collective Pull	2.00	1.52	Maximum Horsepower
			Cyclic Push	2.65	0.02	Flapping
			Collective + Cyclic Push	2.15	-0.02	Flapping
			Collective Push	7.50	-0.05	Flapping

TABLE XL - CONTINUED

Wing Incidence (Deg)	Wing Area (Ft^2)	Maneuver Description			Sustained Load Factor (g)	Limiting Criteria
		Airspeed (KTAS)	Control Type	Amount (Deg)		
9.5	70	195	Cyclic Pull	1.67	2.31	Flapping
			Cyclic Push	1.75	0.17	Flapping
		167	Cyclic Pull	2.20	2.47	Flapping
			Cyclic Push	2.30	0.11	Flapping
		150	Cyclic Pull	2.70	2.50	Flapping
			Collective + Cyclic Pull	1.80	2.62	Flapping
			Collective Pull	2.10	1.55	Maximum Horsepower
			Cyclic Push	2.35	0.03	Flapping
			Collective + Cyclic Push	2.30	-0.07	Flapping
			Collective Push	7.50	0.03	Flapping
	105	195	Cyclic Pull	1.85	2.38	Flapping
			Cyclic Push	1.30	0.37	Flapping
		167	Cyclic Pull	2.35	2.55	Flapping
			Cyclic Push	1.75	0.34	Flapping
		150	Cyclic Pull	2.75	2.55	Flapping
			Collective + Cyclic Pull	1.90	2.70	Flapping
			Collective Pull	1.80	1.45	Maximum Horsepower
			Cyclic Push	2.40	0.12	Flapping
			Collective + Cyclic Push	2.00	0.05	Flapping
			Collective Push	7.25	0	Flapping

TABLE XL. - CONTINUED

Wing Incidence (Deg)	Wing Area (Ft^2)	Maneuver Description			Sustained Load Factor (g)	Limiting Criteria
		Airspeed (KTAS)	Control Type	Amount (Deg)		
12.5	70	195	Cyclic Pull	1.80	2.40	Flapping
			Cyclic Push	1.65	0.24	Flapping
		167	Cyclic Pull	2.30	2.52	Flapping
			Cyclic Push	2.20	0.15	Flapping
		150	Cyclic Pull	2.65	2.55	Flapping
			Collective + Cyclic Pull	1.75	2.65	Flapping
			Collective Pull	1.40	1.40	Maximum Horsepower
			Cyclic Push	2.60	0.10	Flapping
			Collective + Cyclic Push	2.10	0	Flapping
			Collective Push	7.25	-0.02	Flapping
	105	195	Cyclic Pull	2.00	2.50	Flapping
			Cyclic Push	1.15	0.45	Flapping
		167	Cyclic Pull	2.55	2.65	Flapping
			Cyclic Push	1.65	0.30	Flapping
		150	Cyclic Pull	2.90	2.60	Flapping
			Collective + Cyclic Pull	2.05	2.80	Flapping
			Collective Pull	1.70	1.40	Maximum Horsepower
			Cyclic Push	2.25	0.17	Flapping
			Collective + Cyclic Push	1.30	0.15	Flapping
			Collective Push	6.75	0.07	Flapping

APPENDIX V
TASK III - MANEUVER RESULTS, BASIC DATA

TABLE XLI. RESULTS OF PULLUP AND PUSHOVER MANEUVERS, TASK III - 1.50g DESIGN

Maneuver Description			Sustained Load Factor (g)	Limiting Criteria
Airspeed (KTAS)	Control Type	Amount (Deg)		
195	Cyclic Pull	0.47	1.33	Incipient Stall
	Cyclic Push	2.00	0.05	Flapping
177, V_{NRP}	Cyclic Pull	0.85	1.45	Incipient Stall
	Collective + Cyclic Pull	0.45	1.40	Incipient Stall
	Cyclic Push	2.20	0.08	Flapping
150	Cyclic Pull	1.95	1.76	Incipient Stall
	Collective + Cyclic Pull	1.10	1.73	Incipient Stall
	Collective Pull	2.50	1.68	Incipient Stall
	Cyclic Push	2.80	0.05	Flapping
	Collective + Cyclic Push	1.95	0	Flapping
	Collective Push	6.00	-0.10	Flapping
120	Cyclic Pull	2.55	1.76	Zero Horsepower
	Collective + Cyclic Pull	2.40	2.14	Flapping
	Collective Pull	4.20	1.84	Maximum Horsepower
	Cyclic Push	3.70	0.05	Flapping
	Collective + Cyclic Push	2.70	-0.10	Flapping
	Collective Push	9.00	-0.29	Flapping
89	Cyclic Pull	3.85	1.75	Zero Horsepower
	Collective + Cyclic Pull	3.10	2.05	Pitch Rate
	Collective Pull	3.90	1.50	Maximum Horsepower
	Cyclic Push	4.85	-0.08	Pitch Rate
	Collective + Cyclic Push	3.95	-0.25	Flapping
	Collective Push	10.00	-0.18	Extreme Flight Conditions
56	Collective + Cyclic Pull	3.10	1.65	Pitch Rate
	Collective Pull	3.50	1.30	Maximum Horsepower
	Collective + Cyclic Push	4.75	-0.17	Pitch Rate
	Collective Push	10.00	0.22	Extreme Flight Conditions
0	Collective Pull	1.50	0.15	Maximum Horsepower

TABLE XLII. RESULTS OF PULLUP AND PUSHOVER MANEUVERS, TASK III - 1.75g DESIGN

Maneuver Description			Sustained Load Factor (g)	Limiting Criteria
Airspeed (KTAS)	Control Type	Amount (Deg)		
195	Cyclic Pull	0.55	1.50	Incipient Stall
	Cyclic Push	1.70	0	Flapping
175, V_{NRP}	Cyclic Pull	1.00	1.70	Incipient Stall
	Collective + Cyclic Pull	0.65	1.70	Incipient Stall
	Cyclic Push	1.95	0.03	Flapping
150	Cyclic Pull	1.90	1.97	Zero Horsepower
	Collective + Cyclic Pull	1.25	1.96	Flapping
	Collective Pull	3.35	1.92	Maximum Horsepower
	Cyclic Push	2.40	0	Flapping
	Collective + Cyclic Push	1.80	-0.05	Flapping
	Collective Push	6.00	-0.07	Flapping
120	Cyclic Pull	2.30	1.79	Zero Horsepower
	Collective + Cyclic Pull	2.65	2.40	Pitch Rate
	Collective Pull	4.00	1.80	Maximum Horsepower
	Cyclic Push	3.30	-0.07	Flapping
	Collective + Cyclic Push	2.55	-0.15	Flapping
	Collective Push	8.50	-0.20	Flapping
89	Cyclic Pull	3.85	1.82	Pitch Rate
	Collective + Cyclic Pull	2.90	2.06	Pitch Rate
	Collective Pull	3.85	1.51	Maximum Horsepower
	Cyclic Push	4.25	-0.10	Pitch Rate
	Collective + Cyclic Push	3.75	-0.25	Flapping
	Collective Push	10.00	-0.14	Extreme Flight Conditions
56	Collective + Cyclic Pull	3.00	1.68	Pitch Rate
	Collective Pull	3.75	1.30	Maximum Horsepower
	Collective + Cyclic Push	4.40	-0.10	Pitch Rate
	Collective Push	10.00	0.23	Extreme Flight Conditions
0	Collective Pull	1.40	1.17	Maximum Horsepower

TABLE XLIII. RESULTS OF PULLUP AND PUSHOVER MANEUVERS, TASK III - 2.00g DESIGN

Maneuver Description			Sustained Load Factor (g)	Limiting Criteria
Airspeed (KTAS)	Control Type	Amount (Deg)		
195	Cyclic Pull	0.57	1.75	Flapping
	Cyclic Push	1.30	-0.06	Zero Horsepower
170, V_{NRP}	Cyclic Pull	1.10	2.03	Flapping
	Collective + Cyclic Pull	0.75	2.00	Flapping
	Cyclic Push	1.50	0	Zero Horsepower
150	Cyclic Pull	1.60	2.07	Zero Horsepower
	Collective + Cyclic Pull	1.30	2.30	Flapping
	Collective Pull	3.25	1.95	Maximum Horsepower
	Cyclic Push	1.95	-0.06	Zero Horsepower
	Collective + Cyclic Push	1.75	-0.23	Flapping
	Collective Push	6.65	-0.19	Flapping
120	Cyclic Pull	2.10	1.90	Zero Horsepower
	Collective + Cyclic Pull	2.25	2.43	Pitch Rate
	Collective Pull	3.65	1.76	Maximum Horsepower
	Cyclic Push	2.75	-.15	Zero Horsepower
	Collective + Cyclic Push	2.45	-0.30	Flapping
	Collective Push	9.00	-0.26	Flapping
89	Cyclic Pull	3.30	1.85	Pitch Rate
	Collective + Cyclic Pull	2.60	2.10	Pitch Rate
	Collective Pull	3.60	1.50	Maximum Horsepower
	Cyclic Push	3.45	-0.08	Pitch Rate
	Collective + Cyclic Push	3.55	-0.38	Flapping
	Collective Push	10.00	-0.12	Extreme Flight Conditions
56	Collective + Cyclic Pull	2.80	1.58	Maximum Horsepower
	Collective Pull	3.70	1.28	Maximum Horsepower
	Collective + Cyclic Push	4.00	-0.10	Pitch Rate
	Collective Push	10.00	0.23	Extreme Flight Conditions
0	Collective Pull	1.50	1.18	Maximum Horsepower